BAROTROPIC INSTABILITY OF AN INITIAL VALUE PROBLEM

by

GODELIEVE DEBLONDE

B. Sc. -- McGill University (1980)

M. Sc. -- McGill University (1981)

SUBMITTED TO THE DEPARTMENT OF
EARTH, ATMOSPHERE AND PLANETARY SCIENCES
IN PARTIAL FULFILLMENT OF THE REQUIREMENTS
FOR THE DEGREE OF

MASTER OF SCIENCE IN METEOROLOGY

at the

MASSACHUSETTS INSTITUTE OF TECHNOLOGY

September 1984

Signature of Author: _____

Center for Meteorology and PhysicaL Oceanography
Department of Earth, Atmospheric and Planetary Sciences
September 12, 1984

Certified by: _____

Dr. Ka-Kit Tung
Thesis Supervisor

Accepted by: _____

Theodore Madden
Chairman, Departmental Committee on Graduate Students

ACKNOWLEDGEMENTS

This research was sponsored in part by the National Aeronautics and Space Administration

Grant NASA NGR 22-009-727

and

The National Science Foundation

Grant NSF ATM 8217616

BAROTROPIC INSTABILITY OF AN INITIAL VALUE PROBLEM

by

GODELIEVE DEBLONDE

Submitted to the Department of Earth, Atmosphere and Planetary Sciences on September 12, 1984 in partial fulfillment of the requirements for the degree of Master of Science in Meteorology.

ABSTRACT

A numerical study is done on the time-evolution of Rossby waves in a sheared zonal flow in a finite domain. Cases with and without an inflection point in the meridional gradient of the potential vorticity of the basic state are considered. For the case with an inflection point, both stable and unstable (exponentially) cases are considered.

The conclusions on the development of a wave packet as an initial condition drawn by Warsham (1983) using numerical methods and Tung (1983) using asymptotics in an infinite domain are the same provided the wave packet does not interact with the walls.

For the case with an inflection point, using a modified version of the wave packet analysis of Tung (1983) and combining it with the theory of overreflection developed by Lindzen and Tung (1978), one is able to predict and explain qualitatively the time-evolution of an initial condition.

Distinct features (stationary or transient) can be observed in the Fourier spectrum of the vorticity depending on whether the initial condition develops into a normal mode or not respectively.

Thesis Supervisor: Dr. Ka-Kit Tung

Title: Associate Professor of Mathematics

TABLE OF CONTENTS

LIST OF FIGURES

Note: if y = 0, then there is no inflection point in the gradient of vorticity, otherwise there is.

Finite Domain:

Cases for which the initial condition is a stable eigenvector which is a solution of the eigenvalue problem. y = 0.0, K = 1.0, B= 6.0:

Cases for which the initial condition is an unstable eigenvector. y = 5.0, K = 1.25, B = -15.0:

Infinite domain:

Fig. 4.1.1 Orientation of crests of the initial condition on a graph of y vs x.

Couette flow case without inflection point; $\gamma = 0$, $B = 0$ and $y_o = 5$:

Fig. 4.1.2 Magnitude of the vorticity of southward-moving wave where $l_o/k = -2$ for time values ranging from 0 to 8.

Fig. 4.1.3 Magnitude of the vorticity of southward-moving wave where $l_o/k = -2$ for $t = 0$ and 8. Note that the wave does not move, so initial and final values are identical.

Fig. 4.1.4 Magnitude of the vorticity of northward-moving wave where $l_o/k = 2$ for time values ranging from 0 to 8.

Fig. 4.1.5 Magnitude of the vorticity of northward-moving wave where $l_o/k = 2$ fot $t = 0$ and 8. Note that the wave does not move, so initial and final values are identical.

Couette flow case with β-effect without inflection point; $\gamma = 0$, $y_o = 5$.

Fig. 4.1.6 Packet trajectories for $l_o/k = \pm 2$.

Fig. 4.1.7 Magnitude of the vorticity of southward-moving wave where $l_o/k = -2$ for time values ranging from 0 to 8.

Fig. 4.1.8 Magnitude of the vorticity of southward-moving wave where $l_o/k = -2$ for $t = 0$ and 8.

Fig. 4.1.9 Magnitude of the vorticity northward-moving wave where $l_o/k = 2$ for time values ranging from 0 to 8.

Fig. 4.1.10 Magnitude of the vorticity of northward-moving wave where $l_o/k = 2$ for $t = 0$ and 8.

Fig. 4.1.11 Energy of southward-moving wave where l_o/k = -2 for time values ranging from 0 to 8.

Fig. 4.1.12 Energy of northward-moving wave where l_o/k = 2 for time values ranging from 0 to 8.

Finite domain

Couette flow case. The initial condition is a Gaussian. y_o = 5.0, H = 0.75, l_o = 2.67, K = 1.0, B = 0.0, y = 0:

Fig. 4.1.13 Magnitude of the Fourier transform of the vorticity vs l for time values ranging between t=0 and 8.

Fig. 4.1.14 Magnitude of the vorticity vs y for time values ranging between t = 0 and 8.

Fig. 4.1.15 Real part of the streamfunction vs y for time values ranging between t=0 and 8.

Fig. 4.1.16 Energy of the wave vs y for time values ranging between t = 0 and 8.

Couette flow case. The initial condition is a Gaussian. y_o = 5.0, H = 0.75, l_o = 2.67, K = -1.0, B = 0.0, y=0:

Fig. 4.1.17 Magnitude of the Fourier transform of the vorticity vs l for time values ranging between t=0 and 8.

Fig. 4.1.18 Magnitude of the vorticity vs y for time values ranging between t = 0 and 8.

Fig. 4.1.19 Real part of the streamfunction vs y for time values ranging between t=0 and 8.

Fig. 4.1.20 Energy of the wave vs y for time values ranging between t = 0 and 8.

Couette flow with β-effect. The initial condition is a southward-moving Gaussian. y_c inside the domain and y_T outside the domain. yo = 10.5, H = 2.0, l_o = 2.0, y=0, K = -1.0, B = 20.0; $y_c \approx 6.5$, $y_T \approx 26.5$.

Fig. 4.1.21 Magnitude of the Fourier transform of the

vorticity vs l for time values ranging between t=0 and 3.

Fig. 4.1.22 Magnitude of the vorticity vs y for time values ranging between t = 0 and 3.

Fig. 4.1.23 Real part of the streamfunction vs y for time values ranging between t=0 and 3.

Fig. 4.1.24 Energy of the wave vs y for time values ranging between t = 0 and 3.

Fig. 4.1.25 Magnitude of the Fourier transform of the vorticity vs l for t = 0, 1.5 and 3.0.

Couette flow with β-effect. The initial condition is a northward-moving Gaussian. y_c and ys inside the domain. y_o = 8.0, H = 2.0, l_o = 2.0, y = 0.0, k = 1.0, B = 0.0; $y_c \approx 6.0$, $y_T \approx 16.0$.

Fig. 4.1.26 Magnitude of the Fourier transform of the vorticity vs l for time values ranging between t=0 and 8.

Fig. 4.1.27 Magnitude of the vorticity vs y for time values ranging between t = 0 and 8.

Fig. 4.1.28 Real part of the streamfunction vs y for time values ranging between t=0 and 8.

Fig. 4.1.29 Energy of the wave vs y for time values ranging between t = 0 and 8.

Fig. 4.1.30 Magnitude of the Fourier transform of the vorticity vs l for t=0, 2, 4 and 8.

Couette flow with β-effect. The initial condition is a northward-moving Gaussian. y_c outside the domain, y_T inside the domain. y_o = 8.0, H = 2.0, l_o = 1.0, y = 0.0, k = 1.0, B = 20.0; $y_c \approx -2.0$ $y_T \approx 18.0$.

Fig. 4.1.31 Magnitude of the Fourier transform of the vorticity vs l for time values ranging between t=0 and 6.8.

Fig. 4.1.32 Magnitude of the vorticity vs y for time values

ranging between t = 0 and 6.8.

Fig. 4.1.33 Real part of the streamfunction vs y for time

Fig. 4.1.34 Energy of the wave vs y for time values ranging between t = 0 and 6.8.

Fig. 4.1.35 Magnitude of the Fourier transform of the vorticity vs l for t=0, 2 and 4.

Fig. 4.1.36 Magnitude of the Fourier transform of the vorticity vs l for t=6 and 8.

Couette flow with β-effect. The initial condition is a southward-moving Gaussian. y_C and y_T outside the domain. y_o = 8.0, H = 2.0, l_o = 2.0, y = 0.0, K = -1.0, B = 75.0; $y_C \approx -7.0$, $y_T \approx 68.0$.

Fig. 4.1.37 Magnitude of the Fourier transform of the vorticity vs l for time values ranging between t=0 and 6.4.

Fig. 4.1.38 Magnitude of the vorticity vs y for time values ranging between t = 0 and 6.4.

Fig. 4.1.39 Real part of the streamfunction vs y for time values ranging between t=0 and 6.4.

Fig. 4.1.40 Energy of the wave vs y for time values ranging between t = 0 and 6.4.

Fig. 4.1.41 Magnitude of the Fourier transform of the vorticity vs l for t = 0 and 2.

Fig. 4.1.42 Magnitude of the Fourier transform of the vorticity vs l for t = 4 and 6.

Couette flow with β-effect. The initial condition is a northward-moving Gaussian. y_C and y_T outside the domain. y_o = 8.0, H = 2.0, l_o = 2.0, K = 1.0, y = 0.0, B = 75.0; $y_C \approx -7.0$, $y_T \approx 68.0$.

Fig. 4.1.43 Magnitude of the Fourier transform of the vorticity vs l for time values ranging between t=0 and 6.8.

Fig. 4.1.44 Magnitude of the vorticity vs y for time values ranging between t = 0 and 6.8.

Fig. 4.1.45 Real part of the streamfunction vs y for time values ranging between t=0 and 6.8.

Fig. 4.1.46 Energy of the wave vs y for time values ranging between t = 0 and 6.8.

Fig. 4.1.47 Magnitude of the Fourier transform of the vorticity vs l for t=0 and 2.

Fig. 4.1.48 Magnitude of the Fourier transform of the vorticity vs l for t=4 and 6.

Cases with inflection point:

Fig. 4.2.1A Q(y) vs y for $A^2>0$ and $y_c<y_B<y_{Tu}$.

Fig. 4.2.1B Q(y) vs y for $A^2>0$ and $y_{Tu}<y_B<y_c$.

Fig. 4.2.1C Q(y) vs y for $A^2<0$ and $y_{Tu}<y_c<y_B$.

Fig. 4.2.1D Q(y) vs y for $A^2<0$ and $y_B<y_c<y_{Tu}$.

Stable initial condition in a finite domain:

For $y_{Tu}<y_B<y_c<y_o$. y_o = 3.85, H = 0.75, l_o = 5.0, y = 17.8, K = -2.5, B = -62.3; $y_c \approx 3.65$, $y_{Tu} \approx 3.41$, y_B = 3.5, Cgy ≈ -0.16.

Fig. 4.2.2 Magnitude of the Fourier transform of the vorticity vs l for time values ranging between t=0 and 5.6.

Fig. 4.2.3 Magnitude of the vorticity vs y for time values ranging between t = 0 and 5.6.

Fig. 4.2.4 Real part of the streamfunction vs y for time values ranging between t=0 and 5.6.

Fig. 4.2.5 Energy of the wave vs y for time values ranging between t = 0 and 5.6.

Fig. 4.2.6 Magnitude of the Fourier transform of the

vorticity vs l for t=0, 2, 4 and 6.

For $y_{Tu}<y_B<y_c<y_o$. $y_o = 11.0$, $H = 2.0$, $l_o = 2.0$, $y = 1.5$, $k = -1.0$, $B = -15.0$; $y_c \approx 10.7$, $y_{Tu} \approx 8.6$, $y_B = 10.0$, $C_{gy} \approx -0.24$.

Fig. 4.2.7 Magnitude of the Fourier transform of the vorticity vs l for time values ranging between t=0 and 6.0.

Fig. 4.2.8 Magnitude of the vorticity vs y for time values ranging between t = 0 and 6.0.

Fig. 4.2.9 Real part of the streamfunction vs y for time values ranging between t=0 and 6.0.

Fig. 4.2.10 Energy of the wave vs y for time values ranging between t = 0 and 6.0.

Fig. 4.2.11 Magnitude of the Fourier transform of the vorticity vs l for t=0, 1.5, 3.0, 4.5 and 6.0.

Unstable initial condition in a finite domain:

For $y_o<y_c<y_B<y_{Tu}$. $y_o = 2.5$, $H = 1.0$, $l_o = 2.0$, $y = 2.5$, $k = -1.25$, $B = -15.0$; $y_c \approx 2.95$, $y_{Tu} \approx 3.02$, $y_B = 3.0$, $C_{gy} \approx 0.4$.

Fig. 4.2.12 Magnitude of the Fourier transform of the vorticity vs l for time values ranging between t=0 and 15.0.

Fig. 4.2.13 Magnitude of the vorticity vs y for time values ranging between t = 0 and 15.0.

Fig. 4.2.14 Real part of the streamfunction vs y for time values ranging between t=0 and 15.0.

Fig. 4.2.15 Energy of the wave vs y for time values ranging between t = 0 and 15.0.

Fig. 4.2.16 Magnitude of the Fourier transform of the vorticity vs l for t=0, 3 and 6.

Fig. 4.2.17 Magnitude of the Fourier transform of the vorticity vs l for t=6, 9, 12 and 15.

For $y_o < y_c < y_B < y_{Tu}$: y_o = 2.5, H = 1.0, l_o = 2.0, y = 2.5, k = 1.25, B = -15.0; $y_c \approx 2.95$, $y_{Tu} \approx 3.02$, y_B = 3.0, $C_{gy} \approx -0.4$.

Fig. 4.2.18 Magnitude of the Fourier transform of the vorticity vs l for time values ranging between t=0 and 16.0 .

Fig. 4.2.19 Magnitude of the vorticity vs y for time values ranging between t = 0 and 16.0 .

Fig. 4.2.20 Real part of the streamfunction vs y for time values ranging between t=0 and 16.0.

Fig. 4.2.21 Energy of the wave vs y for time values ranging between t = 0 and 16.0.

Fig. 4.2.22 Magnitude of the Fourier transform of the vorticity vs l for t=0, 8 and 16.

Fig. 4.2.23 Real part of the vorticity vs y and vs x for t=0.

Fig. 4.2.24 Real part of the vorticity vs y and vs x for t=1.5.

Fig. 4.2.25 Real part of the vorticity vs y and vs x for t=3.0.

Fig. 4.2.26 Real part of the vorticity vs y and vs x for t=4.5.

Fig. 4.2.27 Real part of the vorticity vs y and vs x for t=6.0.

Fig. 4.2.28 Real part of the vorticity vs y and vs x for t=7.5.

Fig. 4.2.29 Real part of the vorticity vs y and vs x for t=9.0.

Fig. 4.2.30 Real part of the vorticity vs y and vs x for t=10.5.

Fig. 4.2.31 Real part of the vorticity vs y and vs x for t=12.0

Fig. 4.2.32 Real part of the vorticity vs y and vs x for t=15.0.

For $y_C < y_B < y_{Tu} < y_o$, $y_o = 5.0$, $H = 0.75$, $l_o = 2.67$, $\gamma = 17.8$, $K = -2.5$, $B = -62.3$; $y_C \approx 3.0$, $y_{Tu} \approx 3.8$, $y_B = 3.5$, $C_{gy} \approx -0.20$.

Fig. 4.2.33 Magnitude of the Fourier transform of the vorticity vs l for time values ranging between t=0 and 16.

Fig. 4.2.34 Magnitude of the vorticity vs y for time values ranging between t = 0 and 16.

Fig. 4.2.35 Real part of the streamfunction vs y for time values ranging between t=0 and 16.

Fig. 4.2.36 Energy of the wave vs y for time values ranging between t = 0 and 16.

Fig. 4.2.37 Magnitude of the Fourier transform of the vorticity vs l for t=0 and 0.8.

Fig. 4.2.38 Magnitude of the Fourier transform of the vorticity vs l for t=2.4 and 4.0.

Fig. 4.2.39 Magnitude of the Fourier transform of the vorticity vs l for t=6.4 and 8.0.

Fig. 4.2.40 Magnitude of the Fourier transform of the vorticity vs l for t=12 and 16.

Fig. 4.2.41 Real part of the vorticity vs y and vs x for t=0.

Fig. 4.2.42 Real part of the vorticity vs y and vs x for t=1.6.

Fig. 4.2.43 Real part of the vorticity vs y and vs x for t=3.2.

Fig. 4.2.44 Real part of the vorticity vs y and vs x for t=4.8.

Fig. 4.2.45 Real part of the vorticity vs y and vs x for t=6.4.

Fig. 4.2.46 Real part of the vorticity vs y and vs x for t=8.0.

Fig. 4.2.47 Real part of the vorticity vs y and vs x for t=9.6.

Fig. 4.2.48 Real part of the vorticity vs y and vs x for t=11.2.

Fig. 4.2.49 Real part of the vorticity vs y and vs x for t=12.8.

Fig. 4.2.50 Real part of the vorticity vs y and vs x for t=14.4.

Fig. 4.2.51 Real part of the vorticity vs y and vs x for t=16.0.

For $y_{Tu}<y_B<y_C<y_o$. $y_o = 11.0$, $H = 2.0$, $k = 1.0$ $l_o = 2.0$, $y = 1.5$, $B = -15.0$; $y_C \approx 10.7$, $y_{Tu} \approx 8.6$, $y_B = 10.0$, $C_{gy} \approx 0.24$.

Fig. 4.2.52 Magnitude of the Fourier transform of the vorticity vs l for time values ranging between t=0 and 8.0.

Fig. 4.2.53 Magnitude of the vorticity vs y for time values ranging between t = 0 and 8.0.

Fig. 4.2.54 Real part of the streamfunction vs y for time values ranging between t=0 and 8.0.

Fig. 4.2.55 Energy of the wave vs y for time values ranging between t = 0 and 8.0.

Fig. 4.2.56 Magnitude of the Fourier transform of the vorticity vs l for t=0, 2 and 4.

Fig. 4.2.57 Magnitude of the Fourier transform of the vorticity vs l for t=6 and 8.

For $y_{Tu}<y_B<y_C<y_o$. $y_o = 5.0$, $H = 0.75$, $l_o = 2.67$, $y = 4.06$, $k = -1.0$, $B = -12.17$; $y_C \approx 4.0$, $y_{Tu} \approx 2.67$, $y_B = 3.0$, $C_{gy} \approx -0.66$.

Fig. 4.2.58 Magnitude of the Fourier transform of the vorticity vs l for time values ranging between

LIST OF TABLES

Total energy for the case corresponding to the appropriate figure:

I. INTRODUCTION

To study the stability of a shear flow to infinitesimal perturbations, what is usually done is to assume that the solution is of the form of a normal mode. To find the general solution of the problem, one has to solve the initial value problem. To achieve this analytically is very complicated and has not been done yet.

Another way to solve this problem is numerically. The results of numerical solutions are usually hard to interpret and analytic results for a corresponding simplified problem are welcome (i.e. asymptotic analysis, wave packet theory...).

In this thesis, the time-dependent evolution of Rossby waves in a sheared zonal flow in a finite domain is studied. The equation used in this model is the linearized barotropic vorticity equation. The solution is considered to be periodic in x. The problem is solved numerically by taking a Fourier transform in y and integrating in time.

In this thesis, it is shown that the equations representing the evolution of an arbitrary initial condition involves the coupling of different wavelengths. This coupling is due to the presence of the walls. The importance of this coupling will be studied by paying a special attention to the evolution of the solution in Fourier space. This is also why the problem is

solved by using a Fourier transform.

Tung (1983) has studied the evolution of an initial value problem where the initial condition is a wave packet with central wavenumber $\vec{K}_o = (K_o, l_o)$ in an infinite domain with uniform shear. He has shown that even though the initial disturbances that constitute the wave packet in general do not have a well-defined phase speed, during the later stages of its evolution, the wave packet behaves as a whole, from kinematic considerations, as if there exists a well defined phase speed c. He has shown that a packet with positive (l_o/K_o) has a different trajectory than a packet with negative (l_o/K_o). For $(l_o/K_o) > 0$, the initial shape moves first northward untill it reaches a turning point where the group velocity in the meridional direction vanishes. The packet then moves southward, and eventually stagnates at the stagnation level which is equal to the critical level. For the case where $(l_o/K_o) < 0$, the packet trajectory is monotone; the initial shape moves south without changing direction towards the same stagnation level. Worsham (1983) solving the above problem numerically has shown that his results agree with Tung's analytical results.

For the problem in an infinite domain, no normal mode solutions are possible. In a finite domain, normal modes can develop. We want to study what physical quantities control the onset of this development.

In chapter II of this thesis, the problem formulation is described. In chapter III, the numerical methods are presented together with a test case. In chapter IV, we first present the results of Worsham (1983) in an infinite domain for a Couette flow (i.e. uniform shear without β-effect), then with the β-effect. These results are compared with the finite domain case where first the waves do not interact with the walls and second, where the waves do interact with the walls. In particular, the change in shape of the Fourier spectrum of the vorticity is discussed. Further, the effect of the presence of an inflection point (which is a necessary condition for instability) is studied. The expressions for the prediction of the stagnation level and the turning point found by Tung (1983) are modified in consequence. Also, the theory of overreflection developed by Lindzen and Tung (1978) is applied. The prediction of the position of the critical level combined with the overreflection theory permits one to explain the time evolution of the wave packet.

II. PROBLEM FORMULATION

2.1 Constant shear case

To study the time-dependent evolution of Rossby waves in a zonal flow with shear U(y), the following linearized barotropic vorticity equation is taken as the model equation:

$$\left(\frac{\partial}{\partial t} + U(y)\frac{\partial}{\partial x}\right)\zeta + (\beta - U_{yy})\frac{\partial \Psi}{\partial x} = 0 \qquad (2.1.1)$$

where Ψ is the perturbation streamfunction and

$\zeta \equiv (\partial^2/\partial x^2 + \partial^2/\partial y^2)\Psi = \nabla^2\Psi$

is the perturbation vorticity.

Equation (2.1.1) is to be solved subject to the initial condition

$$\zeta(x, y, t=0) = \zeta_0(x, y). \qquad (2.1.2)$$

The boundary conditions are

$$\zeta = 0 \quad (y = 0, 2D) \qquad (2.1.3)$$

where ζ is periodic in x with a period of

$2\pi a \cos \Theta_0$;

the length of the zonal circle at latitude $\Theta = \Theta_0$.

The shear is taken as $U(y) = \alpha y$. Since U_{yy} would be zero, the additional assumption that $\beta - U_{yy}$ is of the form $\sigma(y - b)$ is made. b is the so-called inflection point,

i.e. the location where the mean vorticity gradient changes sign.

The resulting equation is then

$$\left(\frac{\partial}{\partial t} + \alpha y \frac{\partial}{\partial x}\right) \nabla^2 \Psi + \sigma (y - b) \frac{\partial \Psi}{\partial x} = 0 \qquad (2.1.4)$$

To solve equation (2.1.1), we take a Fourier sine transform of the equation so that the boundary conditions $\zeta = 0$ at $y=0$, 2D will be satisfied. The coefficients of the above partial differential equation are not constant, and once the Fourier transform of the equation is taken, we obtain a system of first order linear differential equations. This is demonstrated here. Let $\Psi = \psi e^{ikx}$, then equation (2.1.4) becomes:

$$\left(\frac{\partial}{\partial t} + \alpha y i k\right) \left(\frac{\partial^2}{\partial y^2} - k^2\right) \psi + \sigma (y - b)\ ik\psi = 0 \qquad (2.1.5)$$

To be able to satisfy the boundary conditions, let

$$\psi = \sum_{n=0}^{\infty} \sin l_n y\ \tilde{\psi}(l_n, t);\quad l_n = n\pi/2D\ ,\ n=1, 2\ldots \qquad (2.1.6)$$

Replace ψ defined in (2.1.6) in eq. (2.1.5) and also drop the index n:

$$0 = \sum_{l} \{ (l^2+k^2) \frac{\partial \tilde{\psi}}{\partial t} + \sigma b i k \tilde{\psi} + i y k (\alpha (l^2+k^2) - \sigma) \tilde{\psi} \} \sin ly. \qquad (2.1.7)$$

Then

$$(1/D)\int_0^{2D} \sin l'y \ (\text{eq. } (2.1.7))\, dy = (l'^2+k^2)\frac{\partial \tilde{\psi}}{\partial t}(l', t)$$

$$+ \sigma bik\tilde{\psi}(l', t) + (1/D)\sum_{l}\left[\int_0^{2D} \sin l'y \sin ly\, dy\, y\, ik\right.$$

$$\left. \cdot \tilde{\psi}(l, t)\,(\alpha(l^2+k^2) - \sigma)\right] = 0 \qquad (2.1.8)$$

Now $\sin ly \sin l'y = 1/2\{\cos (l-l')y - \cos (l+l')y\}$.

Let $A \equiv \int_0^{2D} y \sin ly \sin l'y\, dy = 1/2 \int_0^{2D} y\, dy \cos (l-l')y - 1/2 \int_0^{2D} y\, dy \cos (l+l')y.$

Then if $l \neq l'$:

$$A = 1/2 \left.\frac{\cos (l-l')y}{(l-l')^2}\right|_0^{2D} - 1/2 \left.\frac{\cos(l+l')y}{(l+l')^2}\right|_0^{2D}$$

$$+ 1/2\, y \left.\frac{\sin (l-l')y}{(l-l')^2}\right|_0^{2D} - 1/2\, y \left.\frac{\sin (l+l')y}{(l+l')^2}\right|_0^{2D}$$

Also $\cos (l-l')\, 2D = (-1)^{n-n'}$, and $\sin (l-l')2D = 0$.

Then we get

$$A = 1/2 \left[\frac{(-1)^{n-n'}}{(l-l')^2} - \frac{1}{2}\right] - 1/2 \left[\frac{(-1)^{n+n'}}{(l+l')^2} - \frac{1}{2}\right]$$

And if $l = l'$, then $A = D^2$.

Equation (2.1.8) becomes:

$$0 = \frac{\partial\tilde{\psi}}{\partial t}(l', t) + \tilde{\psi}(l', t)\left\{\frac{\sigma\, ik(b-D)+\alpha ikD}{l'^2+k^2}\right.$$

$$+ \sum_{\substack{l=0 \\ l\neq l'}} \left[\frac{\alpha(l^2+k^2)-\sigma}{l'^2+k^2}\right](ik/2D)\left\{\left[\frac{(-1)^{n-n'}-1}{(l-l')^2}\right]\right.$$

$$\left.\left. -\left[\frac{(-1)^{n+n'}-1}{(l+l')^2}\right]\right\}.\tilde{\psi}(l, t)\right\} \qquad (2.1.9)$$

If we use L as a length scale and $1/\alpha$ as a time scale, then equation (2.1.9) in nondimensional form becomes:

$$\frac{\partial\tilde{\psi}}{\partial t}(l', t) = \tilde{\psi}(l', t)\left\{(B+yd)\frac{ik}{\mu'^2} - ikd\right\}$$

$$+ \sum_{\substack{l=0 \\ l\neq l'}}^{\infty} \left(\frac{\mu^2}{\mu'^2} - \frac{y}{\mu'^2}\right)\frac{ik2d}{\pi^2}\left\{\left[\frac{(-1)^{(n+n')}-1}{(n+n')^2}\right]\right.$$

$$\left. - \left[\frac{(-1)^{(n-n')}-1}{(n-n')^2}\right]\right\}.\tilde{\psi}(l, t) \qquad (2.1.10)$$

where

$$B = -\sigma bL/\alpha, \qquad y = \sigma L^2/\alpha,$$

$$\mu^2 = l^2+k^2, \quad \mu'^2 = l'^2+k^2,$$

$$l' = n'\pi/2d, \qquad l = n\pi/2d, \qquad d = D/L.$$

To study the problem without an inflection point, y has to be set equal to zero. Other interesting quantities to study are the energy and the vorticity.

i) Energy averaged over one cycle in x:

$$E(y,t) = 1/2\ \overline{\left[\left(\mathrm{Re}\ \frac{\partial\Psi}{\partial x}\right)^2 + \left(\mathrm{Re}\ \frac{\partial\Psi}{\partial y}\right)^2\right]}^{x}$$

Let $\Psi(x,y,t) = e^{ikx}\psi(y,t)$;

$$\psi = \psi_R + \psi_I$$

$$\frac{\partial\Psi}{\partial x} = ike^{ikx}\,\psi(y,t)$$

$$\mathrm{Re}\ \frac{\partial\Psi}{\partial x} = -k \sin kx\ \psi_R - k \cos kx\ \psi_I$$

$$\left(\mathrm{Re}\ \frac{\partial\Psi}{\partial x}\right)^2 = k^2 \sin^2 kx\ \psi_R^2 + k^2 \cos^2 kx\ \psi_I^2 + 2k^2 \cos kx \sin kx\ \psi_R\ \psi_I.$$

Let $\psi(y,t) = \sum_{l=0}^{\infty} \sin ly\ \tilde{\psi}(l,t)$.

Then $\Psi(x,y,t) = e^{ikx} \sum_{l=-\infty}^{\infty} e^{ily} F(l,t)$;

where $F(l,t)$ { $= \tilde{\psi}(l,t)/2i, \quad l \geq 0;$ $= -\tilde{\psi}(-l,t)/2i, \ l < 0$.

Also $\frac{\partial\Psi}{\partial y} = e^{ikx} i \sum_{l=-\infty}^{\infty} e^{ily} G(l,t)$

where $G(l,t) = l\,\tilde{\psi}(l,t)/2i$, for all l. So

$$\frac{\partial\Psi}{\partial y} = e^{ikx} i\, W \quad \text{where } W = \sum_{l=-\infty}^{\infty} e^{ily} G(l,t) \qquad (2.1.11)$$

$$\left(\mathrm{Re}\ \frac{\partial\Psi}{\partial y}\right) = -\sin kx\ W_R - \cos kx\ W_I$$

$$(\mathrm{Re}\ \frac{\partial \Psi}{\partial y})^2 = \sin^2 kx\ W_R^2 + \cos^2 kx\ W_I^2 + 2 \sin kx \cos kx\ W_R\ W_I$$

Collecting terms, we get:

$$E(y,t) = \frac{1}{(2\pi/k)} \int_0^{2\pi/k} E(x,y,t)\ dx$$

$$= 1/4\ [\ k^2\ |\psi|^2 + |W|^2\ ].$$

The total energy, i.e., the energy integrated over x and y is defined in the numerical methods section (section 3.3).

ii) Vorticity:

The vorticity

$$\zeta(x,y,t) = \nabla^2 \Psi(x,y,t)$$

$$= e^{ikx}\ (-k^2 + \frac{\partial^2}{\partial y^2})\psi(y,t)$$

$$\equiv e^{ikx}\ \omega(y,t).$$

In terms of sine Fourier transforms:

$$\omega(y,t) = \sum_{l=0}^{\infty} \sin ly\ \tilde{\omega}(l,t)$$

we have:

$$\tilde{\omega}(l,t) = -(k^2 + l^2)\ \tilde{\psi}(l,t).$$

In particular:

$$\tilde{\omega}(l,0) = -(k^2 + l^2)\ \tilde{\psi}(l,0).$$

Then equation (2.1.10) becomes:

$$\frac{\partial\tilde{\omega}}{\partial t}(l',t) = \tilde{\omega}(l',t)\ \{(B + yd)\frac{ik}{\mu'^2} - ikd\ \}$$

$$+ \sum_{\substack{l=0 \\ l\neq l'}}^{\infty} (1-y/\mu^2)\ \frac{ik2d}{\pi^2}\ \{\left[\frac{(-1)^{n+n'}-1}{(n+n')^2}\right]$$

$$-\left[\frac{(-1)^{n-n'}-1}{(n-n')^2}\right]\}\ \tilde{\omega}(l,t) \qquad (2.1.12)$$

Instead of taking a Fourier sine transform to solve the above problem, it is possible to take a complex Fourier transform provided $\tilde{\psi}(-l,t) = -\tilde{\psi}(l,t)$. This condition is demonstrated in the appendix.

2.2 Normal mode problem for the constant shear case

The evolution of an arbitrary initial disturbance into a normal mode is studied. This solution is of the form $e^{ik(x-ct)}\cdot\psi(y)$ and $c = c_r + ic_i$. To know what values to give to the parameters of the problem so that it is unstable (i.e., $c_i > 0$), a study of the normal mode eigenvalue problem and its stability is done.

The eigenvalue problem is solved numerically. A description of the numerical scheme is given in section 3.3. Only the equation and its nondimensional counterpart are given here.

Let $\Psi = e^{ik(x-ct)}\ \psi(y)$, then eq. (2.1.5) becomes:

$$(\alpha y - c)\ \{\frac{d^2\psi}{dy^2} - k^2\} + \sigma(y-b)\ \psi = 0. \qquad (2.2.1)$$

If, again, as before, L = length scale and $1/\alpha$ = time scale, then eq. (2.2.1) becomes:

$$(y-c)\ \{\frac{d^2\psi}{dy^2} - k^2\} + \gamma(y-y_B)\ \psi = 0 \qquad (2.2.2)$$

where $y_B = b/L$ and γ is as defined before.

III. NUMERICAL METHODS

3.1 Initial condition

The initial condition used throughout most of this work is a Gaussian distribution, i.e. in physical space the function is of the form

$$\exp\{-(y-y_o)^2/4H^2\}\ \exp\{il_o y\}.$$

H is given values so that the Gaussian fits inside the domain, i.e. is zero at the boundaries. Varying H can produce a wider or narrower function. The narrower the function is in physical space, the wider it is in Fourier space. To apply wave-packet theory to the problem (Tung, 1983), the function has to be peaked in Fourier space, but it should not be too peaked because the Gaussian function at t=0 in physical space should be localized. This is because the Gaussian function is considered as an "arbitrary" initial condition, and therefore, at t = 0, it should not resemble an eigenmode which, in general, has a global structure.

In an infinite domain, the Fourier transform of a Gaussian is a Gaussian. In a finite domain, this is not the case, but if the initial condition is as described above, then one can consider the function as "Gaussian-like" with l_o as central frequency and y_o as central position in physical space.

3.2 Constant shear case

The program mainly consists of six parts.

1. Take the fast Fourier transform (FFT) of the initial condition which is a Gaussian in physical space for the vorticity. The FFT has N+1 points say.
2. Calculate the corresponding streamfunction in Fourier space.
3. Integrate the streamfunction in time.

   In order to do that, it is necessary to solve a system of N ordinary linear differential equations for a time interval $\Delta t = t_{n+1} - t_n$. To do this, use is made of Gear's method. Gear's method is used to insure numerical stability. It is also used to solve stiff equations (Raphson and Robinowitz, 1978, p. 228). A subroutine from the NAG library was used for this.
4. Calculate $W \equiv G(1, t)$ and $\tilde{\omega}$ (see eqs. 2.1.11 and 2.1.12 respectively).
5. Take the inverse of the Fourier transforms $\tilde{\psi}$, $\tilde{W}$, $\tilde{\omega}$ at each t_n and calculate $E(y, t)$ at each t_n.
6. Calculate $E(t)$ at each t_n. $E(t)$ is defined as:

$$E(t_n) = \frac{1}{d}\left\{\frac{\Delta y}{2} E(y, t_n) + \sum_{i=2}^{M-1} \Delta y\, E(y_i, t_n) + \frac{\Delta y}{2} E(y_M, t_n)\right\}$$

where M = N/2.

At each timestep, the results are plotted out for the following quantities: $|\tilde{\omega}(x=0, l, t)|$, $|\omega(x=0, y, t)|$, $Re(\Psi(x=0, y, t)$ and $E(y, t)$. Also, at each timestep, a plot of $Re(\zeta(x, y, t))$ in three dimensions is available.

In theory, l varies between zero and infinity. To execute a numerical computation, l has to be cut off. Consequently, l varies between zero and a finite value which will here be defined as l_{MAX}. If the amplitude of the function in Fourier space becomes significantly different from zero around l_{MAX} the integration in time has to be stopped to avoid aliasing. An example of this is shown on Figure 4.1.36.

There is also a limit on the resolution. In most of the computations, N = 128, which means that in the physical domain $y \in [0, 2D]$, there are 64 intervals, and the same number is used for the antisymmetric extension $y \in [-2D, 0]$. Therefore, waves smaller than (D/16) cannot be represented.

To verify the accuracy of the numerical integration, different values of the local error for Gear's method have been taken. The values for the tolerance was first set to 10^{-4} and then 10^{-8}. Cases for which the total energy decayed continuously in time showed the lowest accuracy. In general, for a qualitative study of the behavior of the problem, a tolerance of 10^{-4} was more than enough. The need to set a higher tolerance depends also on how long the integration is

executed.

3.3 Normal mode problem for the constant shear case

a) *Eigenvalue problem*

Rewriting equation (2.2.2) we have:

$$y\left[\frac{d^2\psi}{dy^2} - k^2\psi\right] + R(y)\psi = c\left[\frac{d^2\psi}{dy^2} - k^2\right] \qquad (3.3.1)$$

where $R(y) = y(y-y_B)$.

If we use a second-order finite differencing to evaluate

$$\frac{d^2\psi}{dy^2} \approx \frac{\psi_{n+1} - 2\psi_n + \psi_{n-1}}{(\Delta y)^2}$$

then the L.H.S. of the above equation becomes:

$$y_n \left[\frac{\psi_{n+1} - 2\psi_n + \psi_{n-1}}{(\Delta y)^2} - k^2\psi_n\right] + R_n\psi_n$$

or multiplying by $(\Delta y)^2$:

$$y_n\psi_{n+1} + \psi_n\left[-2y_n - k^2(\Delta y)^2 y_n + R_n(\Delta y)^2\right] + y_n\psi_{n-1}.$$

Also, $\psi_o = 0$ and $\psi_{N+1} = 0$ from the boundary

conditions.

Let $V_n = [-2y_n - k^2(\Delta y)^2 y_n + R_n(\Delta y)^2]$.

In matrix form, we then have for the L.H.S.:

$$\begin{vmatrix} V_1 & y_1 & & & & \\ y_2 & V_2 & y_2 & & & \\ & & & y_n\ V_n\ y_n & & \\ & & & & y_N\ V_N & \end{vmatrix} \begin{vmatrix} \psi_1 \\ \psi_2 \\ \\ \psi_n \\ \\ \psi_N \end{vmatrix} \equiv M \underset{\sim}{\psi}$$

The R.H.S. of eq. (3.3.1) is

$$c\left[\frac{d^2\psi}{dy^2} - k^2\psi\right]$$

which becomes after multiplication by $(\Delta y)^2$:

$$c\left[\psi_{n+1} + \{-2-k^2(\Delta y)^2\}\psi_n + \psi_{n-1}\right]$$

Let $Z \equiv -2 - k^2(\Delta y)^2$, then the R.H.S. is:

$$c \begin{vmatrix} Z & 1 & & & \\ 1 & Z & 1 & & \\ & \ddots & \ddots & \ddots & \\ & & & 1 & Z \end{vmatrix} \begin{vmatrix} \psi_1 \\ \psi_2 \\ \\ \\ \psi_N \end{vmatrix} \equiv c\,P\,\underset{\sim}{\psi}$$

Finally, $M\underset{\sim}{\psi} = cP\underset{\sim}{\psi}$ or $P^{-1}M\underset{\sim}{\psi} = c\underset{\sim}{\psi}$

To solve this problem, a subroutine from the NAG library was used to find the eigenvalues c and also the eigenvectors $\underset{\sim}{\psi}$ if needed. With this program, eigenvalues for the problem without an inflection point and with an inflection point can be found. Recall that the inflection point is equal to y_B.

The eigenvalue problem without an inflection point is

always stable. This follows from the Rayleigh-Kuo theorem. Only neutral modes are obtained numerically with phase speeds smaller than zero. With the vorticity gradient

$$\beta - U_{yy} = \alpha(y-y_B),$$

the Rayleigh-Kuo theorem says that a necessary condition for instability is that the inflection point lies inside the domain. Fjortoft's theorem can also be applied. The short-wave cutoff for instability can be shown to be

$$(\gamma-\pi^2/4D^2)^{1/2} = k_{MAX}$$

(see Pedlosky (1979) for a similar derivation). For the eigenvalue problem with an inflection point, a graph of the growth rate (kc_i) versus the wavenumber for different values of γ is shown on Fig. 3.3.1. This diagram is for a nondimensional domain of size = 2. The most unstable wave occurs when y_B is at the center of the domain. Lines of constant growth rate are shown in Fig. 3.3.2. The zero growth rate line is very wiggly; this should not be the case and is due to an insufficient amount of data points for the plotting routine. This graph is only meant to give a qualitative idea about the instability properties.

b) *Eigenvector as an initial condition*

To test the numerical method, the initial condition is set equal to an eigenvector which was found by solving the eigenvalue problem. The eigenvectors in the case without an inflection point and with an inflection point were both calculated. An eigenvector given as an initial condition should always remain a solution to the initial value problem.

Figure 3.3.3-4 illustrate the magnitude of the Fourier transform of the vorticity and the magnitude of the vorticity. These should both be conserved in time.

Figure 3.3.5 illustrates the real part of the streamfunction. The oscillation in time is present because the complex streamfunction is of the form $\exp[-ikc_r t]$. Figure 3.3.6 shows the energy as a function of y and t which should be conserved in time. In an eigenvalue problem the accuracy of the eigenvalue is larger than that of the eigenvector. Since there is some error in the eigenvector, it will need some time to adjust to the initial value problem. This is the main reason for the discrepancies observed in the figures mentioned above.

Another check is that the total energy E(t) has to be conserved. This is the case (see Table 1). The phase speed c_r could also be verified using x vs y vs Re(vort(x, y, t,)) diagrams.

Figures 3.3.7-11 illustrate the unstable eigenvector. The same variables as for the case above are illustrated. The total energy grows like $\exp[2kc_i t]$ which it has to (see Table 2). Here also the phase speed c_r turned out to be the same as predicted.

FIG. 3.3.1

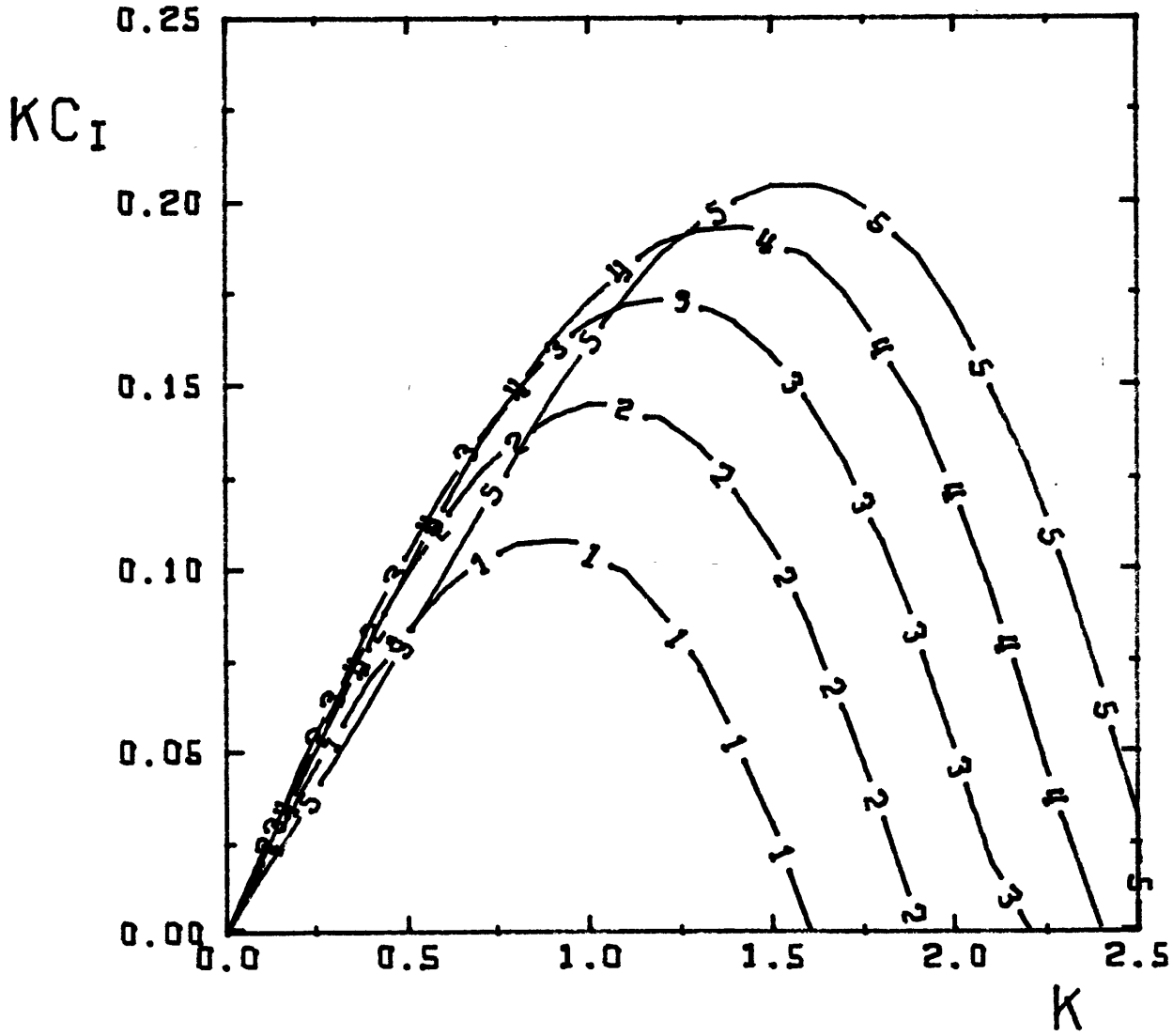

YB=1.00

-1- $\gamma = 5.0$
-2- $\gamma = 6.0$
-3- $\gamma = 7.0$
-4- $\gamma = 8.0$
-5- $\gamma = 9.0$

$U = \alpha Y$
$D = 1.0$

FIG. 3.3.2

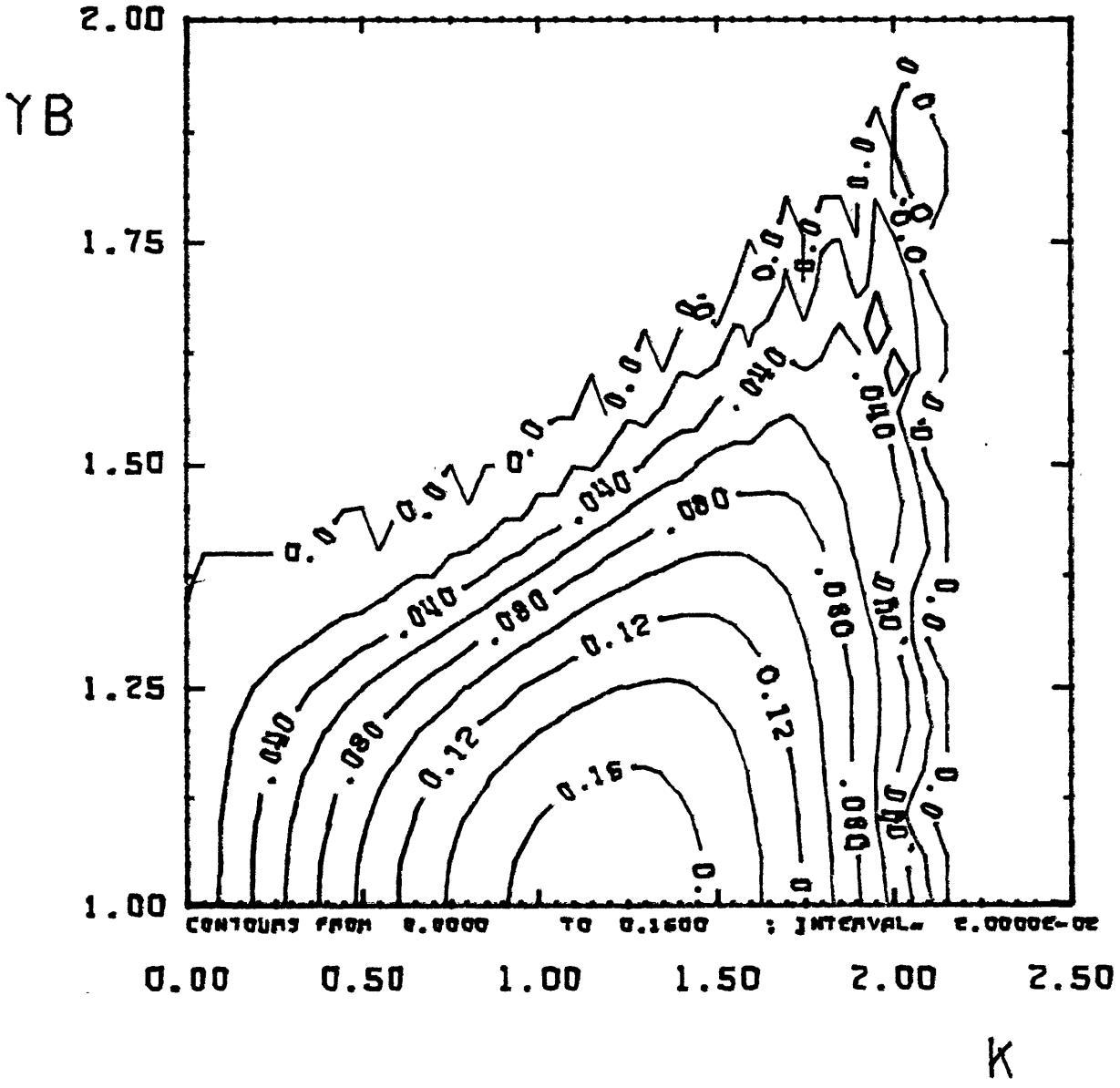

LINES OF CONSTANT KC_1 $\gamma = 7.0$ $U = \alpha y$, $D = 1.0$

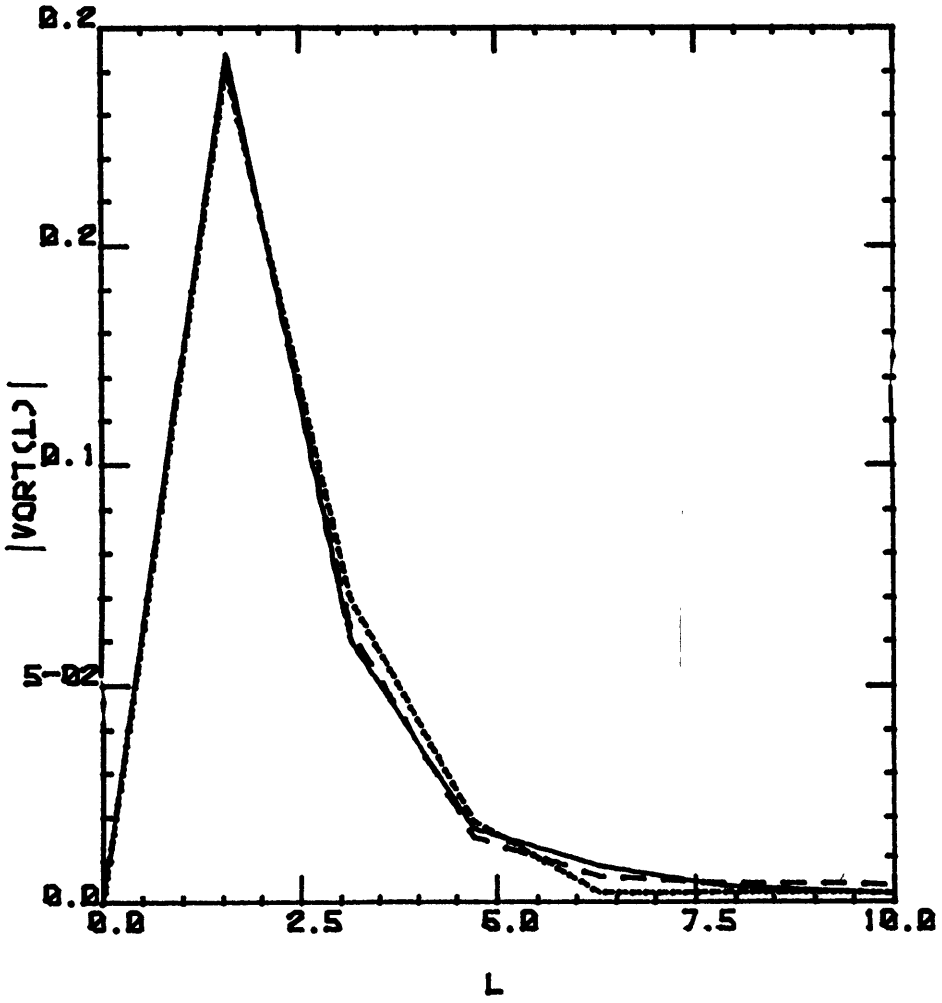

FIG. 3.3.3

γ = 0.0
k = 1.0
B = 6.0
$l \in [0.0, 100.5]$
—— T = 0.0
--- T = 2.5
– – T = 5.0

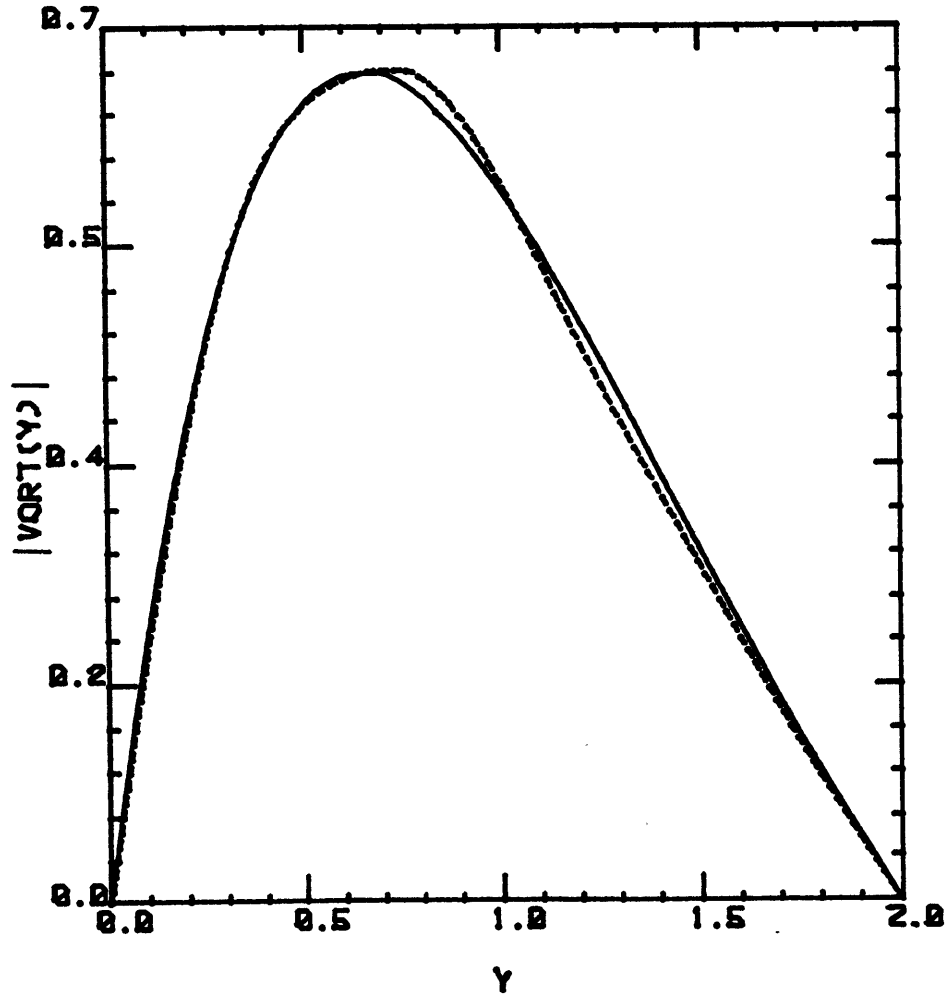

FIG. 3.3.4

γ = 0.0
k = 1.0
B = 6.0
——— T = 0.0
----- T = 5.0

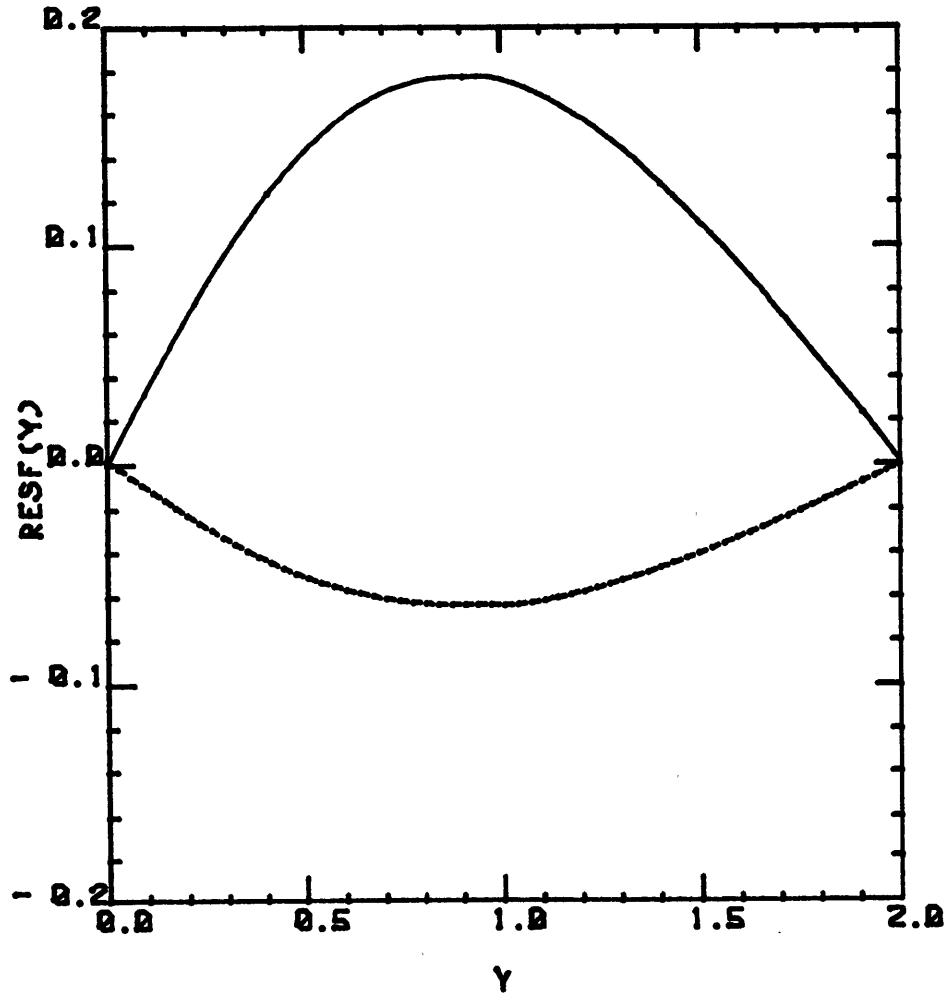

FIG. 3.3.5

$\Upsilon = 0.0$
k = 1.0
B = 6.0
—— T = 0.0
---- T = 5.0

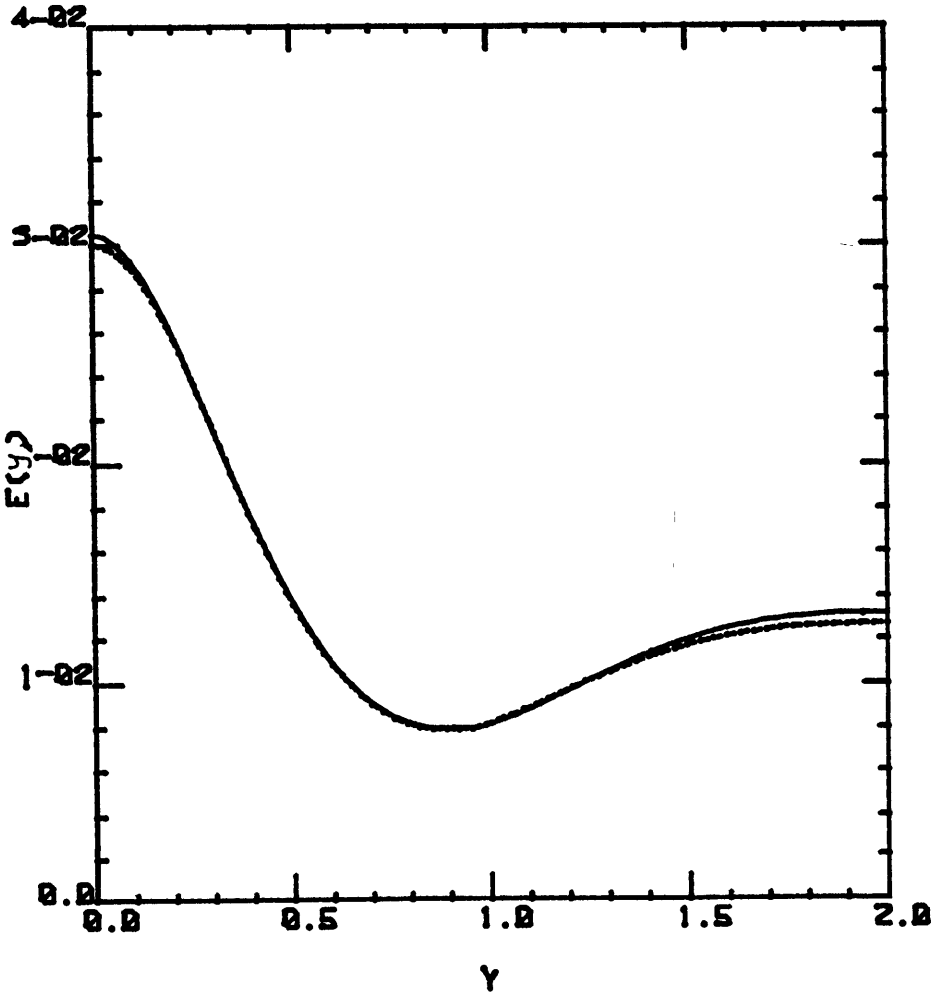

FIG. 3.3.6

γ = 0.0
k = 1.0
B = 6.0
—— T = 0.0
---- T = 5.0

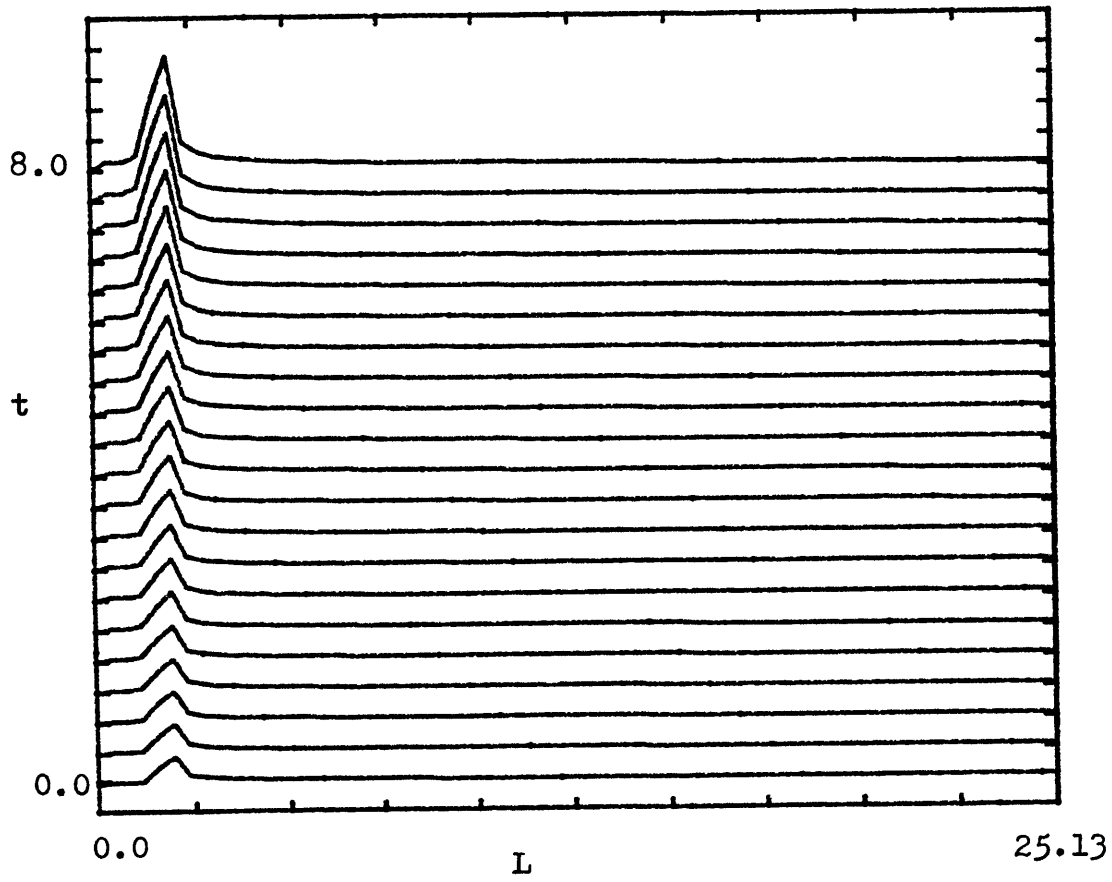

FIG. 3.3.7

γ = 5.0
k = 1.25
B = -15.0

|Vort(L)|

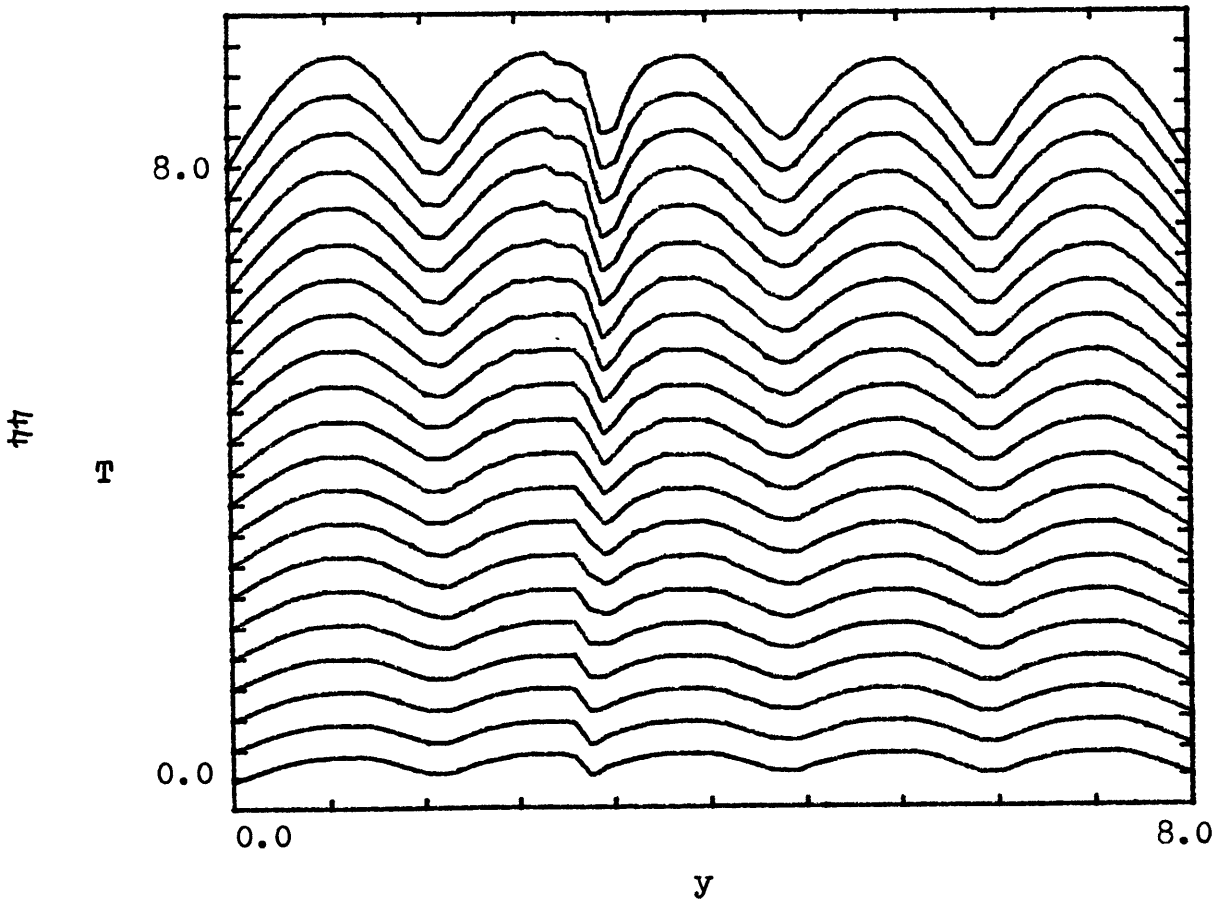

FIG. 3.3.8

γ=5.0
k=1.25
B=-15.0

|Vort(y,T)|

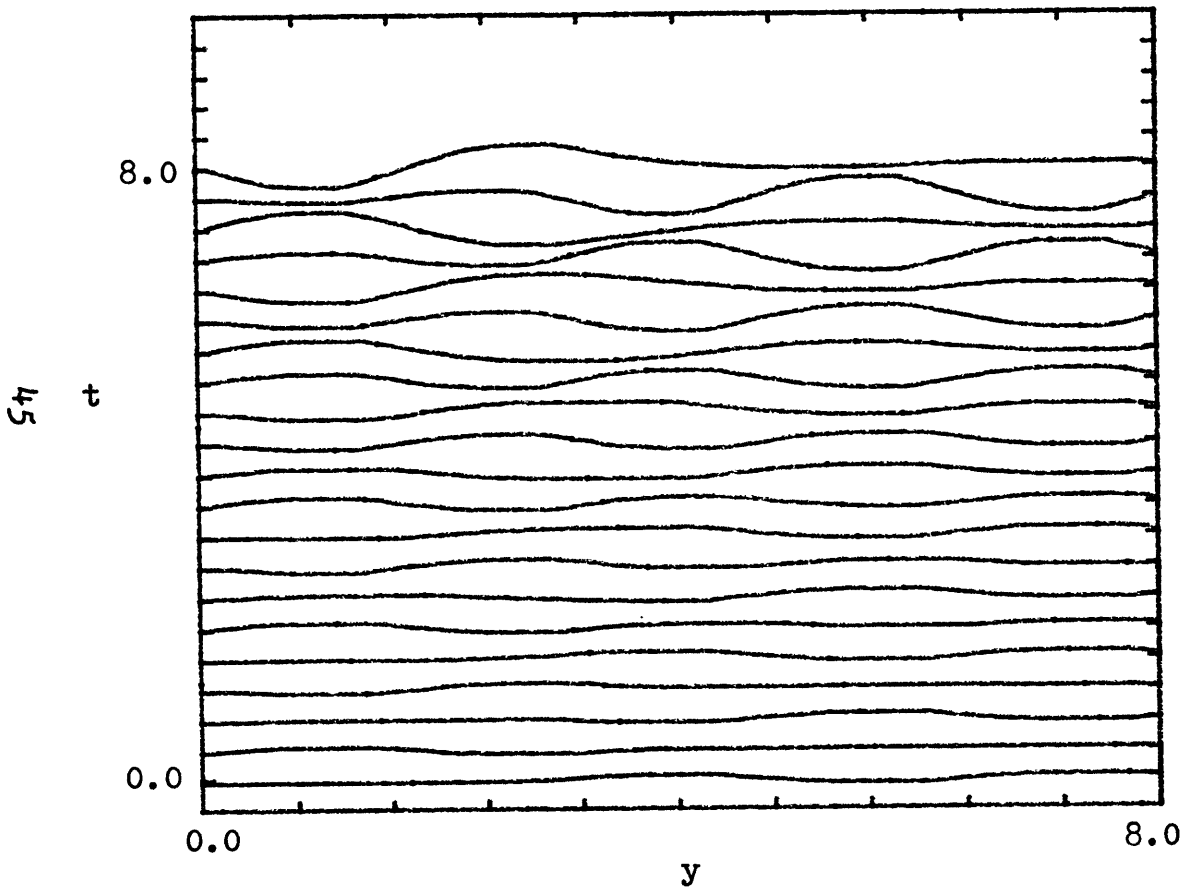

FIG. 3.3.9

$\gamma = 5.0$
$k = 1.25$
$B = -15.0$

Re sf(y,t)

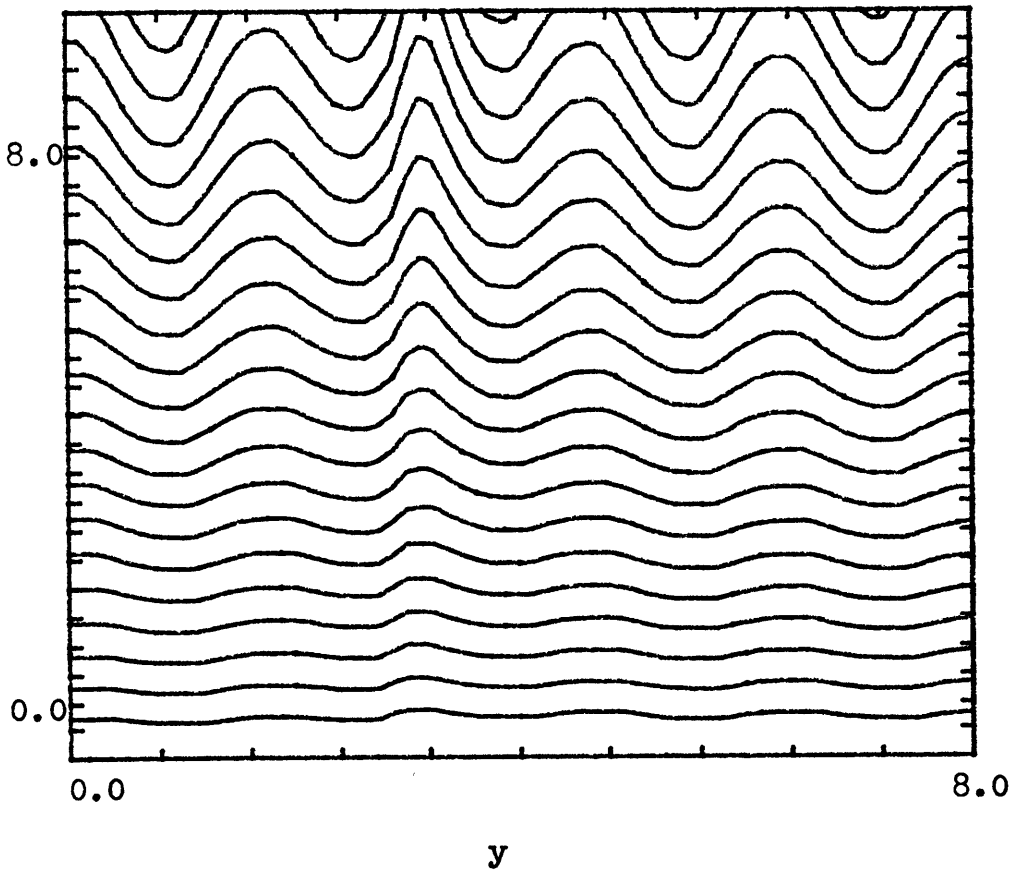

FIG. 3.3.10

$\gamma = 5.0$
$k = 1.25$
$B = -15.0$

E(y,t)

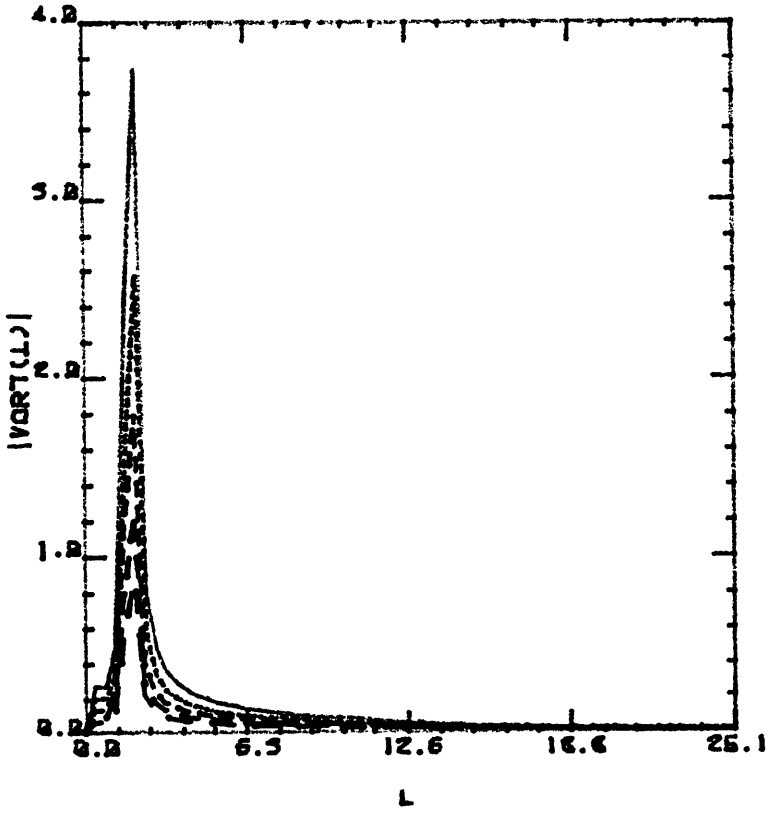

FIG. 3.3.11

$\gamma = 5.0$
$k = 1.25$
$B = -15.0$

—— $t = 0.0$
----- $t = 2.0$
---- $t = 4.0$
--- $t = 6.0$
— — $t = 8.0$

IV. RESULTS AND DISCUSSIONS

4.1 Constant shear case without an inflection point

4.1.1. Infinite domain.

For the constant shear case in an infinite domain with β-effect, the solution in moving coordinates is (Tung (1983)):

$$\zeta = (1/2\pi) \int_{-\infty}^{\infty} e^{ik\xi + i\eta M} \, \tilde{\zeta}(k, M, \tau) \, dM \qquad (4.1.1)$$

where $\xi = x - \alpha y t$, $\eta = y$, $\tau = t$ and

$$\tilde{\zeta}(k, M, \tau) = \tilde{\zeta}_0(k, M) \exp\{\frac{i\beta}{\alpha k} \cdot [tg^{-1}(\alpha t - M/k) + tg^{-1}(M/k)]\} \qquad (4.1.2)$$

If one takes the magnitude of both sides of the above equation, one obtains:

$$|\tilde{\zeta}(k, M, \tau)| = |\tilde{\zeta}_0(k, M)| \qquad (4.1.3)$$

In fixed coordinates :

$$\zeta(x, y, t) = (1/2\pi) e^{ikx} \int_{-\infty}^{\infty} e^{ily} \, \tilde{\zeta}(k, l+\alpha k t, t) \, dl$$

and equation (4.1.3) becomes:

$$|\tilde{\zeta}(k, l+\alpha k t, t)| = |\tilde{\zeta}_0(k, l+\alpha k t)| \qquad (4.1.4)$$

Equation (4.1.4) shows that $|\tilde{\zeta}|$ depends on $l+\alpha k t$. This means that a particular wavenumber of the spectrum is

displaced in time by the shear at a uniform rate αk.

Consider the evolution in time of the central wavenumber $l_o(t)$ of the wave-packet (see Figure 4.1.1). If $(l_o(0)/k) > 0$ then the orientation of the crest of the wave at t=0 is north-west. The effect of the shear will then be to increase the y-scale of the wave (i.e. decrease l_o), when the orientation is north-south, the y-scale is infinity and $l_o = 0$. This happens at a time t^* such that

$$l_o(0) - \alpha k t^* = 0.$$

Thus $t^* = l_o(0)/\alpha k$.

When the orientation becomes north-east, then the scale of y decreases i.e. $|l_o|$ will increase.

If $(l_o(0)/k) < 0$, the orientation of the crest of the wave is north-east. The effect of the shear is to decrease the y - scale and hence increase the wavenumber.

a) *Couette flow*

For the Couette flow $\beta = 0$, the effect of the shear is the same as described above since equation (4.1.4) does not depend on β. It is also possible from the differential equation to show that $|\zeta(x, y, t)|$ is conserved with time. This is illustrated in figures 4.1.2 and 4.1.3 for which $(l_o/k) > 0$. Figures 4.1.4 and 4.1.5 also show that $|\zeta(x, y, t)|$ is constant for the case $(l_o/k) < 0$. These

figures were calculated by Worsham (1983).

The kinetic energy density averaged over x for one wavenumber l is:

$$(1/4)\,(k^2 + l^2)\,|\tilde{\psi}|^2$$

and

$$\tilde{\psi} = -\tilde{\zeta}(k, l+\alpha k t, t) \;/\; (k^2+l^2).$$

Therefore, using eq. (4.1.4):

$$E = (1/4)\,|\tilde{\zeta}_0(k, l+\alpha k t)|^2/(k^2+l^2).$$

As before, consider the time-evolution of the central wavenumber $l_0(t)$ of a wave-packet with small spectral spread. Then substitute $l \equiv l_0(t) = l_0(0) - \alpha k t$ in E. One obtains

$$E \sim [k^2 + (l_0(0) - \alpha k t)^2]^{-1}.$$

When $(l_0(0)/k) < 0$ the energy always decays and when $(l_0(0)/k) > 0$ the energy increases untill $t = t^*$ and then decreases. t^* is the same as defined above.

b) *Couette flow with β-effect*

When β is different from zero, the waves can move in the y direction. Tung (1983) studied the evolution of a wave-packet in an infinite domain where the initial spectrum $\tilde{\zeta}_0(k, l)$ is peaked about the central wavenumber $\vec{k}_0 = (k_0, l_0)$. There is a small spectral spread $\Delta\vec{k}_0$

about the central wavenumber. He showed that

$$y_c = y_o - \beta/(k^2+l_o^2)$$

and

$$y_T = y_o + \beta(l_o^2/k^2)/(k^2+l_o^2)$$

We recall that y_o is the position of the centroid of the Gaussian initial wave-packet. y_c is the critical level and is the point where the wave-packet eventually stagnates. It is determined by the location where $U(y)-c = 0$. c is the barotropic wave speed in the absence of shear. It is called the nominal phase speed of the packet. Even though the initial disturbance (here a Gaussian distribution) that constitutes the wave-packet, in general do not have a well-defined phase speed, Tung (1983) has shown that during the later stages of its evolution, the wave-packet behaves as if there exists a well - defined phase speed c. Worsham (1983) has shown numerically that this is the case.

y_T is the turning point and is the location where the group velocity in the meridional direction changes sign. This occurs at $\alpha t^* = l_o/K$. The group velocity is

$$C_{gy} = 2\beta K l_o / (k^2+l_o^2)^2.$$

Figures 4.1.6 to 4.1.12 were computed by Worsham (1983). Figure 4.1.6 illustrates the packet trajectories for $l_o/K = \pm 2$. For $l_o/K=2$, the wave-packet is moving northwards untill it hits the turning point and then moves south towards the critical level. For $l_o/K = -2$, the wave-packet moves

south towards the critical level. Figures 4.1.7 - 4.1.8 illustrate the magnitude of the vorticity of a wave packet moving south towards the critical level. Figures 4.1.9 - 4.1.10 illustrate the magnitude of the vorticity of a wave-packet moving north, hitting the turning point and then moving south towards the critical level. Figure 4.1.11 illustrates the energy for a southward-moving wave-packet. The energy always decays as discussed before. Figure 4.1.12 illustrates the energy for a wave-packet moving north. When the wave moves north, the energy increases and when the wave moves south, the energy decays. The reasons for the behaviour of the energy is basically the same as the one described for the Couette flow.

4.1.2 Finite domain

a) *Couette flow* ($\beta=0$)

For the Couette flow in a finite domain, it is also possible to show that $|\zeta(x, y, t)|$ is conserved. This can be seen on figures 4.1.14 and 4.1.18 which illustrate $|\zeta(x=0, y, t)|$ for $(l_o/k)>0$ and $(l_o/k)<0$ respectively.

Figures 4.1.16 and 4.1.20 show the evolution of the energy $E(y, t)$ for $(l_o/k)>0$ and $(lo/k)<0$ respectively. (Also

see tables 3 and 4) The behaviour of the energy is the same as the one predicted for the Couette flow in an infinite domain. The waves in physical space do not move so that the walls at y=0 and 2D are basically not felt.

The magnitude of the Fourier spectrum of the vorticity is illustrated in figures 4.1.13 and 4.1.17 for $(l_o/k)>0$ and $(l_o/k)<0$. Consider first the case $(l_o/k)<0$. Roughly one can say that the behaviour of the function in Fourier space is the same as for the infinite domain. The change in l with time is due to the shear and was described in section 4.1.1a. One has also to consider the fact that the Fourier spectrum is made up of values of $l \in [0,\infty]$ and also $l \in [-\infty,0]$. The function for $l<0$ is the antisymmetric extension of the function for $l>0$. It is the inverse of the Fourier transform of these two functions which make up a function in physical space which satisfies the boundary conditions. In a finite domain, there is an interaction between different wavenumbers. This is due to the coupling terms in the system of differential equations. This coupling which is present because of the walls can explain the development of longer waves of the spectrum which is observed as time increases (i.e. broadening of the Fourier spectrum towards smaller wavenumbers). The longer waves are the first ones to feel the walls.

Consider the case for which $(l_o/k)>0$. At t=0, the initial condition has a Gaussian-like shape. As t increases, since

both the function and its virtual image move towards $l=0$, the functions while passing each other will superpose. So the function which was initially in the region $l<0$ will now be in the region with $l>0$ and vice versa. Therefore, the effect of the shear on the scale of l in a finite domain is roughly the same as for the infinite domain (i.e. if one excludes the broadening effects).

Only transient waves make up the Fourier spectrum, i.e. the l-scale is continuously changing.

Also, one can conclude that the decay of the wave is associated with the function in Fourier spectrum which is moving towards larger l's. This particular structure will be called the part of the Fourier spectrum associated with the decay of the wave.

b) *Couette flow with β-effect*

Consider first the cases where the effects of the walls are almost not felt. This is possible because of the presence of y_c and y_T.

In a finite domain, one can place the walls so that y_c and y_T are inside or outside the domain.

When only y_c is inside the domain and y_c is to the south of y_o (where y_o is the centroid of the wave - packet) and the initial group velocity of the wave-packet is negative, then the centroid of the wave-packet will stagnate at y_c and will not be able to travel to the wall. This is shown in figure 4.1.22. As time increases, small scale structures appear. These are due to the presence of the wall. The tail end of the packet feels the wall and moves very slowly as time increases (i.e. it is only when $t \to \infty$ that $C_{gy} \to 0$). The behaviour of the wave is basically the same as for the infinite domain case. As expected, the Fourier spectrum is the same as for the Couette flow ($\beta=0$).

The energy of the wave-packet decays as it moves south (see figure 4.1.24 and table 5). This is due to the effect of the shear acting on the wave-packet near the stagnation level.

If y_c and y_T are both inside the domain, i.e.

$$y_C < y_O < y_T$$

and $C_{gy}(t=0) > 0$, then the wave-packet moves north untill it hits the turning point and then moves south and stagnates at the critical level. Again in this way the wave-packet did not enter in contact with the walls and one obtains the same overall behaviour as for the infinite domain case. Figure 4.1.29 shows the behaviour of the energy. The energy of the wave increases as it moves north ans then decreases as it moves south as predicted. Also see table 6. Again the magnitude of the Fourier transform of the vorticity has the same behaviour as for the Couette flow.

Consider now cases where the presence of the walls is felt considerably.

If y_T is inside the domain ($0 < y_O < y_T < 2D$) and $C_{gy}(t=0) > 0$, then the wave-packet moves north untill it hits the turning point and then moves south and feels the left wall. Figures 4.1.31-4.1.36 illustrate this case. The energy increases as the wave goes north and then decreases as the wave goes south (see also table 7). It then increases again as the wave goe's north and increases and decays in a "harmonic fashion".

By bouncing back and forth against the walls, eigenvectors are set up. Since the eigenvectors are neutral for this problem, waves with different phase speeds are present and all have a phase speed $c_r < U_{min}$. Before and untill the wave-packet hits the turning point, the Fourier spectrum has

the same shape as for the case without walls considered before. When the waves enter in contact with the walls, distinct smaller wavenumbers develop. As the neutral waves are being set up, the part of the Fourier spectrum associated with the decay of the wave fades away (it is smeared out over larger and larger wavenumbers).

The development of the smaller wavenumbers as mentioned before is due to the fact that the normal modes have a definite structure in the y domain. There is not just one peak but several because of the presence of several neutral waves which each have a different phase speed. The left side of the domain in physical space is a lot more wavy than the right side. This seems to indicate that some wavelengths feel a turning point which is to the left of $y_T(l_o)$.

If both y_c and y_T are outside the domain, i.e.

$$y_c < 0 < y_o < 2D < y_T$$

then the wave-packet will come directly in contact with the wall. Consider first the case $(l_o/k) < 0$. As time evolves, two distinct structures appear one after the other in Fourier space. At first, only the part of the Fourier spectrum associated with the decay of the wave is present; as for the Couette flow, this is due to the effect of the shear. When the wave-packet in physical space enters in contact with the wall, distinct wavenumber peaks appear for the lower wavenumber part of the spectrum. This structure of the spectrum persists while

the part of the spectrum associated with the decay of the wave fades away as for the case described just before.

Figures 4.1.37-4.1.42 illustrate this case. The total energy decays while the wave is going south, then increases once the wave has entered in contact with the wall. After that, the energy decays and again increases and decays in a "rythmic fashion" (see table 8). The fact that the energy increases and decays in a so- called "rythmic fashion" suggests the presence of several neutral waves. The initial condition has a spread of wavenumbers around l_o. The walls can contain structures with different wavenumbers each thus having a different phase speed. What we observe in physical space as well as in Fourier space is a superposition of these waves. Again, as in the previous case $c_r(l)$ should be smaller than U_{min} for a solution to exist. In the case where several normal modes are present, it is not possible to determine numerically what c_r is.

Consider now the case $(l_o/K) > 0$. Figures 4.1.43-4.1.48 illustrate this case. For the first seven timesteps, one can again observe the same general behaviour of the Fourier spectrum as for the Couette flow with $(l_o/K) > 0$. For the latest timesteps during this time, one can see the development of distinct wavenumber peaks and as time goes on this structure becomes more and more developed (i.e. normal modes are present). Again, as time evolves the part of the Fourier spectrum

associated with the decay of the wave fades away. As the wave goes north untill it hits the wall, the energy increases (this is consistent with the Couette flow case). Then the energy decreases untill the wave hits the left wall and increases again, then decreases and finally increases and decays in a "rythmic fashion". This also indicates the development of normal modes. See also table 9. Again, $c_r < U_{min}$. Comparing the solution for $(l_o/k) > 0$ and $(l_o/k) < 0$, one can conclude that they have the same general form. The final Fourier spectra are similar as well as the solution in Fourier space. This is to be expected since y_C and y_T are outside the domain (so that the waves have no obstacles) and the initial conditions are the same.

In the three last cases mentioned above, the presence of the walls cause the development of distinct wavenumbers in the lower wavenumber part of the spectrum which does not shift in time, indicating the presence of a definite structure in physical space which is a superposition of normal modes with different phase speeds.

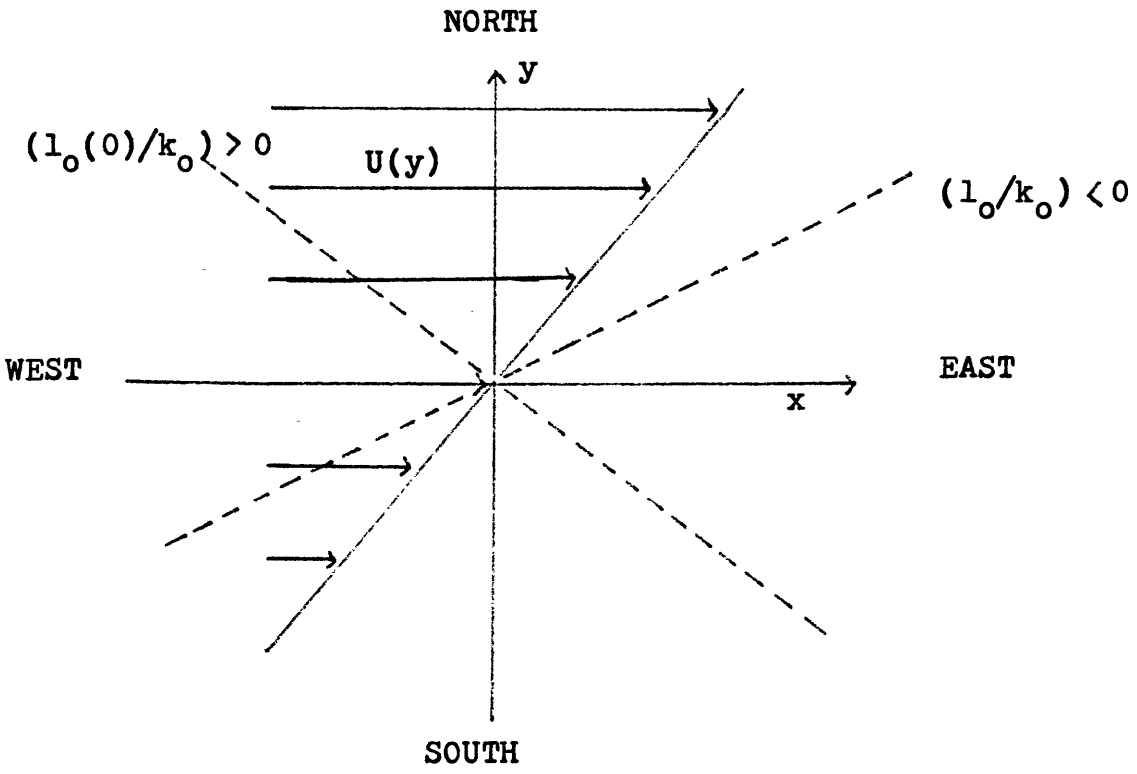

FIG. 4.1.1

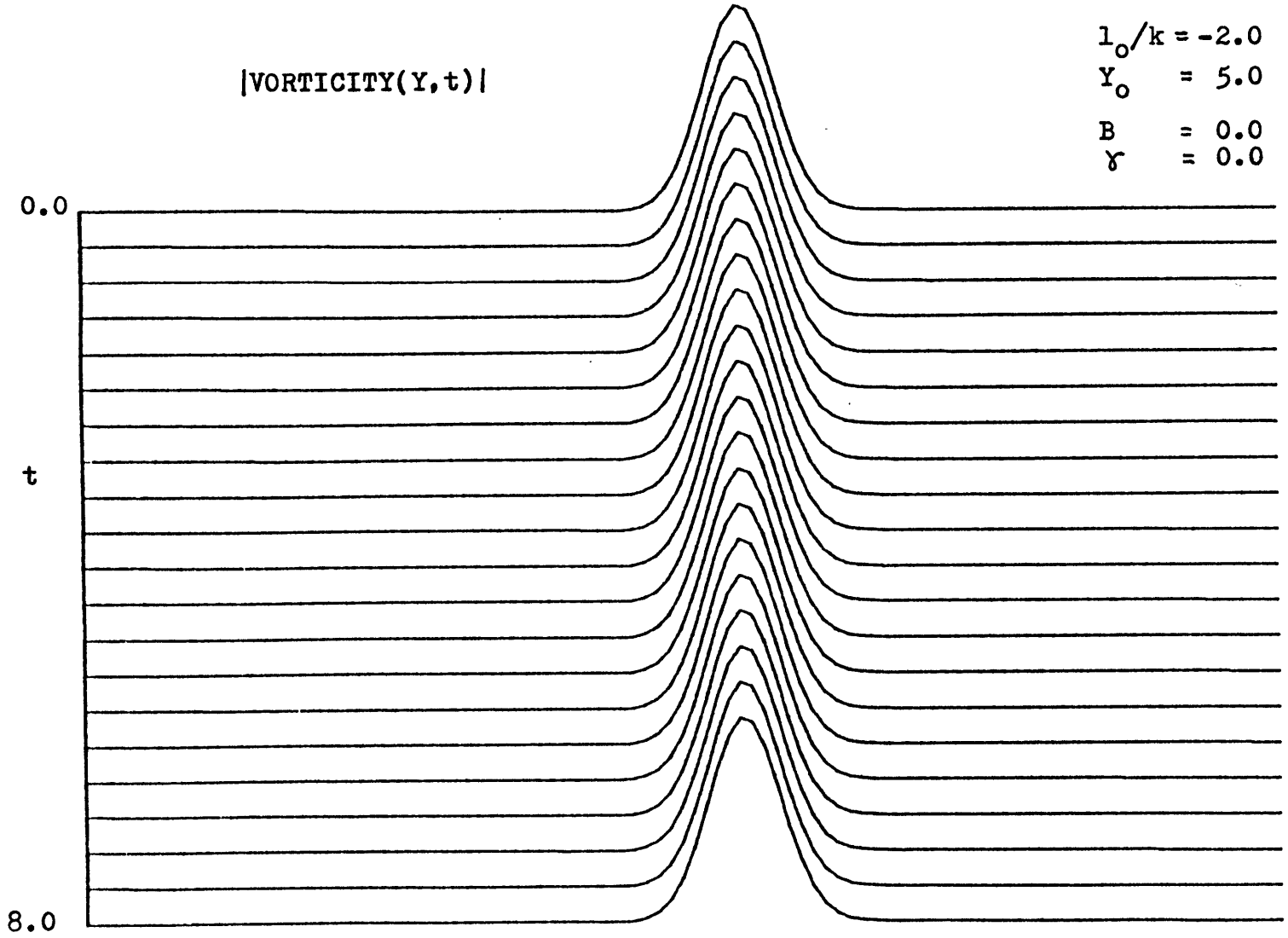

Figure 4.1.2

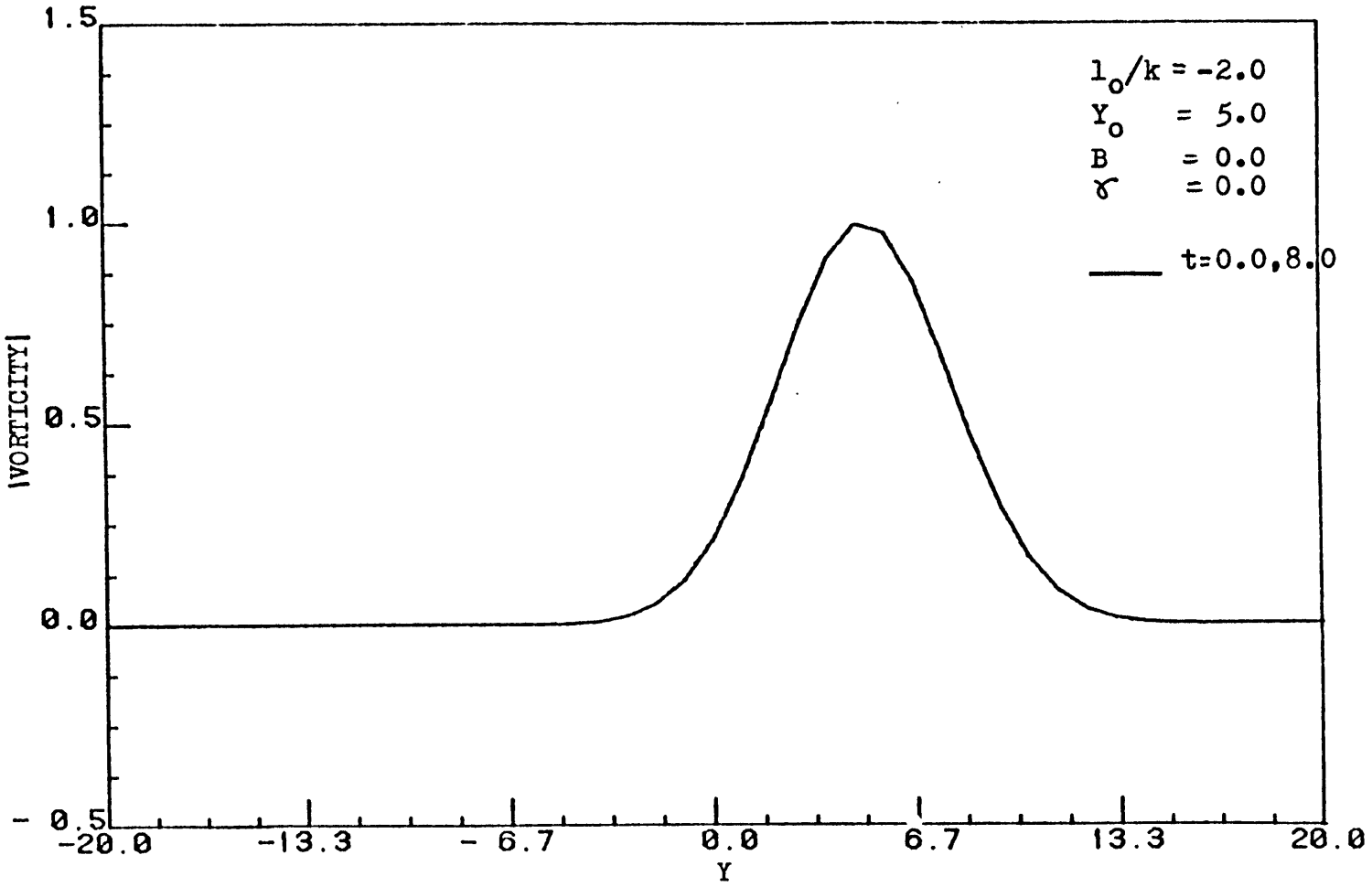
1.5
1.0
0.5
0.0
- 0.5
|VORTICITY|
-20.0
-13.3
- 6.7
0.0
6.7
13.3
20.0
Y
l_o/k = -2.0
Y_o = 5.0
B = 0.0
γ = 0.0
t=0.0,8.0

Figure 4.1.3

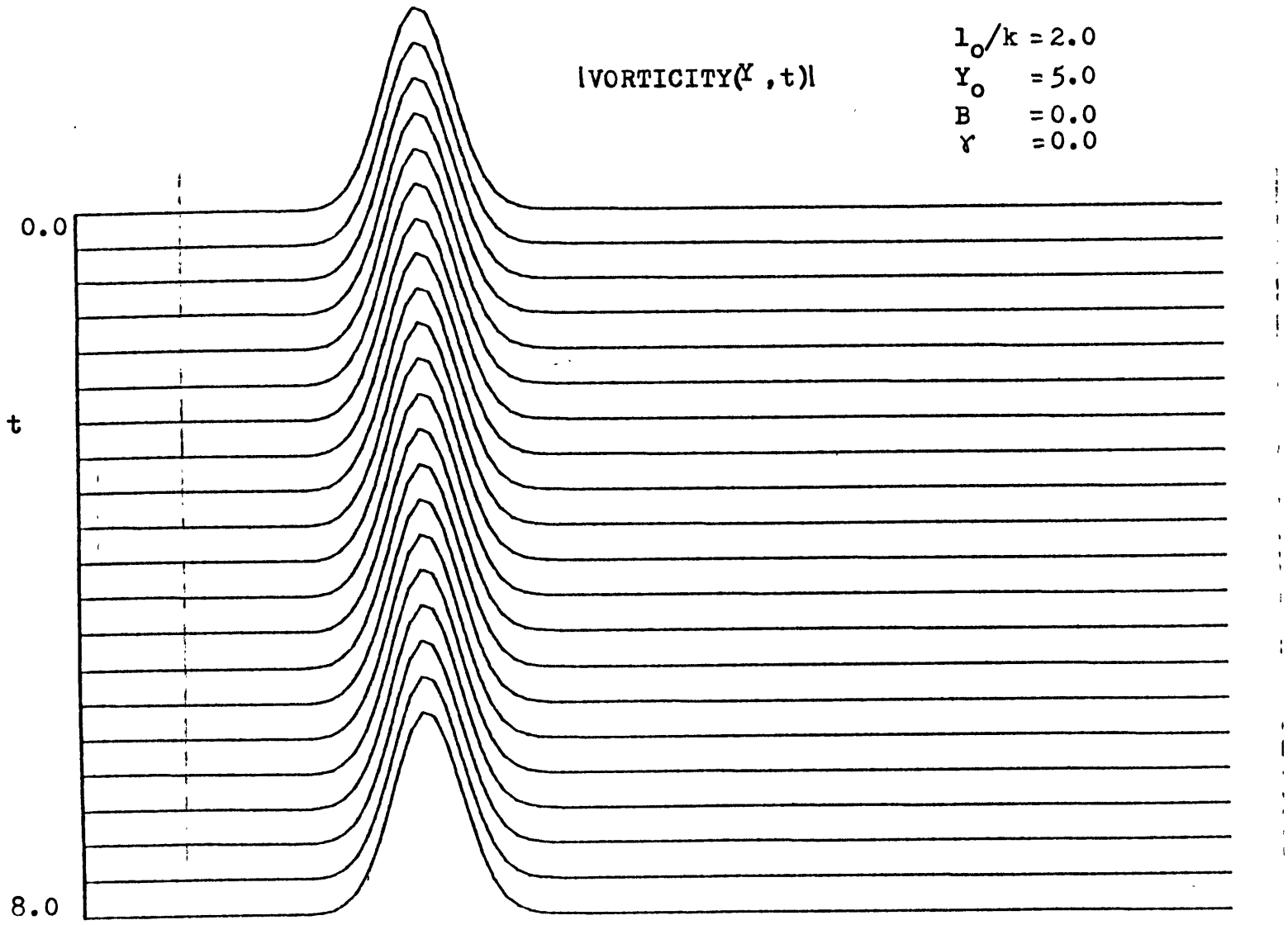

Figure 4.1.4

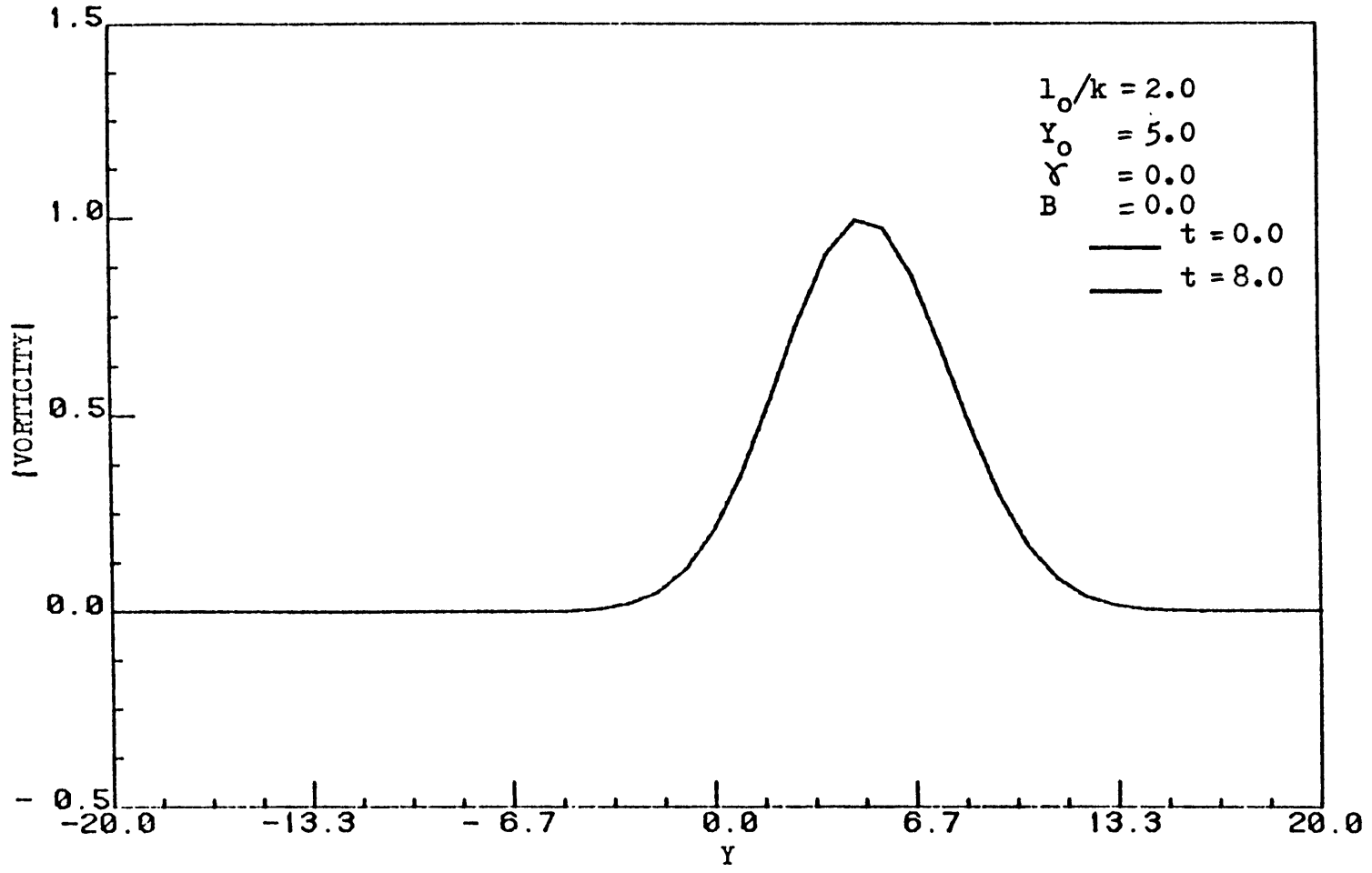
1.5
1.0
0.5
0.0
- 0.5
|VORTICITY|
-20.0
-13.3
- 6.7
0.0
6.7
13.3
20.0
Y
l_o/k = 2.0
Y_o = 5.0
γ = 0.0
B = 0.0
t = 0.0
t = 8.0

Figure 4.1.5

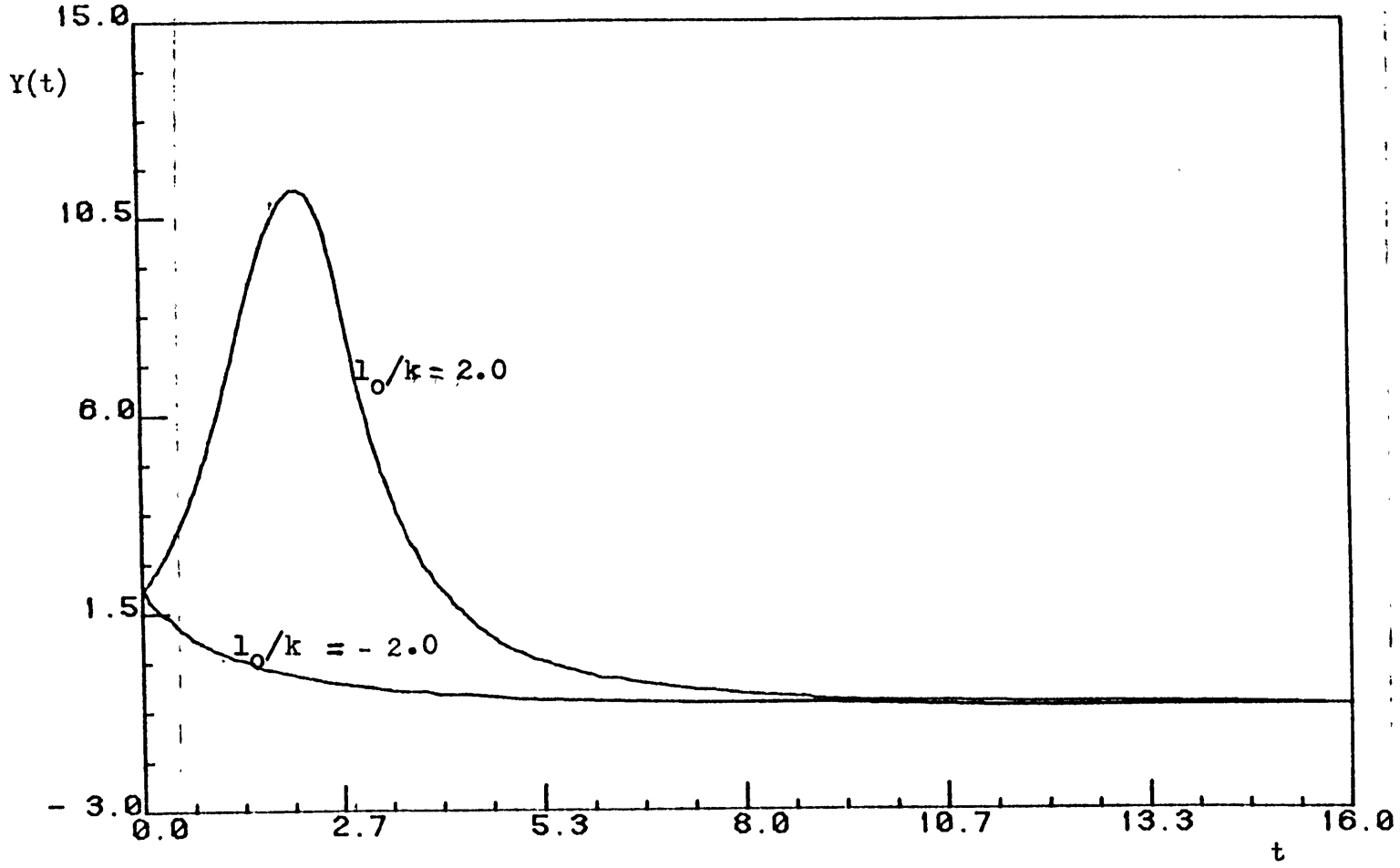

Figure 4.1.6

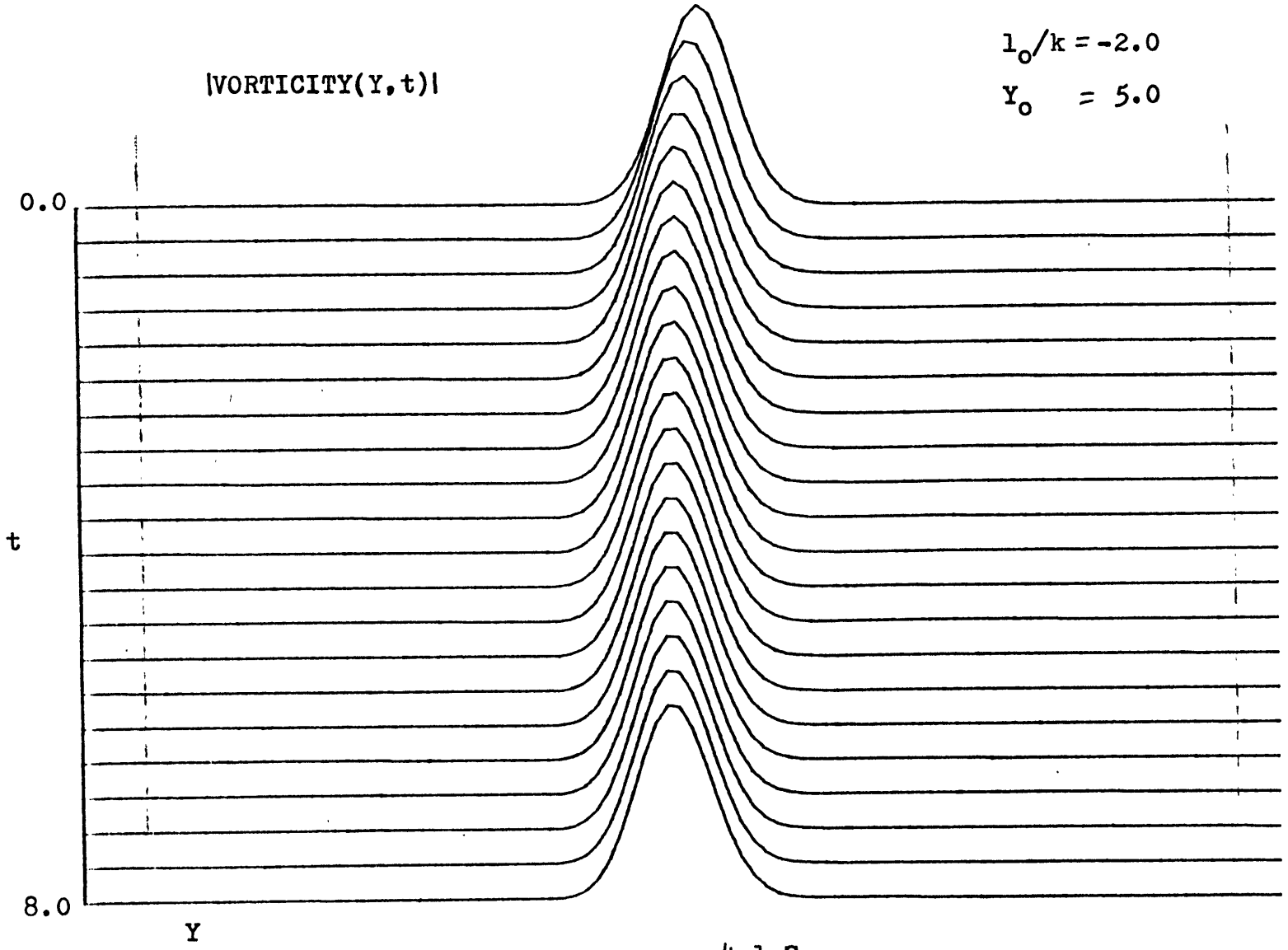

Figure 4.1.7

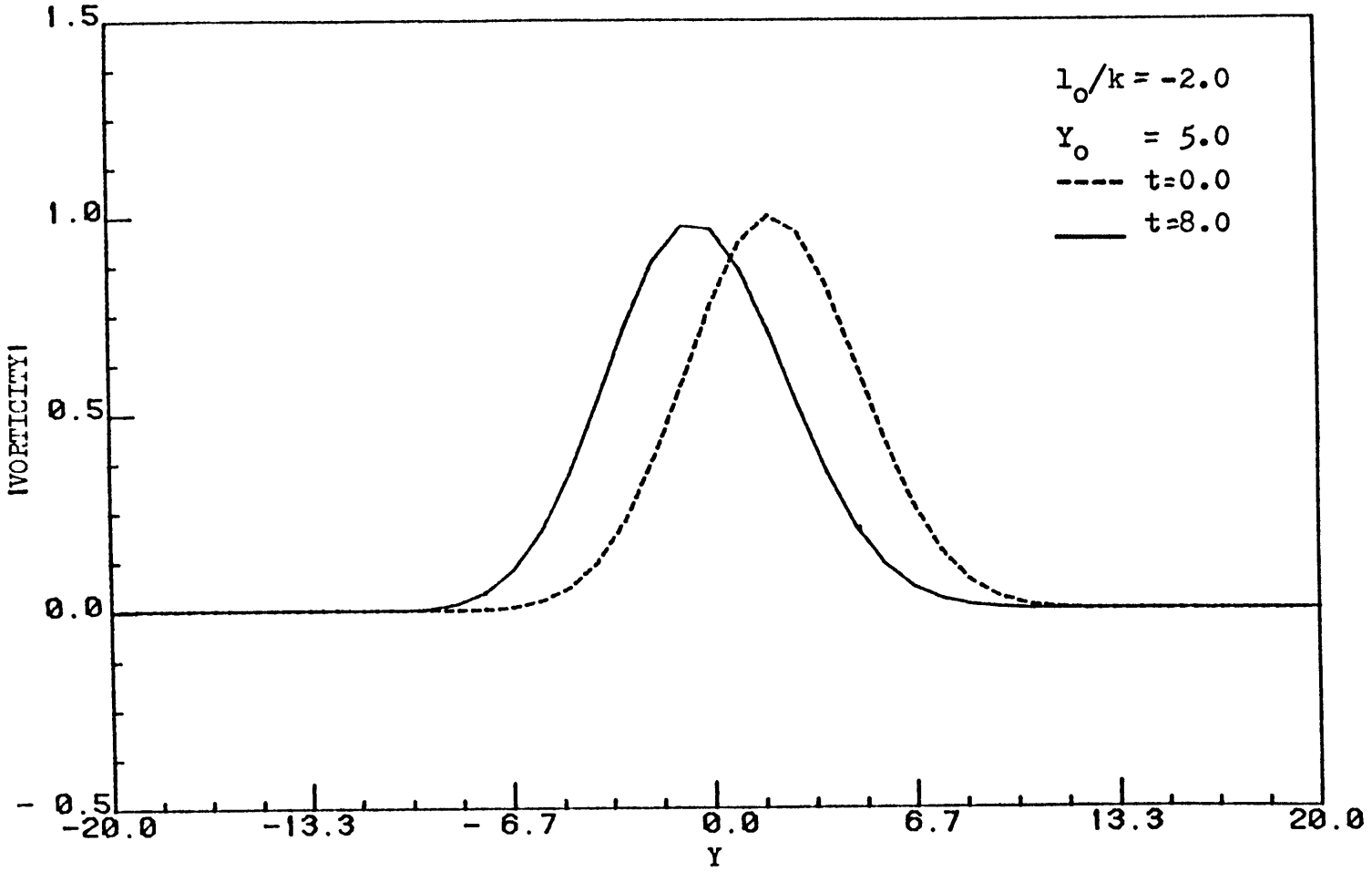
1.5
1.0
0.5
0.0
- 0.5
|VORTICITY|
-20.0
-13.3
- 6.7
0.0
6.7
13.3
20.0
Y
l_o/k = -2.0
Y_o = 5.0
---- t=0.0
____ t=8.0

Figure 4.1.8

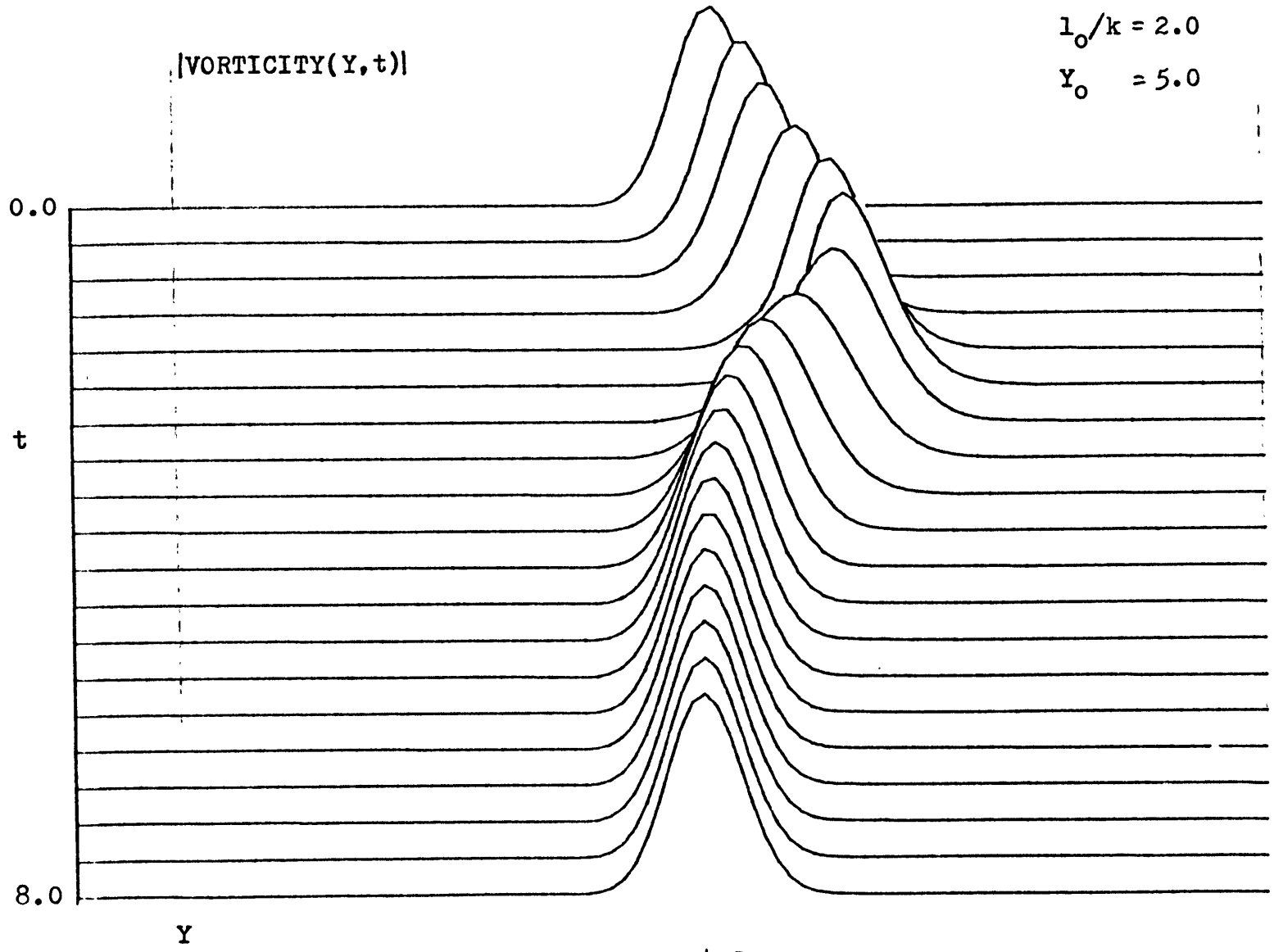

Figure 4.1.9

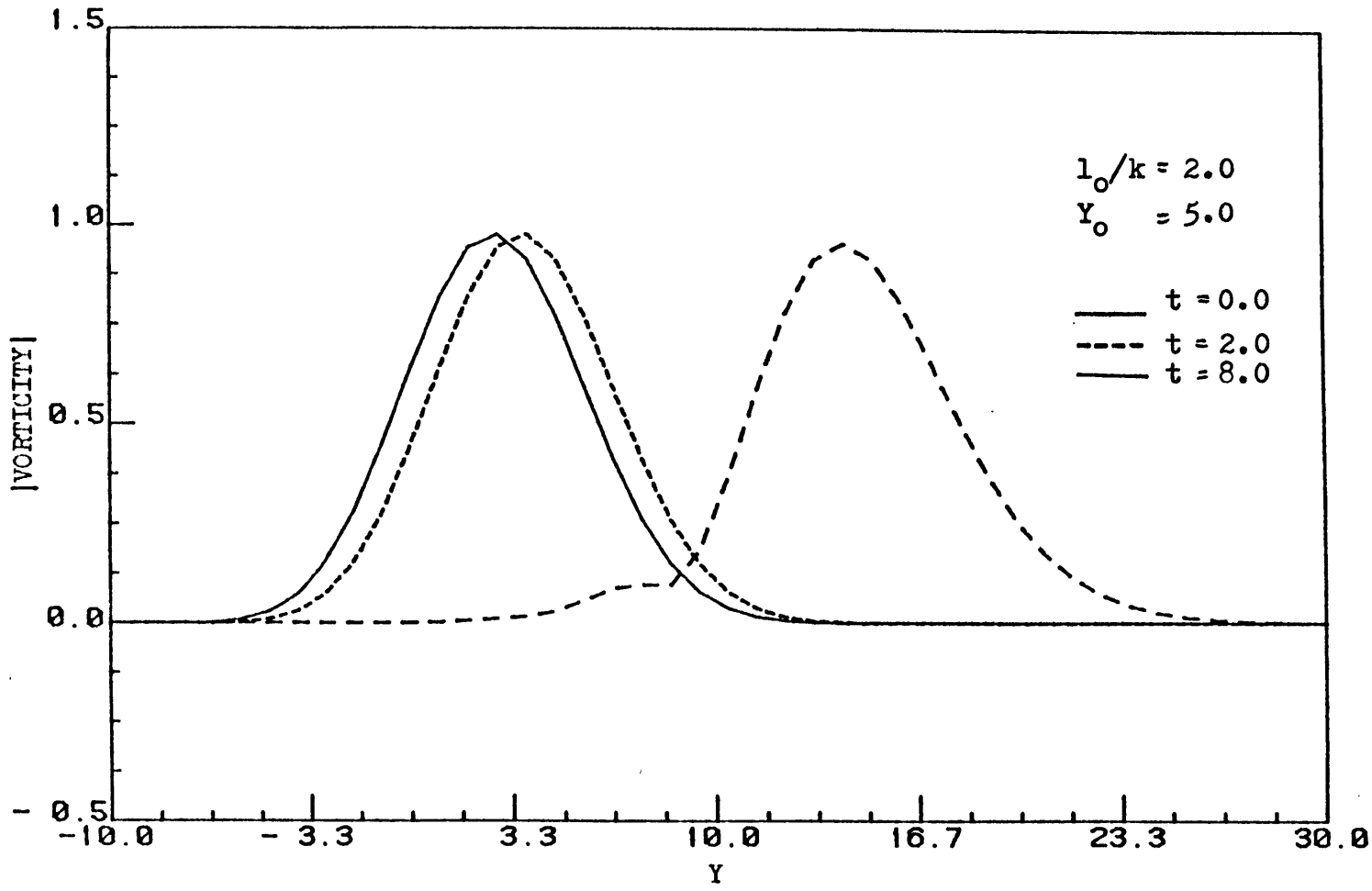
1.5
1.0
0.5
0.0
- 0.5
|VORTICITY|
$l_o/k = 2.0$
$Y_o = 5.0$
t = 0.0
t = 2.0
t = 8.0
-10.0
- 3.3
3.3
10.0
16.7
23.3
30.0
Y

Figure 4.1.10

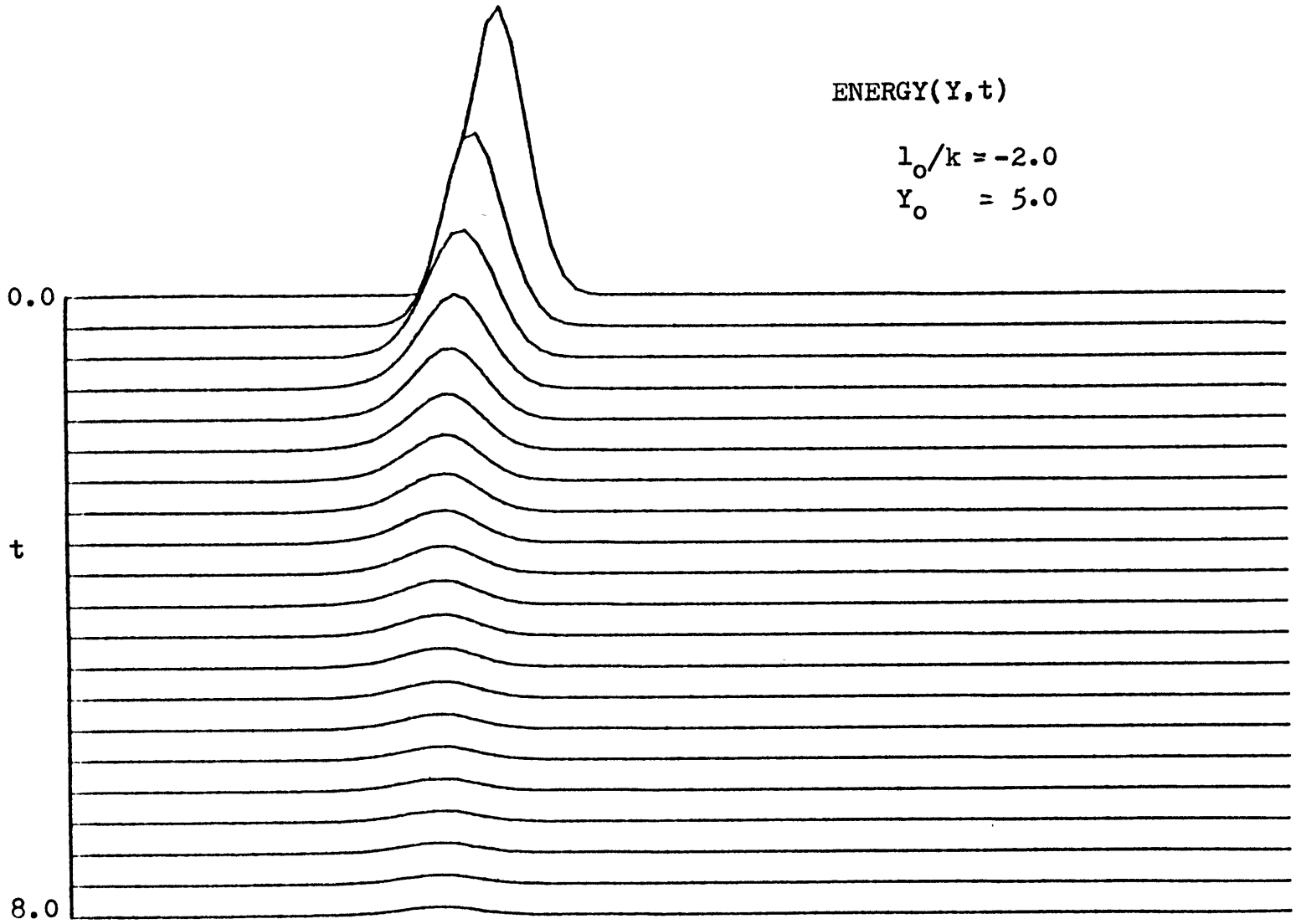

Figure 4.1.11

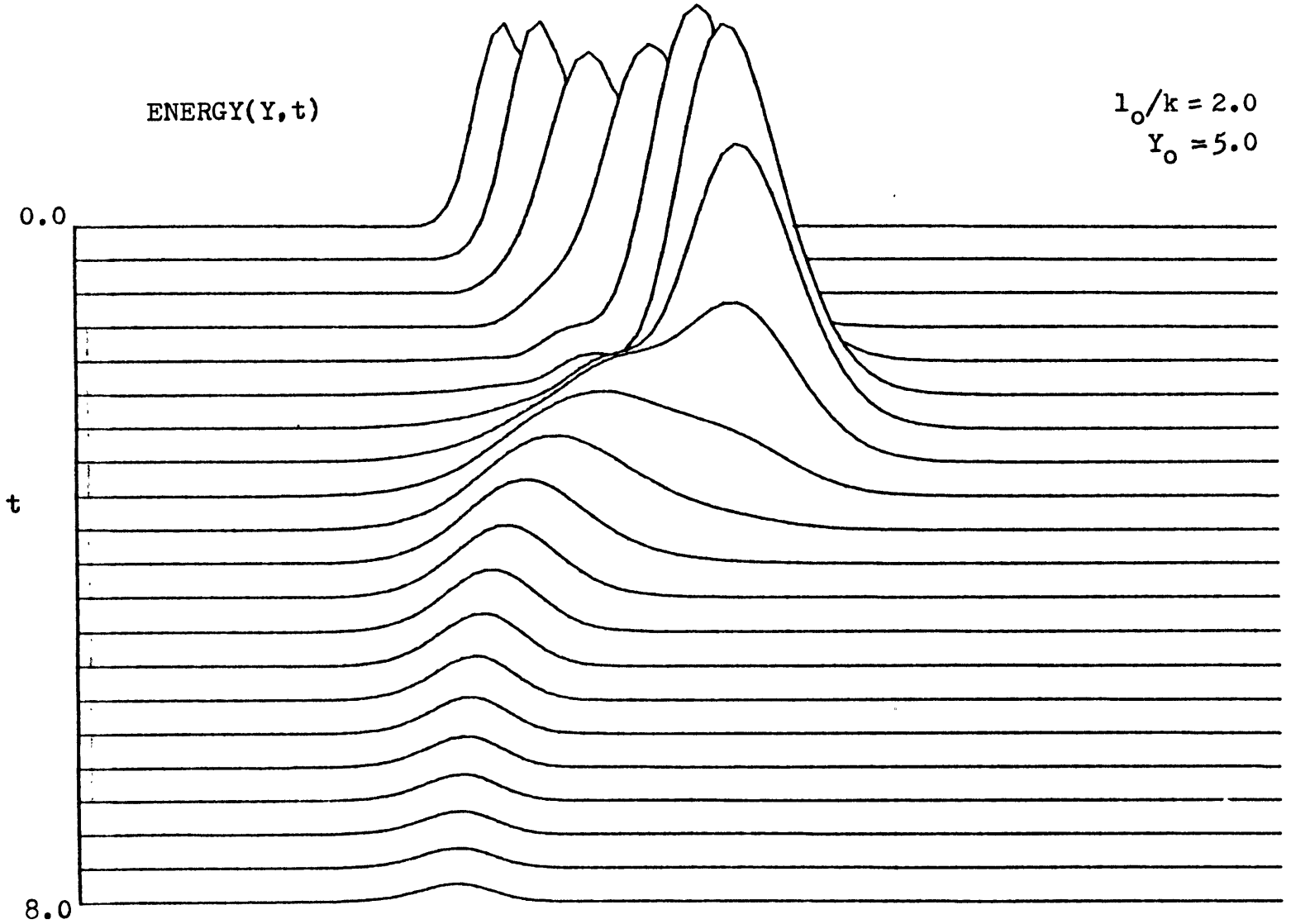

Figure 4.1.12

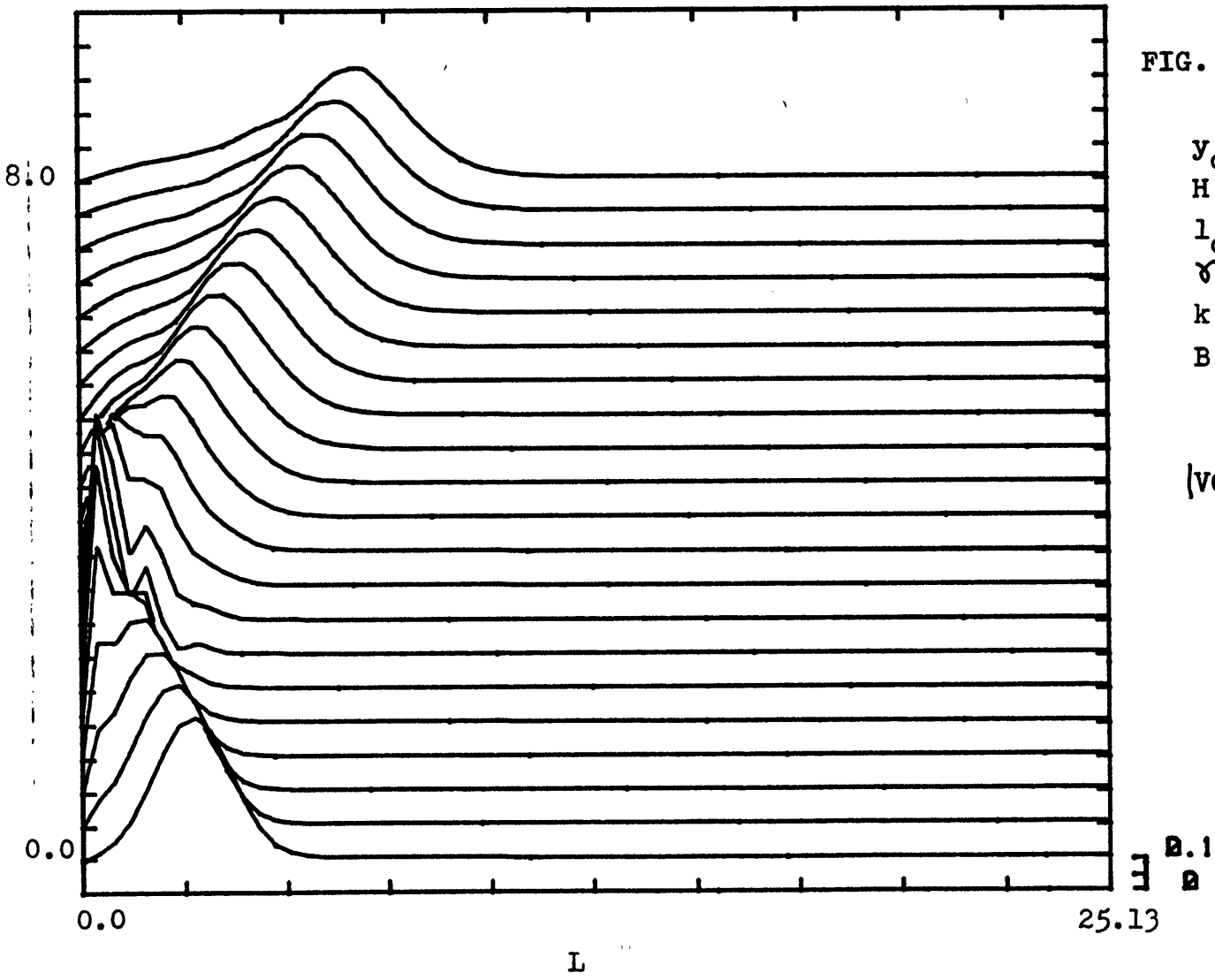

FIG. 4.1.13

$y_o = 5.0$
$H = 0.75$
$l_o = 2.67$
$\gamma = 0.0$
$k = 1.0$
$B = 0.0$

|VORT(L,t)|

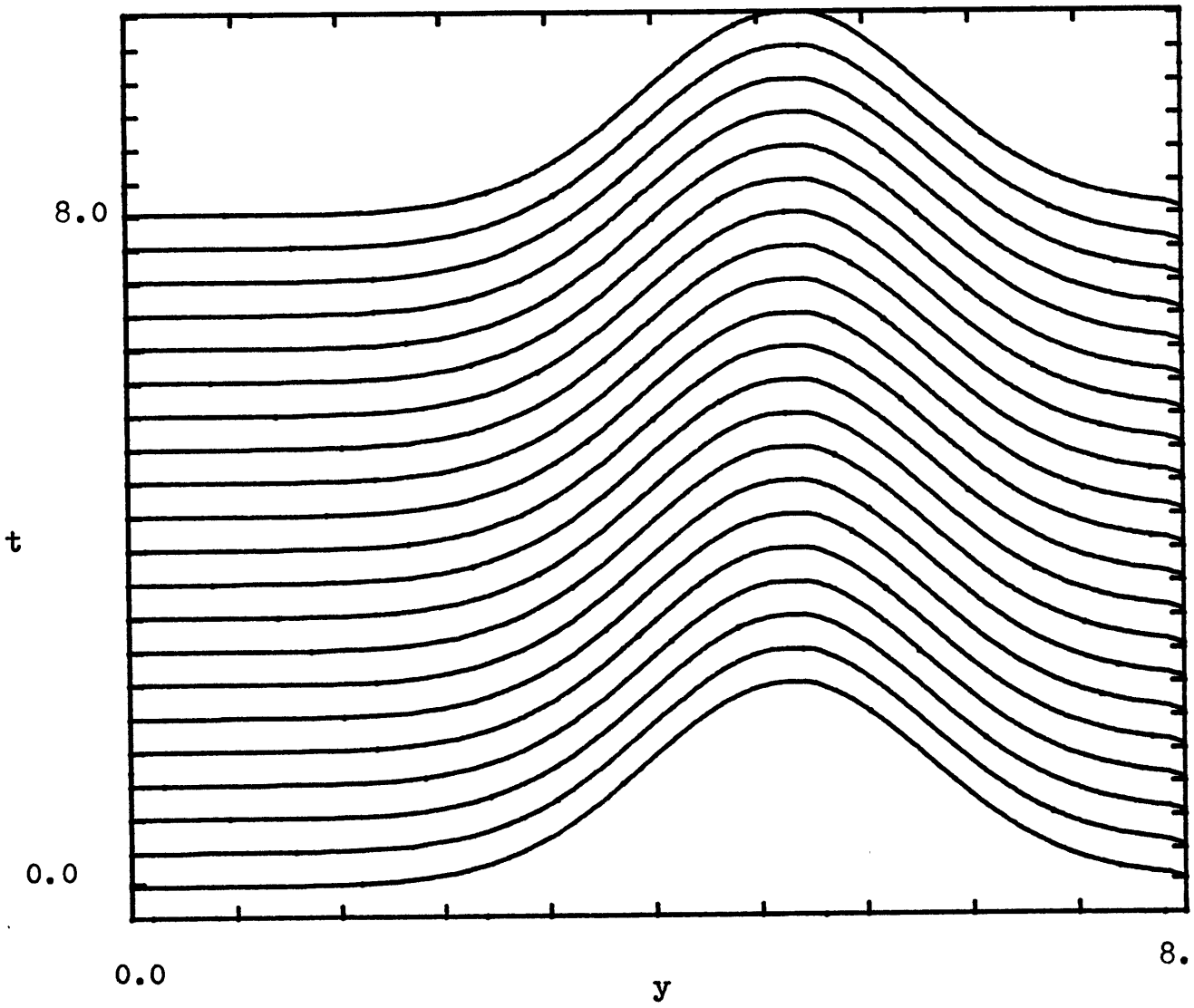

FIG. 4.1.14

$y_o = 5.0$
$H = 0.75$
$l_o = 2.67$
$\gamma = 0.0$
$k = 1.0$
$B = 0.0$

|VORT(y,t)|

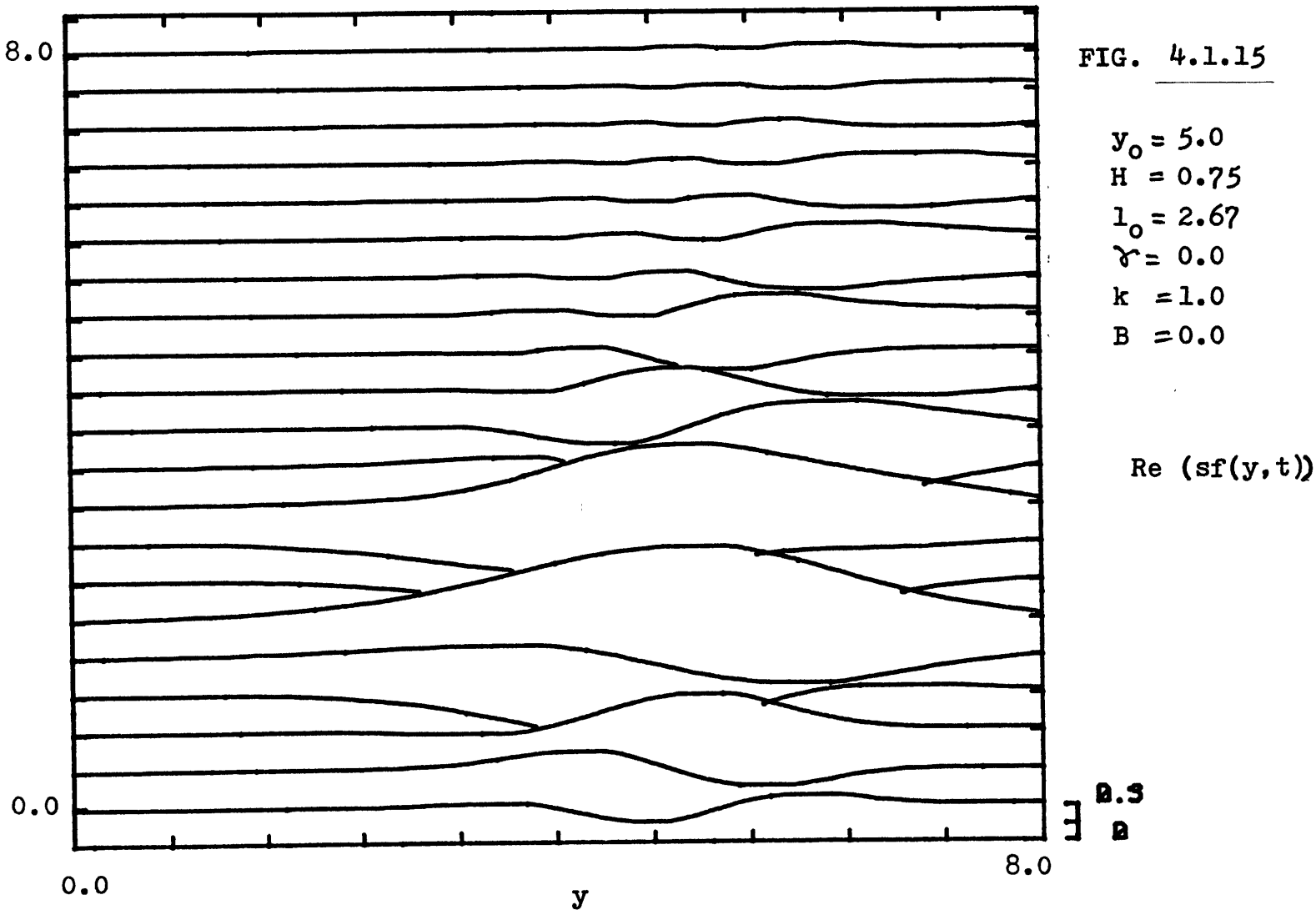

FIG. 4.1.15

$y_o = 5.0$
$H = 0.75$
$l_o = 2.67$
$\gamma = 0.0$
$k = 1.0$
$B = 0.0$

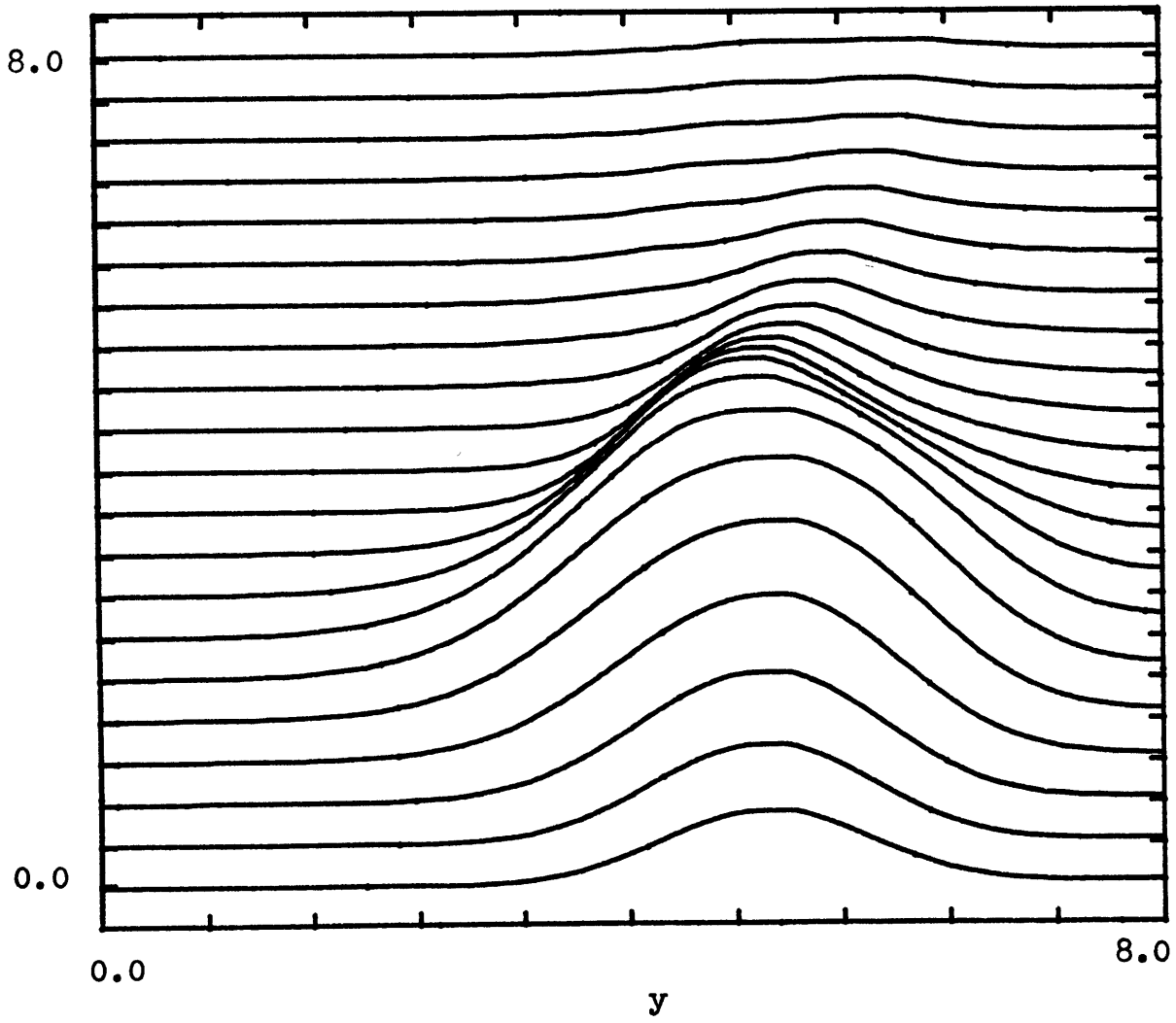

FIG. 4.1.16

$y_o = 5.0$
$H = 0.75$
$l_o = 2.67$
$\gamma = 0.0$
$k = 1.0$
$B = 0.0$

E(y,t)

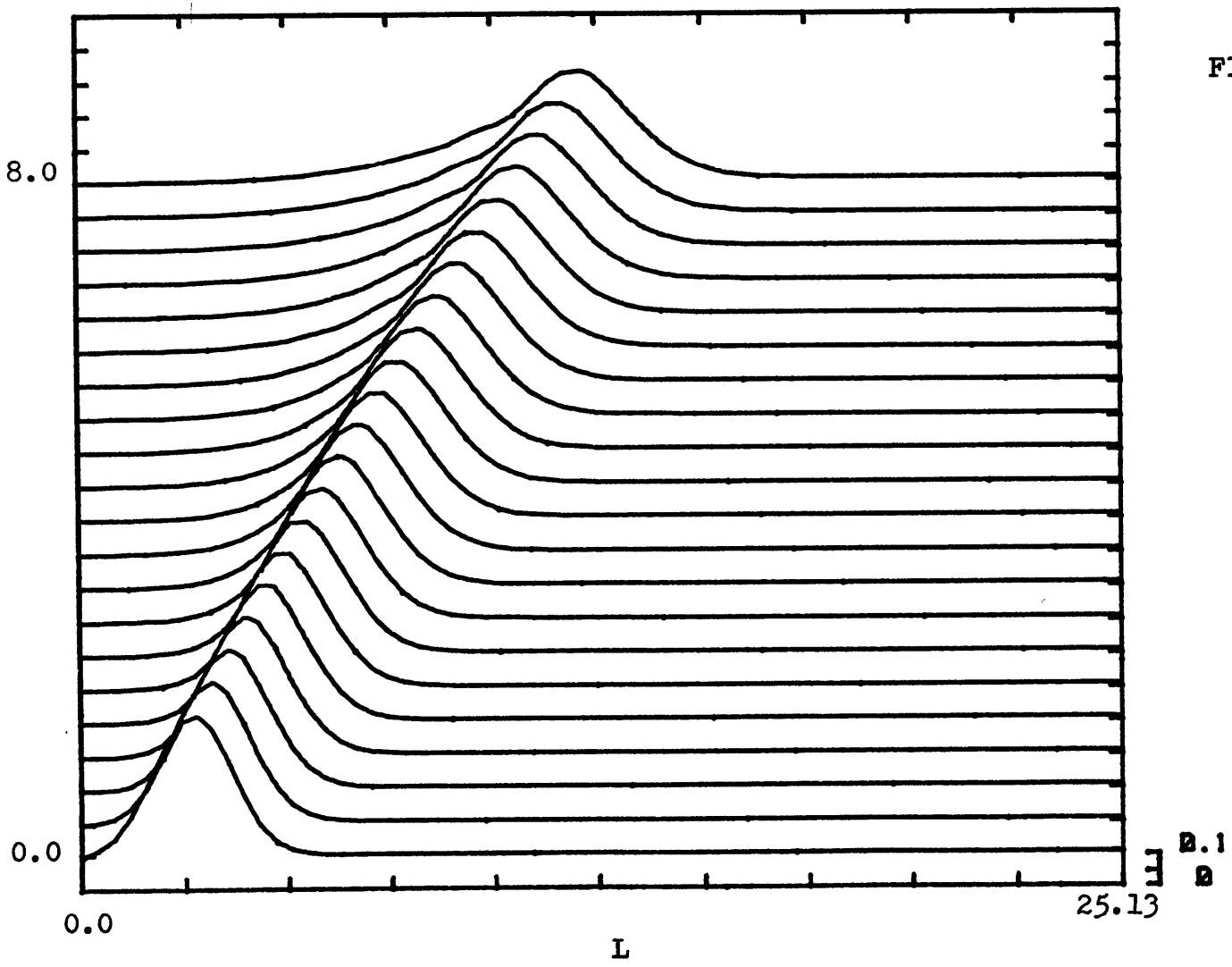

FIG. 4.1.17

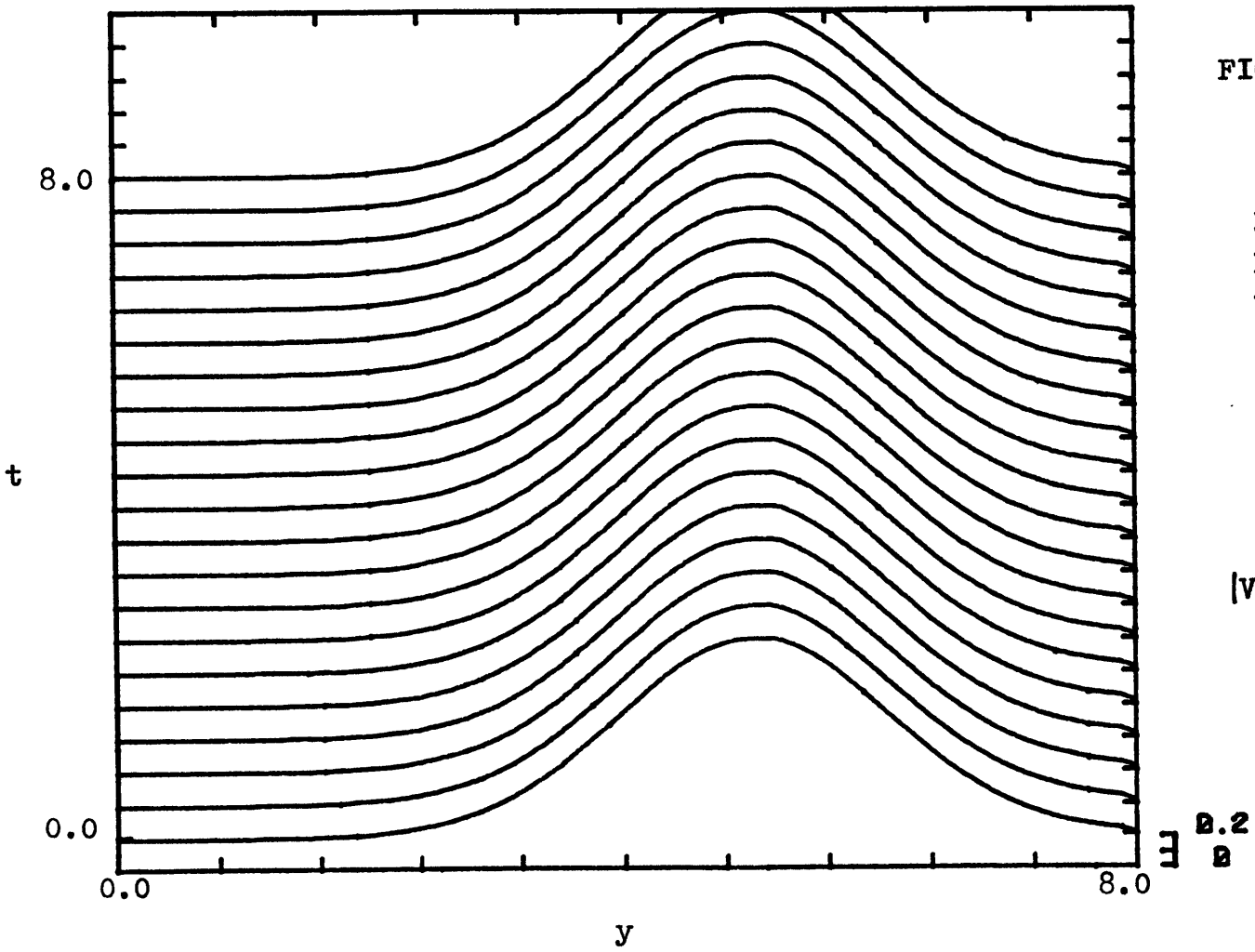

FIG. 4.1.18

$y_o = 5.0$
H = 0.75
γ = 0.0
k = -1.0
B = 0.0

|VORT(y,t)|

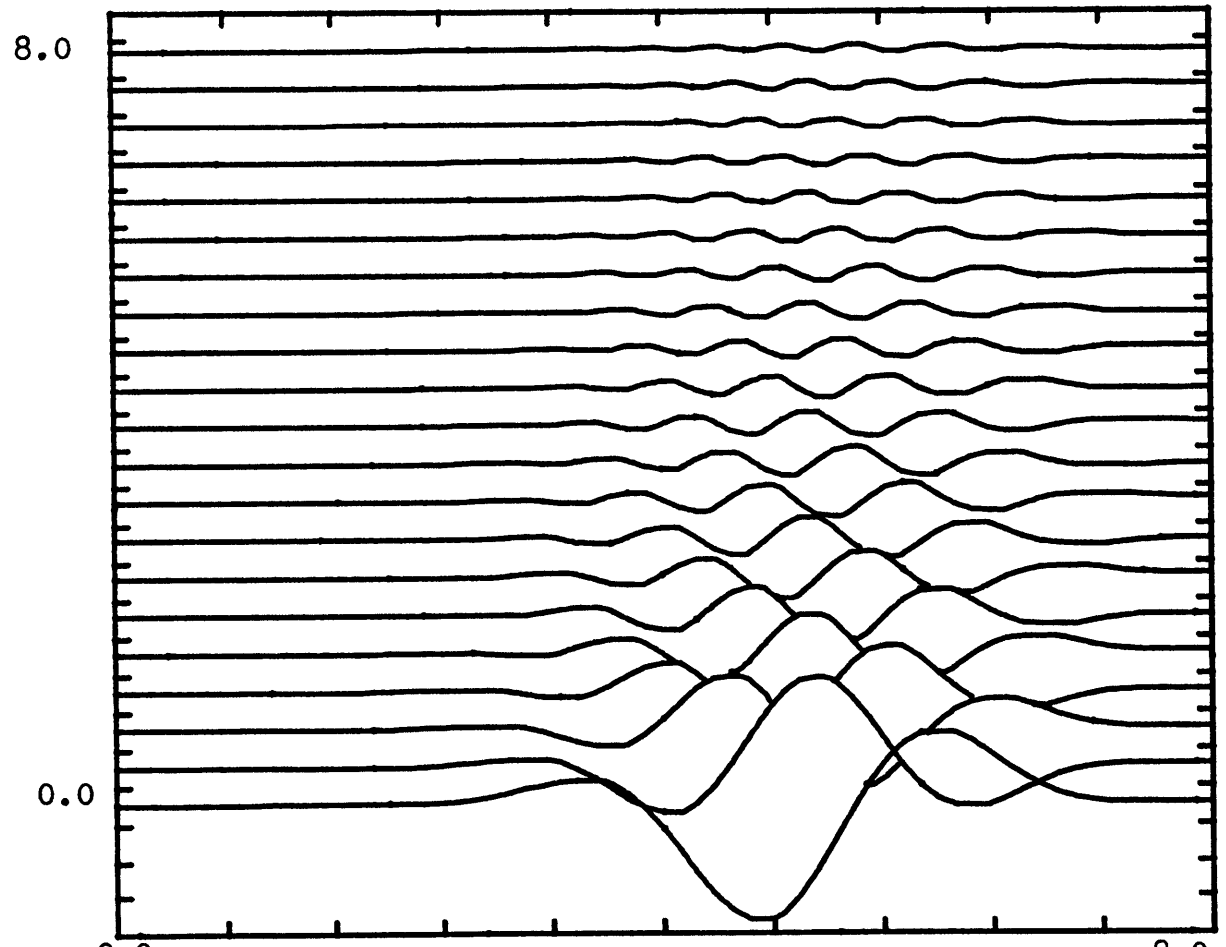

FIG. 4.1.19

$y_o = 5.0$
H = 0.75
$\gamma = 0.0$
k = -1.0
B = 0.0

Re (sf(y,t))

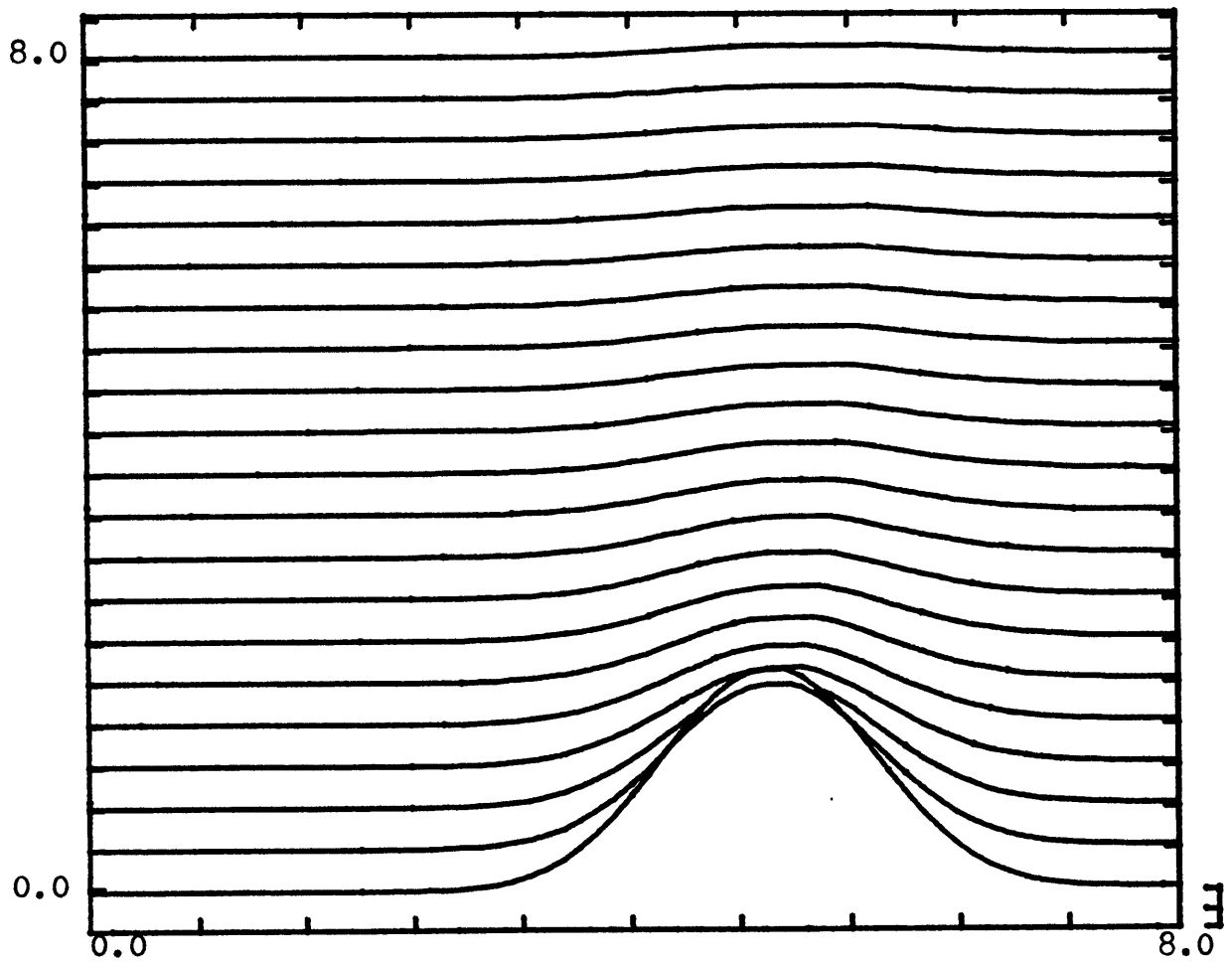

FIG. 4.1.20

$y_o = 5.0$
$H = 0.75$
$\delta = 0.0$
$k = -1.0$
$B = 0.0$

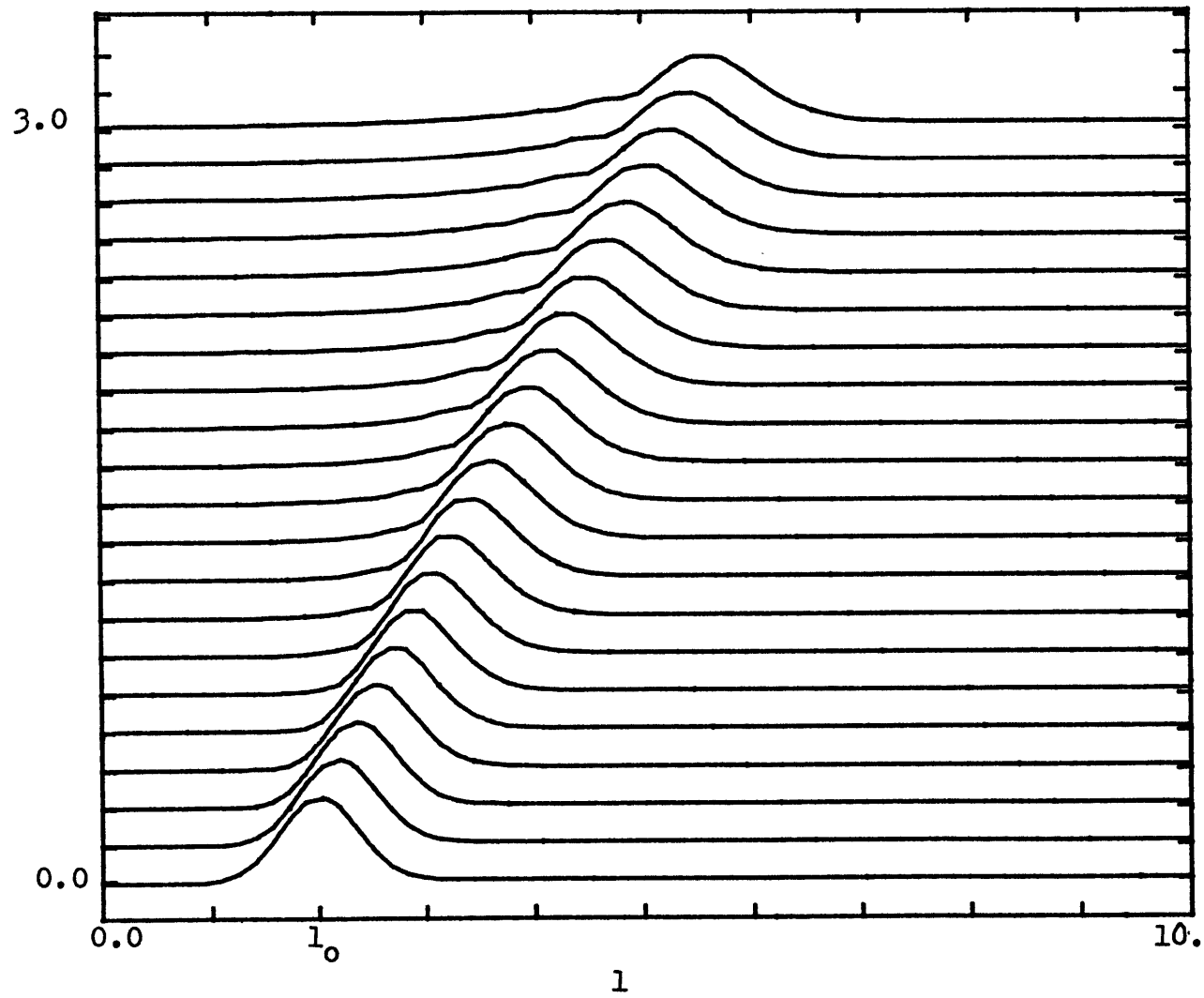

FIG. 4.1.21

$y_o = 10.5$
$H = 2.0$
$l_o = 2.0$
$\gamma = 0.0$
$k = -1.0$
$B = 20.0$
$y_c \cong 6.5$
$y_T \cong 26.5$

|VORT(L,t)|

0.5
0

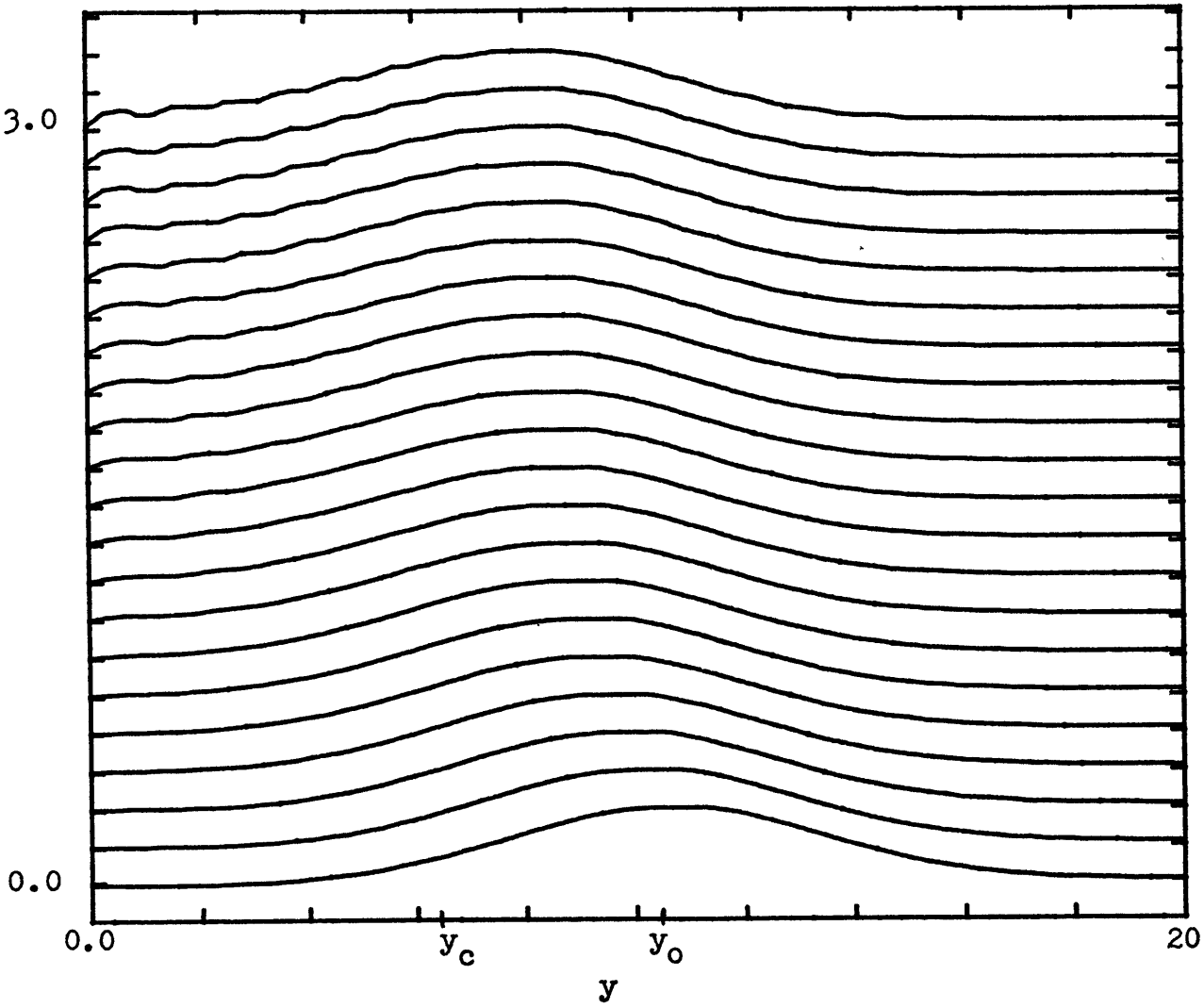

FIG. 4.1.22

$y_o = 10.5$
$H = 2.0$
$l_0 = 2.0$
$\gamma = 0.0$
$k = -1.0$
$B = 20.0$
$y_c \cong 6.5$
$y_T \cong 26.5$

|VORT(y,t)|

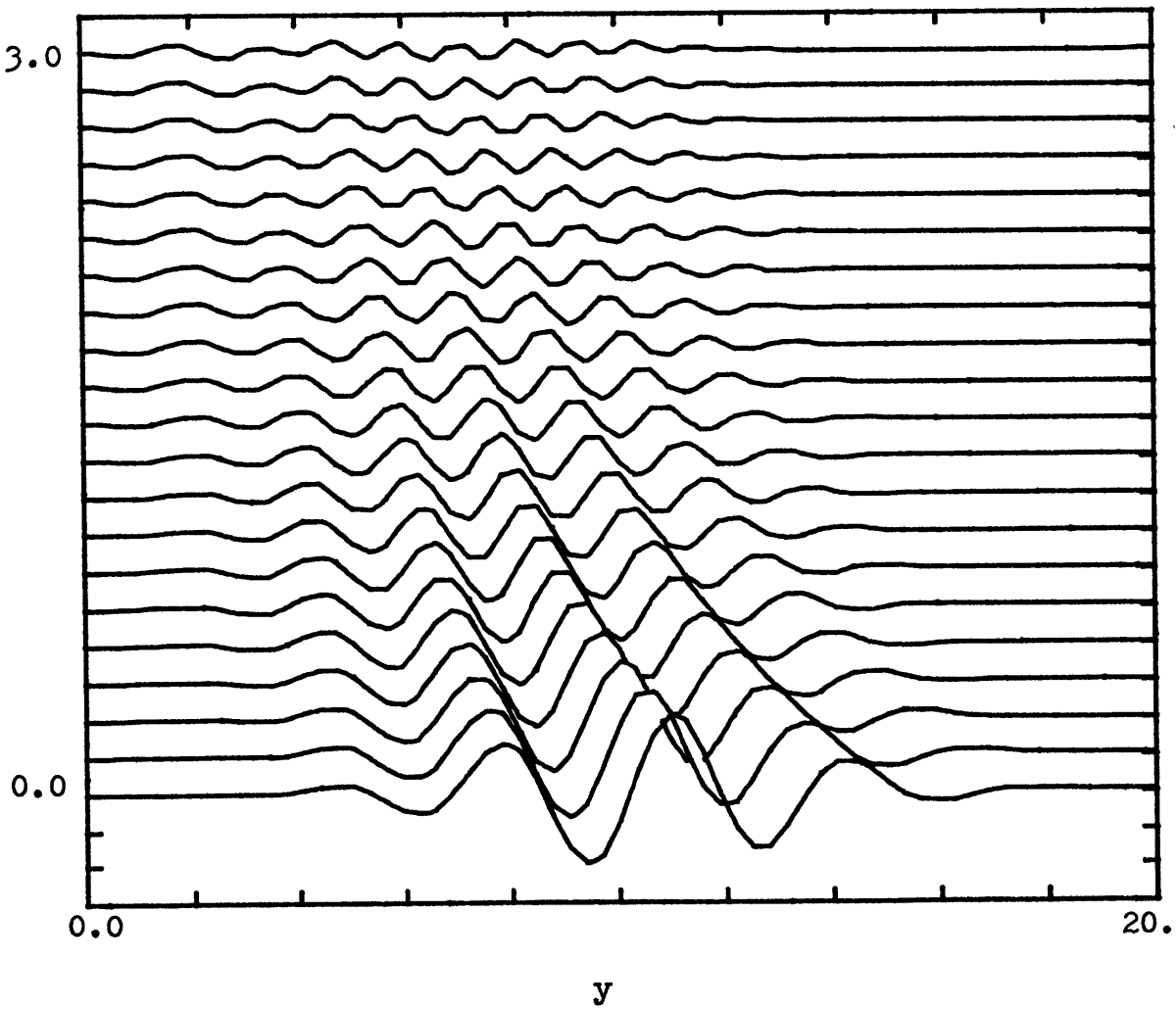

FIG. 4.1.23

$y_o = 10.5$
$H = 2.0$
$l_o = 2.0$
$\gamma = 0.0$
$k = -1.0$
$B = 20.0$
$y_c \hat{=} 6.5$
$y_T \hat{=} 26.5$

Re (sf(y,t))

0.1
0

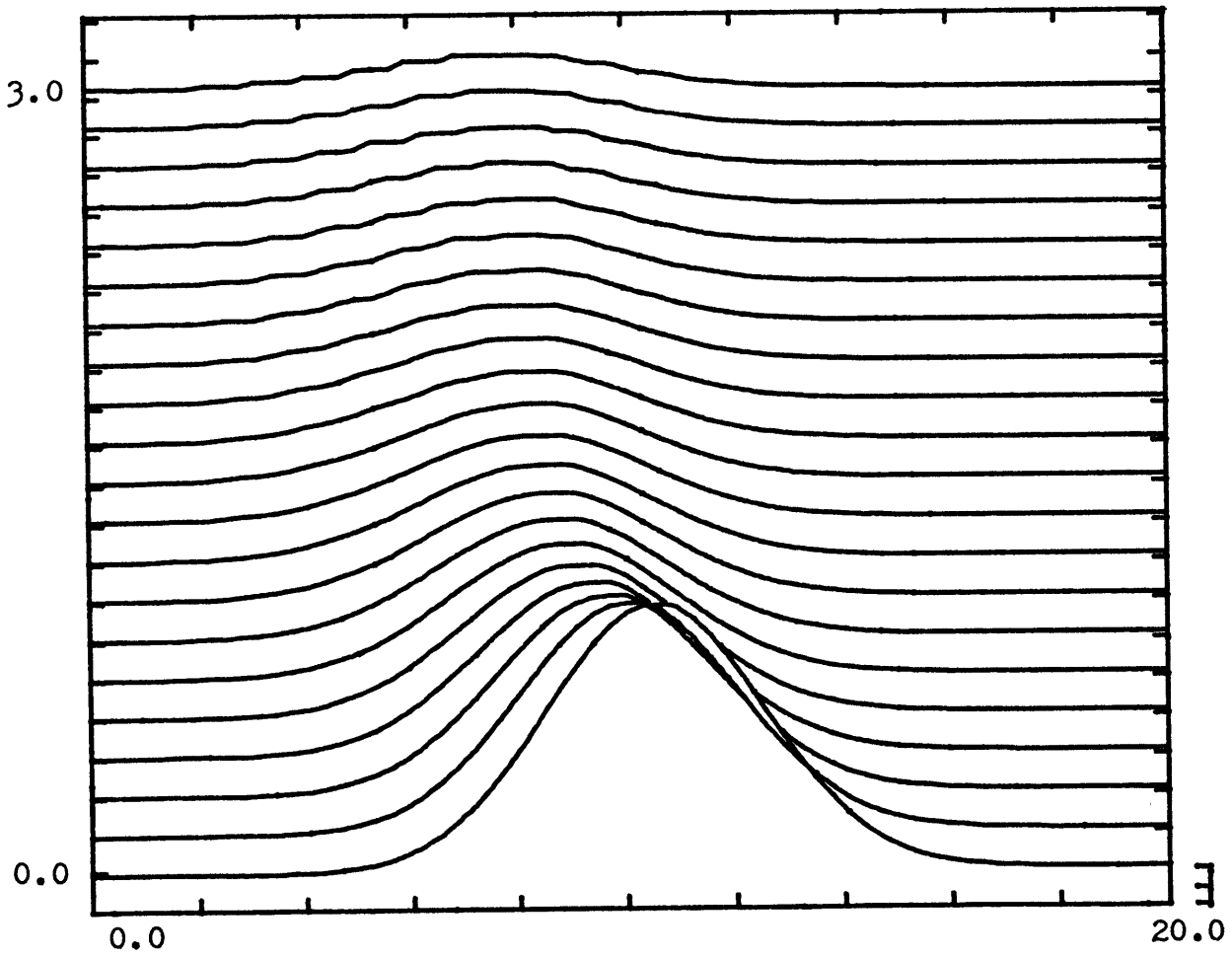

FIG. 4.1.24

$y_o = 10.5$
$H = 2.0$
$l_o = 2.0$
$\gamma = 0.0$
$k = -1.0$
$B = 20.0$
$y_c \cong 6.5$
$y_T \cong 26.5$

E(y,t)

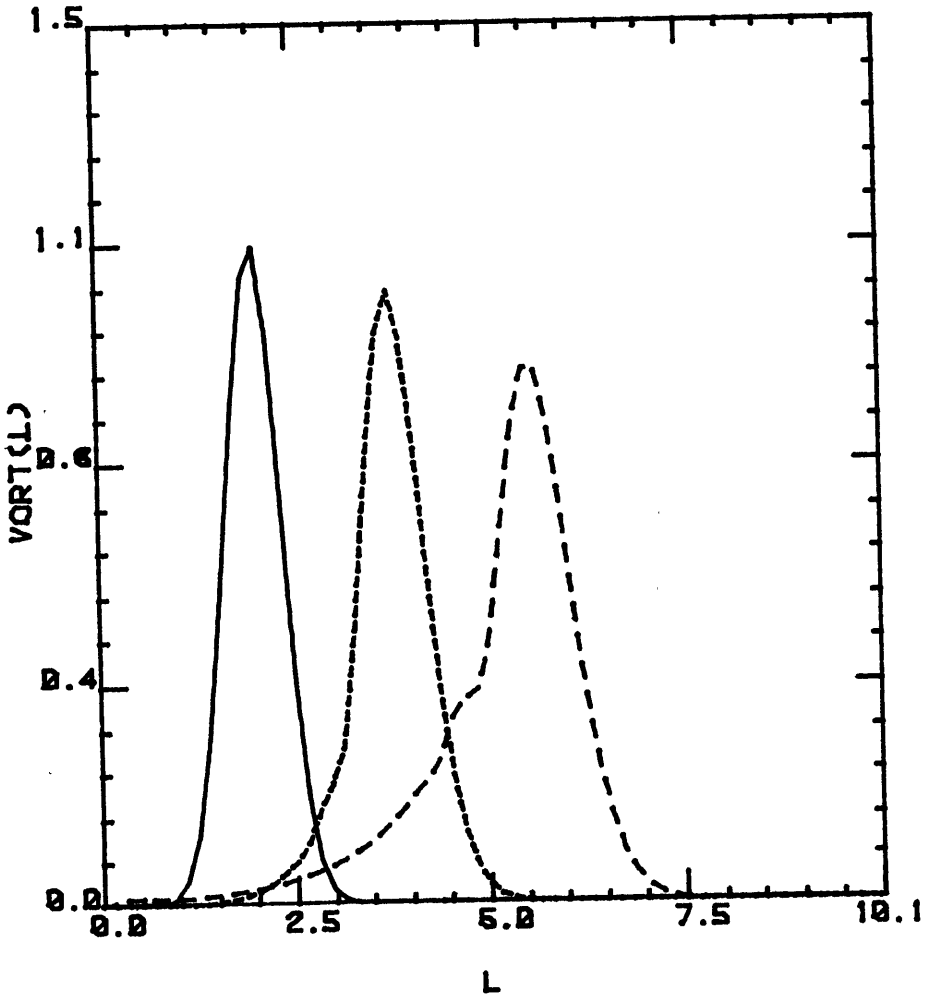

FIG. 4.1.25

$y_o = 10.5$
$H = 2.0$
$l_o = 2.0$
$\gamma = 0.0$
$k = -1.0$
$B = 20.0$
$y_c \cong 6.5$
$y_T \cong 26.5$

—— T = 0.0
----- T = 1.5
----- T = 3.0

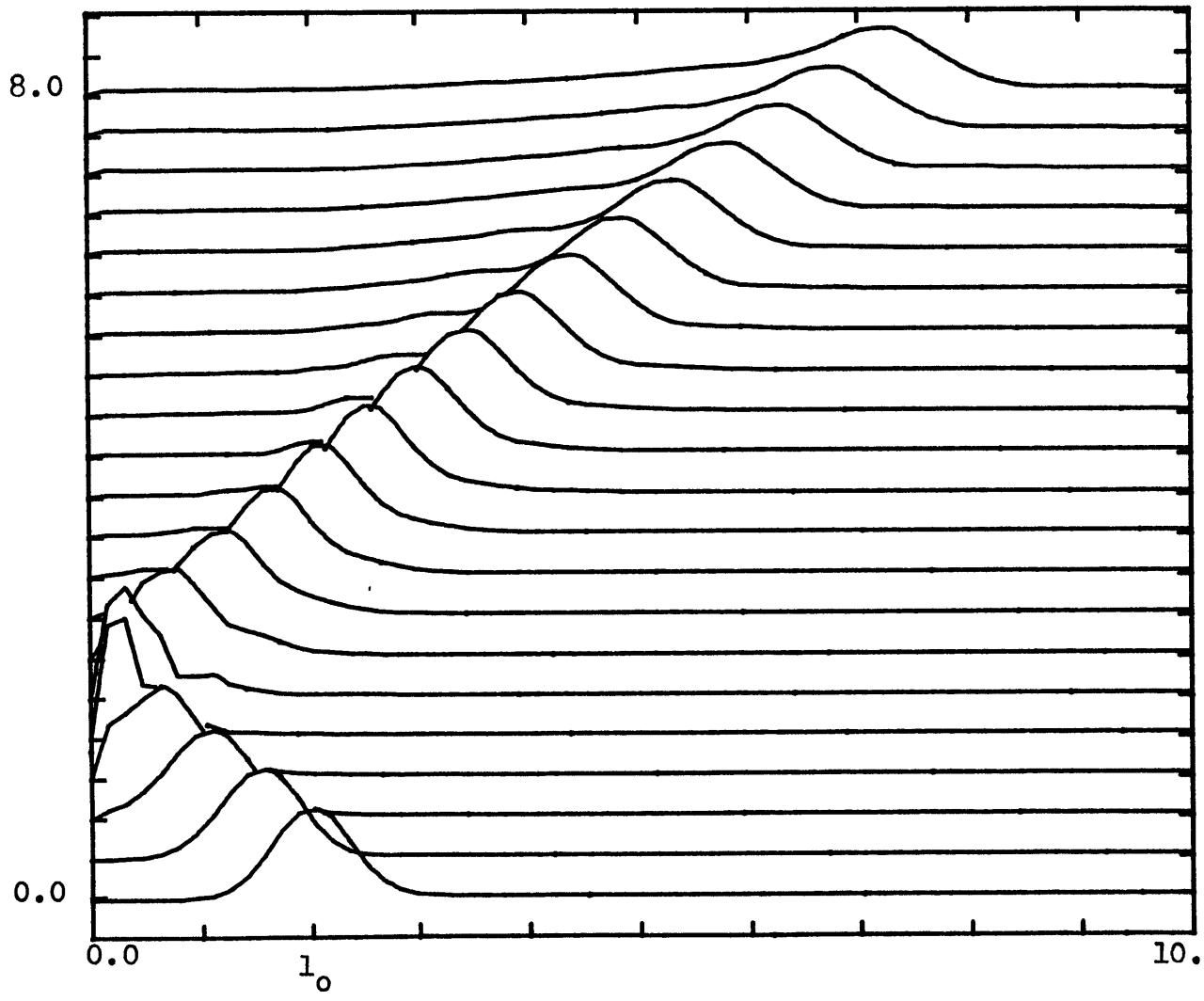

FIG. 4.1.26

$y_o = 8.0$
$H = 2.0$
$l_o = 2.0$
$\gamma = 0.0$
$k = 1.0$
$B = 0.0$
$y_c \cong 6.0$
$y_T \cong 16.0$

|VORT(1,t)|

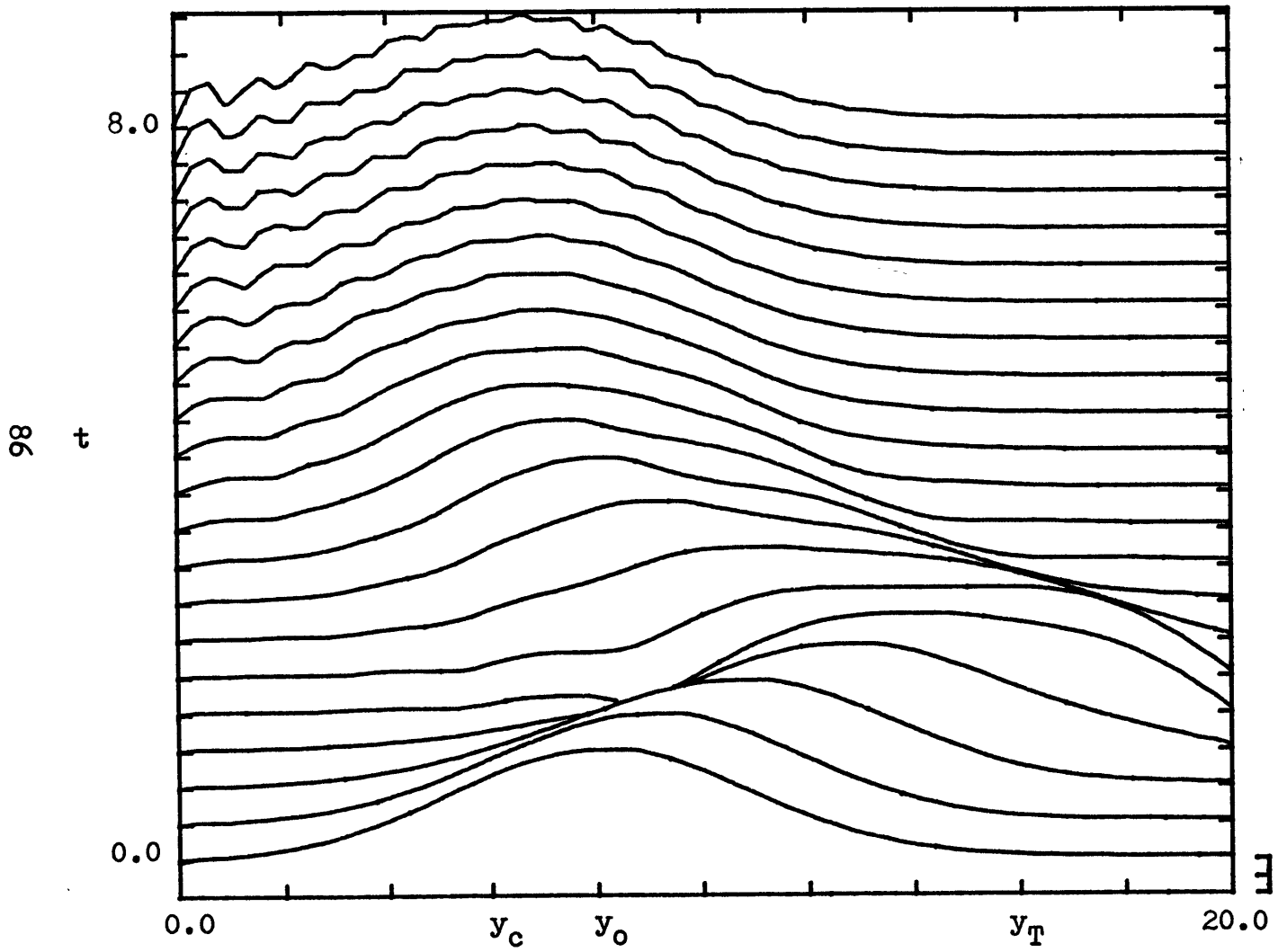

FIG. 4.1.27

$y_o = 8.0$
$H = 2.0$
$l_o = 2.0$
$\gamma = 0.0$
$k = 1.0$
$B = 0.0$
$y_c \cong 6.0$
$y_T \cong 16.0$

|VORT(y,t)|

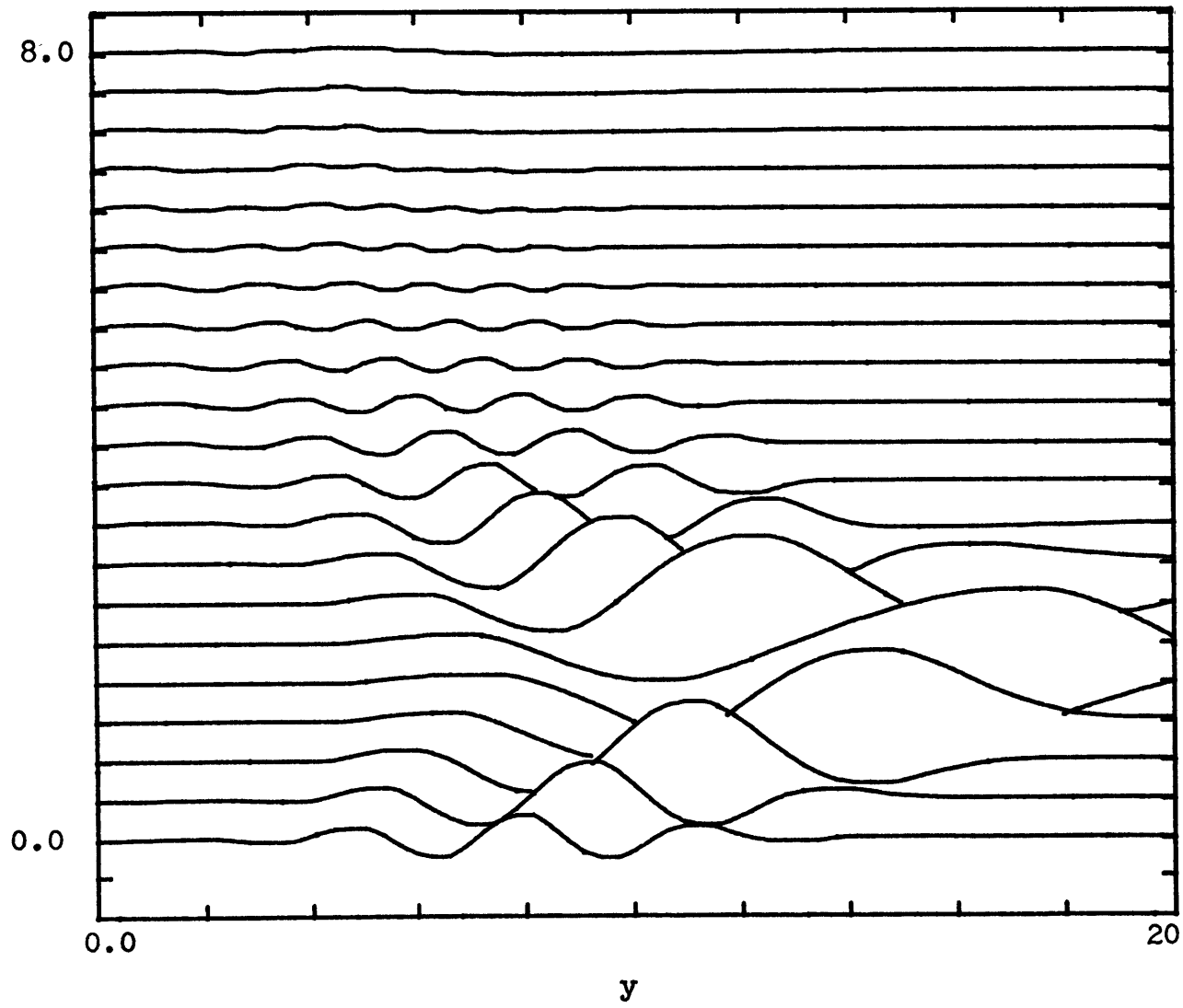

FIG. 4.1.28

$y_o = 8.0$
$H = 2.0$
$l_o = 2.0$
$\gamma = 0.0$
$k = 1.0$
$B = 0.0$
$y_c \cong 6.0$
$y_T \cong 16.0$

Re (sf(y,t))

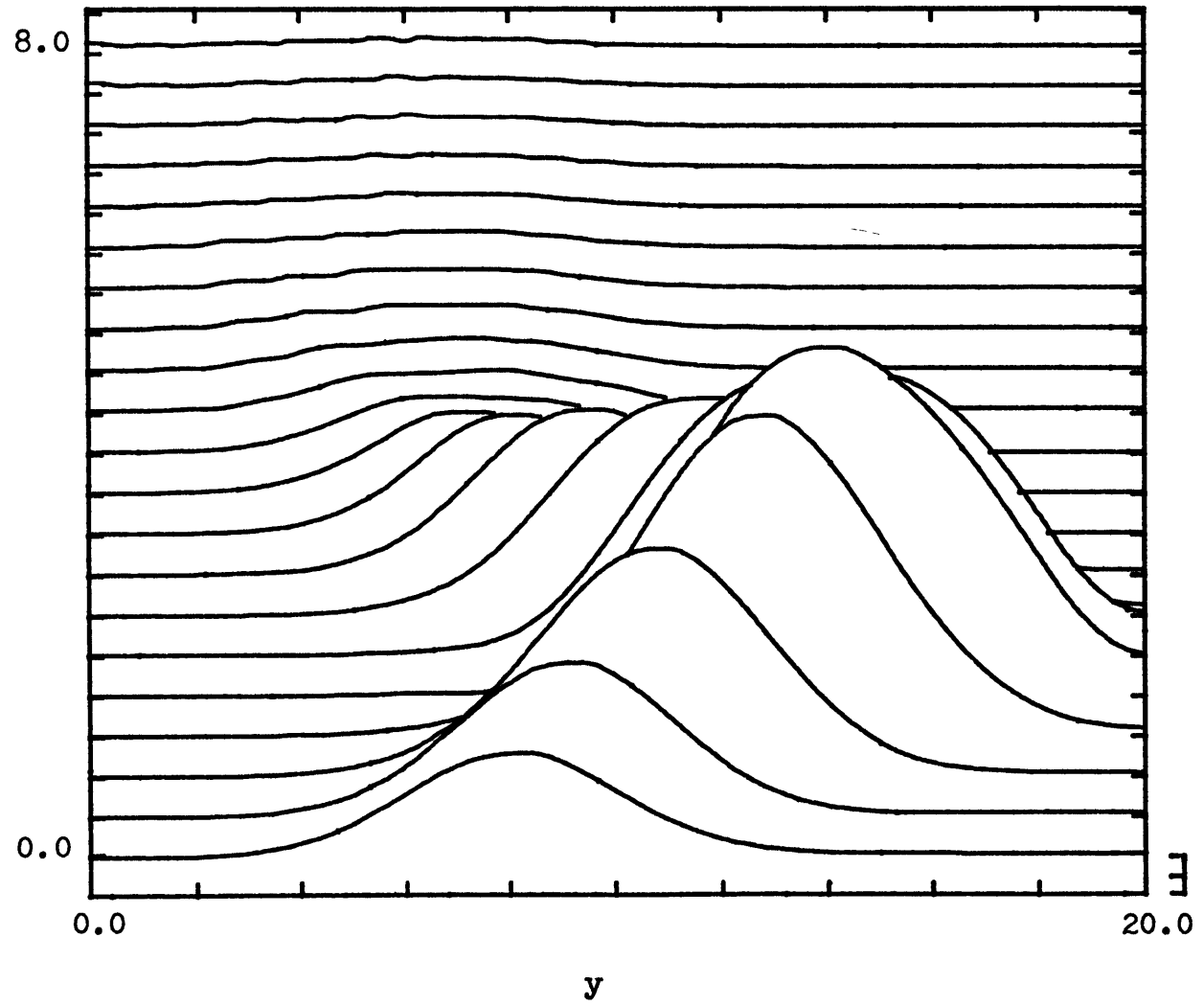

FIG. 4.1.29

$y_o = 8.0$
$H = 2.0$
$l_o = 2.0$
$\gamma = 0.0$
$k = 1.0$
$B = 0.0$
$y_c \cong 6.0$
$y_T \cong 16.0$

E(y,t)

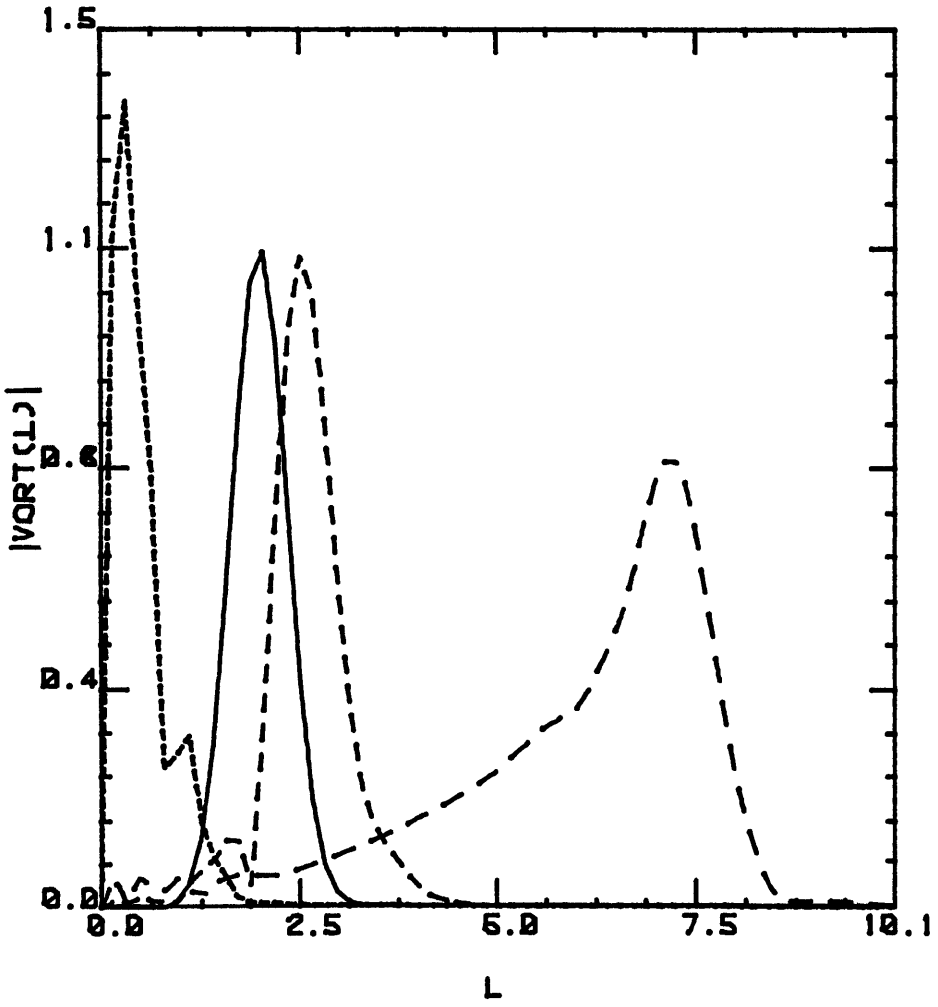

FIG. 4.1.30

$y_o = 8.0$
$H = 2.0$
$l_o = 2.0$
$\Upsilon = 0.0$
$k = 1.0$
$B = 0.0$

$y_c \tilde{=} 6.0$

$y_T \tilde{=} 16.0$

——— T = 0.0
------ T = 2.0
- - - - T = 4.0
— — — T = 8.0

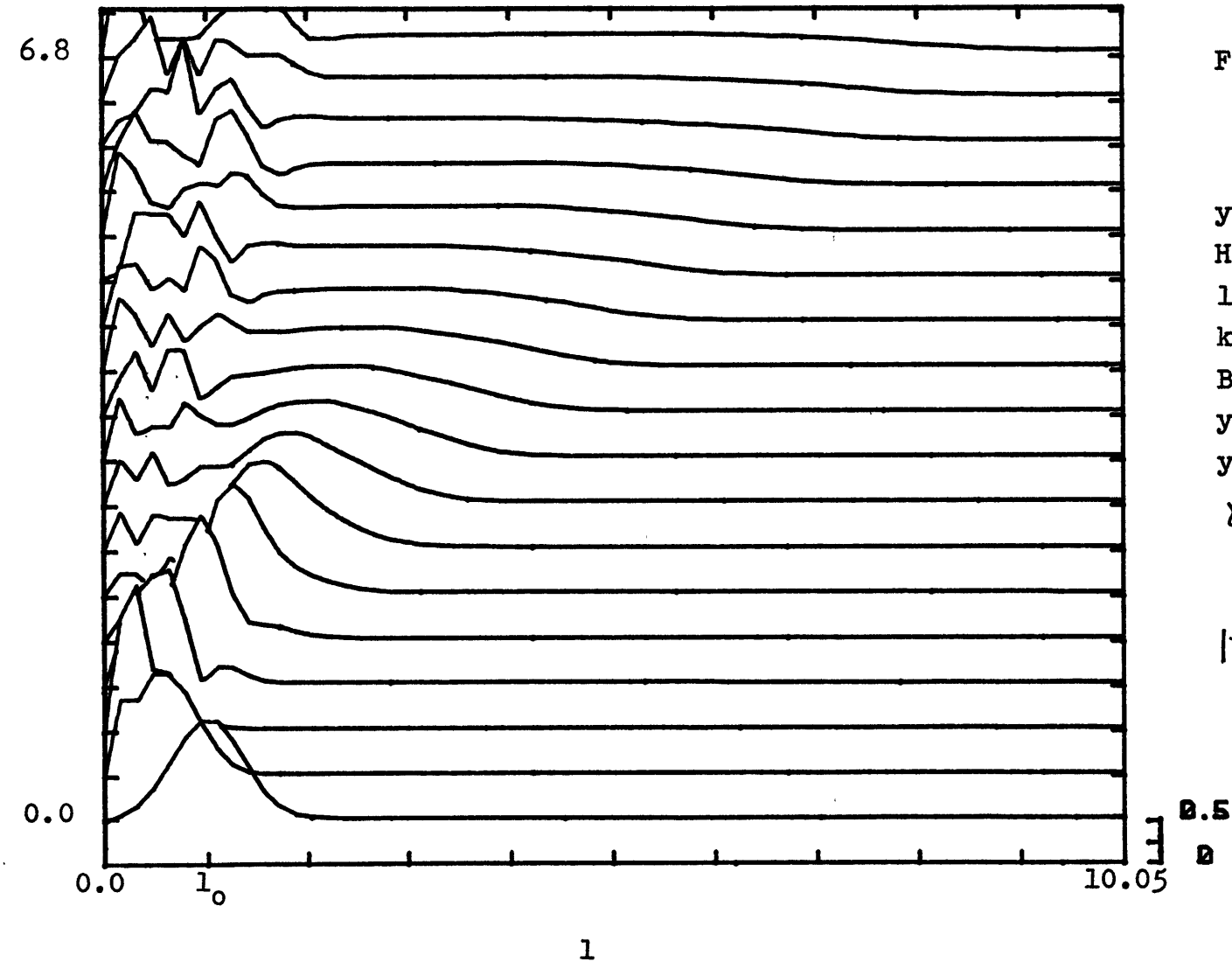

FIG. 4.1.31

$y_o = 8.0$
$H = 2.0$
$l_o = 1.0$
$k = 1.0$
$B = 20.0$
$y_c \cong -2.0$
$y_T \cong 18.0$
$\gamma = 0.0$

|VORT(1,t)|

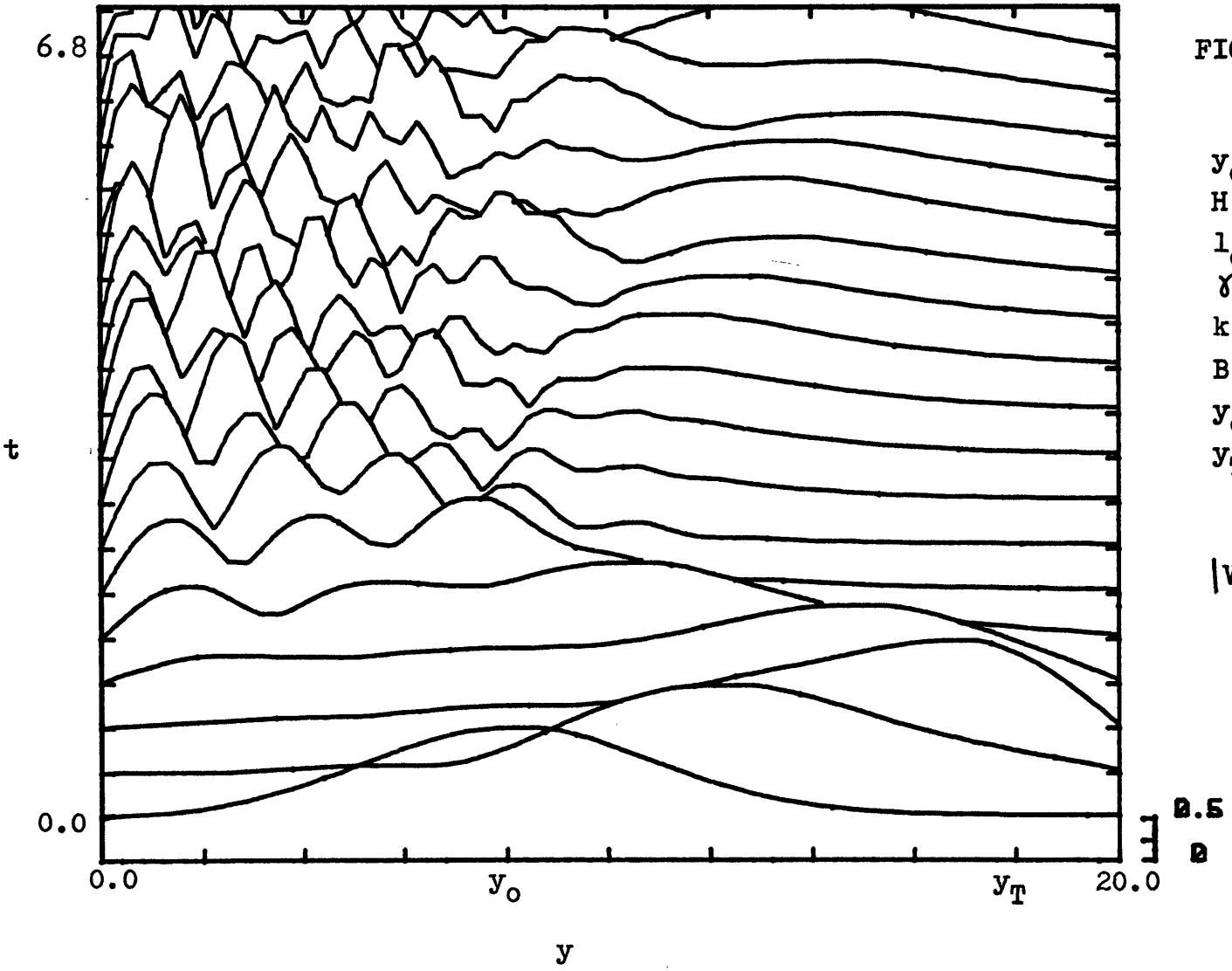

FIG. 4.1.32

$y_o = 8.0$
$H = 2.0$
$l_o = 1.0$
$\gamma = 0.0$
$k = 1.0$
$B = 20.0$
$y_c \cong -2.0$
$y_T \cong 18.0$

|VORT(y,t)|

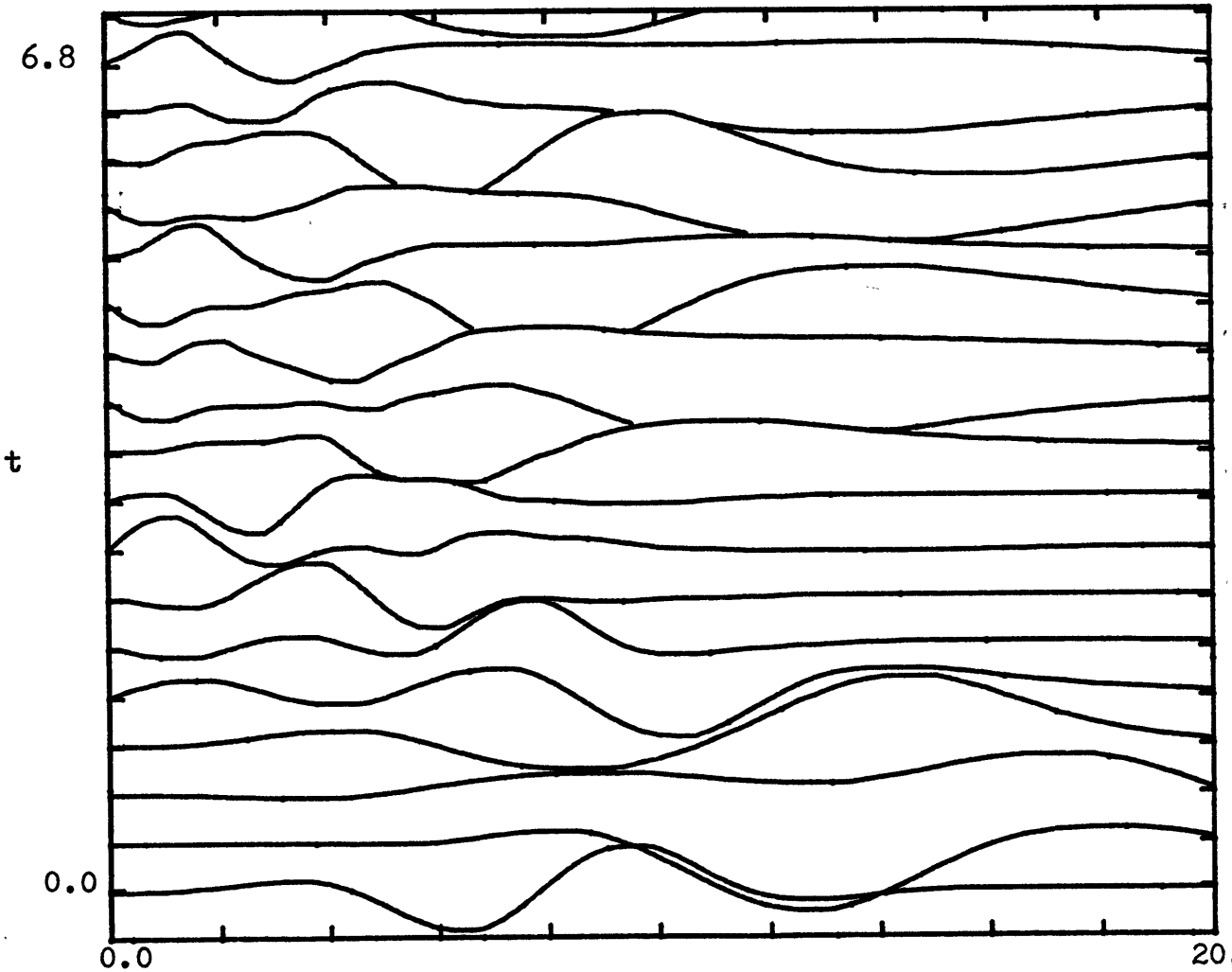

FIG. 4.1.33

$y_o = 8.0$
$H = 2.0$
$l_o = 1.0$
$\gamma = 0.0$
$k = 1.0$
$B = 20.0$
$y_c \cong -2.0$
$y_T \cong 18.0$

Re (sf(y,t))

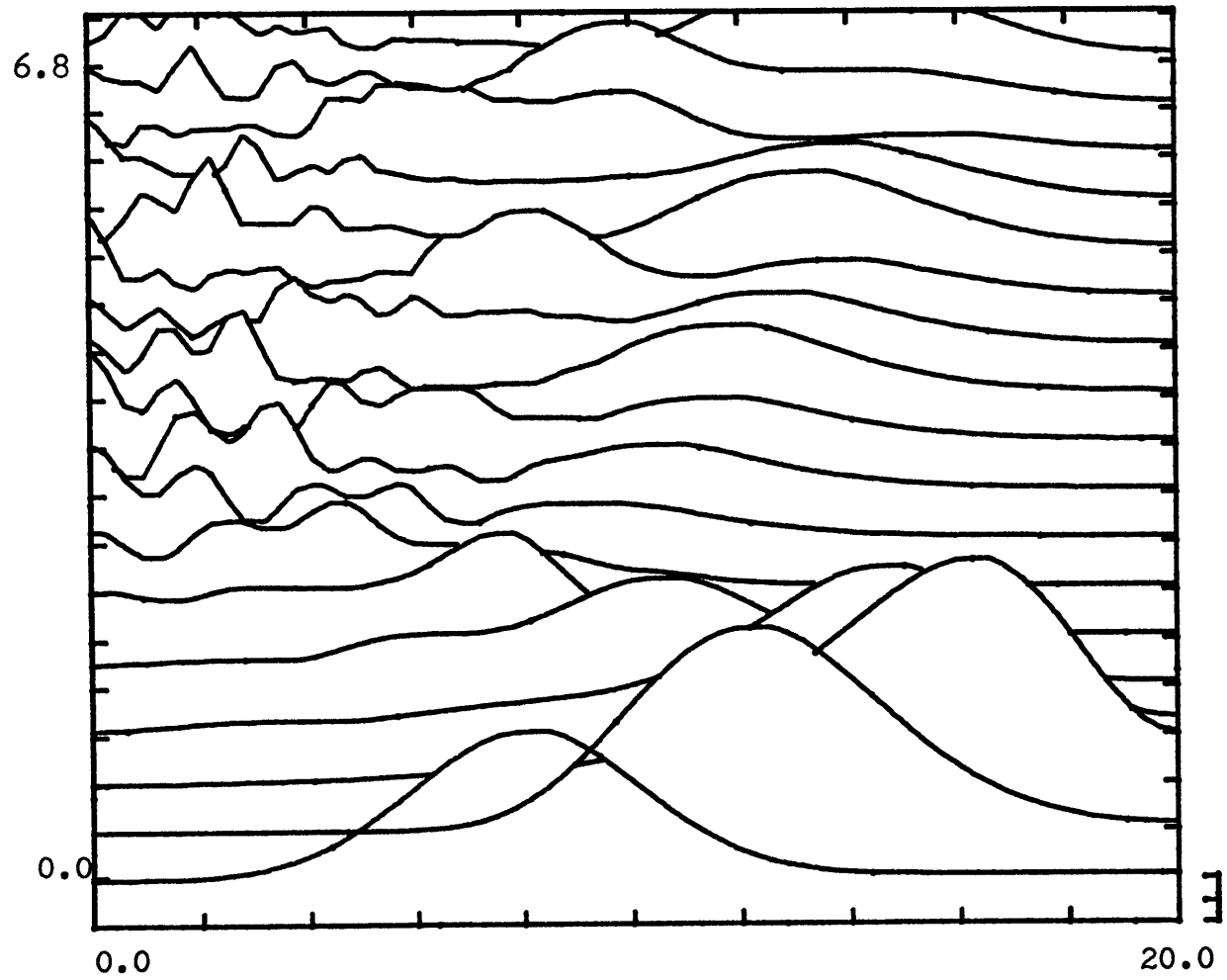

FIG. 4.1.34

$y_o = 8.0$
$H = 2.0$
$l_o = 1.0$
$k = 1.0$
$B = 20.0$
$\gamma = 0.0$
$y_c \cong -2.0$
$y_T \cong 18.0$

E(y,t)

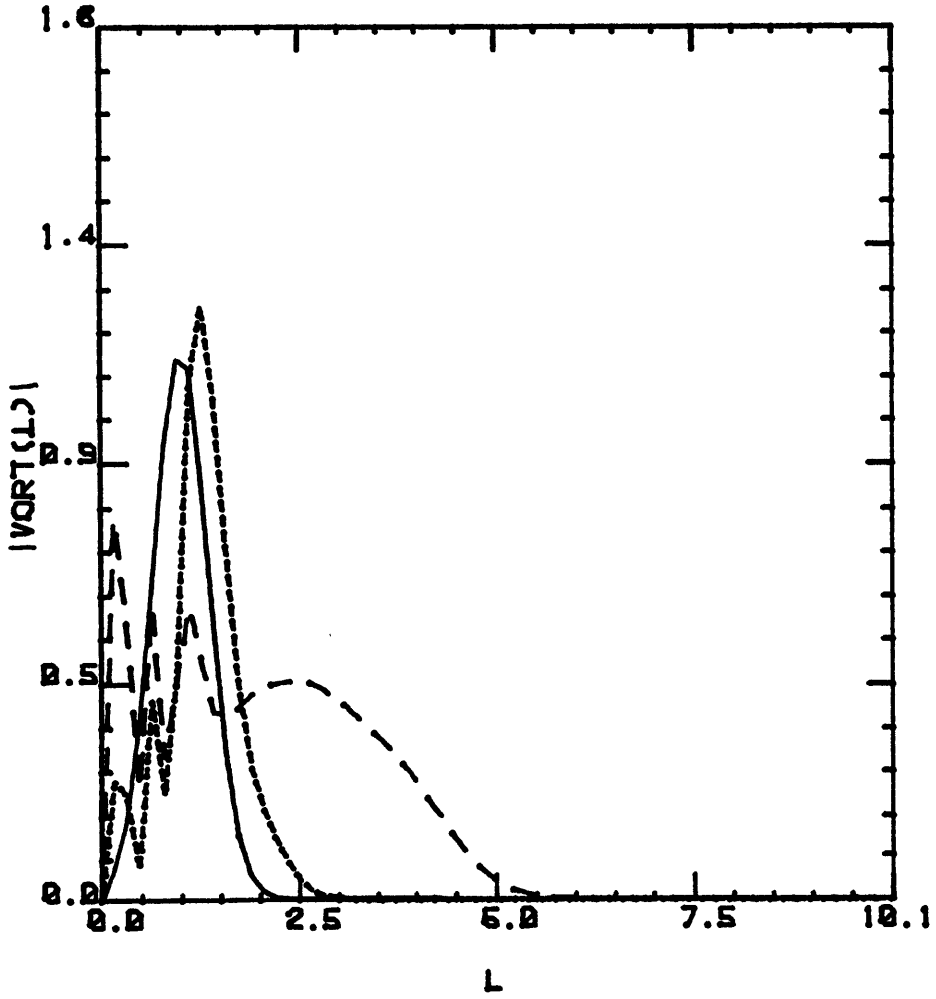

FIG. 4.1.35

$y_o = 8.0$
$H = 2.0$
$l_o = 1.0$
$\gamma = 0.0$
$k = 1.0$
$B = 20.0$
$y_c \cong -2.0$
$y_T \cong 18.0$

—— T = 0.0
----- T = 2.0
– – – T = 4.0

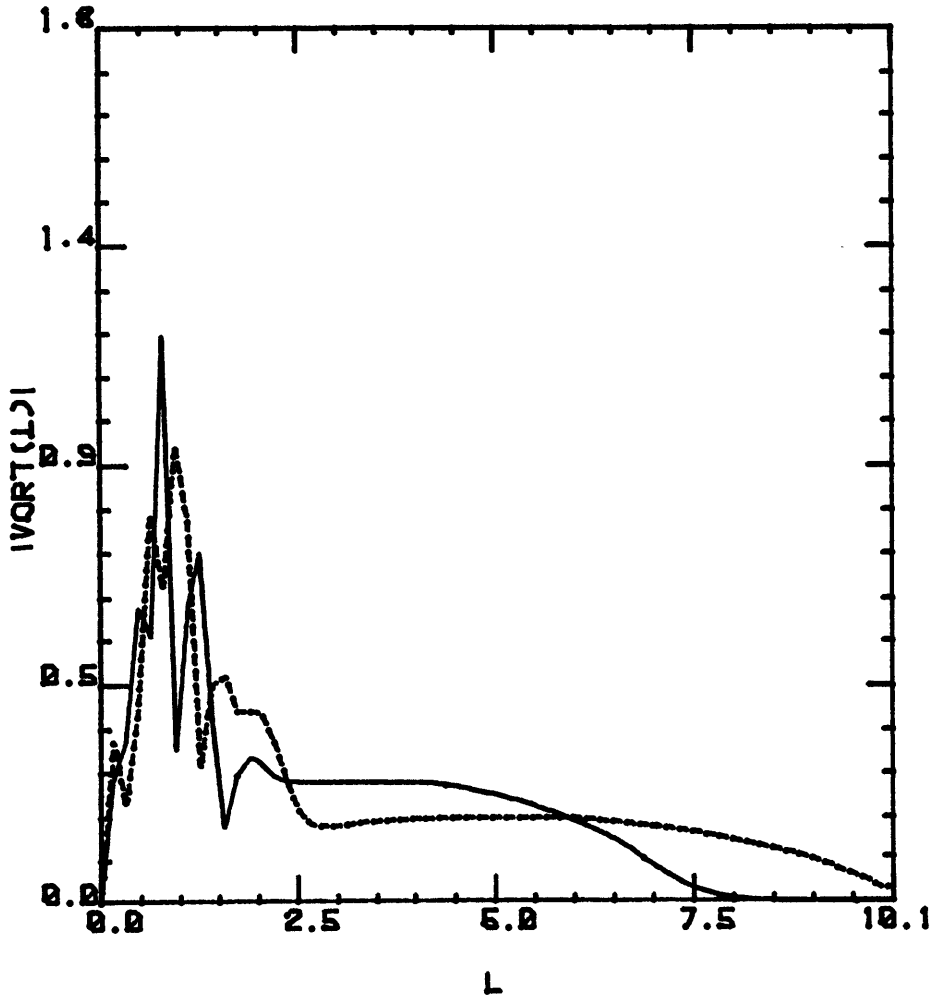

FIG. 4.1.36

$y_o = 8.0$
$H = 2.0$
$l_o = 1.0$
$\gamma = 0.0$
$k = 1.0$
$B = 20.0$
$y_c \cong -2.0$
$y_T \cong 18.0$

—— T = 6.0
---- T = 8.0

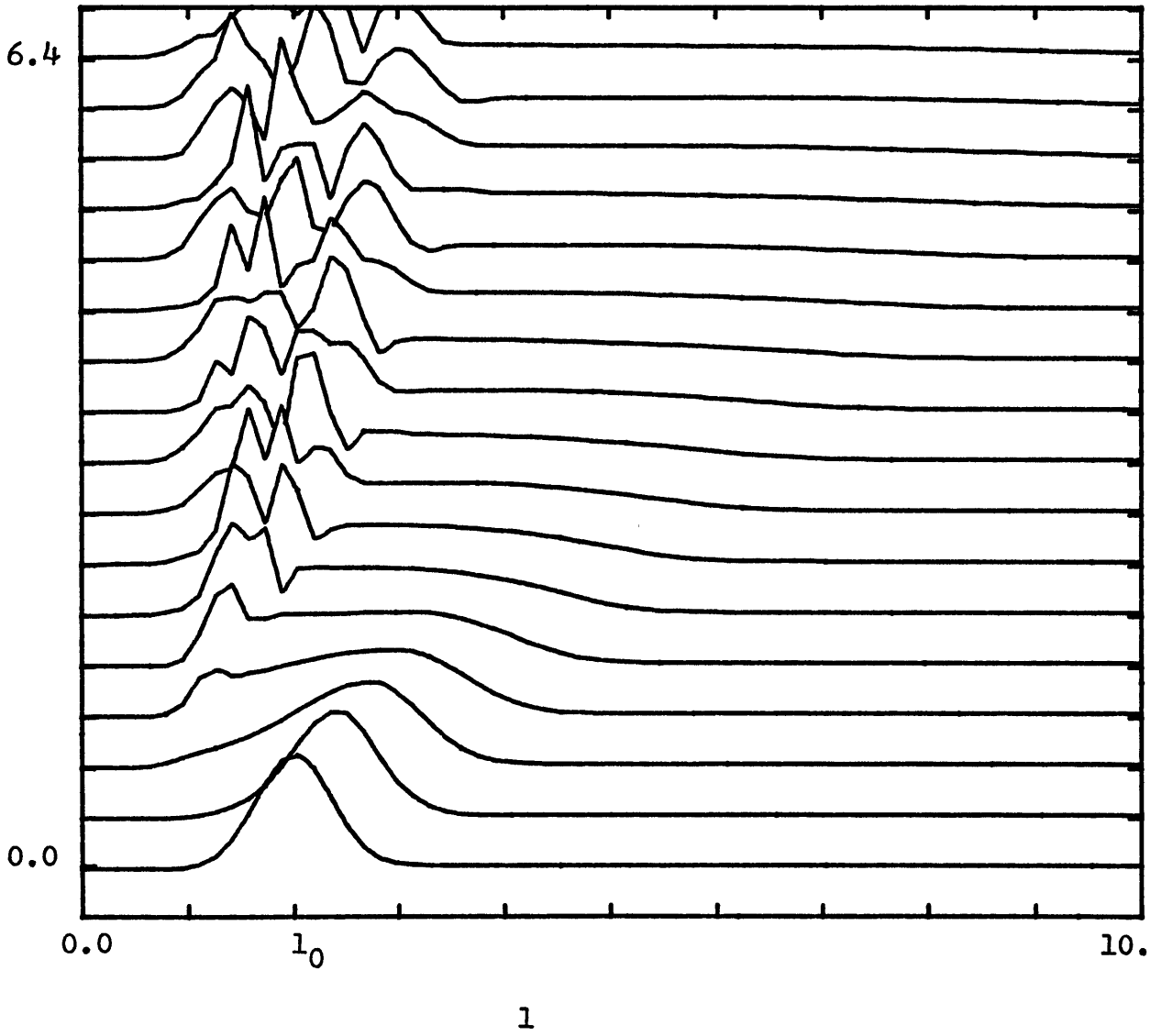

FIG. 4.1.37

$y_0 = 8.0$
$H = 2.0$
$l_0 = 2.0$
$\gamma = 0.0$
$k = -1.0$
$B = 75.0$
$y_c \cong -7.0$
$y_T \cong 68.0$

|VORT(l,t)|

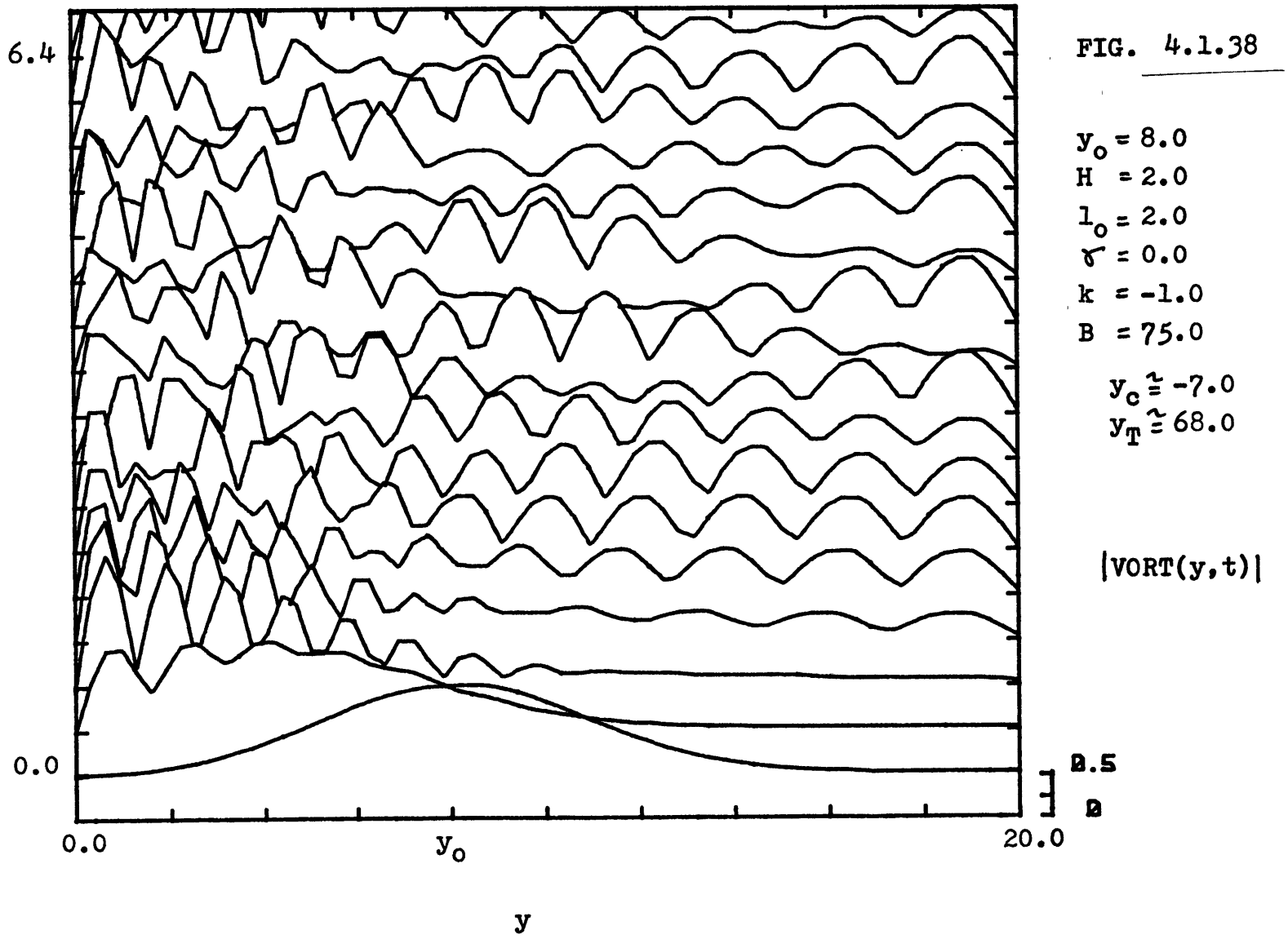

FIG. 4.1.38

$y_o = 8.0$
$H = 2.0$
$l_o = 2.0$
$\gamma = 0.0$
$k = -1.0$
$B = 75.0$

$y_c \cong -7.0$
$y_T \cong 68.0$

|VORT(y,t)|

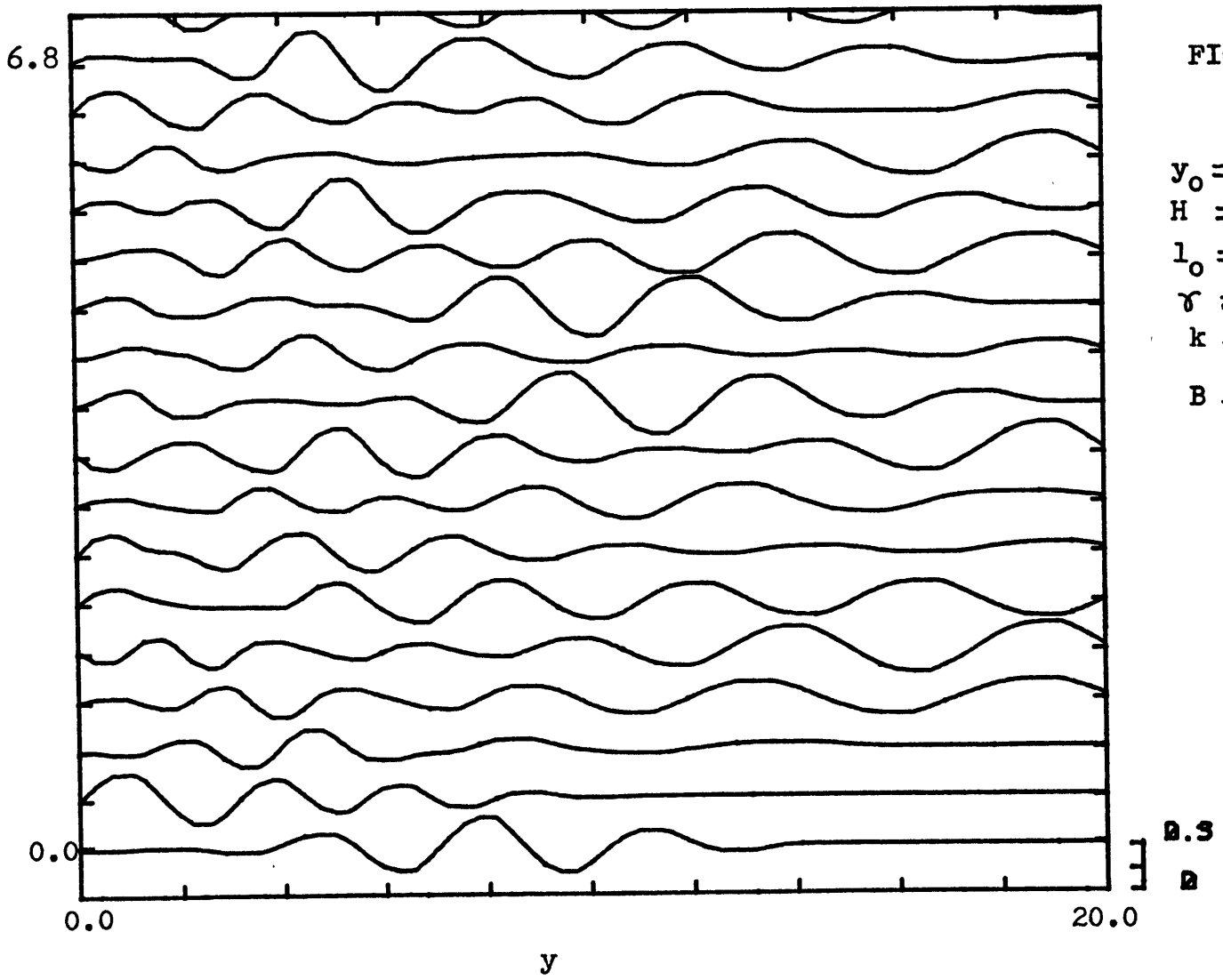

FIG. 4.1.39

$y_o = 8.0$
$H = 2.0$
$l_o = 2.0$
$\gamma = 0.0$
$k = -1.0$
$B = 75.0$
$y_c \cong -7.0$
$y_T \cong 68.0$

Re (sf(y,t))

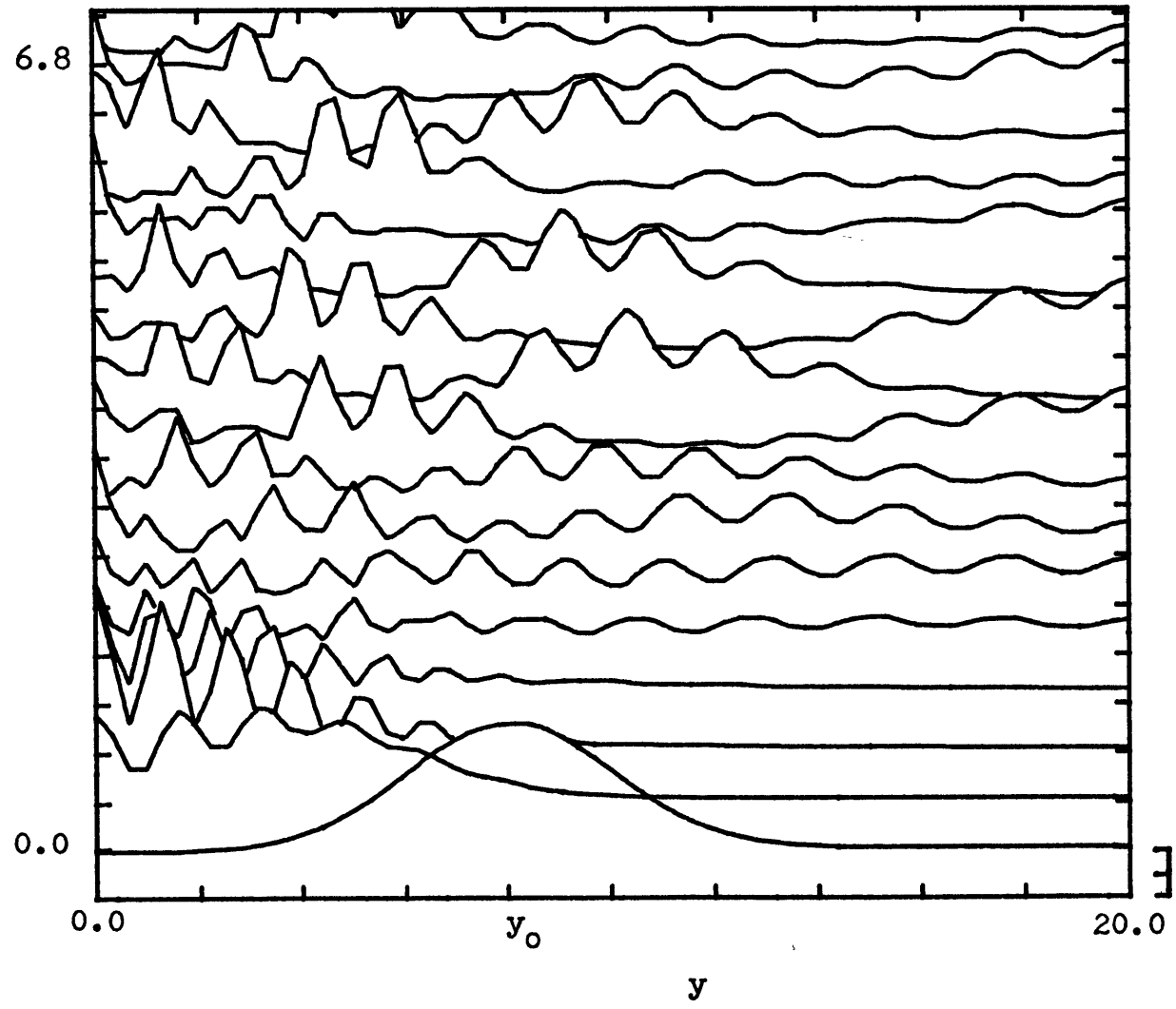

FIG. 4.1.40

$y_o = 8.0$
$H = 2.0$
$l_o = 2.0$
$\gamma = 0.0$
$k = -1.0$
$B = 75.0$
$y_c \cong -7.0$
$y_T \cong 68.0$

E(y,t)

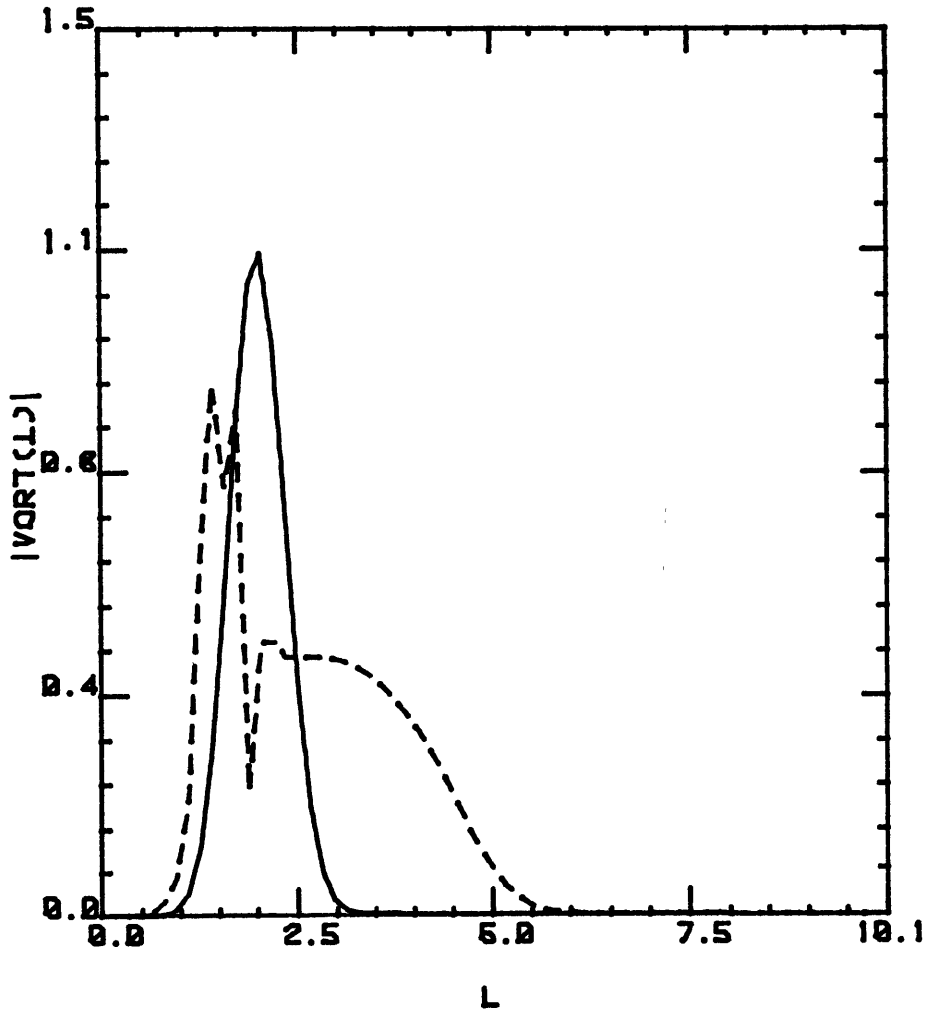

FIG. 4.1.41

$y_o = 8.0$
$H = 2.0$
$l_o = 2.0$
$\gamma = 0.0$
$k = -1.0$
$B = 75.0$
$y_c \cong -7.0$
$y_T \cong 68.0$

——— T = 0.0
----- T = 2.0

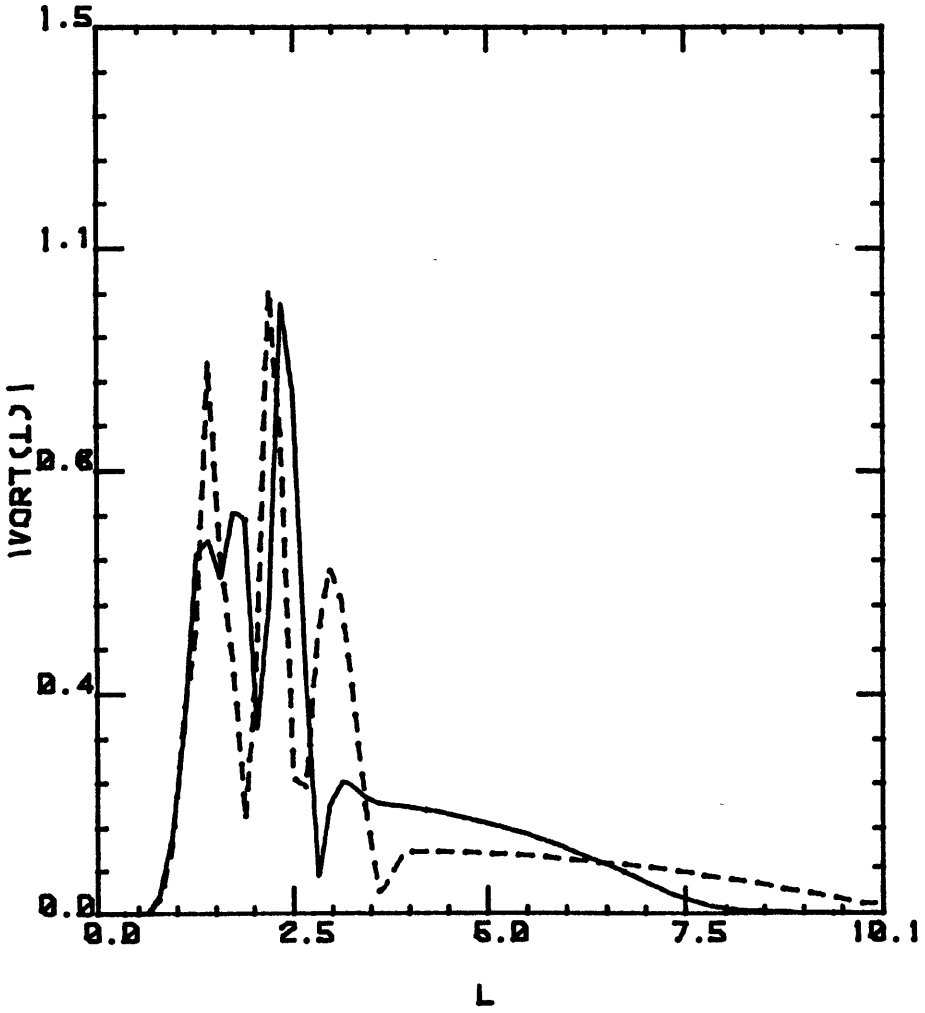

FIG. 4.1.42

y_o = 8.0
H = 2.0
l_o = 2.0
γ = 0.0
k = -1.0
B = 75.0
$y_c \cong$ -7.0
$y_T \cong$ 68.0

—— T 4.0
---- T 6.0

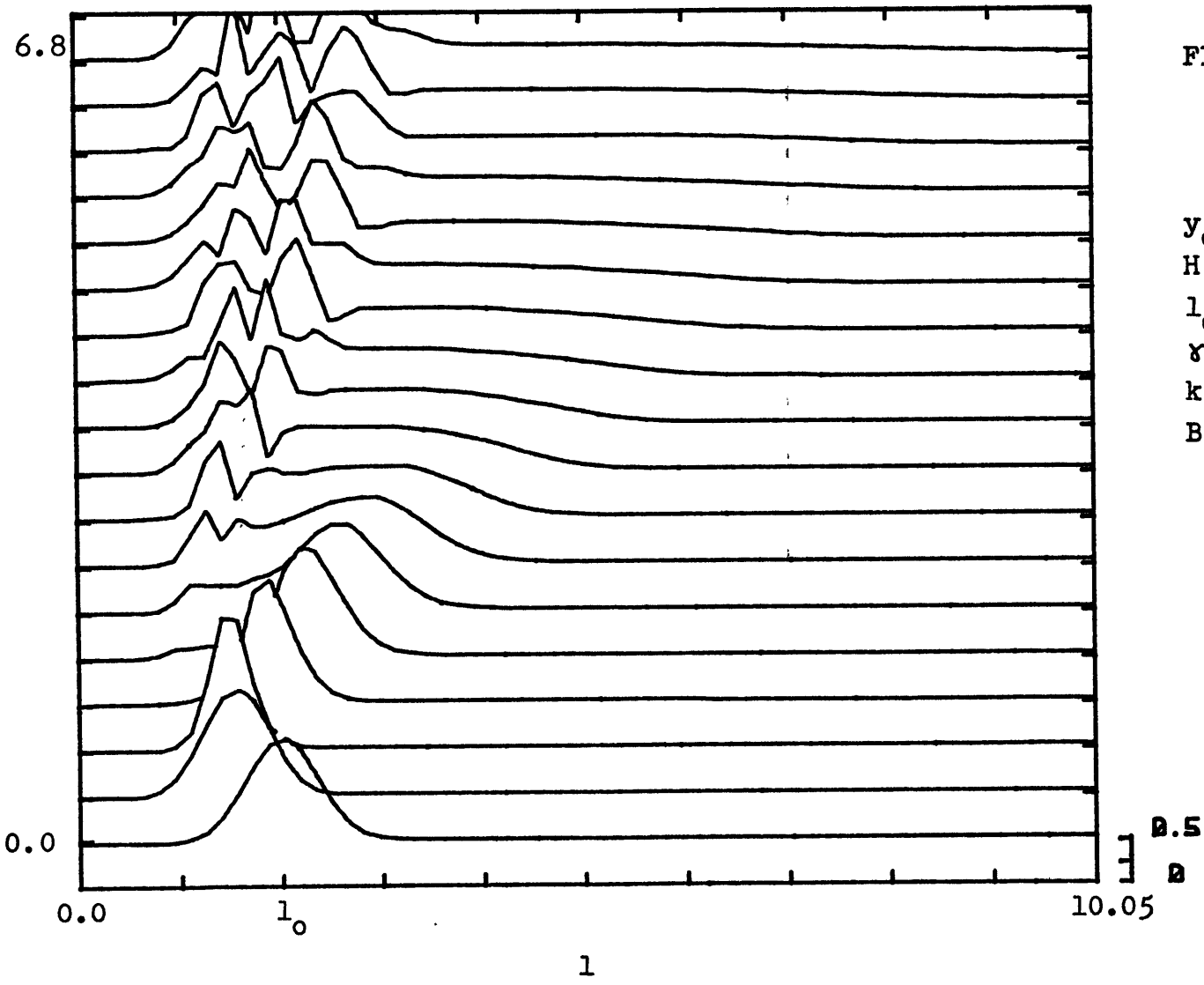

FIG. 4.1.43

$y_o = 8.0$
$H = 2.0$
$l_o = 2.0$
$\gamma = 0.0$
$k = 1.0$
$B = 75.0$

$y_c \cong -7.0$
$y_T \cong 68.0$

|VORT(l,t)|

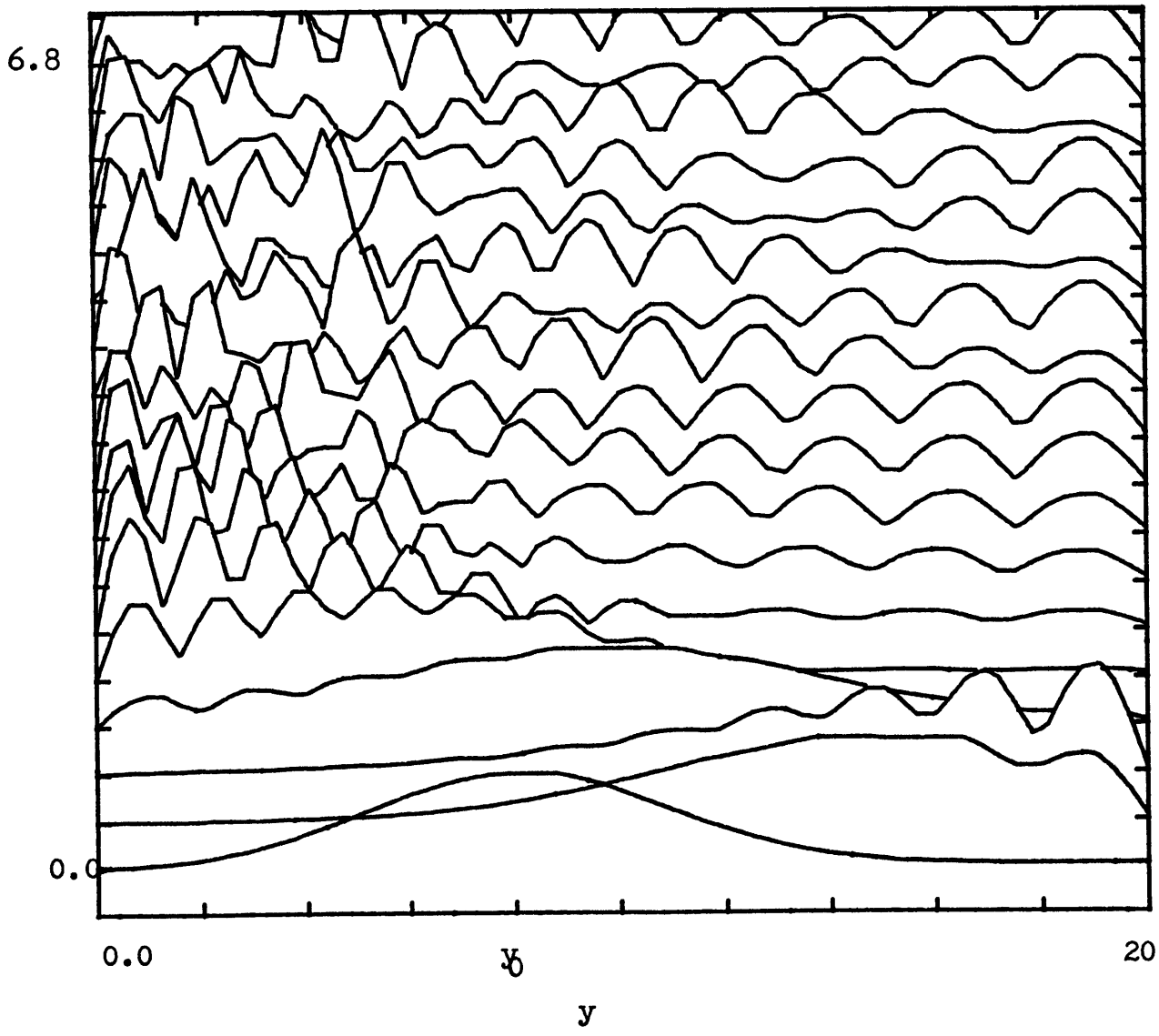

FIG. 4.1.44

$y_o = 8.0$
$H = 2.0$
$l_o = 2.0$
$\gamma = 0.0$
$B = 75.0$

$y_c \cong -7.0$
$y_T \cong 68.0$

$|VORT(y,t)|$

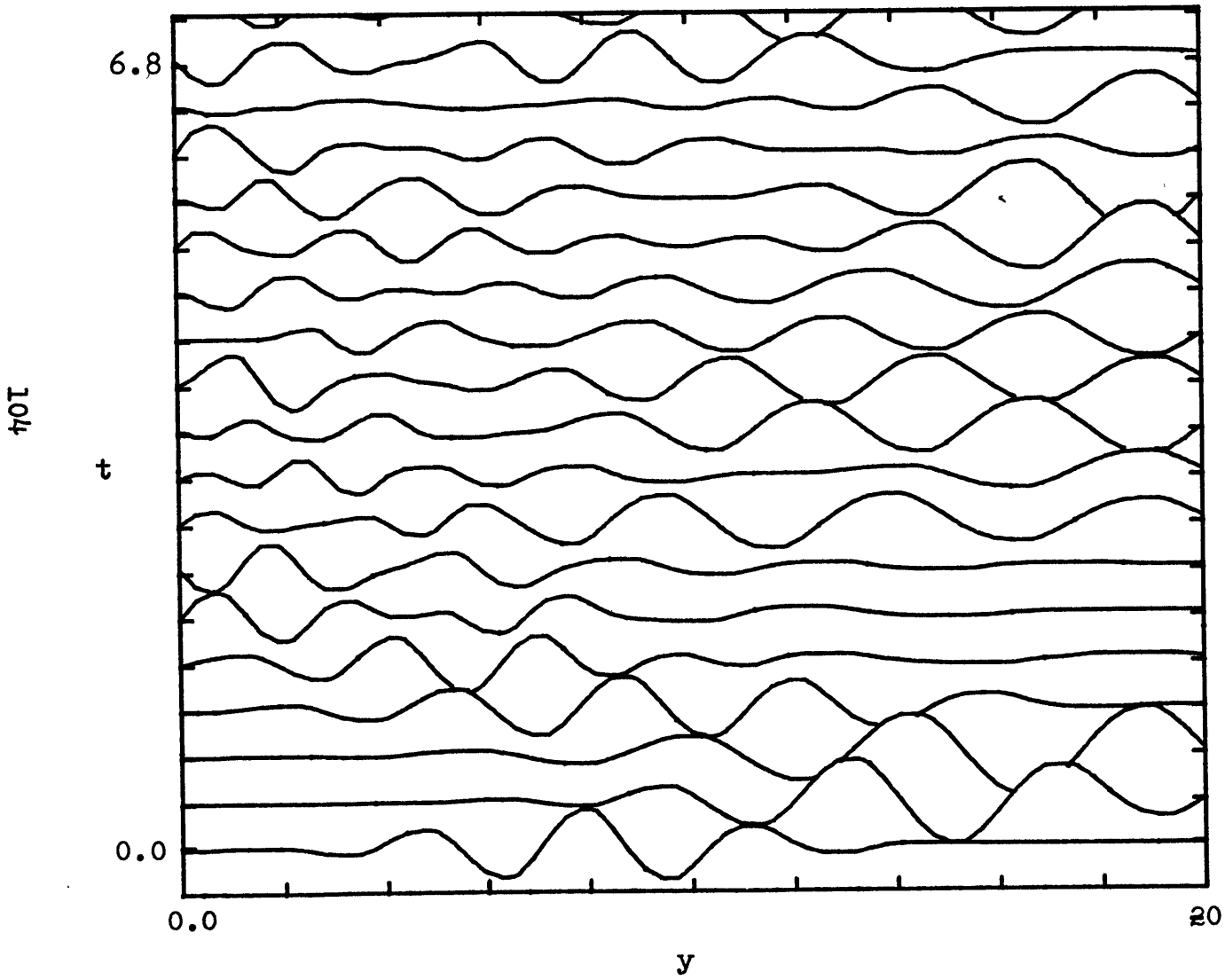

FIG. 4.1.45

$y_o = 8.0$
$H = 2.0$
$l_o = 2.0$
$\gamma = 0.0$
$k = 1.0$
$B = 75.0$

$y_c \cong -7.0$
$y_T \cong 68.0$

Re (sf(y,t))

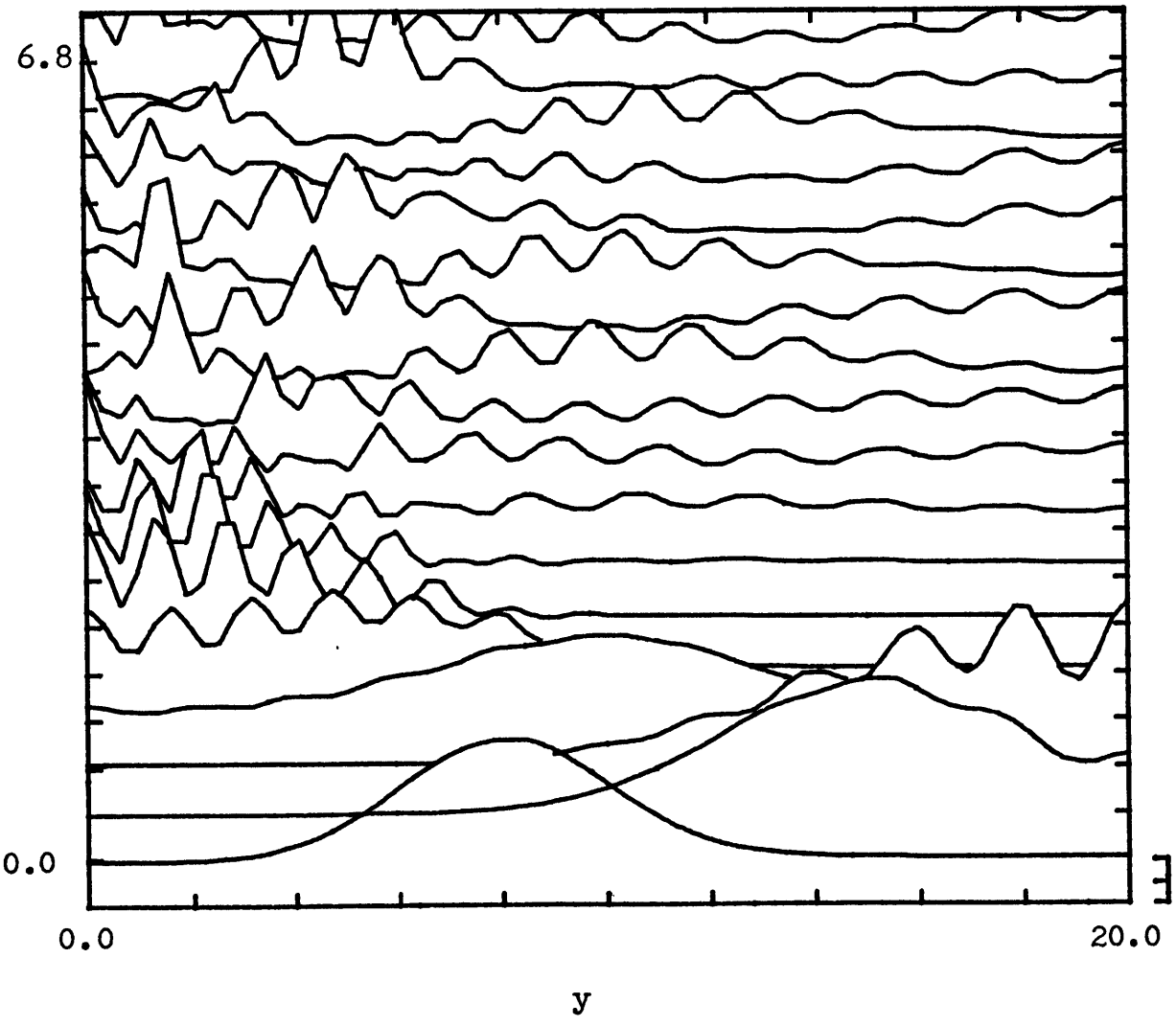

FIG. 4.1.46

$y_o = 8.0$
$H = 2.0$
$l_o = 2.0$
$\gamma = 0.0$
$k = 1.0$
$B = 75.0$

$y_c \cong -7.0$
$y_T \cong 68.0$

E (y,t)

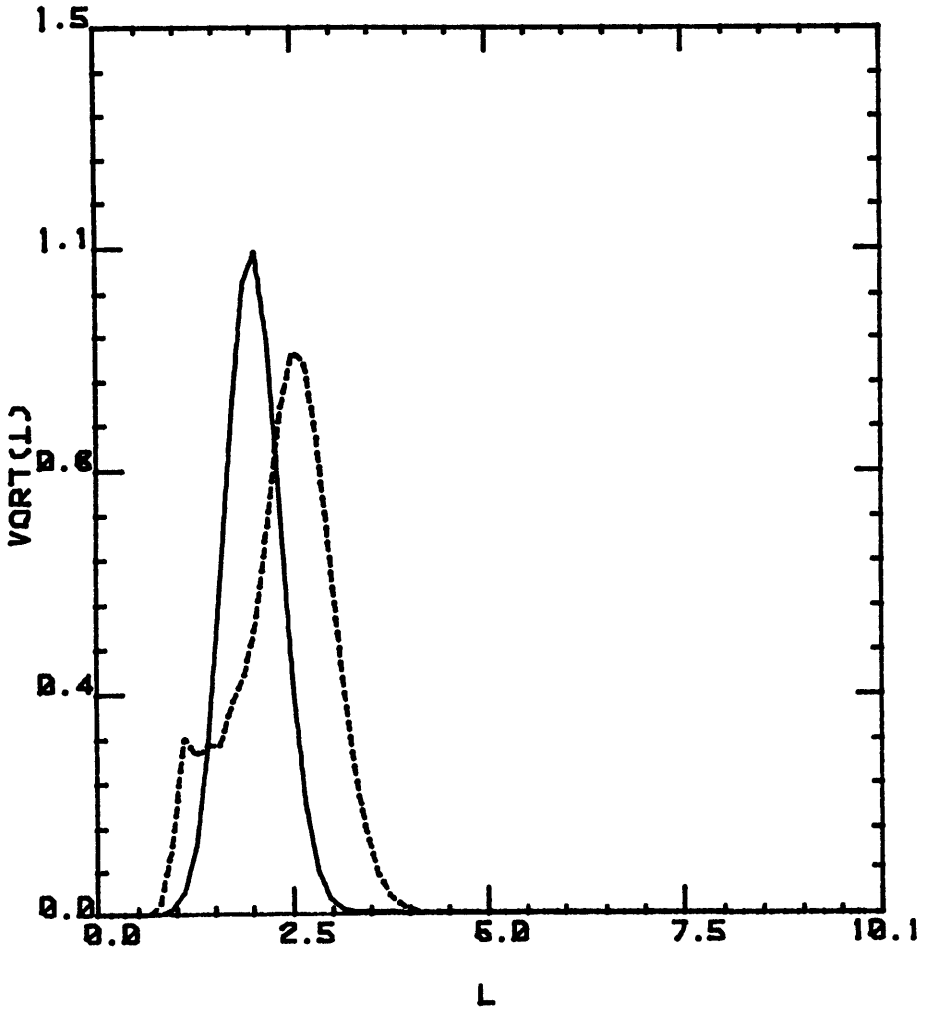

FIG. 4.1.47

$y_o = 8.0$
$H = 2.0$
$l_o = 2.0$
$\gamma = 0.0$
$k = 1.0$
$B = 75.0$
$y_c \cong -7.0$
$y_T \cong 68.0$

——— T = 0.0
----- T = 2.0

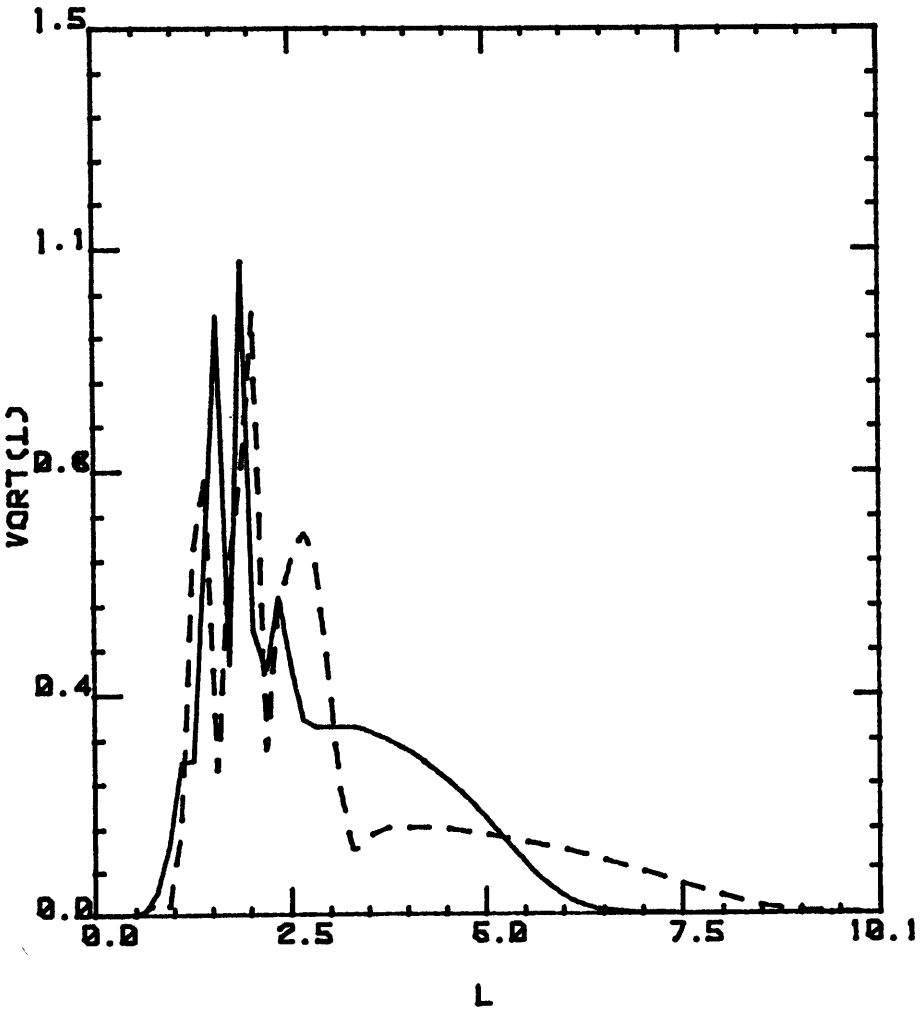

FIG. 4.1.48

$y_o = 8.0$
$H = 2.0$
$l_o = 2.0$
$\gamma = 0.0$
$k = 1.0$
$B = 75.0$
$y_c \cong -7.0$
$y_T \cong 68.0$

——— T=4.0
---- T=6.0

4.2 Constant shear case with an inflection point in a finite domain

4.2.1. Introduction

To be able to predict the development of a wave-packet in a constant shear flow with an inflection point, one can again apply the wave-packet theory developed by Tung (1983) described earlier. Because of the presence of the inflection point the predicted value of y_c will now be:

$$y_c = y_o - \gamma(y_o - y_B)/(k^2+l_o^2) \qquad (4.2.1)$$

whereas before, without an inflection point, it was:

$$y_c = y_o - \beta/(k^2+l_o^2)$$

where y_c is the point where $U(y) = c$.

The initial meridional group velocity becomes:

$$C_{gy} = 2\gamma(y_o - y_B)kl_o/(k^2+l_o^2)^2$$

whereas before, without an inflection point it was:

$$C_{gy} = 2\beta kl_o/(k^2+l_o^2)^2.$$

Note that in the case with an inflection point, the sign of the group velocity also depends on the relative position of y_o and y_B.

If the solution of the initial value problem evolves into a normal mode solution, then the solution is the same as that of the eigenvalue problem described earlier, i.e. governed by the equation

$$\frac{d^2\psi}{dy^2} + Q(y)\ \psi = 0$$

with $\psi = 0$ at $y = 0, 2D$ and where

$$Q(y) = \frac{y(y - y_B)}{(y - y_c)} - k^2.$$

By predicting the value of y_c and then using it in Q(y), one can apply the overreflection theory developed by Lindzen and Tung (1978). Their results make clear the reason why existing stability theorems (i.e. the Rayleigh-Kuo and the Fjortoft theorems) give only necessary conditions for instability insofar as they usually guarantee only overreflection, but not quantization of waves. Overreflection occurs when the magnitude of the coefficient of reflection is larger than 1. Barotropic instability occurs provided overreflection exists and the waves are quantized. Quantization is the condition under which successive overreflections must occur in phase for instability to take the form of a normal mode. The conditions for overreflection as found by Lindzen and Tung (1978) can be applied as a condition on having the right configuration of points y_c, y_B, y_T, the presence of the walls and also the direction in which a wave is sent initially. y_B is the inflection point and

$$y_{Tu} = (yy_B - k^2y_c)/(y-k^2)$$

is the point where $Q(y) = 0$. y_{Tu} reduces to y_B if $k^2=0$. y_{Tu} is also called a "turning point" and should not be confused with y_T.

All the possible arrangements of points (y_C, y_B, y_{Tu}) are shown on figure 4.2.1 A, B, C and D. Only two of these figures can satisfy the conditions for overreflection and these are figures 4.2.1 A, B for which $A^2 > 0$ where

$$A^2 \equiv \lim_{y->\infty} Q(y) = \gamma - k^2.$$

To be able to guarantee overreflection the condition is that a wave has to come in from the right onto y_{Tu} as in figure 4.2.1 A or from the left onto y_{Tu} as in figure 4.2.1 B. In both cases the critical level will be able to overreflect an incoming wave.

Also in our problem, there is the presence of a wall to the right of y_{Tu} and to the left of y_C in figure 4.2.1 A and to the left of y_{Tu} and the right of y_C in figure 4.2.1 B.

Thus, the presence of walls (at the positions specified) as well as the arrangement of points corresponding to figures 4.2.1 A, B and sending waves in the appropriate direction as described above will guarantee overreflection, which is a necessary condition for barotropic instability. On figures 4.2.1 A-D, E and W regions indicate evanescent (i.e. $Q(y) < 0$) and wavy ($Q(y) > 0$) regions respectively.

Another numerical tool which is used in this problem is that it is possible to solve the eigenvalue problem corresponding to the initial value problem. The program to solve for

the eigenvalues has only a small accuracy and therefore was used mainly as a guide. Also, the quality of the results depends on the particular case studied, thus on the values of the parameters.

4.2.2 Stable initial condition

Consider a case which is potentially unstable (i.e. a case where the eigenvalue problem showed that the solution was unstable for a particular set of parameters; also an initial value problem has been shown to become unstable (which will be discussed later) for the same parameter set. The arrangement of points corresponds to figure 4.2.1 B. The wave-packet is moving from the left onto y_c. Figures 4.2.2 - 6 illustrate this case. With this arrangement no overreflection is supposed to take place. The wave should be absorbed at the critical level.

Figures 4.2.5 shows that the energy of the wave is decaying (also see table 10). Figure 4.2.3 shows the slow development in time of a stationary structure in the y direction. It also shows that $y_c \approx 3.65$, i.e. the same as predicted by equation (4.2.1). Figure 4.2.2, which shows the time-evolution of the Fourier transform of the vorticity, has two distinct features.

I. There is a part of the Fourier spectrum associated with

the decay of the wave due to the absorption of the wave by the critical level. This is similar to the transient wave of the Couette flow case in a finite domain.

II. The development of a distinct peak for $l \approx 3.4$. Since this peak after a while does not grow with time, and since it is stationary in y, it must be representing a neutral mode. Between those two structures, the part of the Fourier spectrum associated with the decay of the wave dominates by far.

Neutral waves which have a phase speed inside the range of the velocity profile (i.e. in this case $0<c_r<2D$) have their critical level equal to y_B so that Q(y) reduces to

$$\gamma - k^2.$$

The equation predicting the value of y_c can also predict the value of l for which $y_c=y_B$. This l will be called l_φ, i.e.

$$y_B = y_c = y_o - \frac{\gamma(y_o - y_B)}{k^2 + l_\varphi^2}$$

from which: $l_\varphi^2 = \gamma - k^2$.

If one thinks of a wave-packet as a superposition of delta functions then equation (4.2.1) predicts a different y_c for each l. This would then also mean that all the l's which are smaller than l_φ would see an arrangement as in figure 4.2.1 A instead of the arrangement of figure 4.2.1 B.

In the example given above, $l_\varphi = l_o - 2.4\sigma_s$ where $\sigma_s = 1/2H$ is the standard deviation of the initial Gaussian spectrum. This means that only ≈ 1% of the Fourier spectrum sees arrangement B. That is why the wave is absorbed at the critical level. For this case then also, there is practically no projection of the initial condition onto the normal modes. There seems to be enough projection to enable the development of a neutral mode. Note that it takes a relatively long time before the normal mode develops.

Another case similar to the above is illustrated in figures 4.2.7-11 (also see table 11). The wave-packet again approaches y_c through a wavy region and is absorbed there, $y_c \approx 10.7$ as predicted. Note that in this case, there is no development of a neutral mode. The l_φ predicted in this case is equal to 0.71 and $l_\varphi = l_o - 5.16\sigma_s$. In the case where l_φ is $5.16\sigma_s$ away from l_o one can conclude that there is no projection of the initial Fourier condition onto normal modes.

For this last case, the author has not been able to show numerically (i.e. by solving for the eigenvalues) that the problem was potentially unstable (i.e. $c_r > 0$). c_i did not converge. The main reason is that the size of the domain is large and the numerical scheme only has an accuracy of order $(\Delta y)^2$. Since k is smaller than the cut-off k_{MAX}, but not too small, chances are that the profile is unstable. The

growth rate will be small since γ is small.

4.2.3 Unstable initial condition

Figures 4.2.12-17 and table 12 illustrate a case where

$$y_o < y_c < y_B < y_{Tu}.$$

These points have an arrangement as in figure 4.2.1 A. y_o is to the left of y_c and the initial group velocity of the wave-packet is positive so that it moves towards y_c.

A question readily asked is: why is not the wave stagnating at y_c? In the case of an unstable wave, one can show at least numerically that c_r is close to y_B if $y_B \neq D$. Therefore, as for the stable case, $y_B \approx y_c$ for $l = l_\varphi$. If one studies the Fourier spectrum of the initial condition one can show that $l_\varphi = l_o - 0.3\sigma$. Therefore, a large part of the spectrum will see arrangement B instead of A and overreflection is possible as well as the development of an unstable normal mode.

One can also note that there is a considerable projection of the initial condition onto normal modes. The growth of the normal mode is quite fast. Note that y_c and y_{Tu} are close so that the process of overreflection is efficient. In

this example $(l_o/k) < 0$ and the Fourier spectrum has a part which is associated with the decay of the wave. This part will never see the walls. A distinct structure is present around y_c in the physical domain and tends to disappear with time.

As the initial wave moves north, the energy decays and after a few timesteps starts growing. After a while, the growth rate becomes exponential.

As time evolves from t=0, one can observe the development of a distinct structure in Fourier space which becomes stationary. This shows the presence of unstable normal modes which are stationary waves in physical space. This part of the spectrum is due to the presence of the walls. With time, the stationary part of the Fourier spectrum becomes much larger than the part which causes decay. The growth rate found by solving the eigenvalue problem is the same as the one computed using the time-evolution of the energy ($c_i \approx 0.12$).

Figures 4.2.18-32 and table 13 illustrate a case where all the values of the parameters are the same as for the last case considered except for the group velocity which has a different sign. Now, the initial packet will see the wall before it sees y_c. This effect can be seen in the development of the Fourier spectrum. When the initial condition sees the walls first, the development of a stationary structure occurs sooner than in the case above and therefore also exponential growth occurs sooner. The effect of the wall is to convert more and

more of the spectrum into waves with an arrangement so that overreflection can take place. For this example $(l_o/k) > 0$ and the Fourier spectrum does not have a part which is associated with the decay of the wave. There is no distinct structure around y_c in physical space as for the last case studied. The phase speed of the normal mode was shown to be the same as the one determined from the eigenvalue problem. The phase speed can be measured by following the maximum of Re Vort(x, y, t). This can be seen in figures 4.2.23-4.2.32. c_r was found to be = 2.95. Note that one has to wait a while before c_r becomes constant.

As expected, no matter what the sign of the initial group velocity is, the final normal mode solution has the same structure.

Figures 4.4.33-4.4.51 (also see tables 14a and 14b) show an example in which the arrangement of points is as in figure 4.2.1.A. For this example, the wave-packet for small times moves towards y_{Tu}. Here $l_\varphi = l_o + 1.1\sigma_s$ and so this is an excellent candidate for overreflection. On the vorticity diagram, at the second timestep, one can observe that part of the wave is reflected but also part of it is transmitted. Since $(l_o/k) < 0$, one again has the presence of a transient decaying wave but the exponential growth of the wave soon takes over.

For this example, the time for exponential growth to deve-

lop is longer than for the second unstable case considered. This is because the effect of the walls is not as strong and also because the distance between y_{Tu} and y_c is larger than in the second unstable case considered.

Here again, the phase speed could be deduced from the 3 dimensional figures ($c_r \approx 3.5$).

Figures 4.2.52-57 and table 15 illustrate a case which has the same parameter set as the second case described in section 4.2.2. Only the sign of the group velocity is different. In this case, there is a development of a normal mode, even if the projection of the initial spectrum is small (this was discussed in the earlier case). The fact that a normal mode does develop can be explained as follows.

Here $(1_o/k) > 0$, so that the 1's first decay. The effect of the walls then generates a stationary part in the Fourier spectrum. It takes a long time before this stationary part develops. This is because most of the wavenumbers in the initial spectrum have an arrangement of points which do not allow overreflection. Again, the effect of the walls is to generate a spectrum which have waves with a proper arrangement of points for overreflection. If the walls were not present, only the transient waves would be present.

Figures 4.2.58-62 and table 16 illustrate a case for which there is a strong absorption of energy at the critical level, but the other remaining waves still manage to develop into

normal modes. For this case $l_\varphi = l_o - 1.4\sigma_s$.

A small part of the Fourier spectrum, i.e. 8% of the surface will see an arrangement where y_{Tu} comes first, therefore allowing overreflection to take place. The total energy first decays and it takes a long time before it starts to grow. The effect of y_c is considerable as can be seen in particular on figure 4.2.59 which shows the magnitude of the vorticity and roughly has the same shape as for the Couette flow without an inflection point. The development of the stationary part of the Fourier spectrum takes a while to develop.

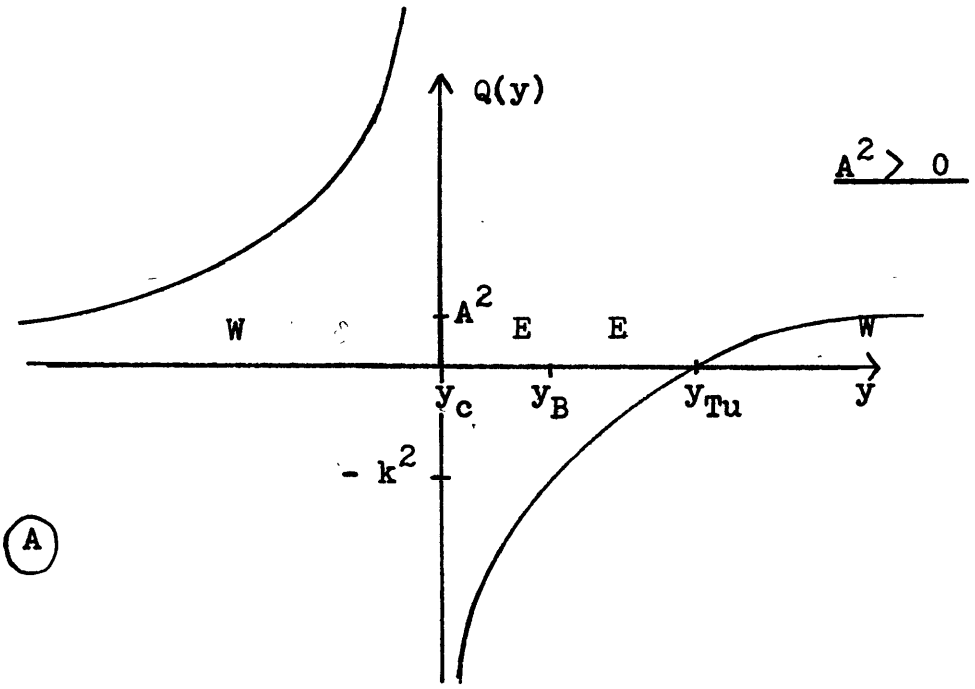

$$Q(y) = \frac{\gamma(y-y_B)}{(y-y_c)} \quad -k^2 \quad ; \quad \lim_{y \to \infty} Q(y) = A^2 = \gamma - k^2$$

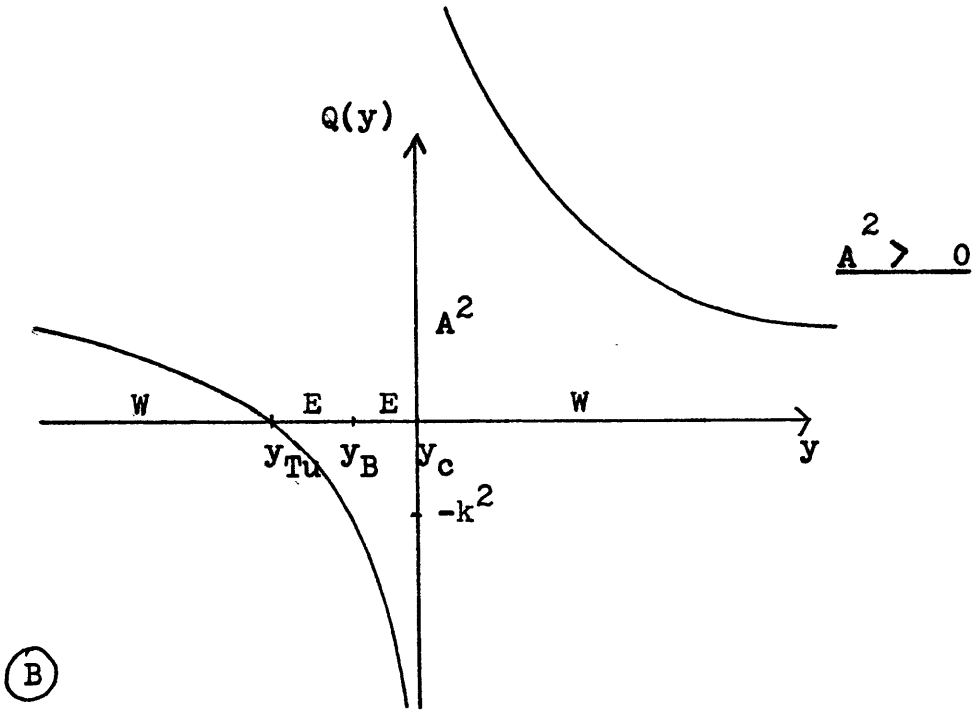

FIG. 4.2.1

$A^2 < 0$

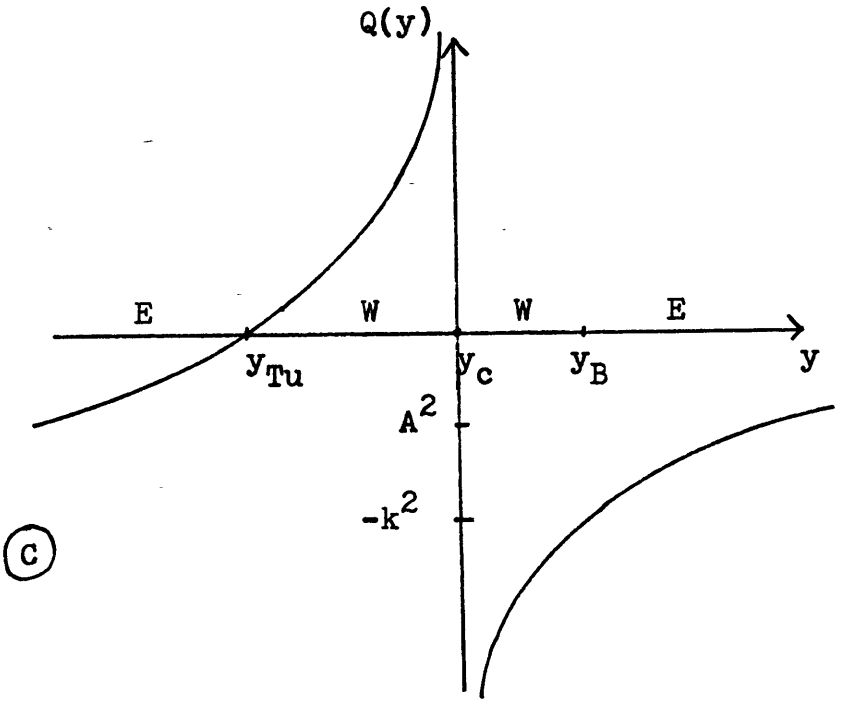

C

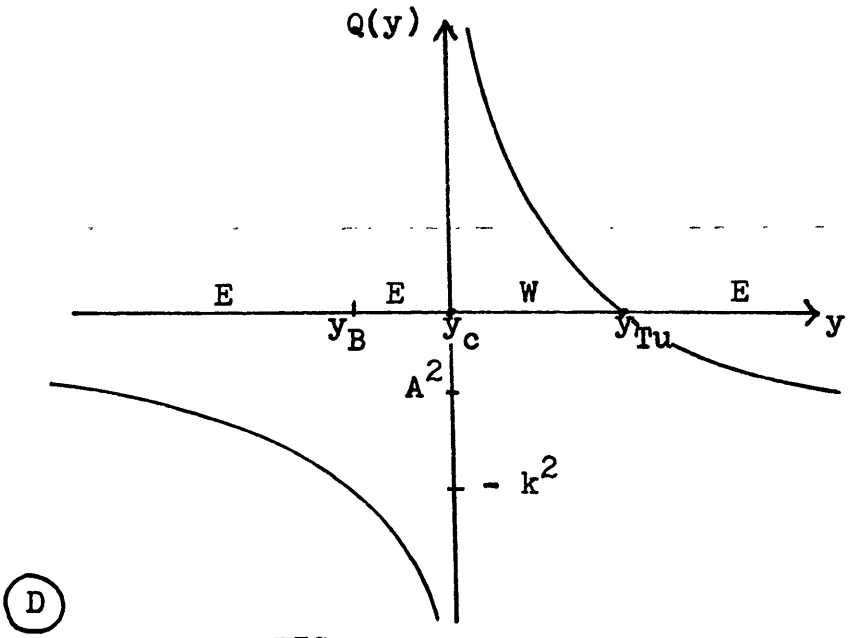

$A^2 < 0$

D

FIG. 4.2.1

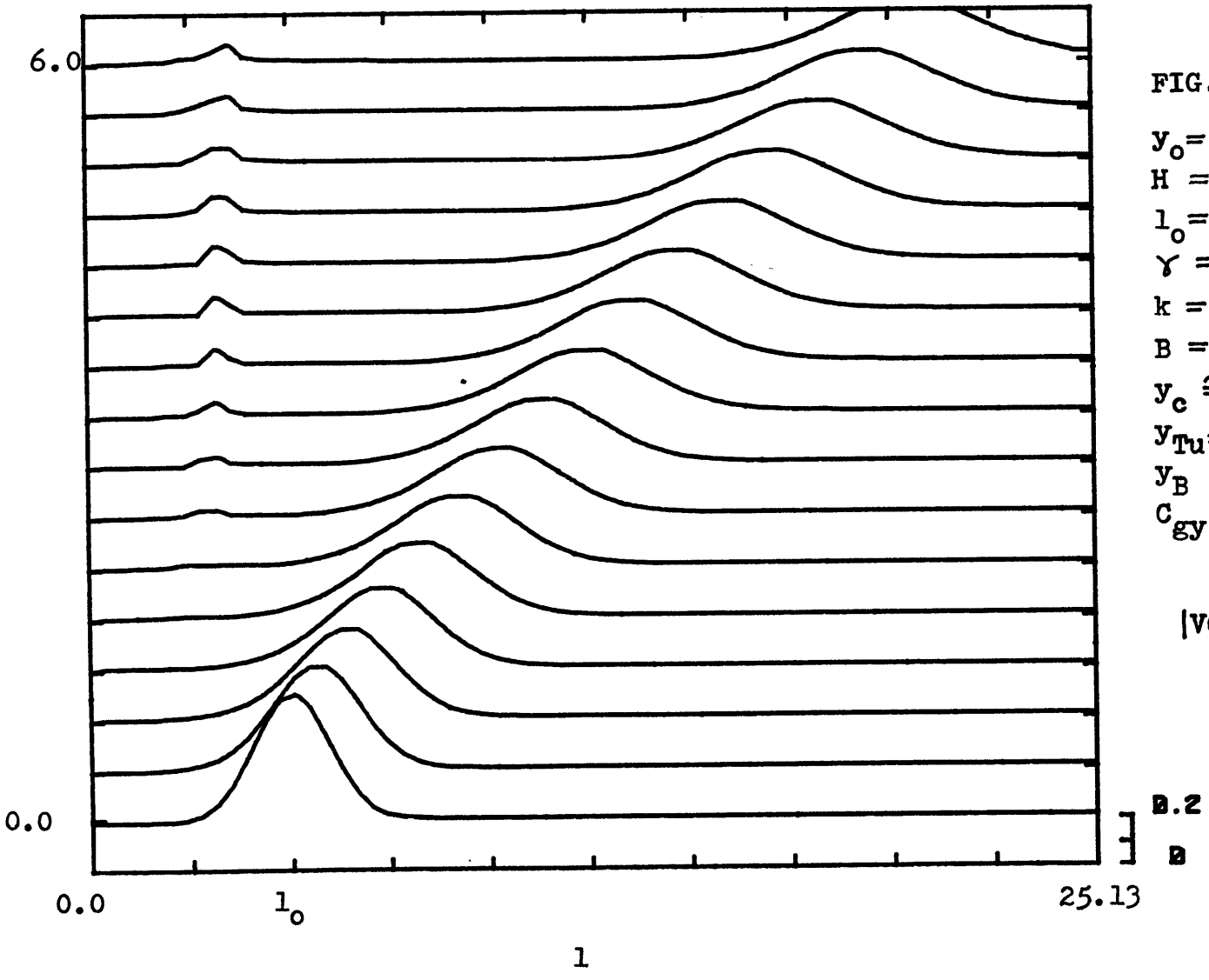

FIG. 4.2.2

$y_o = 3.85$
$H = 0.75$
$l_o = 5.0$
$\gamma = 17.8$
$k = -2.5$
$B = -62.3$
$y_c \cong 3.65$
$y_{Tu} \cong 3.41$
$y_B = 3.5$
$C_{gy} \cong -0.16$

$|VORT(l,t)|$

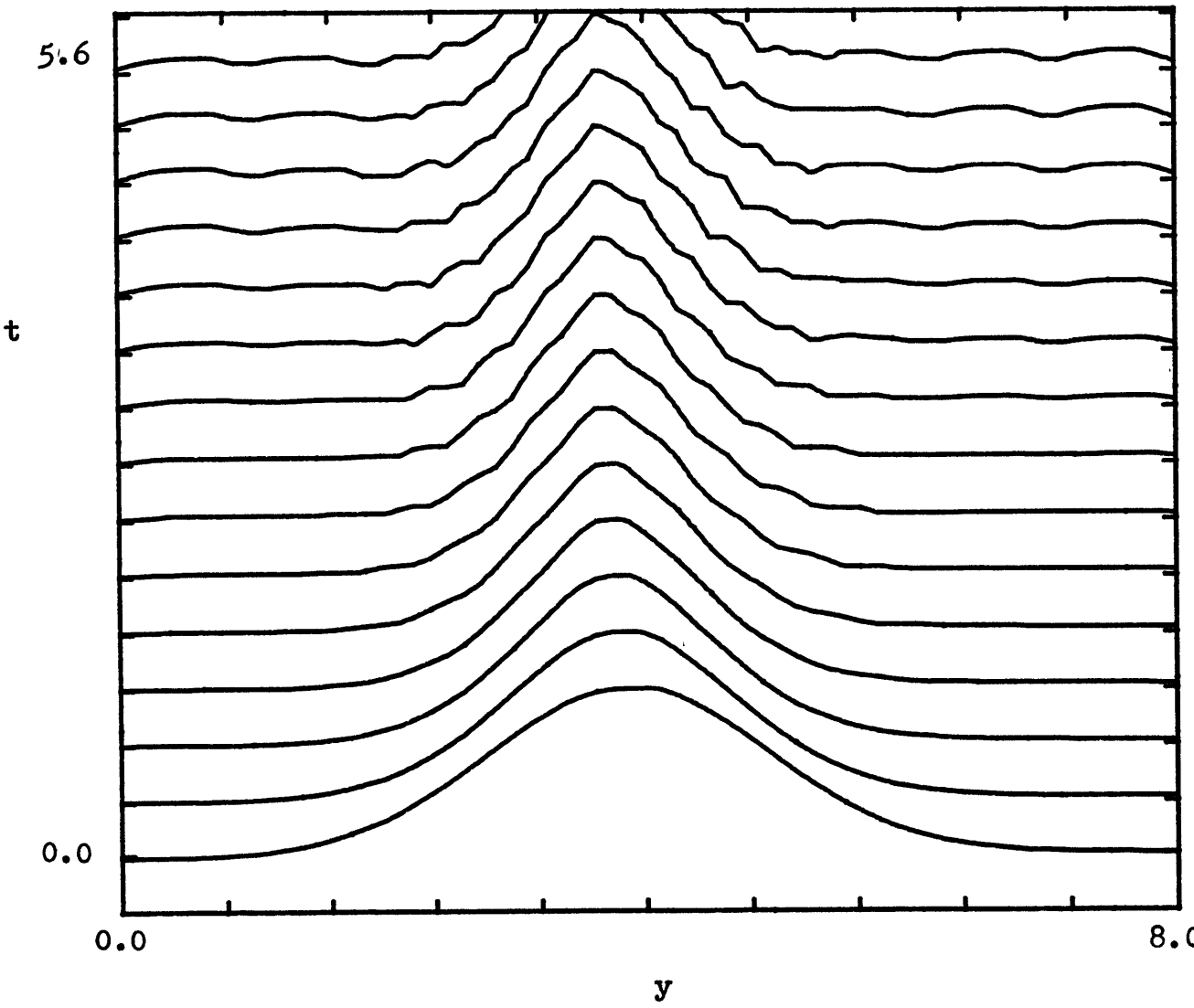

FIG. 4.2.3

$y_o = 3.85$
$H = 0.75$
$l_o = 5.0$
$\gamma = 17.8$
$k = -2.5$
$B = -62.3$
$y_c \cong 3.65$
$y_{Tu} \cong 3.41$
$y_B = 3.5$
$C_{gy} \cong 0.16$

|VORT(y,t)|

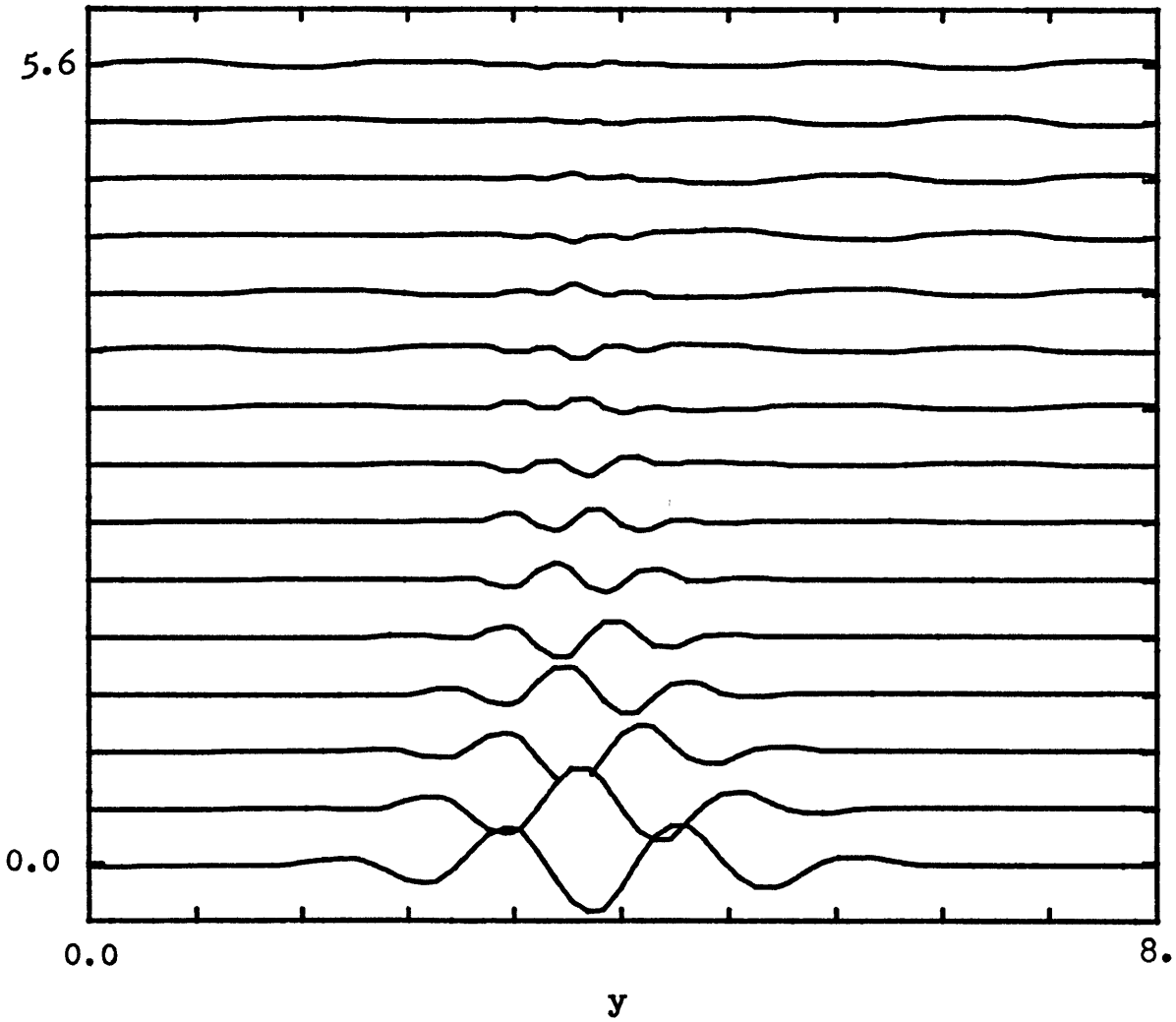

FIG. 4.2.4

$y_o = 3.85$
$H = 0.75$
$l_o = 5.00$
17.8
$k = -2.5$
$B = -62.3$
$y_c \cong 3.65$
$y_{Tu} \cong 3.41$
$y_B = 3.50$
$C_{gy} \cong -0.16$

Re (sf(y,t))

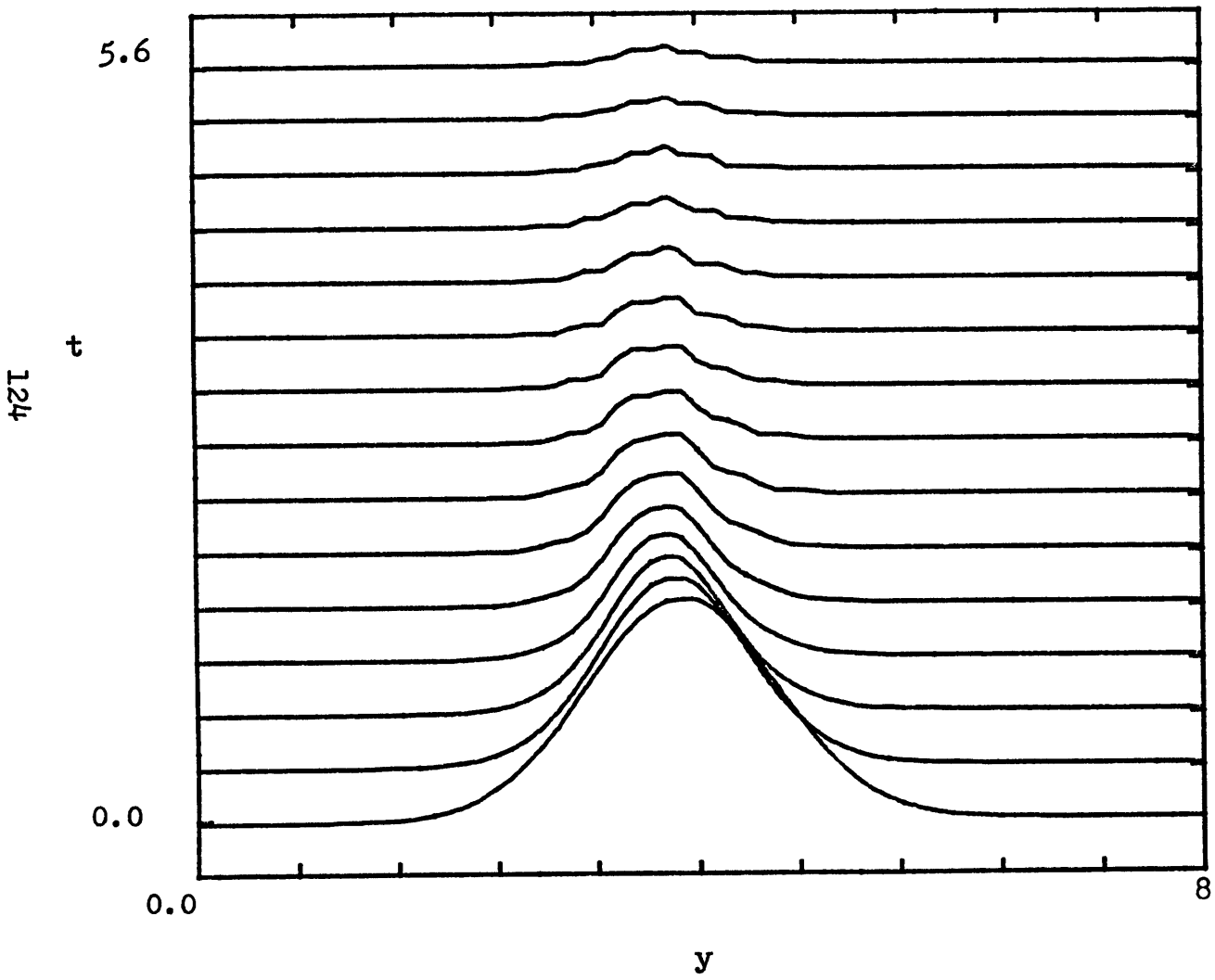

FIG. 4.2.5

$y_0 = 3.85$
$H = 0.75$
$l_o = 5.00$
$\gamma = 17.8$
$k = -2.5$
$B = -62.3$
$y_c \cong 3.65$
$y_{Tu} \cong 3.41$
$y_B = 3.5$
$C_{gy} \cong -0.16$

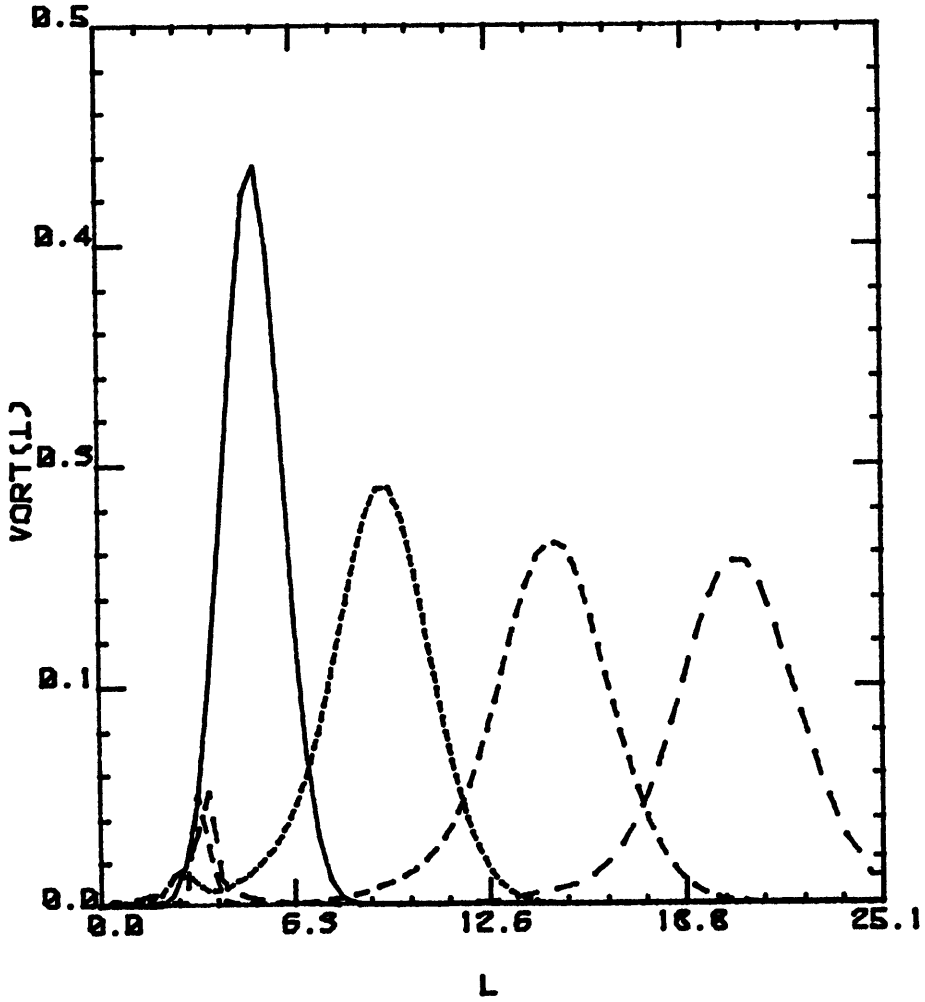

FIG. 4.2.6

$y_o = 3.85$
$H = 0.75$
$l_o = 5.00$
$\gamma = 17.8$
$k = -2.5$
$B = -62.3$
$y_c \cong 3.65$
$y_{Tu} \cong 3.41$
$y_B = 3.5$
$C_{gy} \cong 0.16$

—— T = 0.0
---- T = 2.0
--- T = 4.0
—— T = 6.0

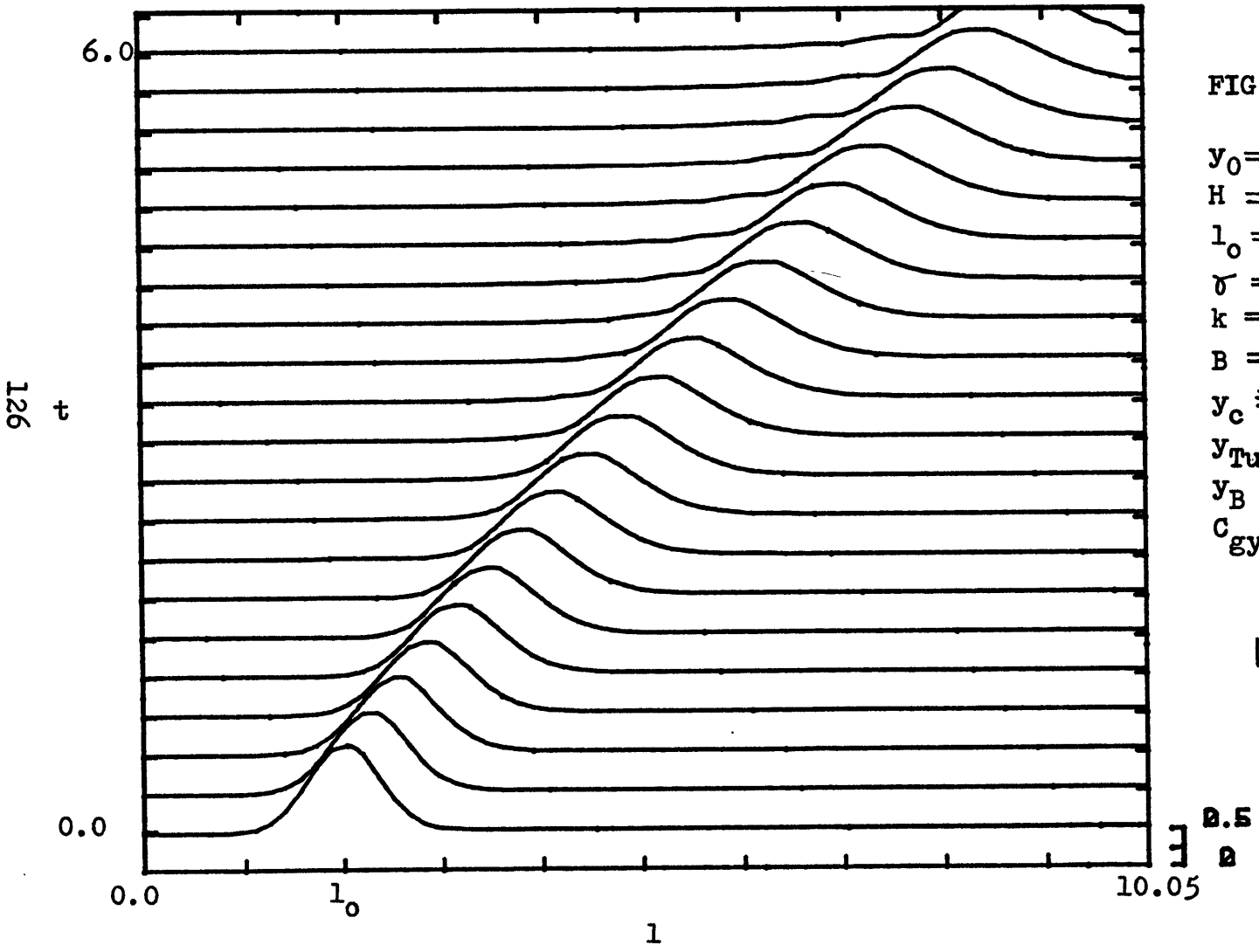

FIG. 4.2.7

$y_0 = 11.0$
$H = 2.0$
$l_o = 2.0$
$\sigma = 1.5$
$k = -1.0$
$B = -15.0$
$y_c \cong 10.7$
$y_{Tu} \cong 8.6$
$y_B = 10.0$
$C_{gy} \cong -0.24$

|VORT(l,t)|

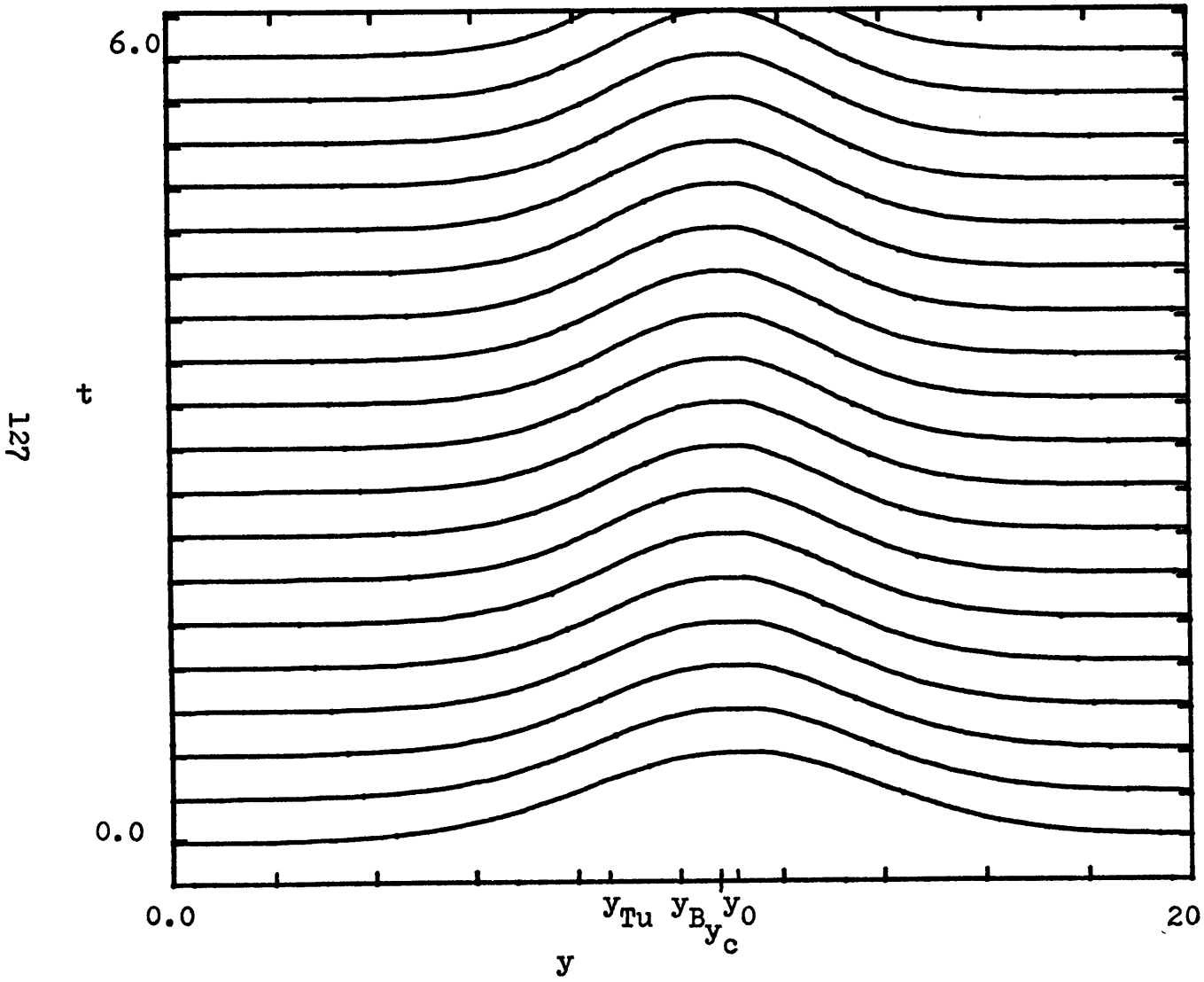

FIG. 4.2.8

$y_o = 11.0$
$H = 2.0$
$l_o = 2.0$
$\gamma = 1.5$
$k = -1.0$
$B = -15.0$
$y_c \cong 10.7$
$y_{Tu} \cong 8.6$
$y_B = 10.0$
$c_{gy} \cong -0.24$

|VORT(y,t)|

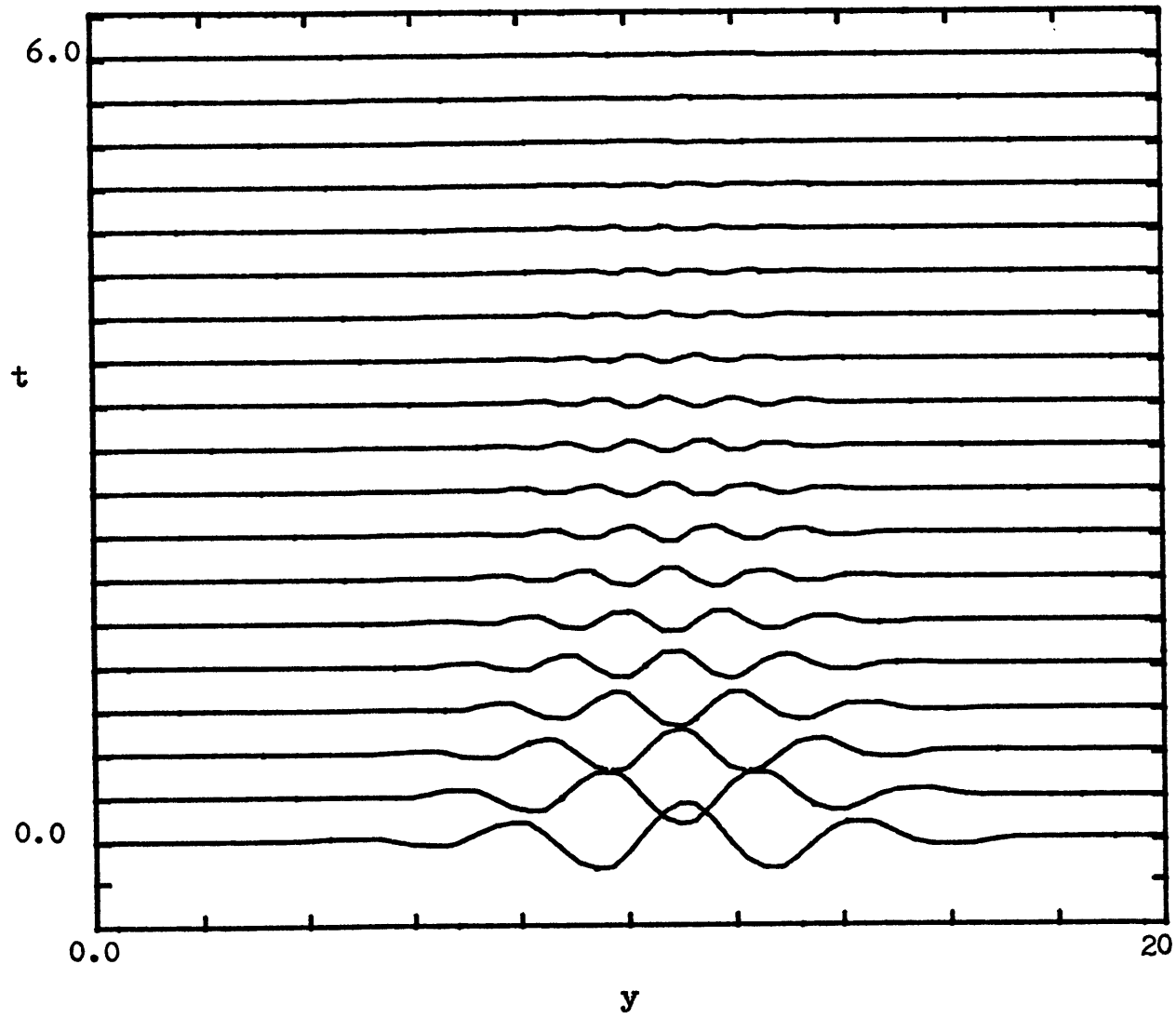

FIG. 4.2.9

$y_o = 11.0$
$H = 2.0$
$l_o = 2.0$
$\gamma = 1.5$
$k = -1.0$
$B = -15.0$
$y_c \cong 10.7$
$y_{Tu} \cong 8.6$
$y_B = 10.0$
$C_{gy} \cong -0.24$

Re (sf(y,t))

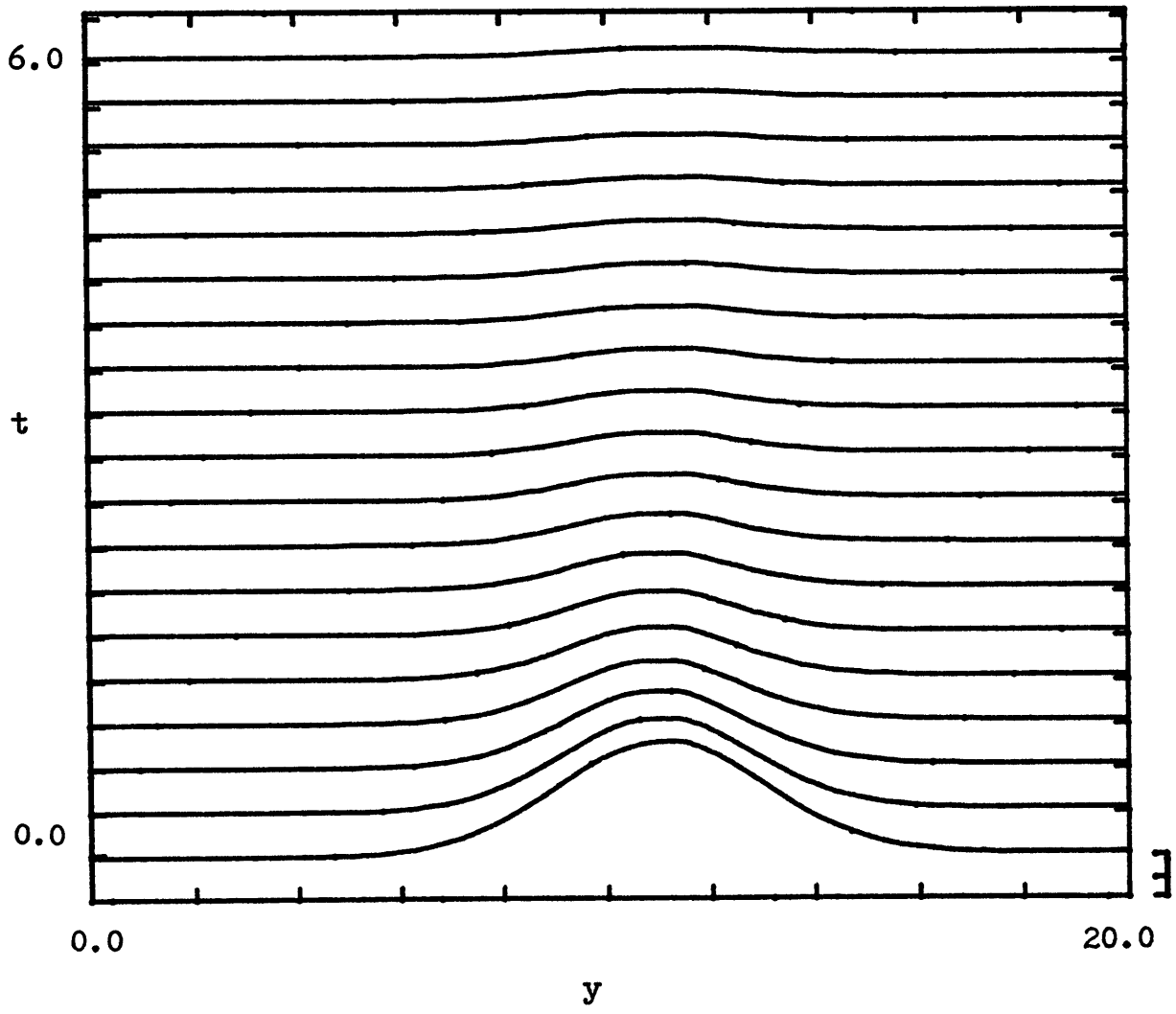

FIG. 4.2.10

$y_o = 11.0$
$H = 2.0$
$l_o = 2.0$
$\gamma^o = 1.5$
$k = -1.0$
$B = -15.0$
$y_c \cong 10.7$
$y_{Tu} \cong 8.6$
$y_B = 10.0$
$C_{gy} \cong -0.24$

E(y,t)

0.02
0

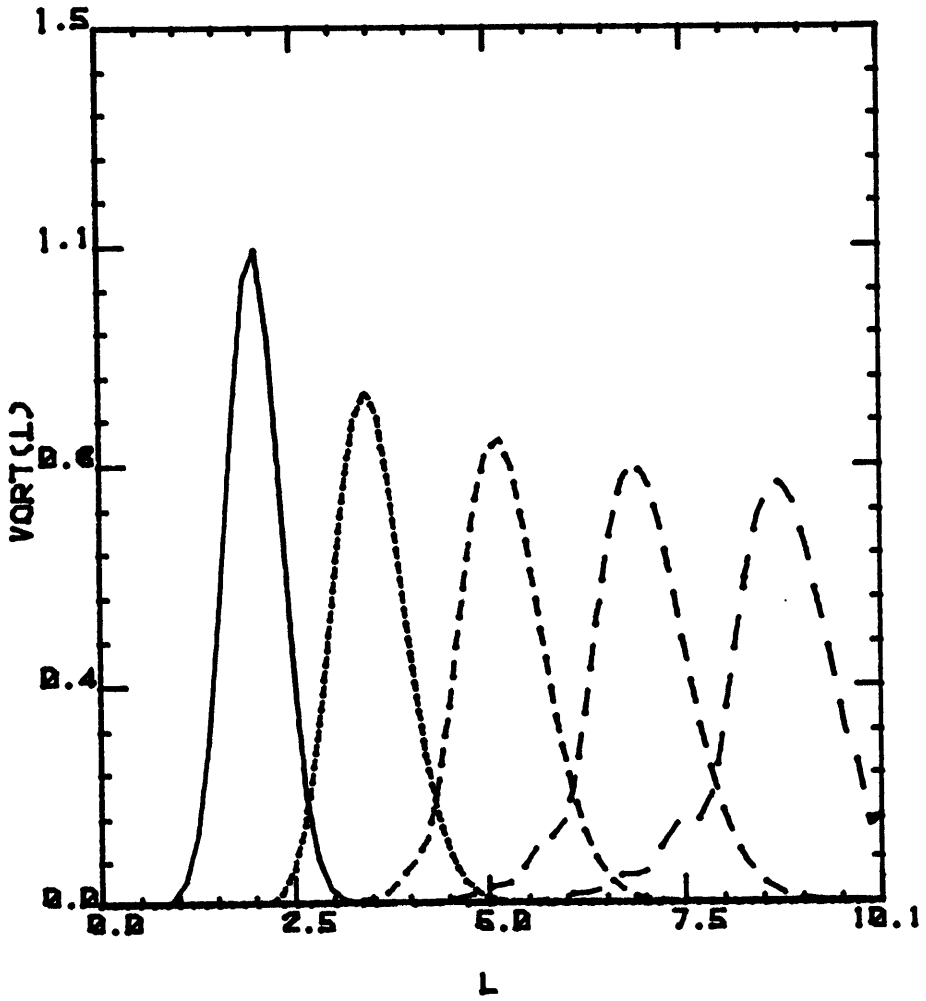

FIG. 4.2.11

$y_o = 11.0$
$H = 2.0$
$l_o = 2.0$
$\delta = 1.5$
$k = -1.0$
$B = -15.0$
$y_c \cong 10.7$
$y_{Tu} \cong 8.6$
$y_B = 10.0$
$C_{gy} \cong -0.24$

——— T = 0.0
----- T = 1.5
--- T = 3.0
— — — T = 4.5
—— T = 6.0

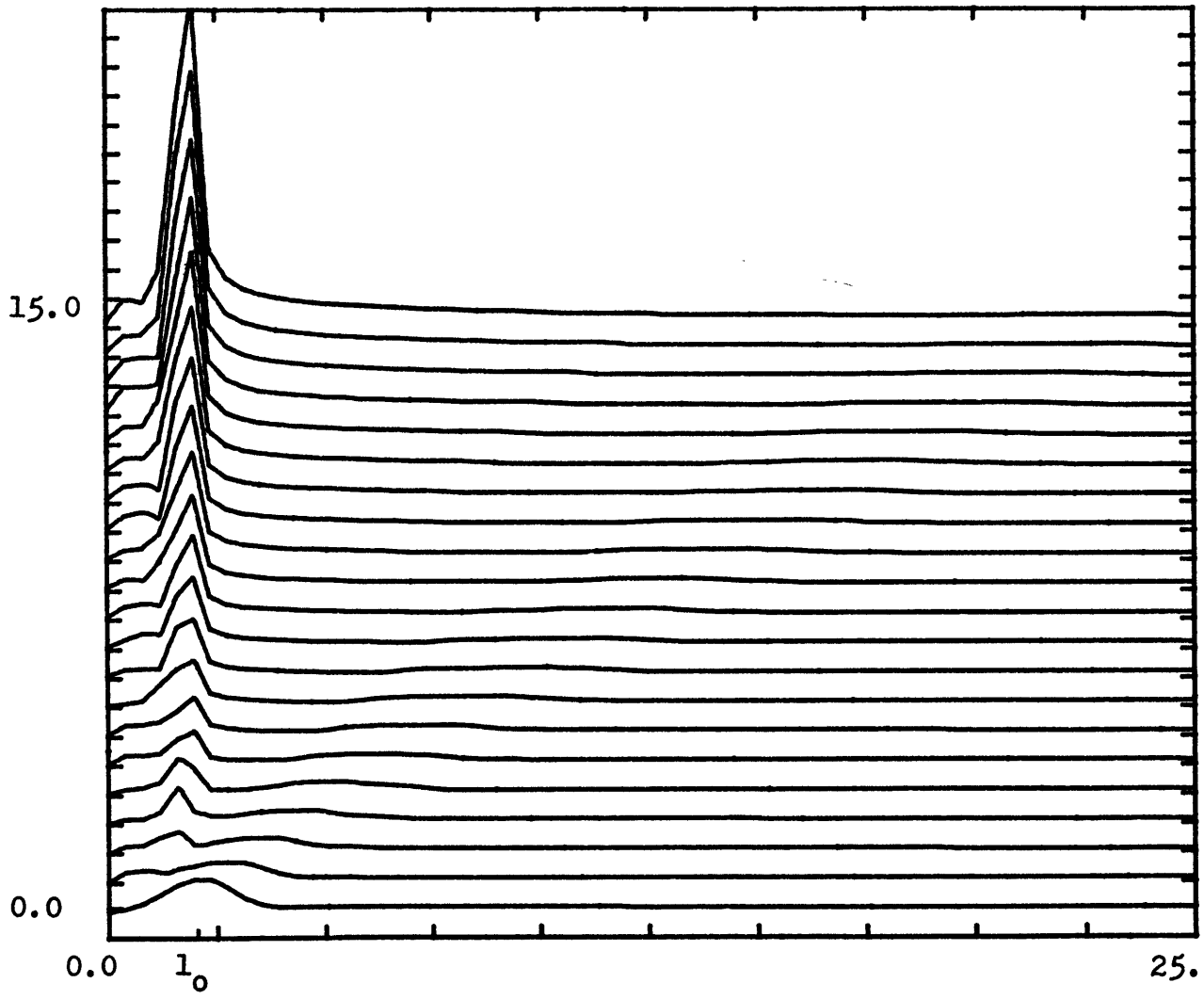

FIG. 4.2.12

$y_o = 2.5$
$H = 1.0$
$l_o = 2.0$
$\gamma = 5.0$
$k = -1.25$
$B = -15.0$
$y_c \cong 2.95$
$y_{Tu} \cong 3.02$
$y_B = 3.0$
$C_{gy} \cong 0.4$

|VORT(l,t)|

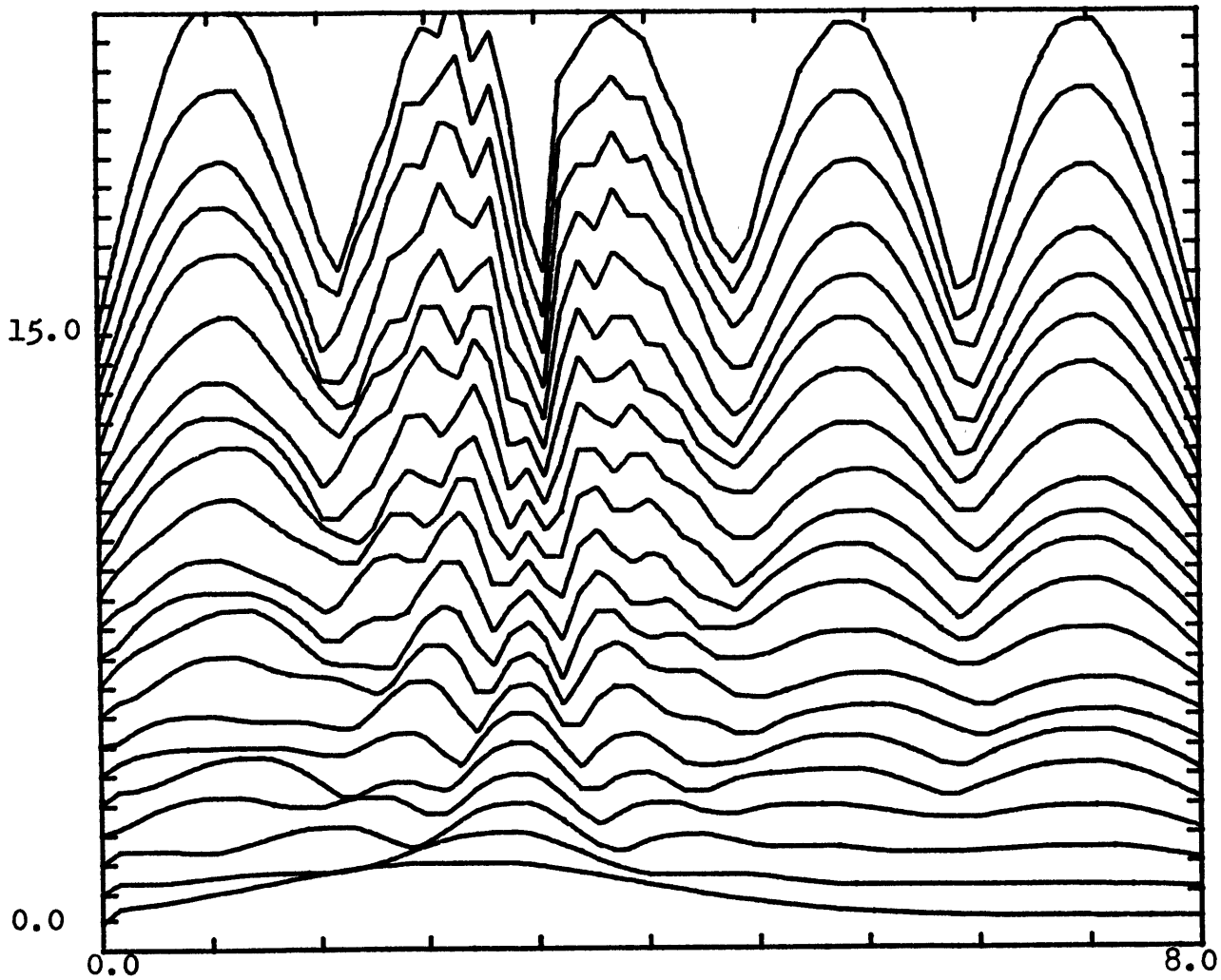

FIG. 4.2.13

$y_0 = 2.5$
$H = 1.0$
$l_o = 2.0$
$\gamma = 5.0$
$k = -1.25$
$B = -15.0$
$y_c \cong 2.95$
$y_{Tu} \cong 3.02$
$y_B = 3.0$
$c_{gy} \cong 0.4$

$|VORT(y,t)|$

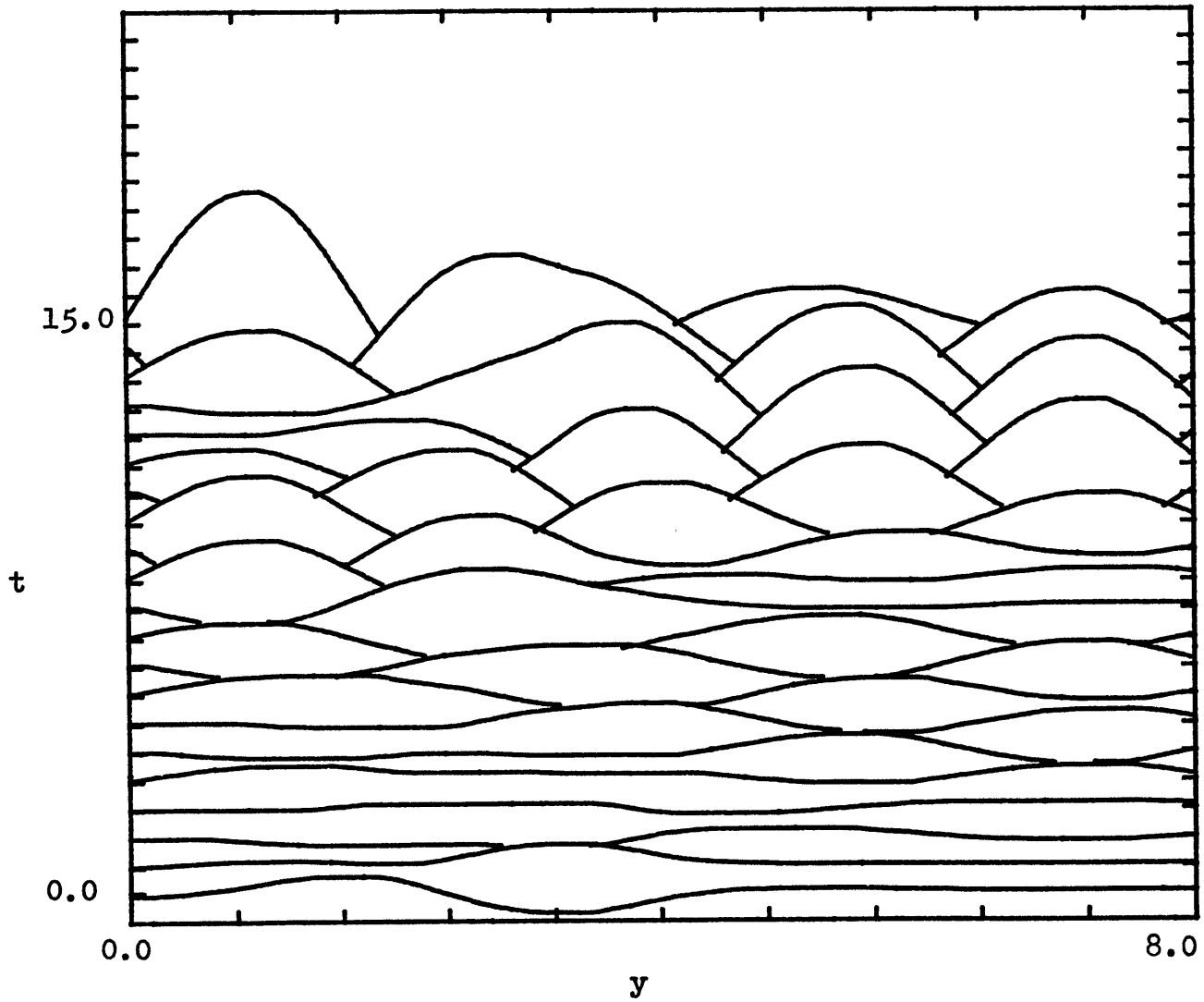

FIG. 4.2.14

$y_o = 2.5$
$H = 1.0$
$l_o = 2.0$
$\gamma = 5.0$
$k = -1.25$
$B = -15.0$
$y_c \cong 2.95$
$y_{Tu} \cong 3.02$
$y_B = 3.0$
$C_{gy} \cong 0.4$

Re (sf(y,t))

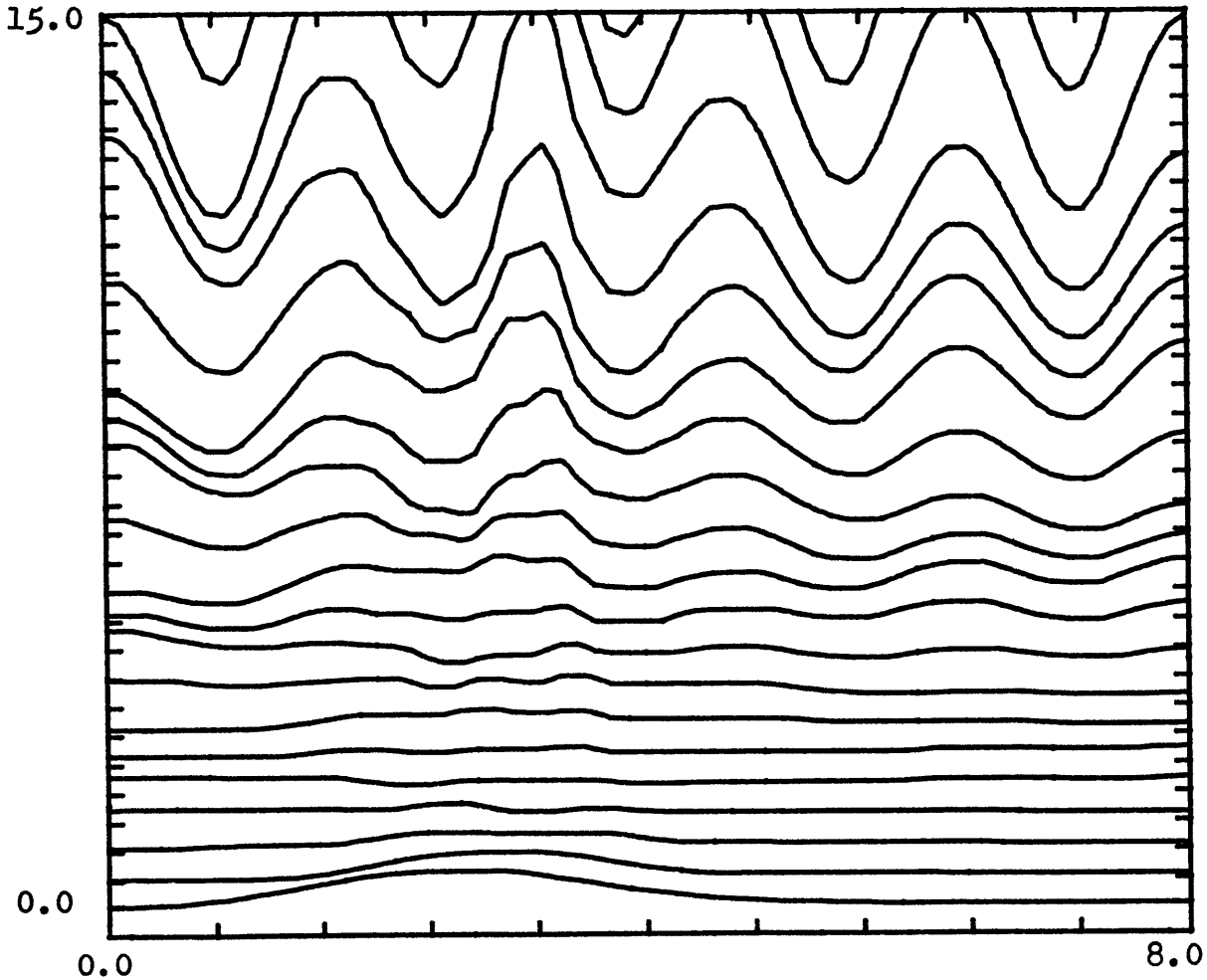

FIG. 4.2.15

$y_o = 2.5$
$H = 1.0$
$l_o = 2.0$
$\gamma = 5.0$
$k = -1.25$
$B = -15.0$
$y_c \cong 2.95$
$y_{Tu} \cong 3.02$
$y_B = 3.0$
$C_{gy} \cong 0.4$

E(y,t)

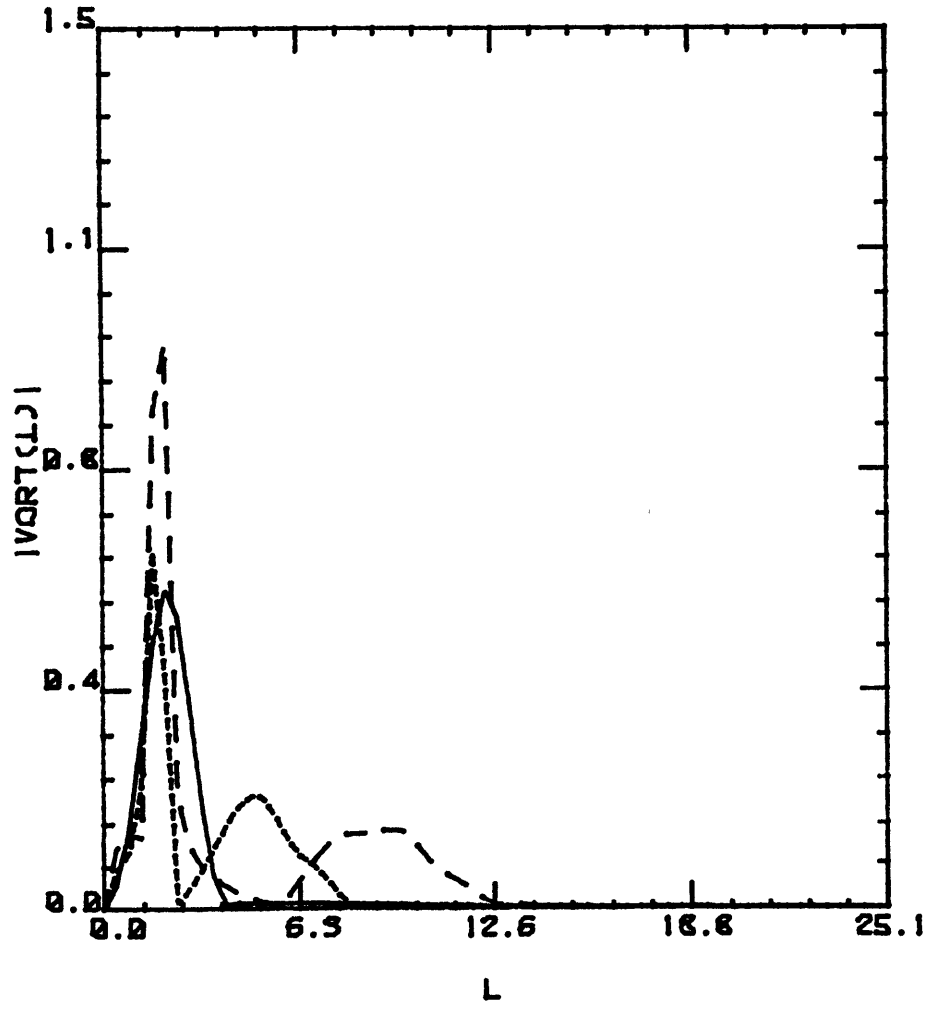

FIG. 4.2.16

$y_o = 2.5$
$H = 1.0$
$l_o = 2.0$
$\gamma_o = 5.0$
$k = -1.25$
$B = -15.0$
$y_c \cong 2.95$
$y_{Tu} \cong 3.02$
$y_B = 3.0$
$C_{gy} \cong 0.4$

—— T = 0.0
---- T = 3.0
– – – T = 6.0

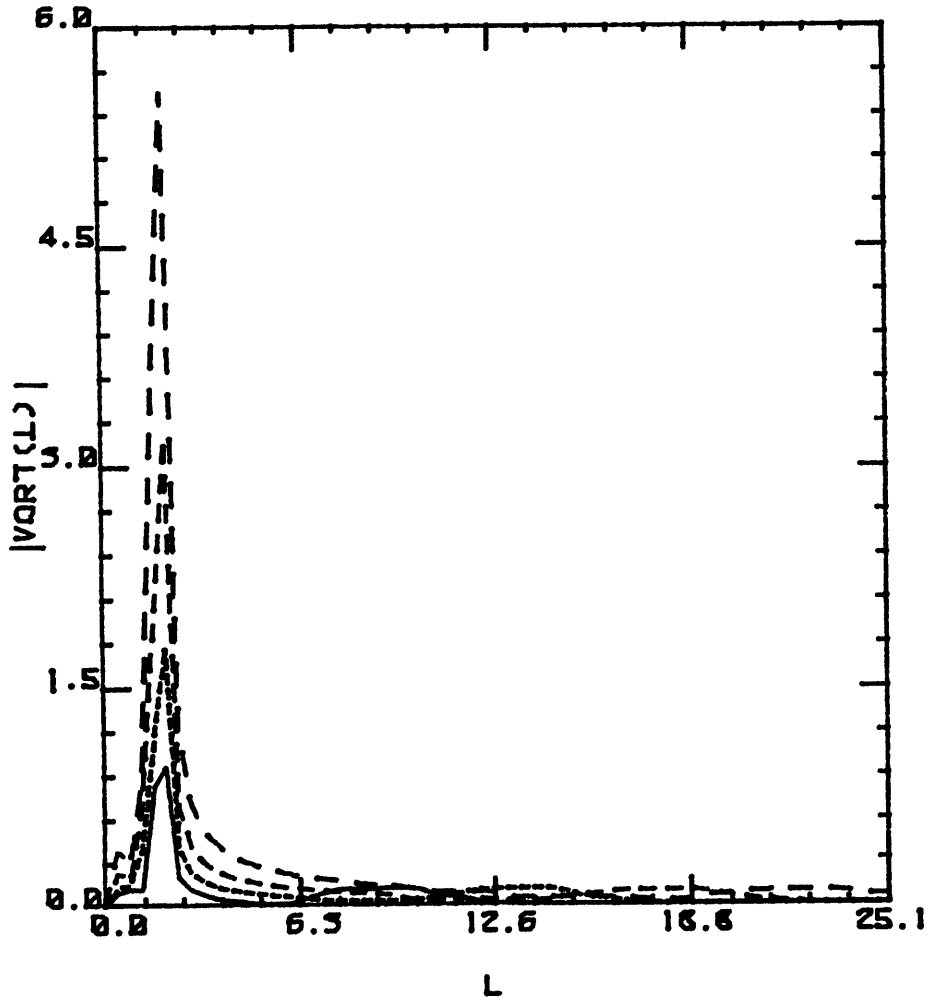

FIG. 4.2.17

$y_o = 2.5$
$H = 1.0$
$l_o = 2.0$
$\gamma = 5.0$
$k = -1.25$
$B = -15.0$
$y_c \cong 2.95$
$y_{Tu} \cong 3.02$
$y_B = 3.0$
$C_{gy} \cong 0.4$

——— T = 6.0
- - - - - T = 9.0
— — — T = 12.0
— — — T = 15.0

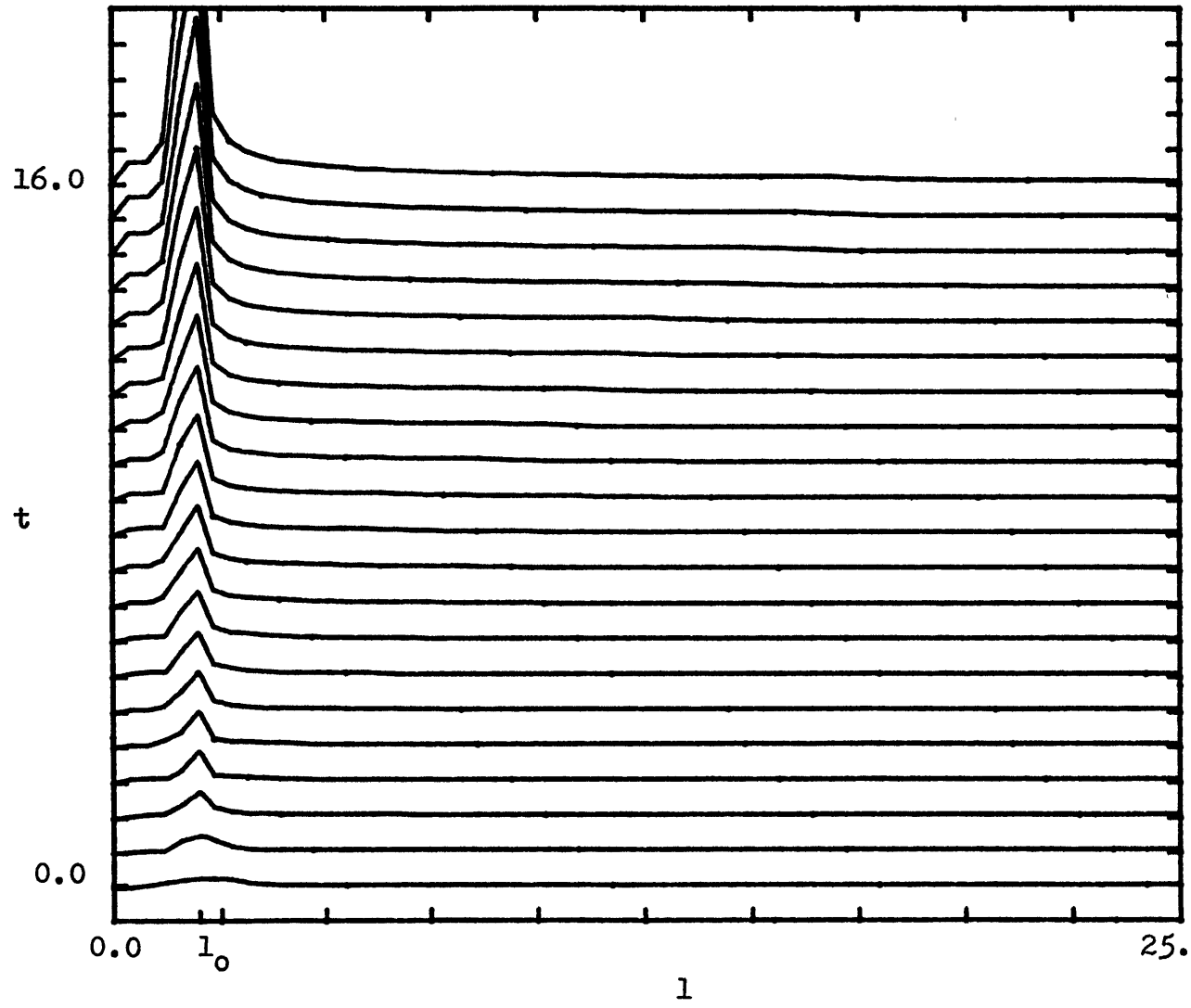

FIG. 4.2.18

$y_o = 2.5$
$H = 1.0$
$l_o = 2.0$
$\gamma = 5.0$
$k = 1.25$
$B = -15.0$
$y_c \cong 2.95$
$y_{Tu} \cong 3.02$
$y_B = 3.0$
$C_{gy} \cong -0.4$

|VORT(l,t)|

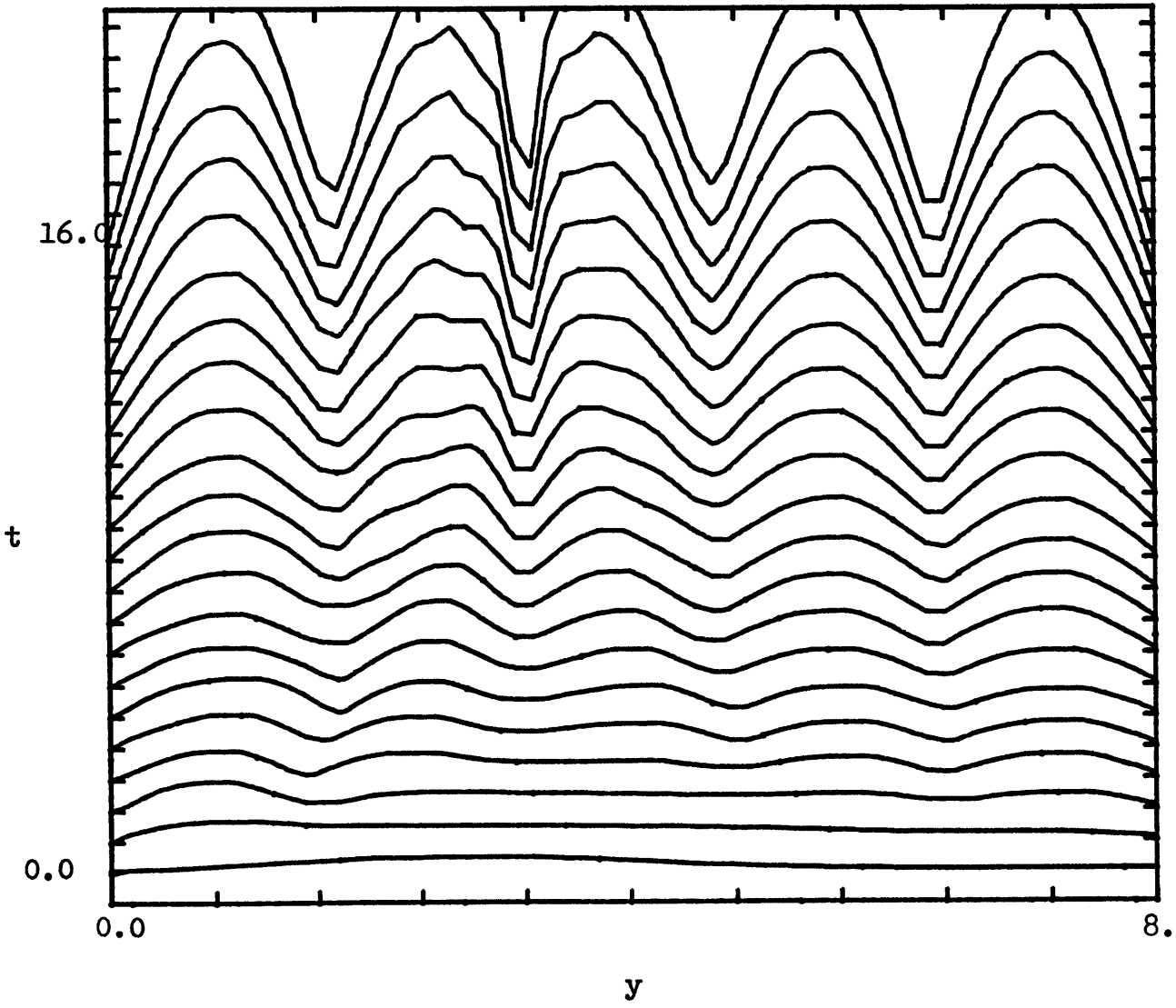

FIG. 4.2.19

$y_o = 2.5$
$H = 1.0$
$l_o = 2.0$
$\delta = 5.0$
$k = 1.25$
$B = -15.0$
$y_c \cong 2.95$
$y_{Tu} \cong 3.02$
$y_B = 3.0$
$C_{gy} \cong -0.4$

$|VORT(y,t)|$

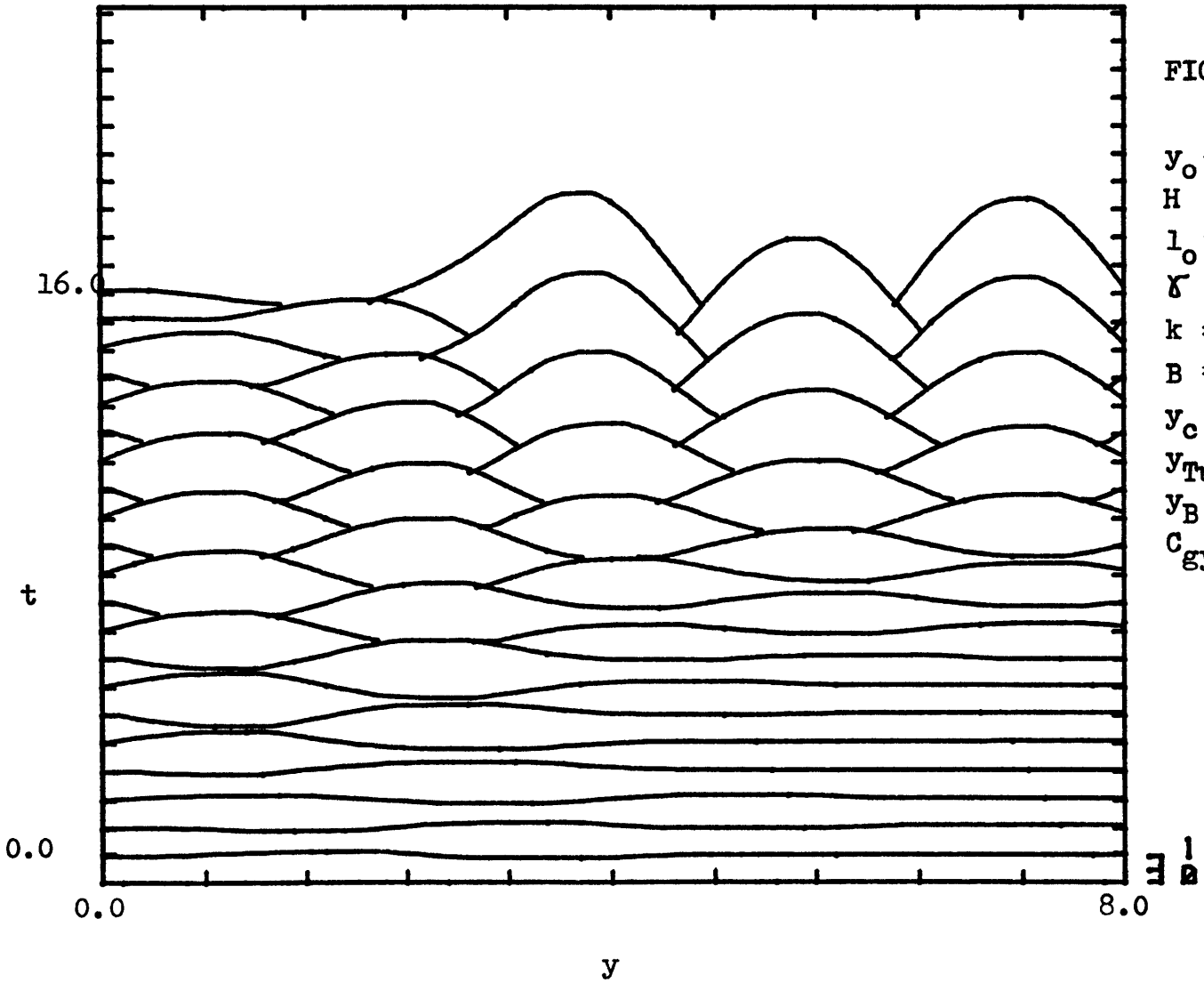

FIG. 4.2.20

$y_o = 2.5$
$H = 1.0$
$l_o = 2.0$
$\gamma = 5.0$
$k = 1.25$
$B = -15.0$
$y_c \cong 2.95$
$y_{Tu} \cong 3.02$
$y_B = 3.0$
$C_{gy} \cong -0.4$

Re (sf(y,t))

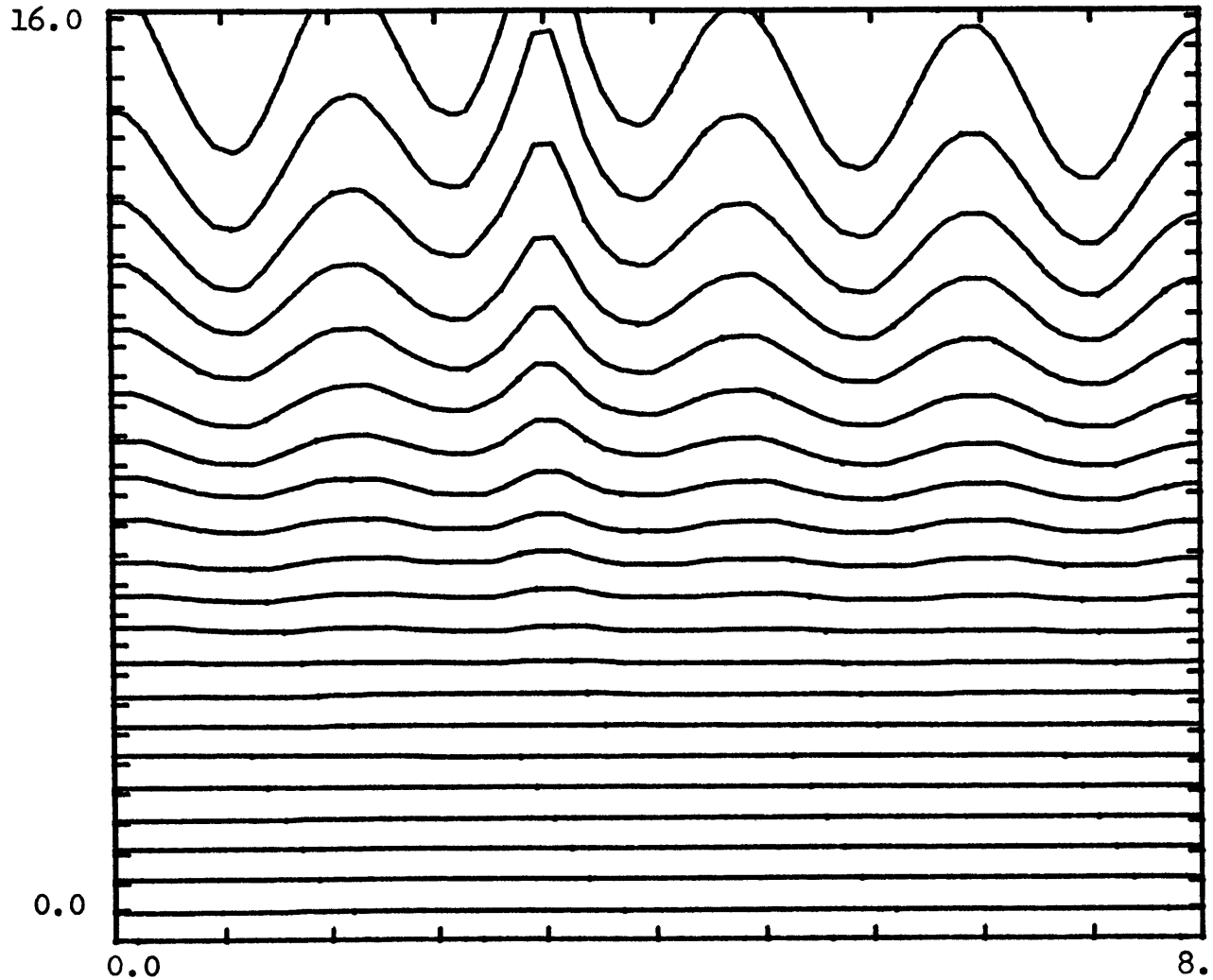

FIG. 4.2.21

$y_o = 2.5$
$H = 1.0$
$l_o = 2.0$
$\gamma = 5.0$
$k = 1.25$
$B = -15.0$
$y_c \cong 2.95$
$y_{Tu} \cong 3.02$
$y_B = 3.0$
$C_{gy} \cong -0.4$

E(y,t)

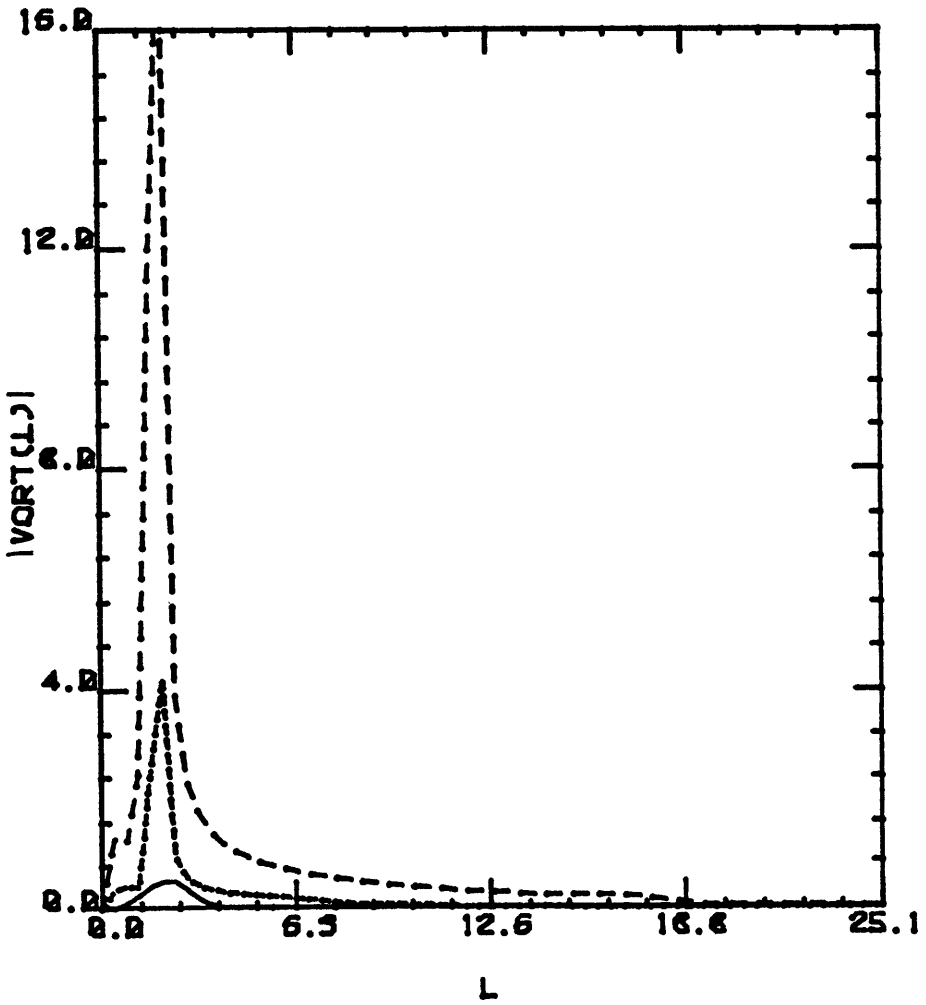

FIG. 4.2.22

$y_o = 2.5$
$H = 1.0$
$l_o = 2.0$
$\gamma = 5.0$
$k = 1.25$
$B = -15.0$
$y_c \cong 2.95$
$y_{Tu} \cong 3.02$
$y_B = 3.0$
$C_{gy} \cong -0.4$

——— T = 0.0
----- T = 8.0
----- T = 16.0

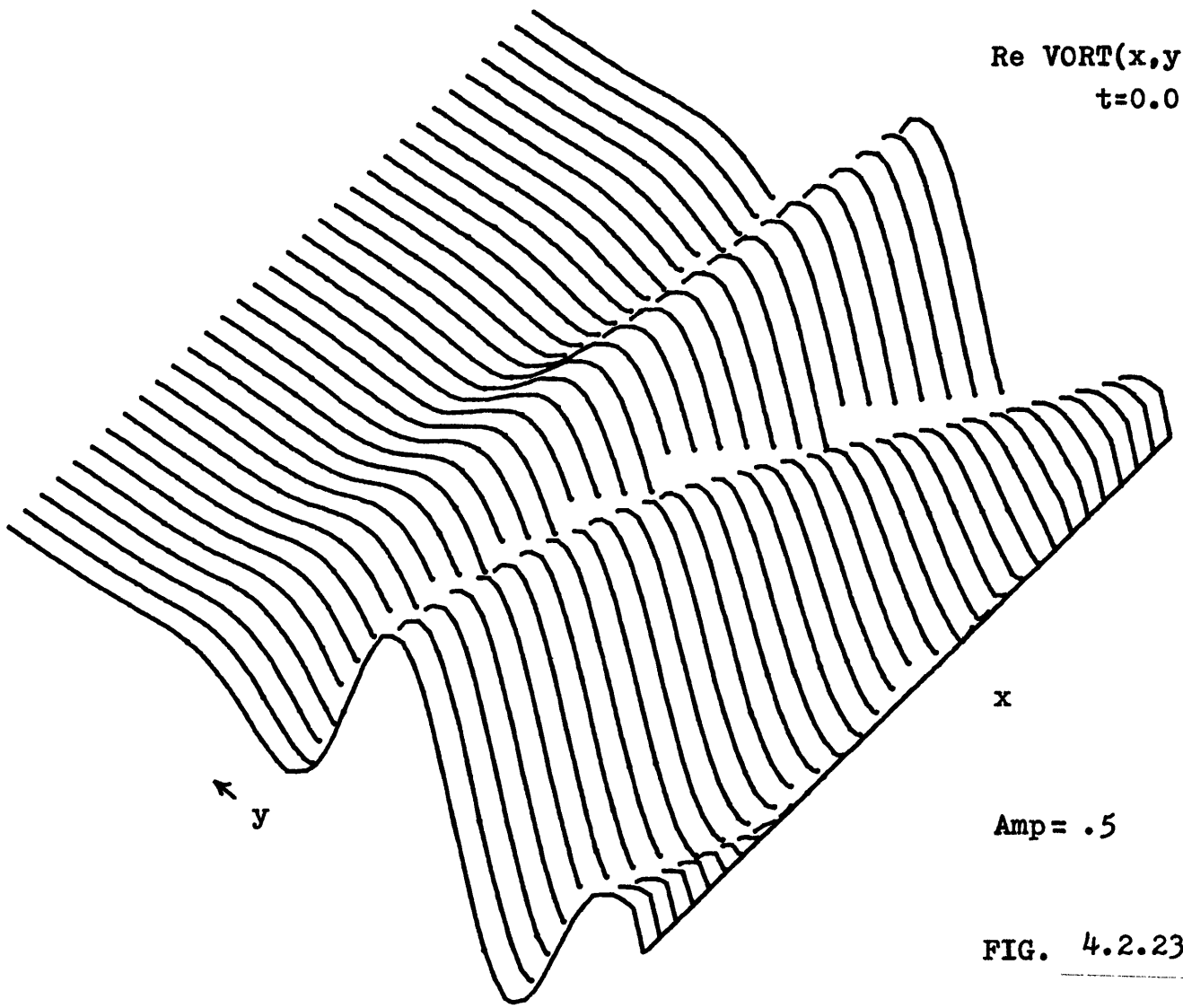

FIG. 4.2.23

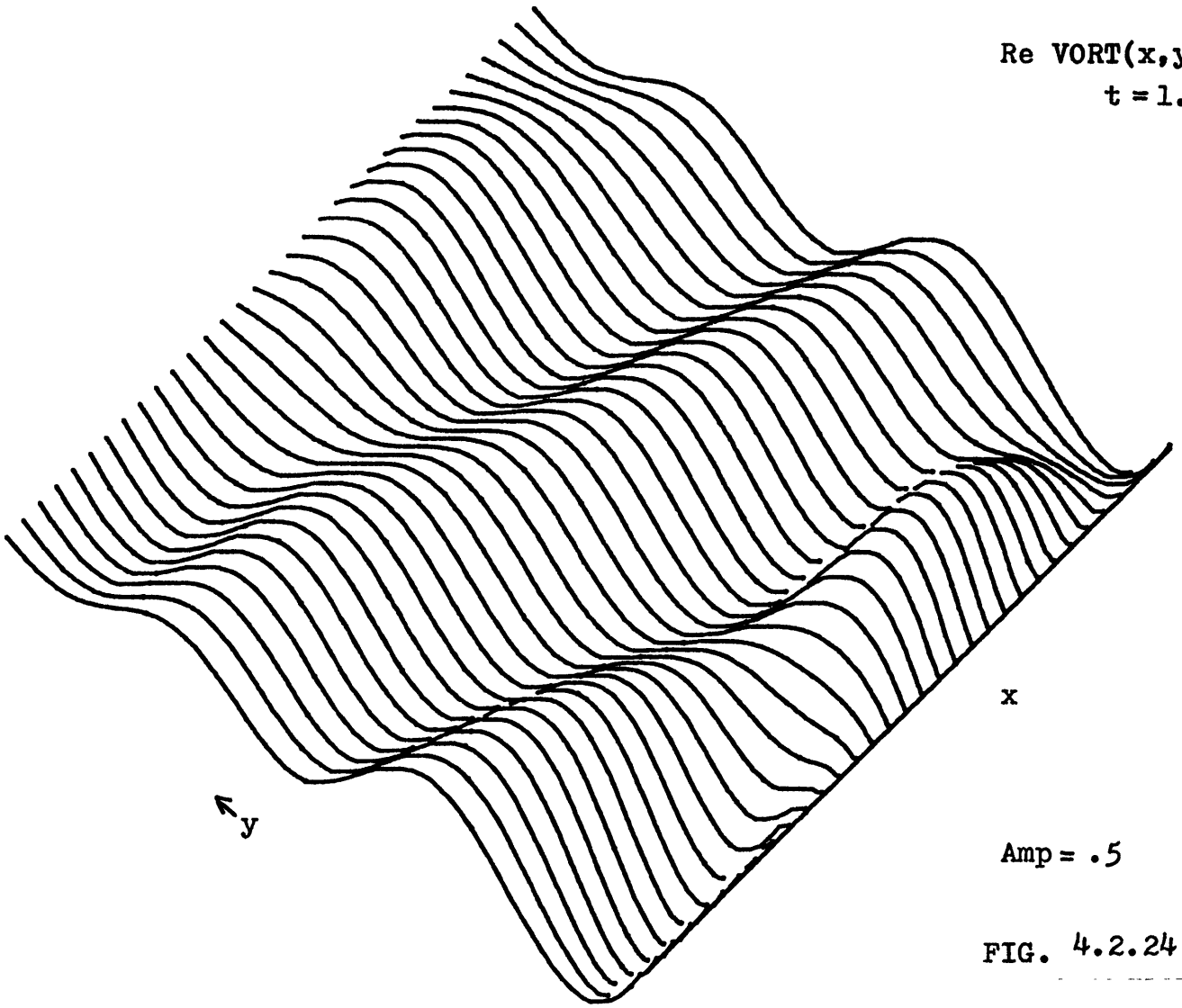

FIG. 4.2.24

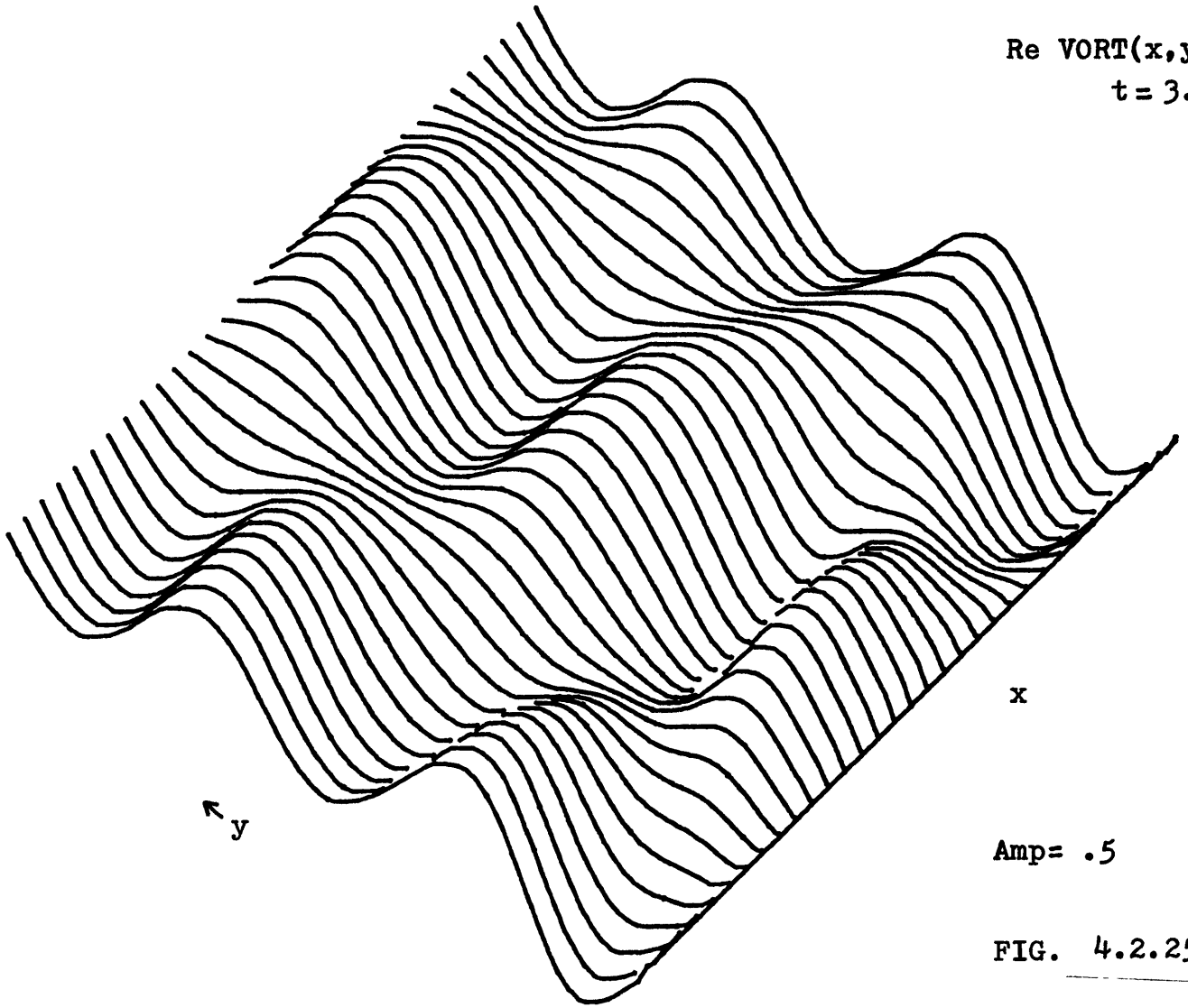

FIG. 4.2.25

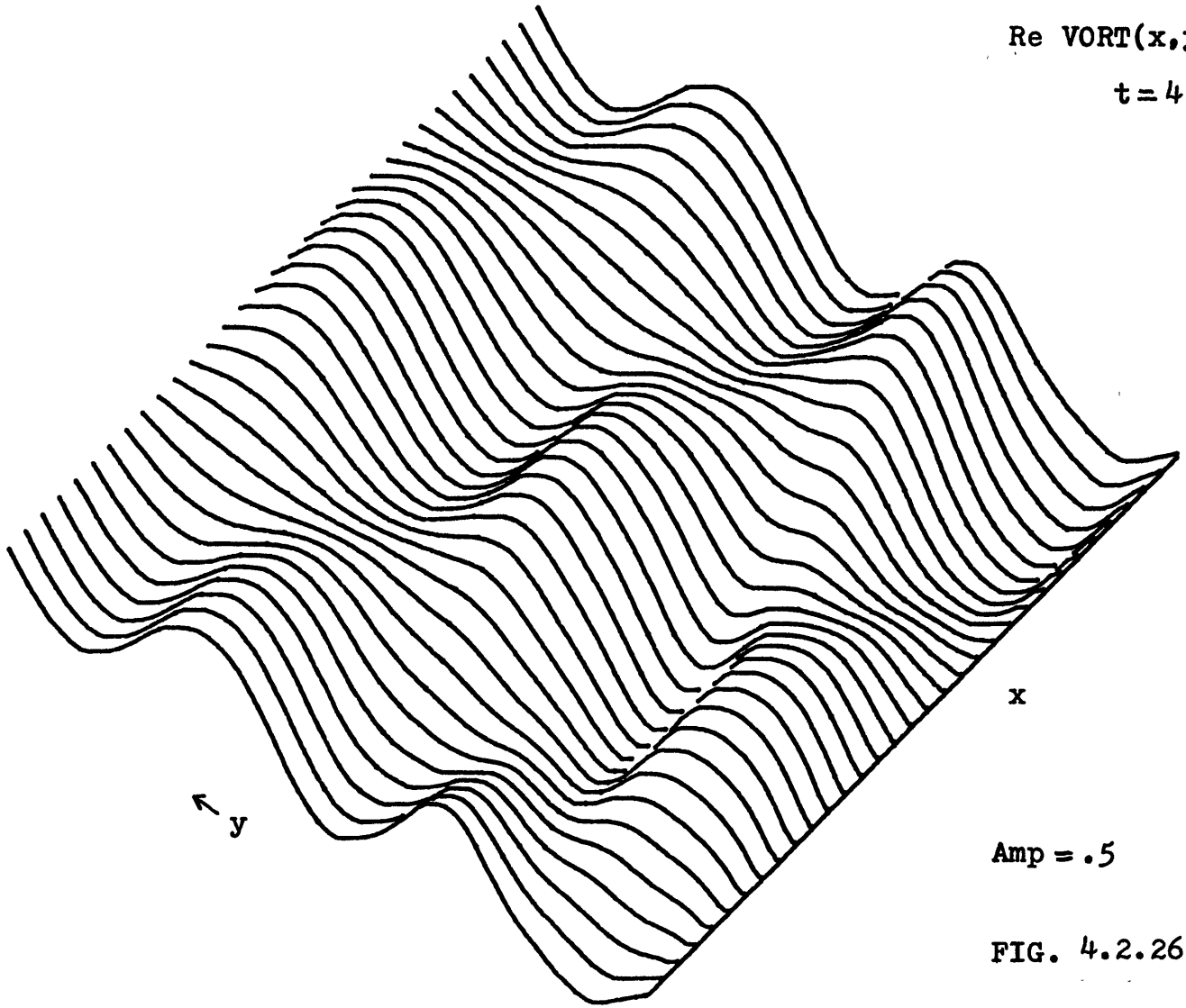

FIG. 4.2.26

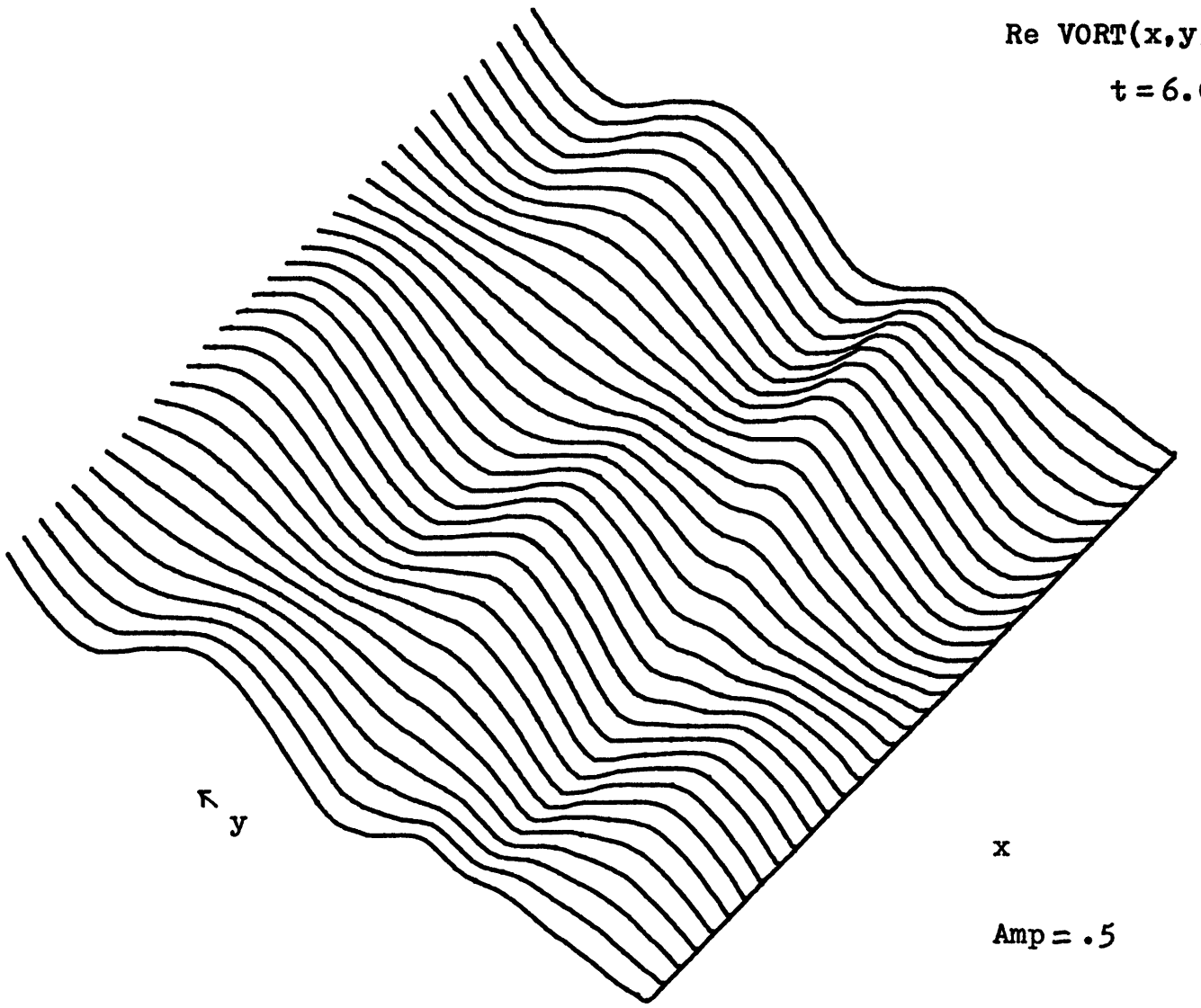

Re VORT(x,y,t)

t = 6.0

Amp = .5

FIG. 4.2.27

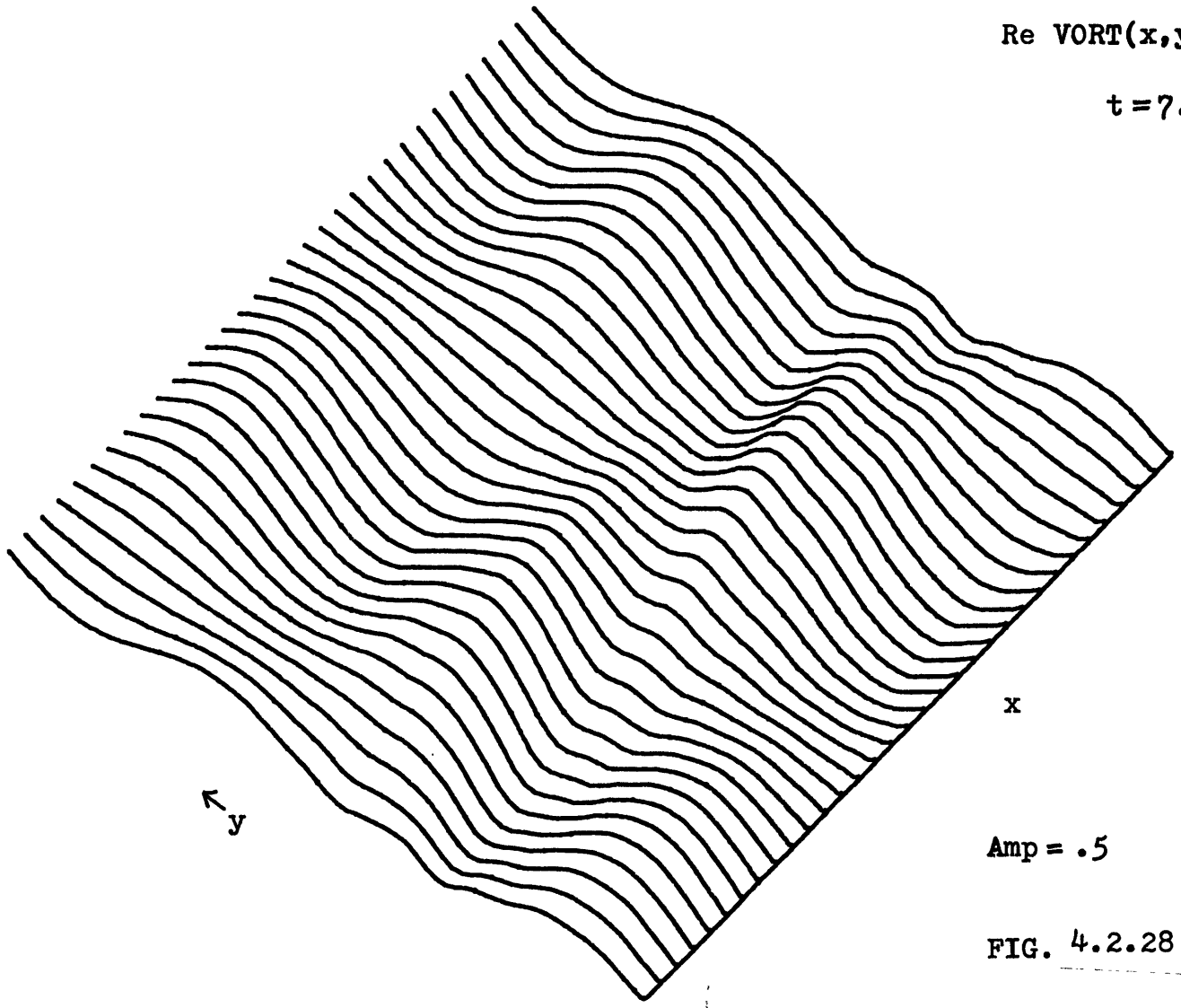

FIG. 4.2.28

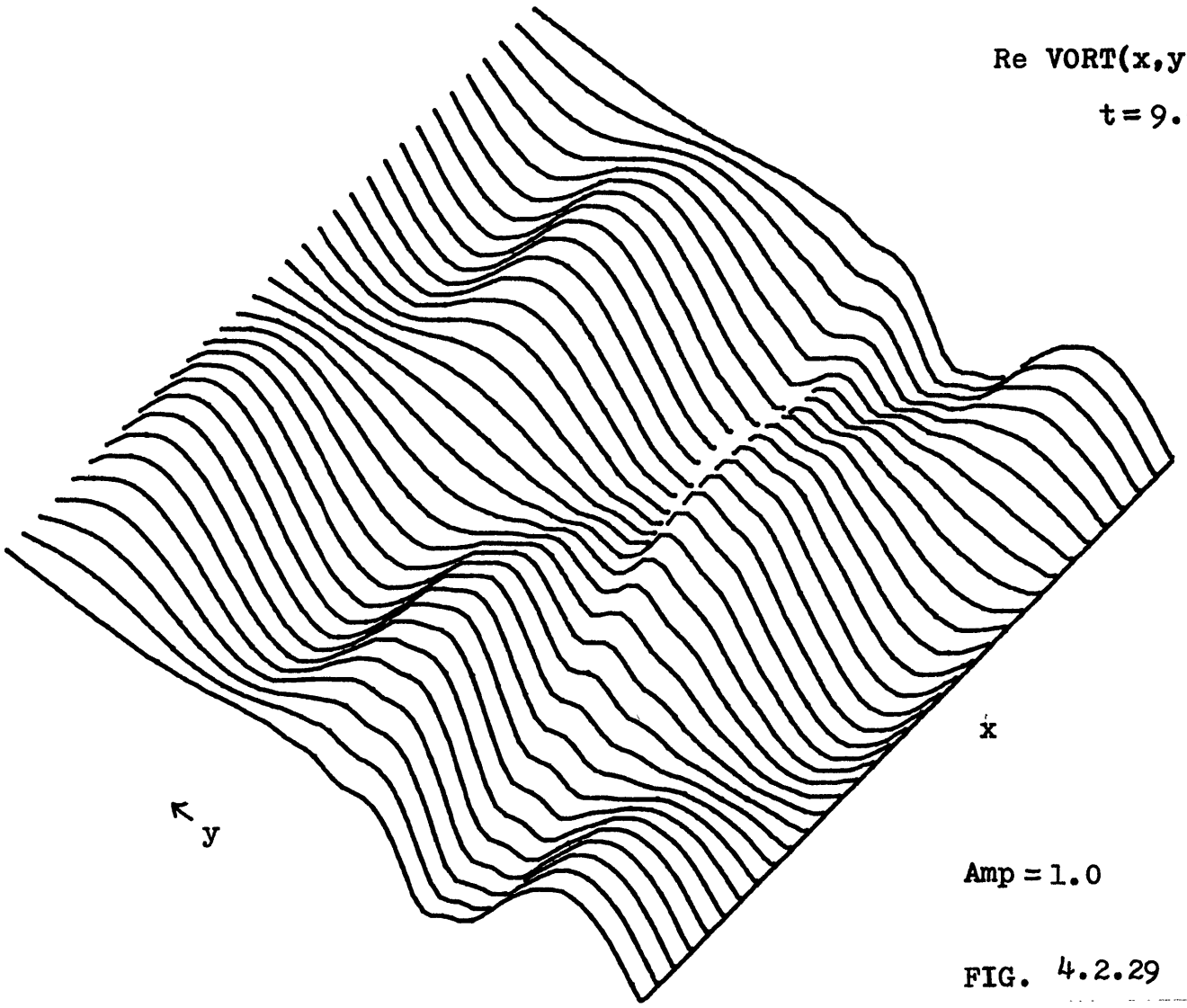

Amp = 1.0

FIG. 4.2.29

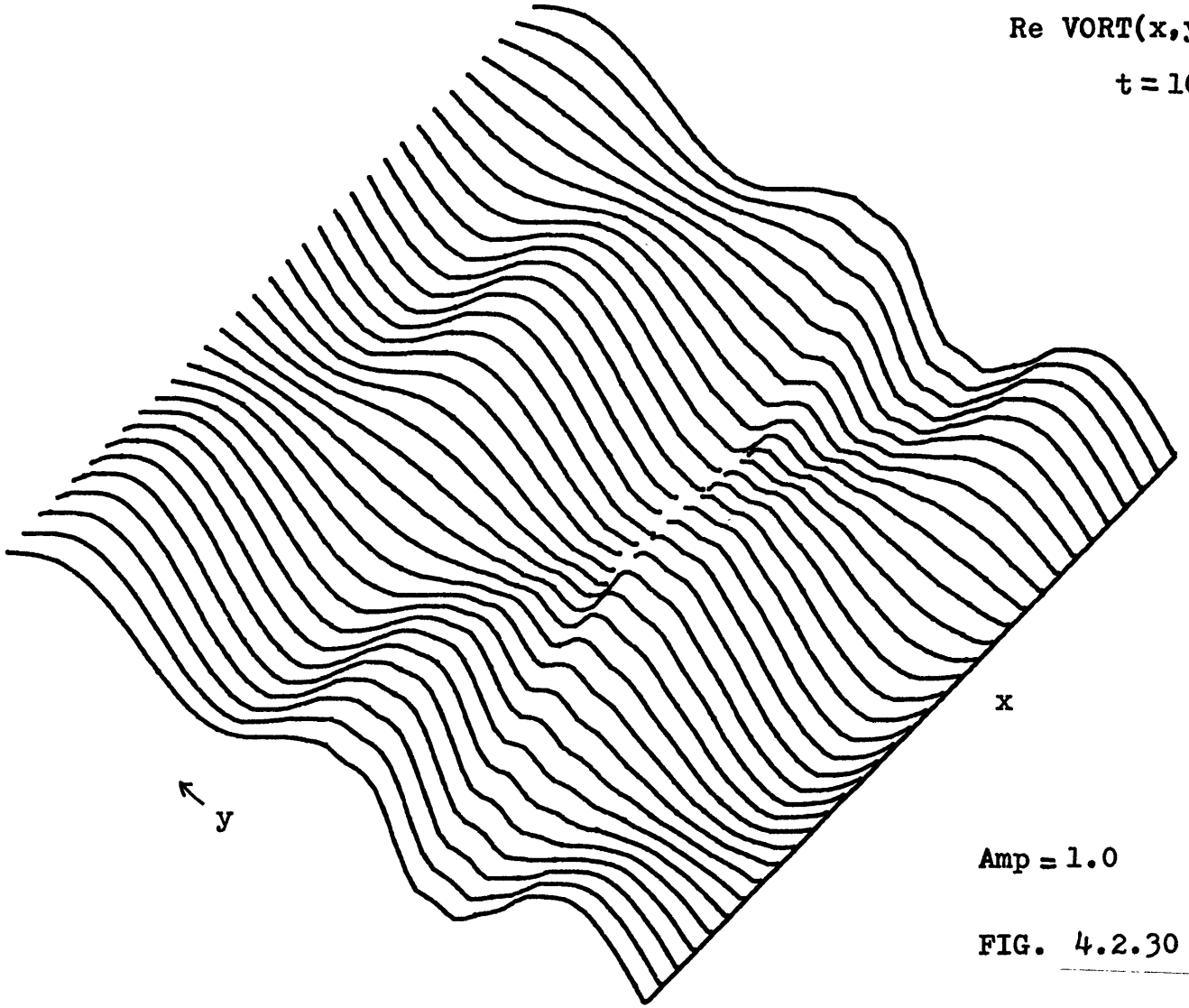

FIG. 4.2.30

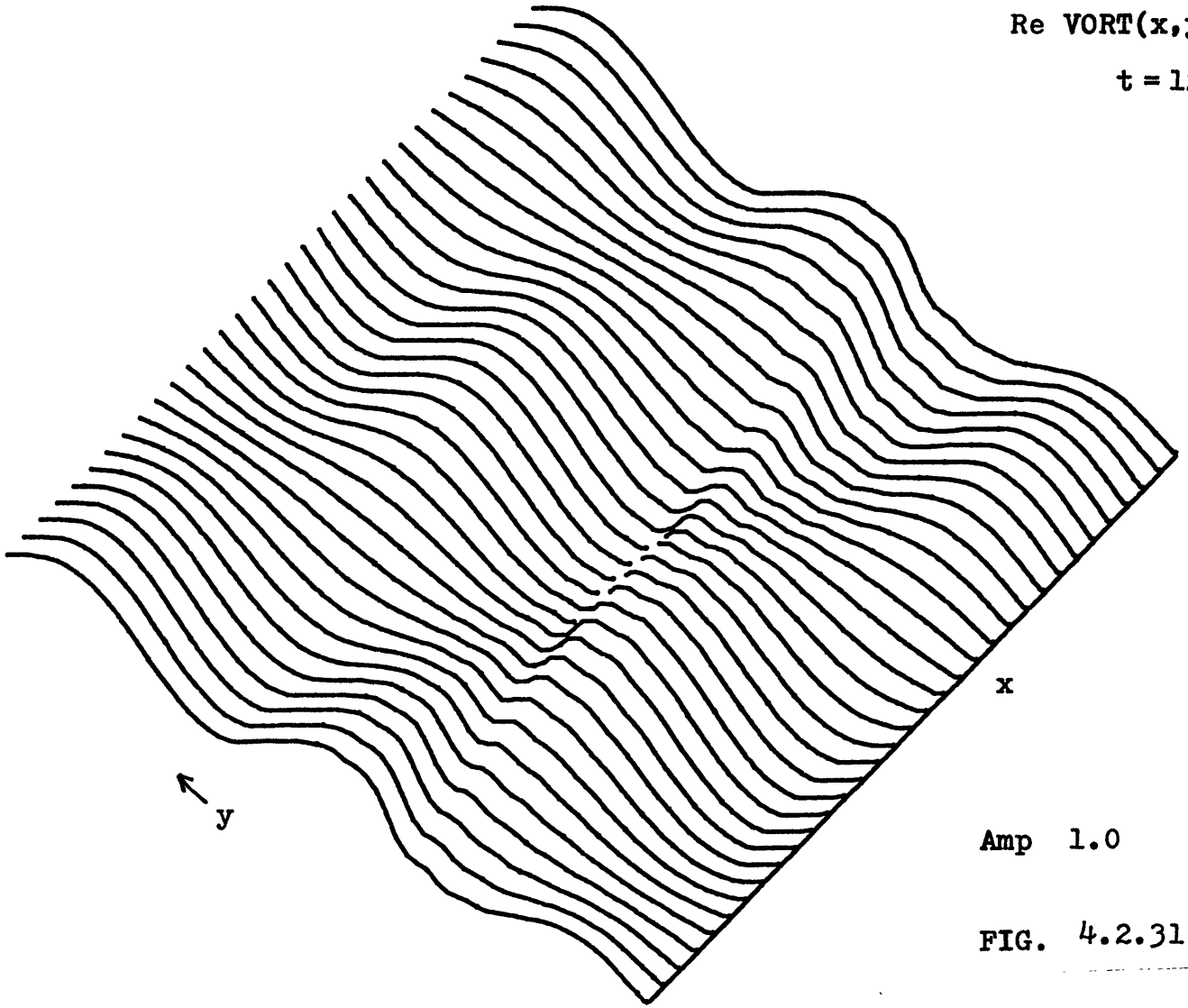

FIG. 4.2.31

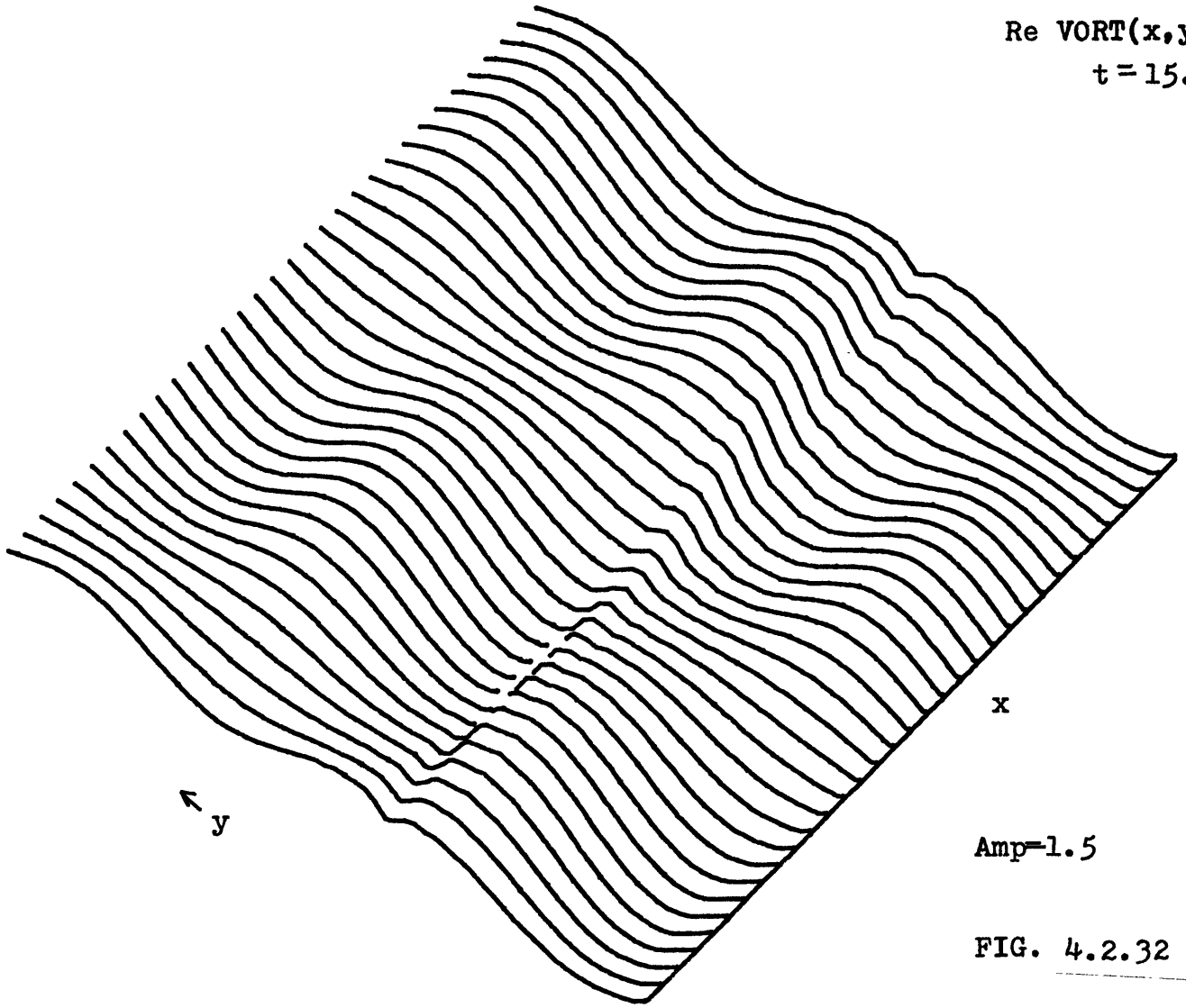

FIG. 4.2.32

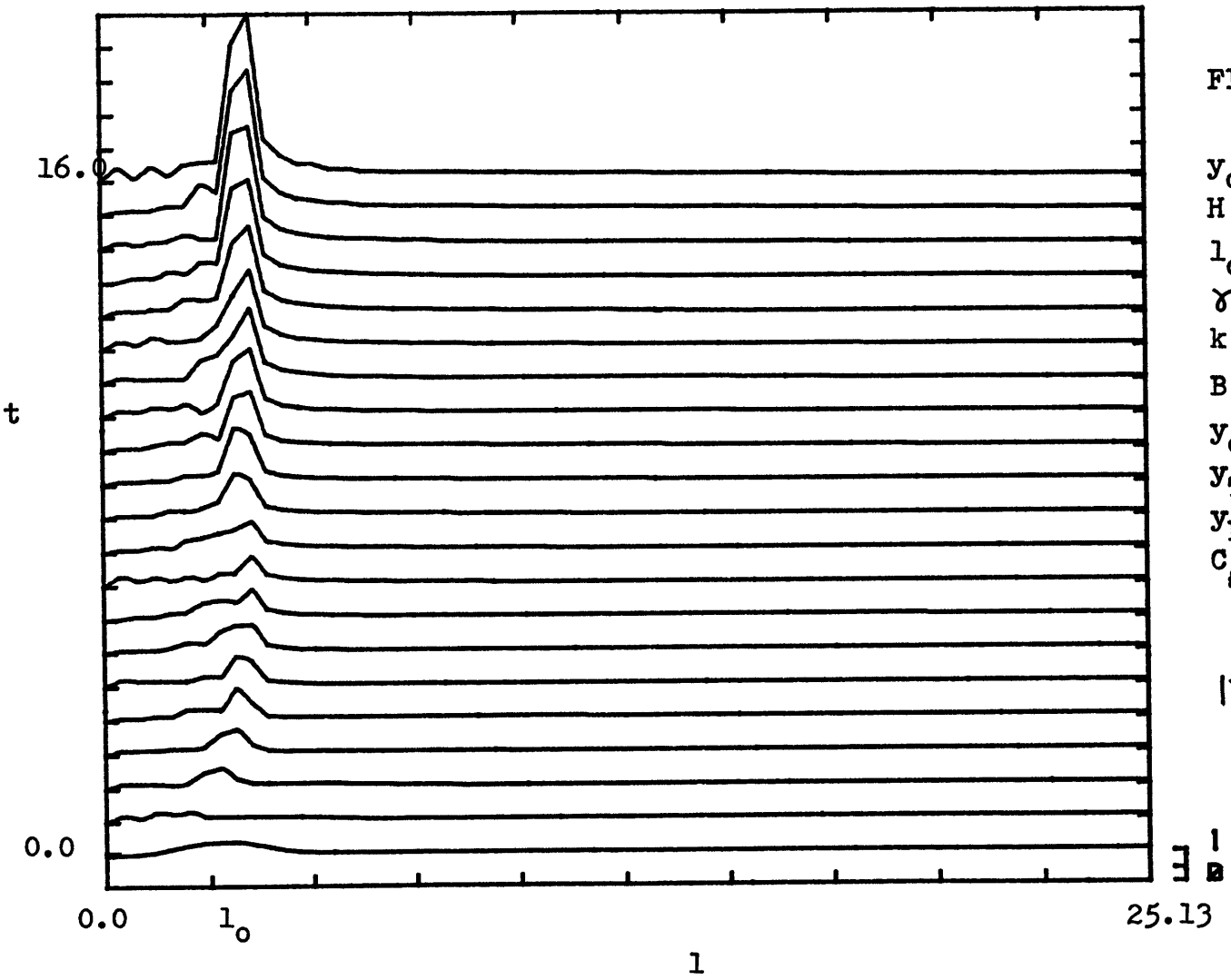

FIG. 4.2.33

$y_o = 5.0$
$H = 0.75$
$l_o = 2.67$
$\gamma = 17.8$
$k = -2.5$
$B = -62.3$
$y_c \cong 3.0$
$y_{Tu} \cong 3.8$
$y_B = 3.5$
$C_{gy} \cong -0.20$

|VORT(l,t)|

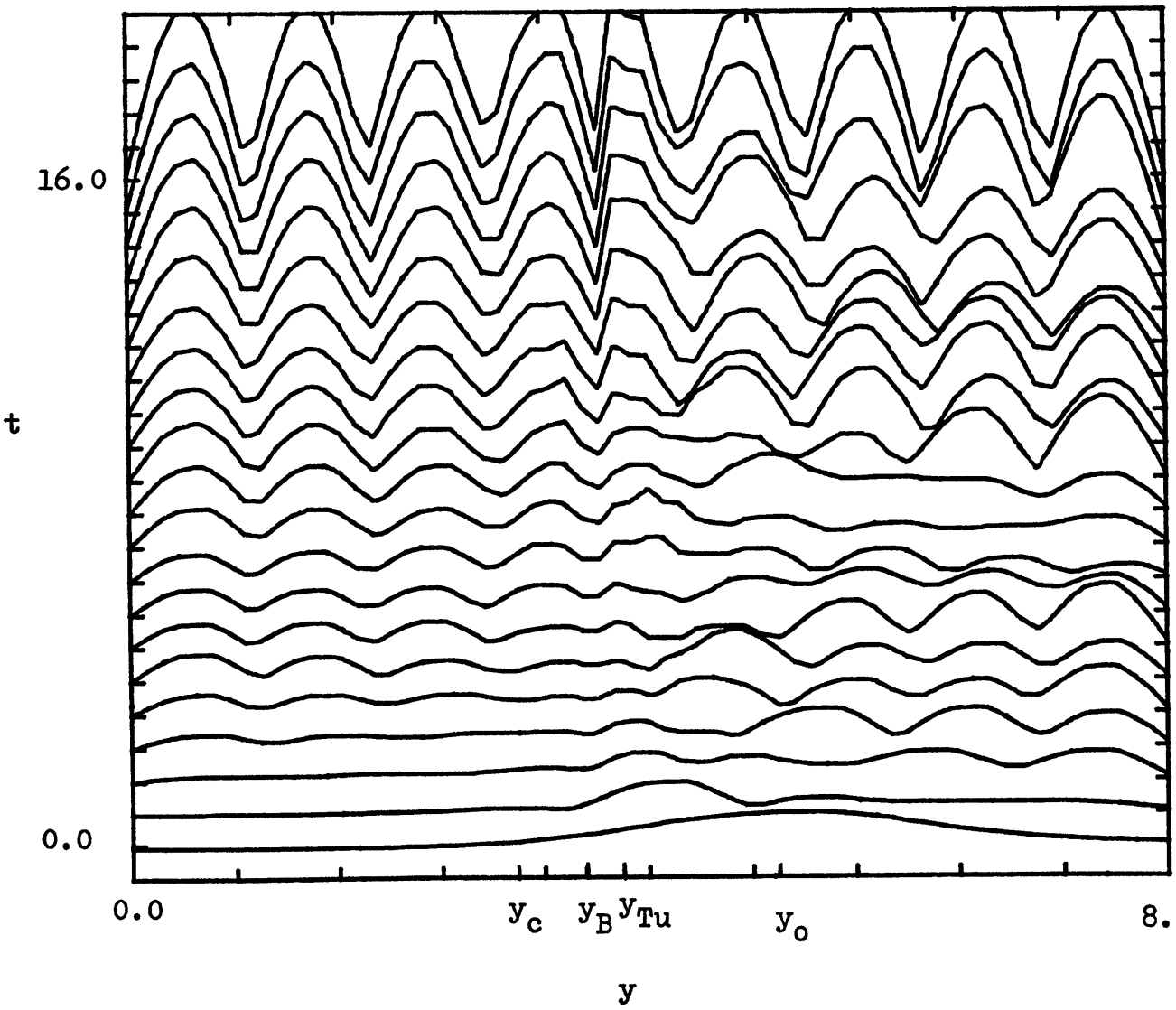

FIG. 4.2.34

$y_o = 5.0$
$H = 0.75$
$l_o = 2.67$
$\gamma = 17.8$
$k = -2.5$
$B = -62.3$

$y_c \cong 3.0$
$y_{Tu} \cong 3.8$
$y_B = 3.5$
$C_{gy} \cong -0.20$

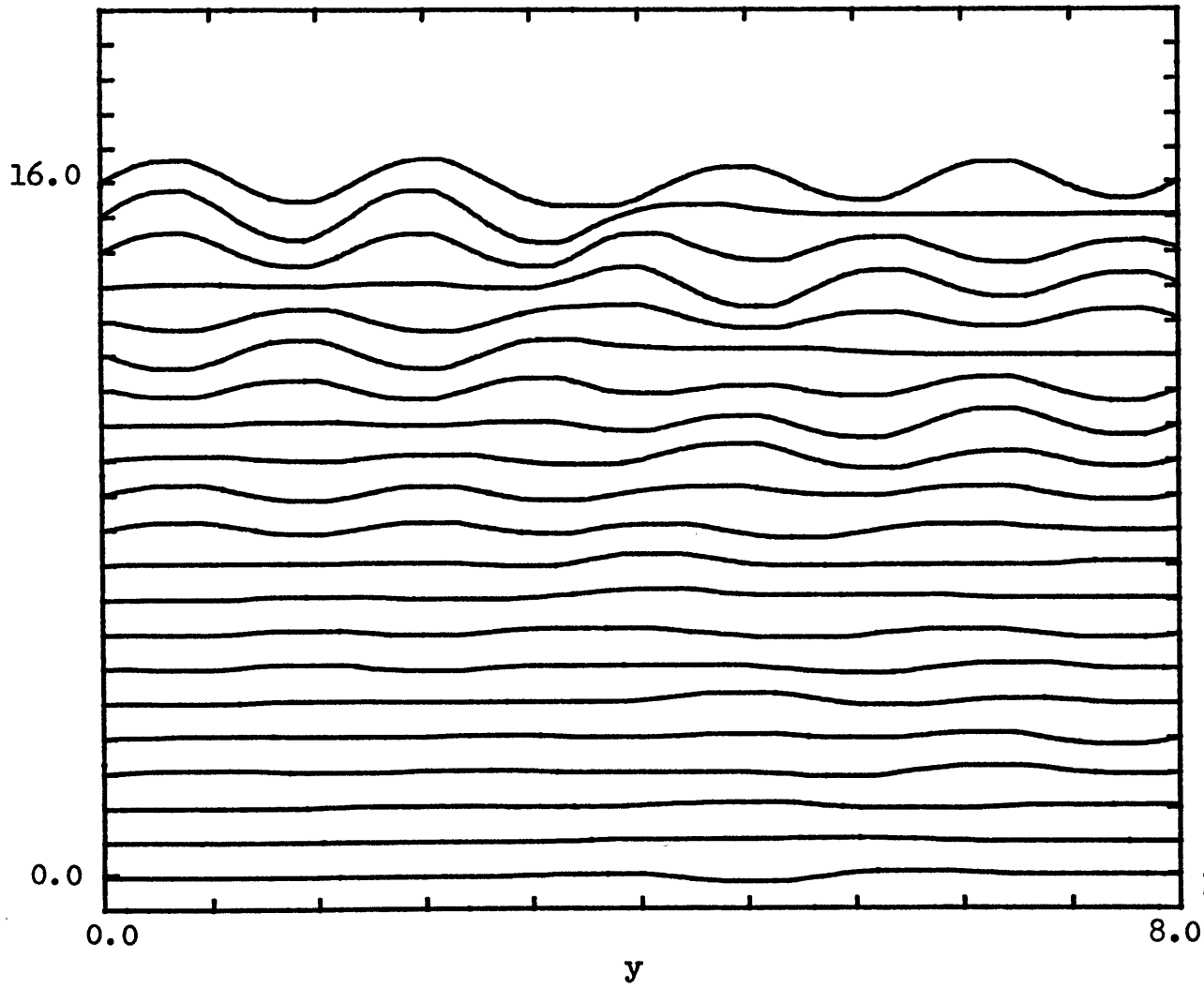

FIG. 4.2.35

$y_o = 5.0$
$H = 0.75$
$l_o = 2.67$
$\gamma = 17.8$
$k = -2.5$
$B = -62.3$
$y_c \cong 3.0$
$y_{Tu} \cong 3.8$
$y_B = 3.5$
$C_{gy} \cong -0.20$

Re (sf(y,t))

0.5
0

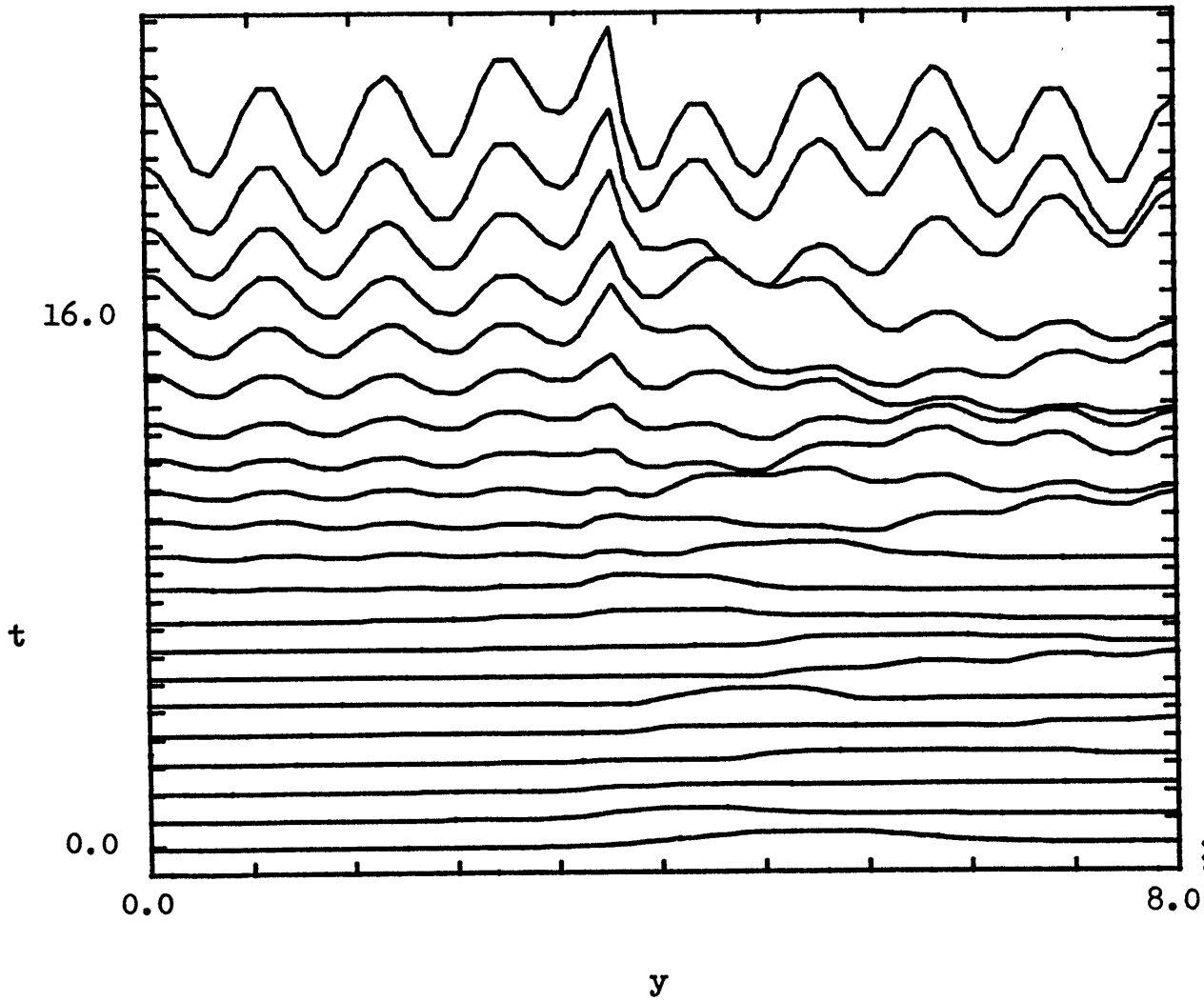

FIG. 4.2.36

$y_o = 5.0$
$H = 0.75$
$l_o = 2.67$
$\gamma = 17.8$
$k = -2.5$
$B = -62.3$
$y_c \cong 3.0$
$y_{Tu} \cong 3.8$
$y_B = 3.5$
$C_{gy} \cong -0.20$

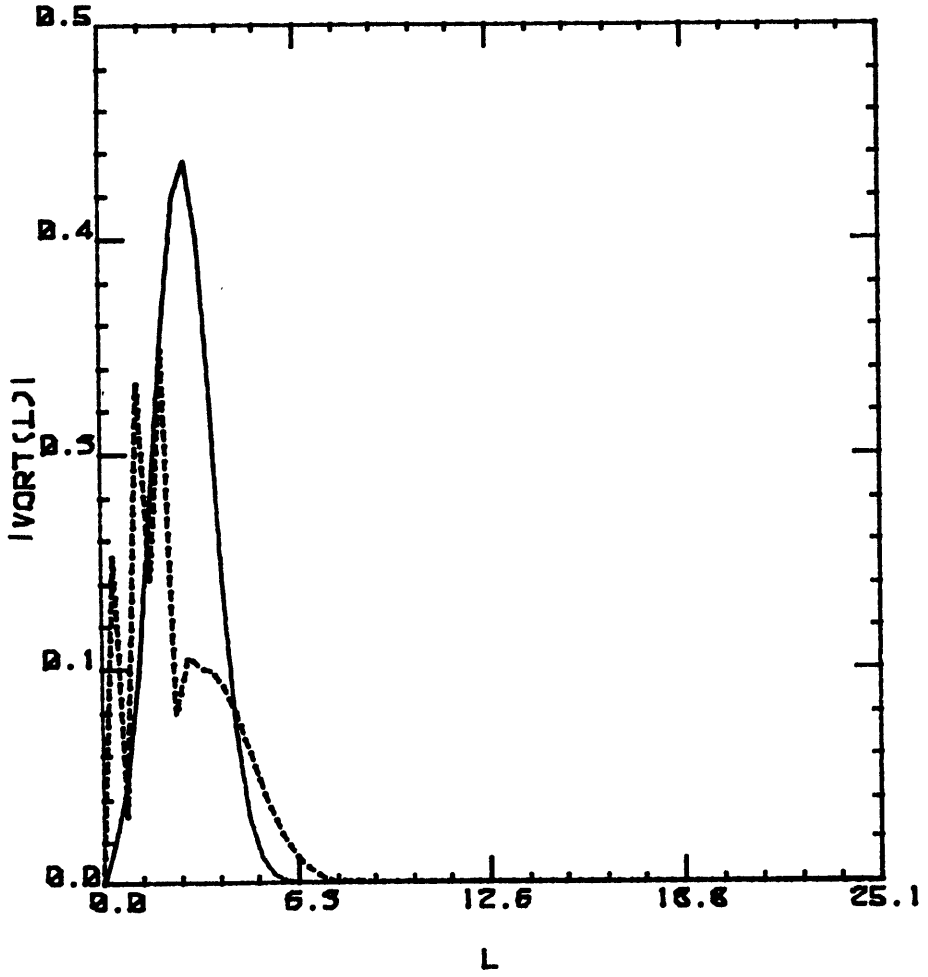

FIG. 4.2.37

$y_o = 5.0$
$H = 0.75$
$l_o = 2.67$
$\gamma = 17.8$
$k = -2.5$
$B = -62.3$
$y_c \cong 3.0$
$y_{Tu} \cong 3.8$
$y_B = 3.5$
$c_{gy} \cong -0.20$

——— T = 0.0
----- T = 0.8

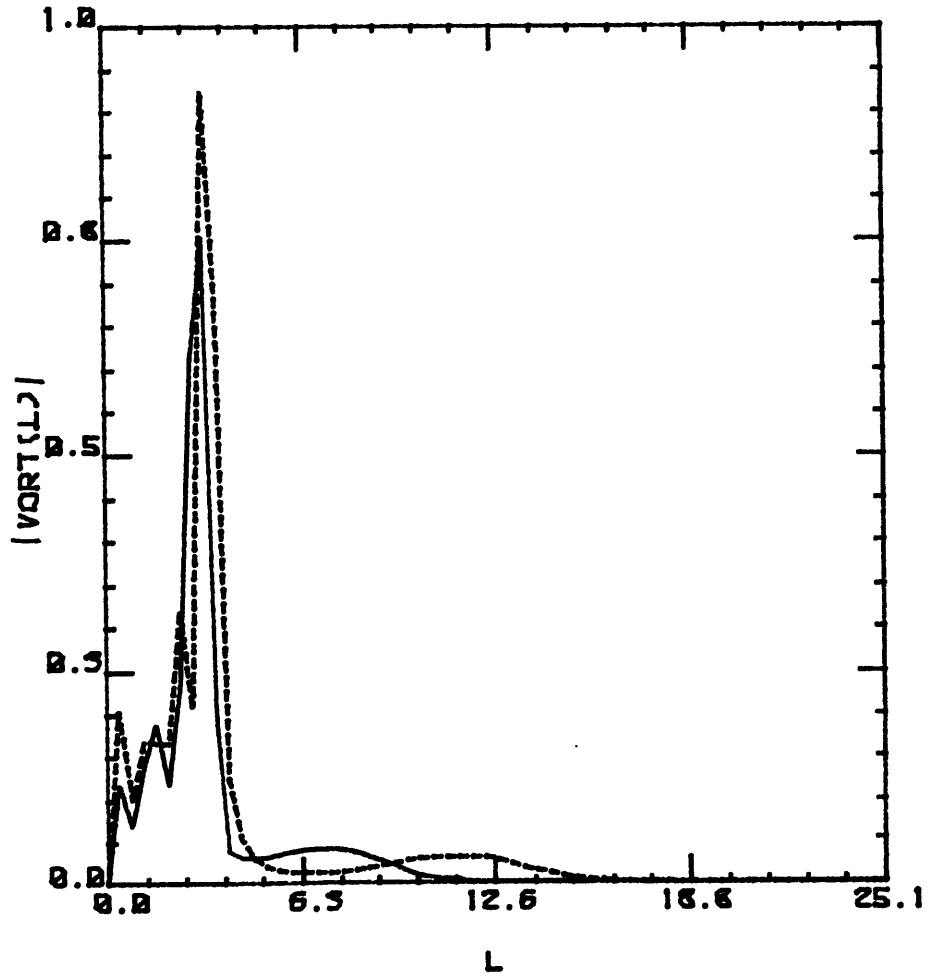

FIG. 4.2.38

$y_o = 5.0$
$H = 0.75$
$l_o = 2.67$
$\gamma = 17.8$
$k = -2.5$
$B = -62.3$
$y_c \cong 3.0$
$y_{Tu} \cong 3.8$
$y_B = 3.5$
$C_{gy} \cong -0.20$

—— T = 2.4
---- T = 4.0

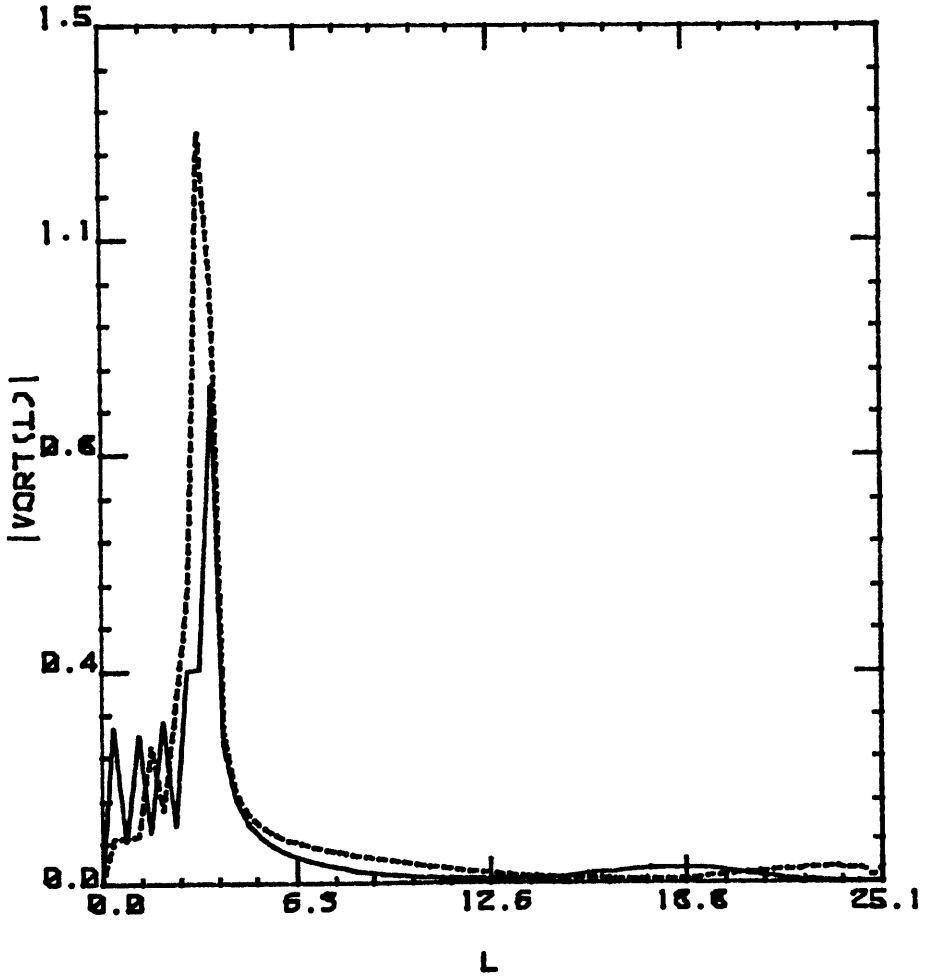

FIG. 4.2.39

$y_o = 5.0$
$H = 0.75$
$l_o = 2.67$
$\gamma = 17.8$
$k = -2.5$
$B = -62.3$

$y_c \cong 3.0$
$y_{Tu} \cong 3.8$
$y_B \cong 3.5$
$C_{gy} \cong -0.20$

——— T = 6.4
----- T = 8.0

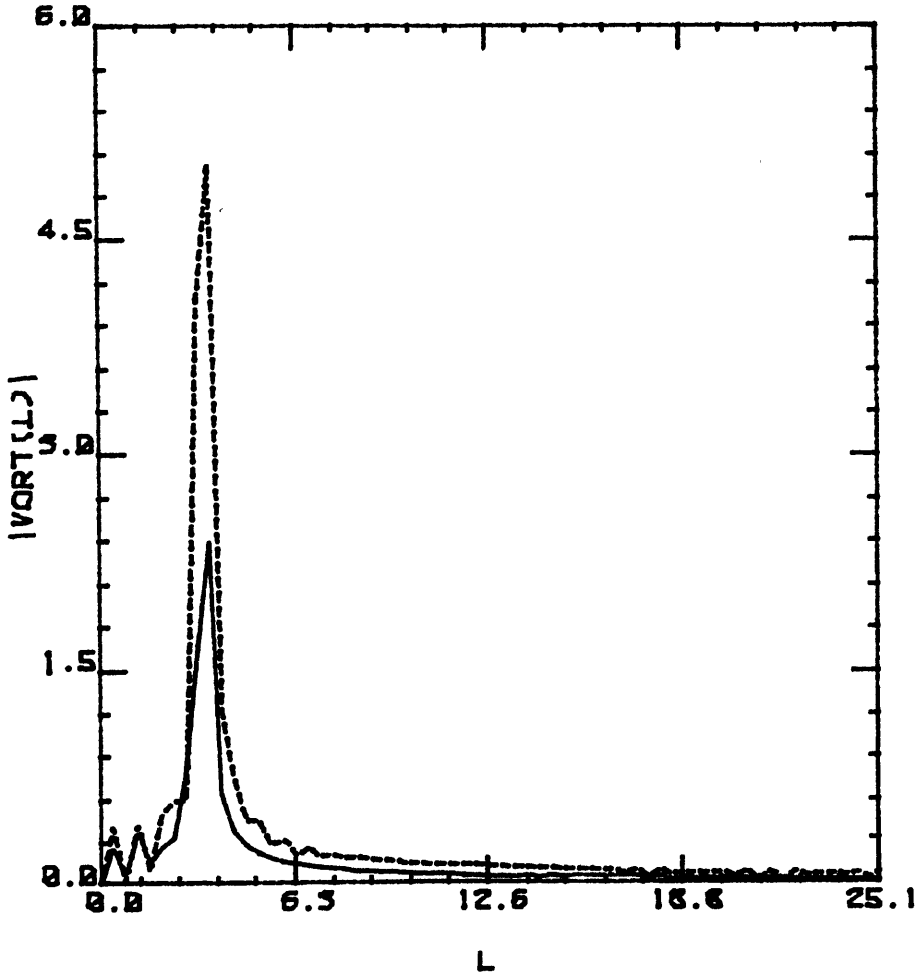

FIG. 4.2.40

$y_o = 5.0$
$H = 0.75$
$l_o = 2.67$
$\gamma = 17.8$
$k = -2.5$
$B = -62.3$
$y_c \cong 3.0$
$y_{Tu} \cong 3.8$
$y_B = 3.5$
$C_{gy} \cong -0.20$

——— T = 12.0
----- T = 16.0

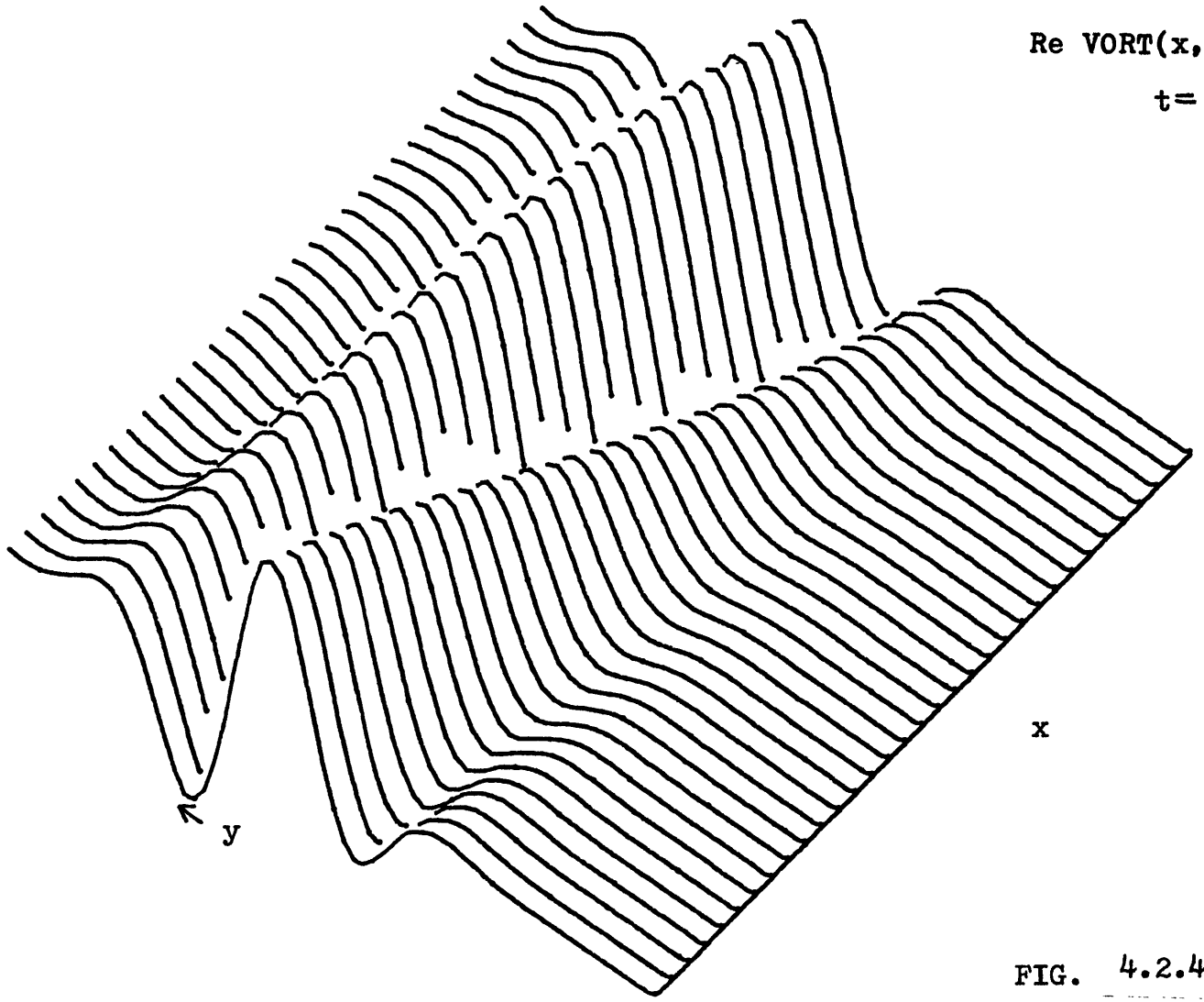

FIG. 4.2.41

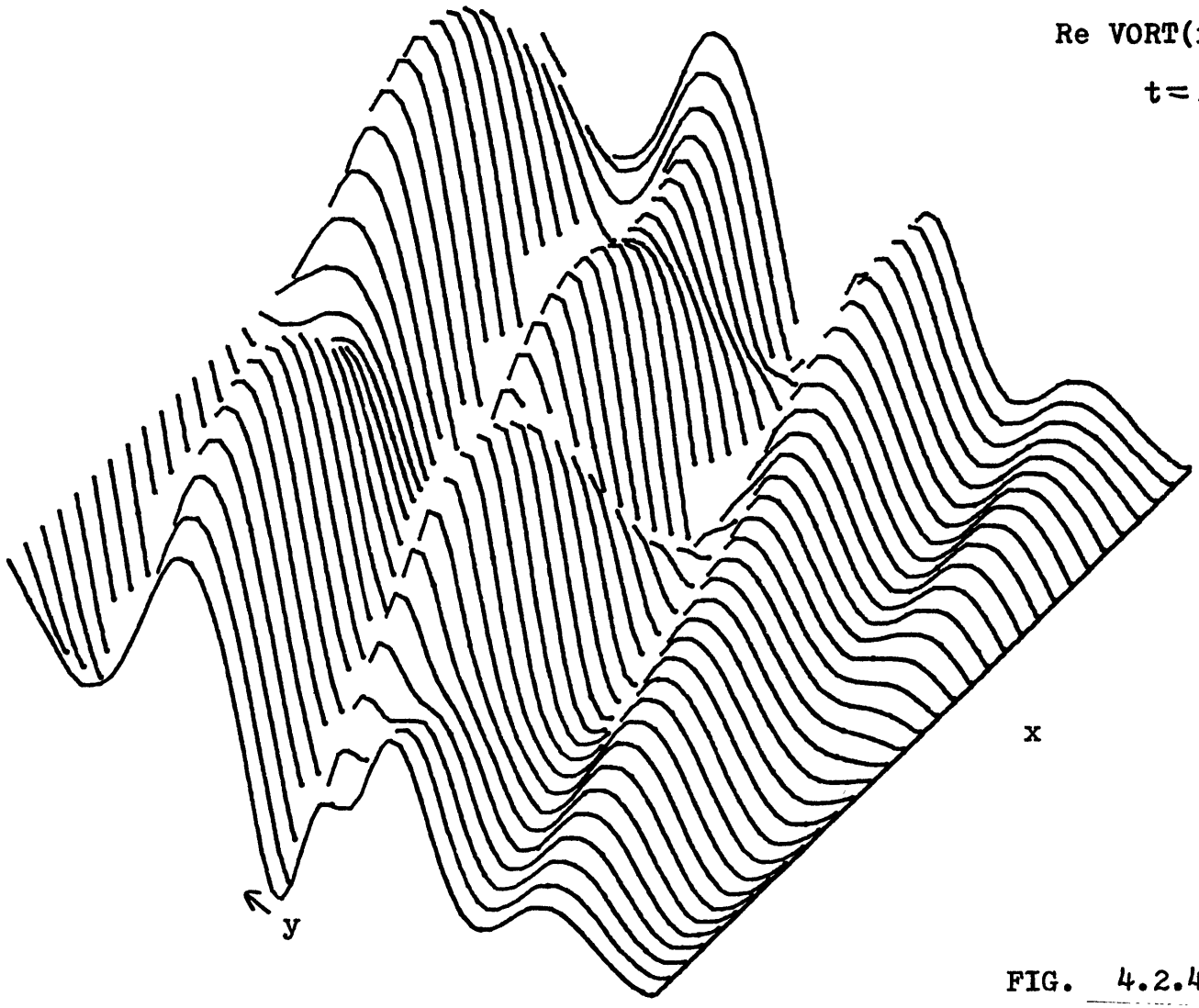

FIG. 4.2.42

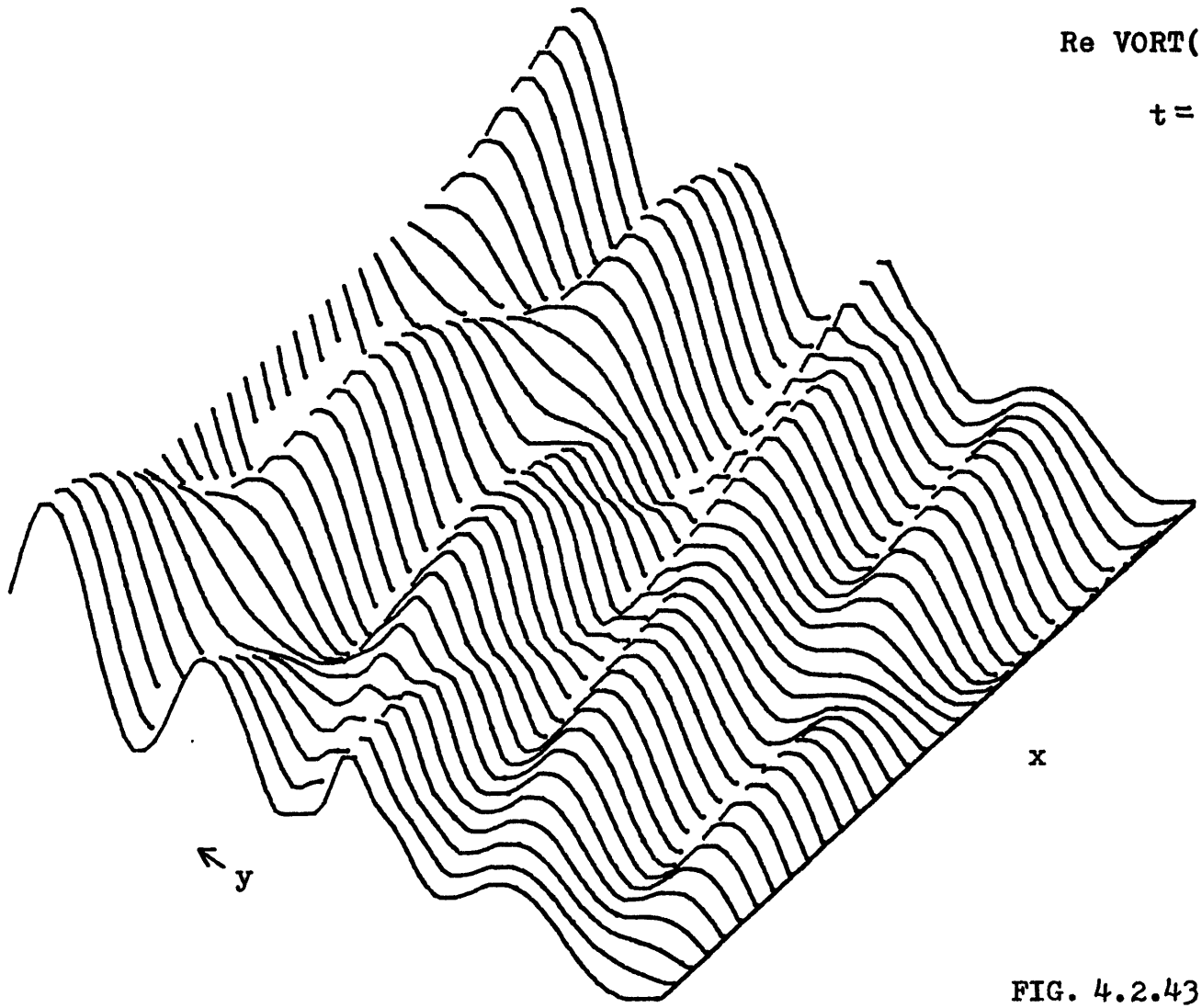

FIG. 4.2.43

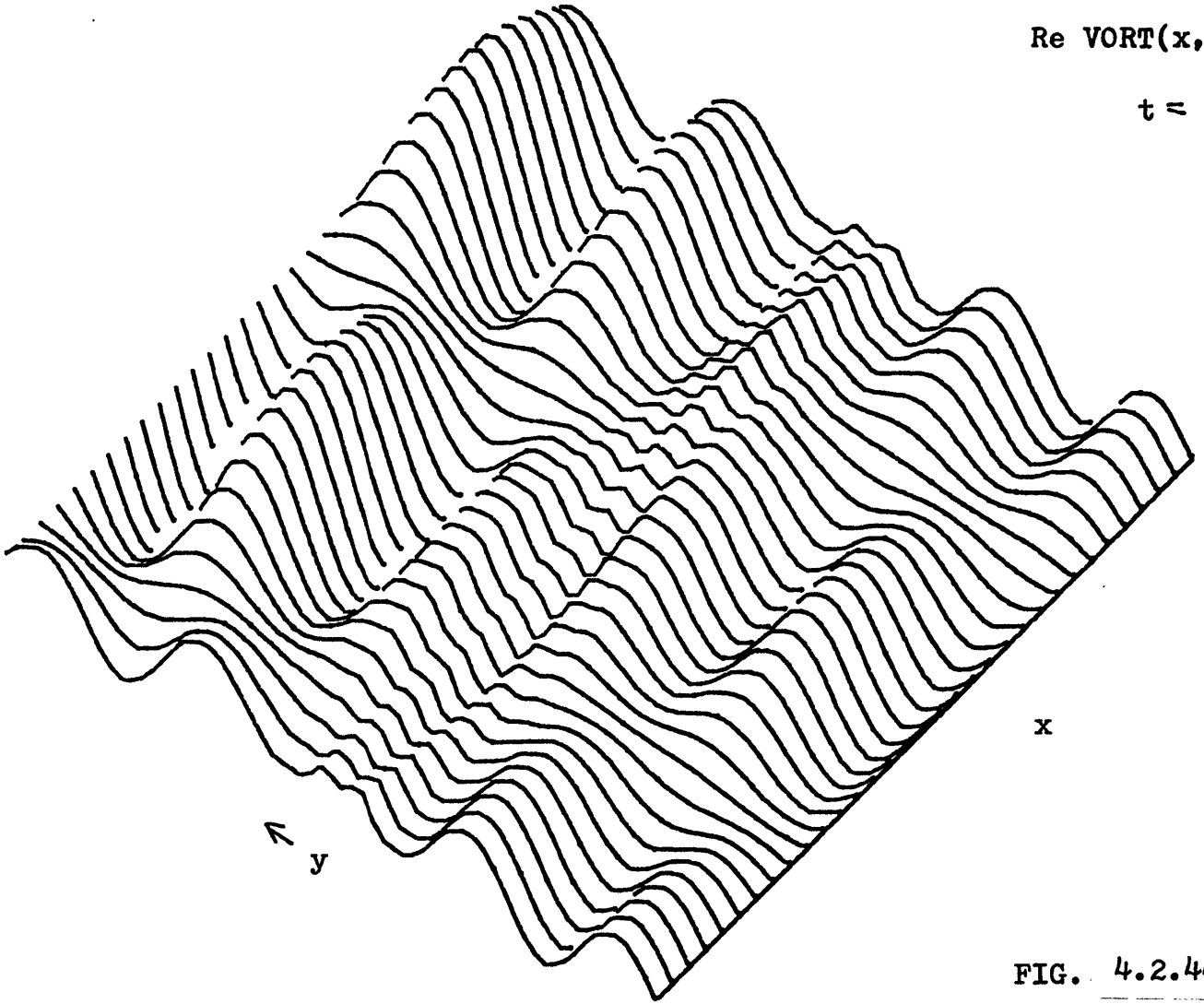

FIG. 4.2.44

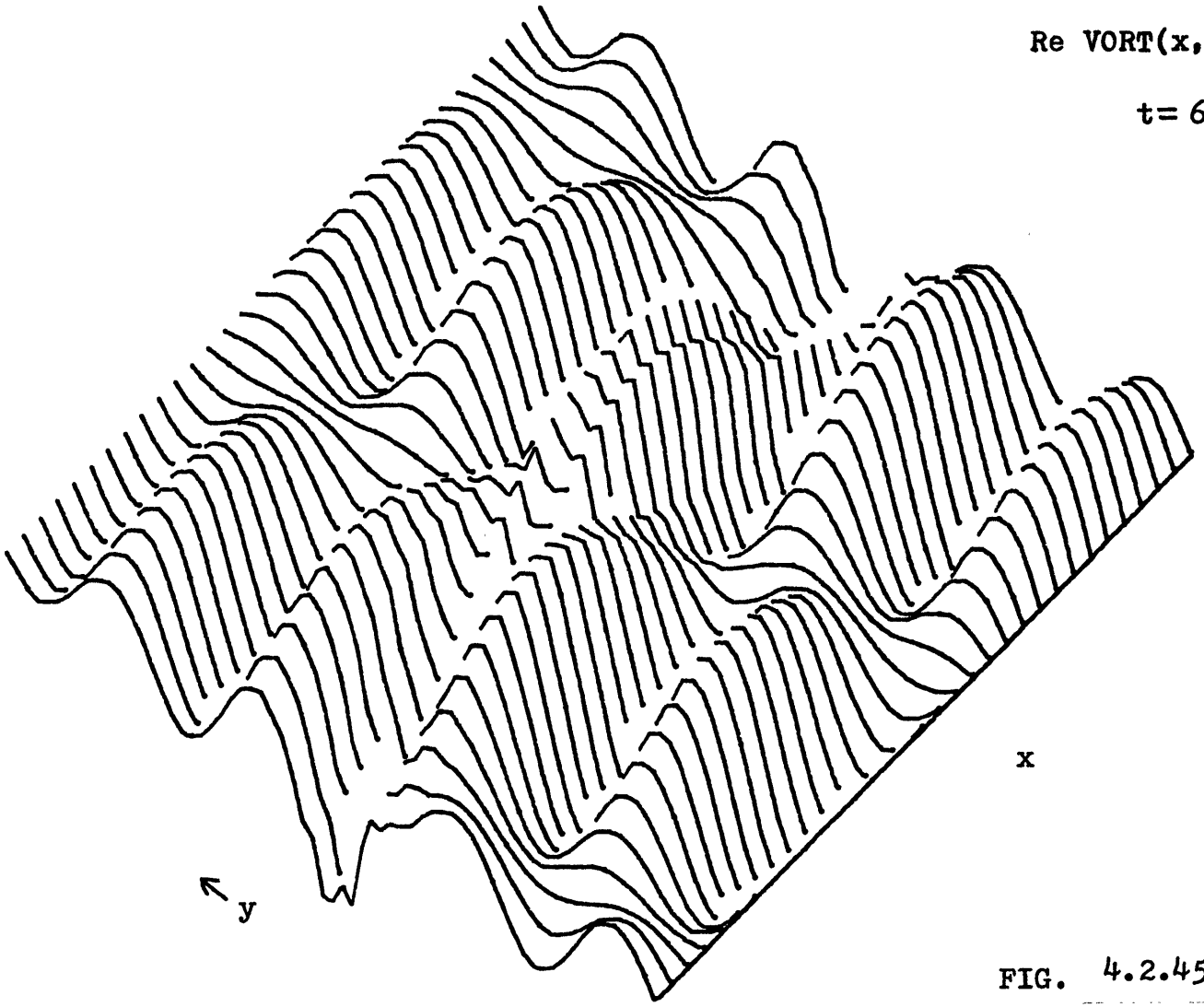

FIG. 4.2.45

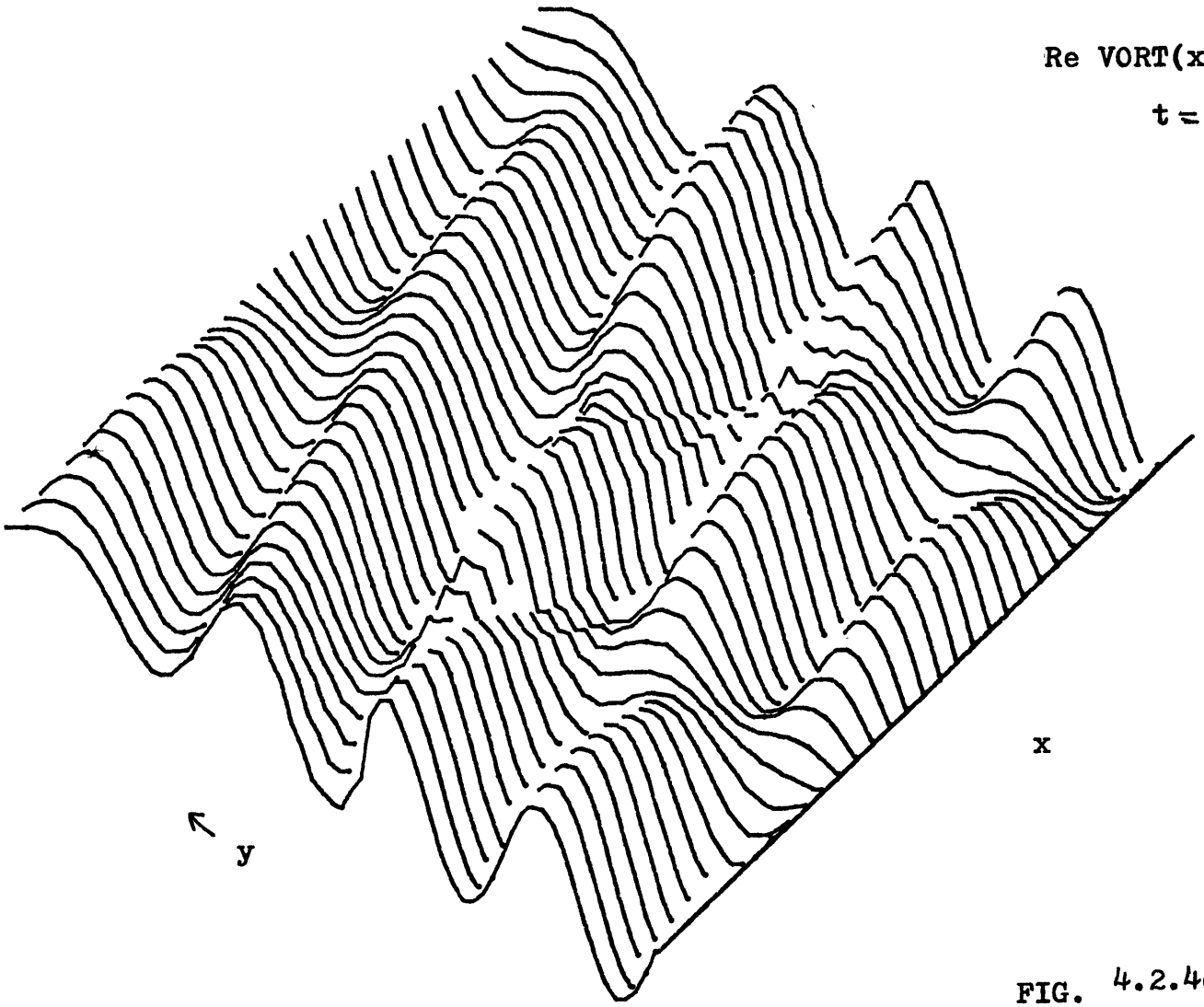

FIG. 4.2.46

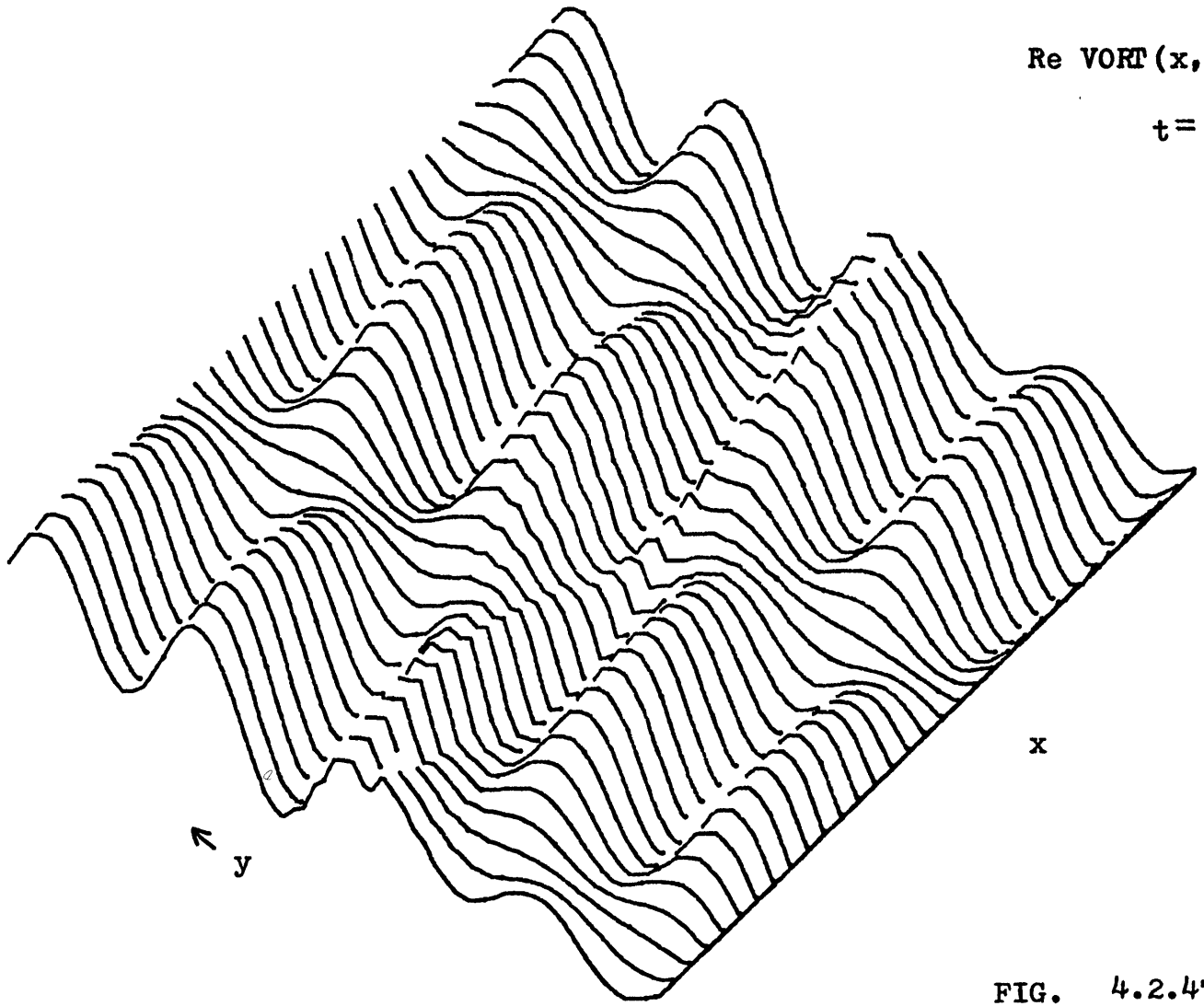

FIG. 4.2.47

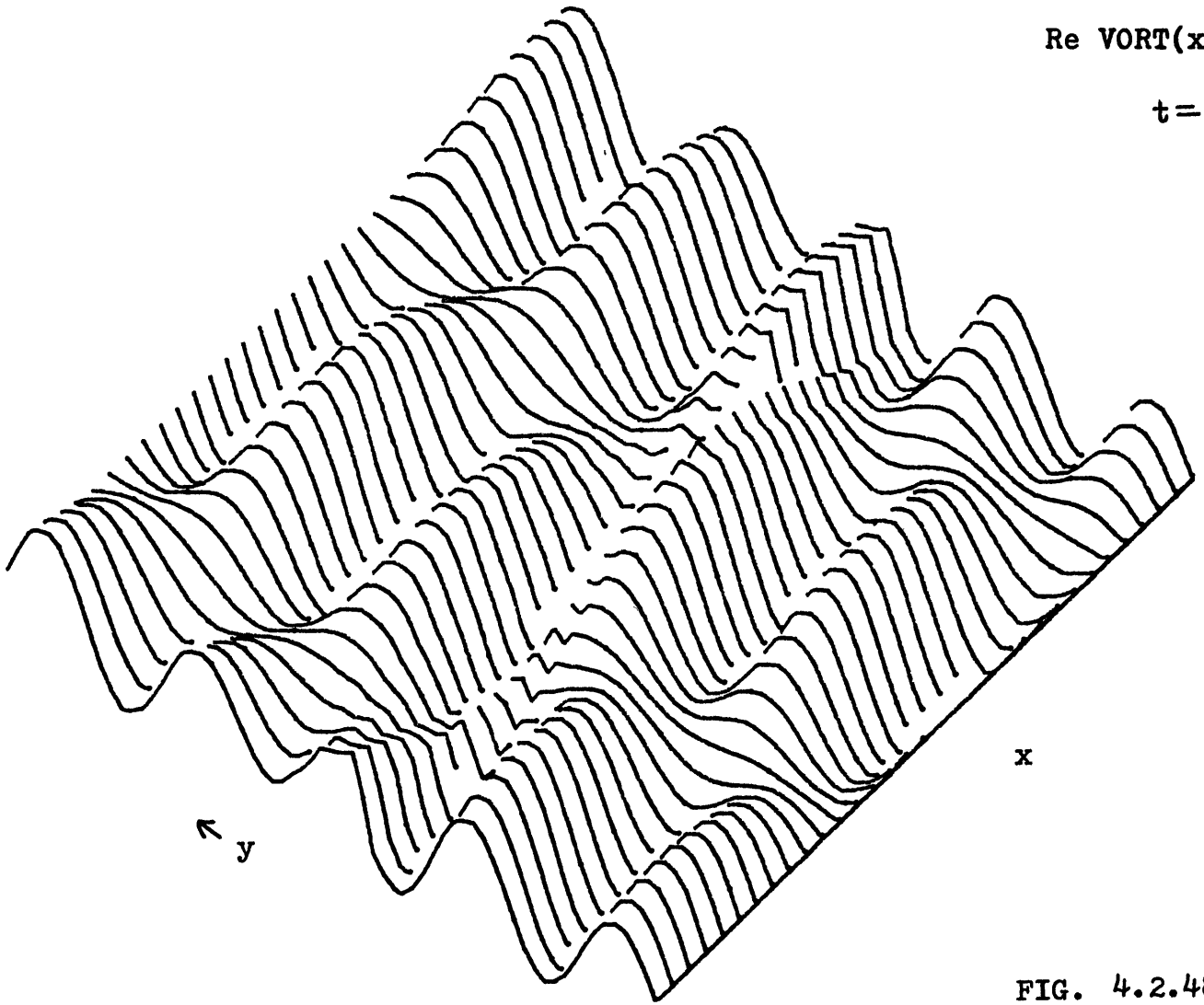

FIG. 4.2.48

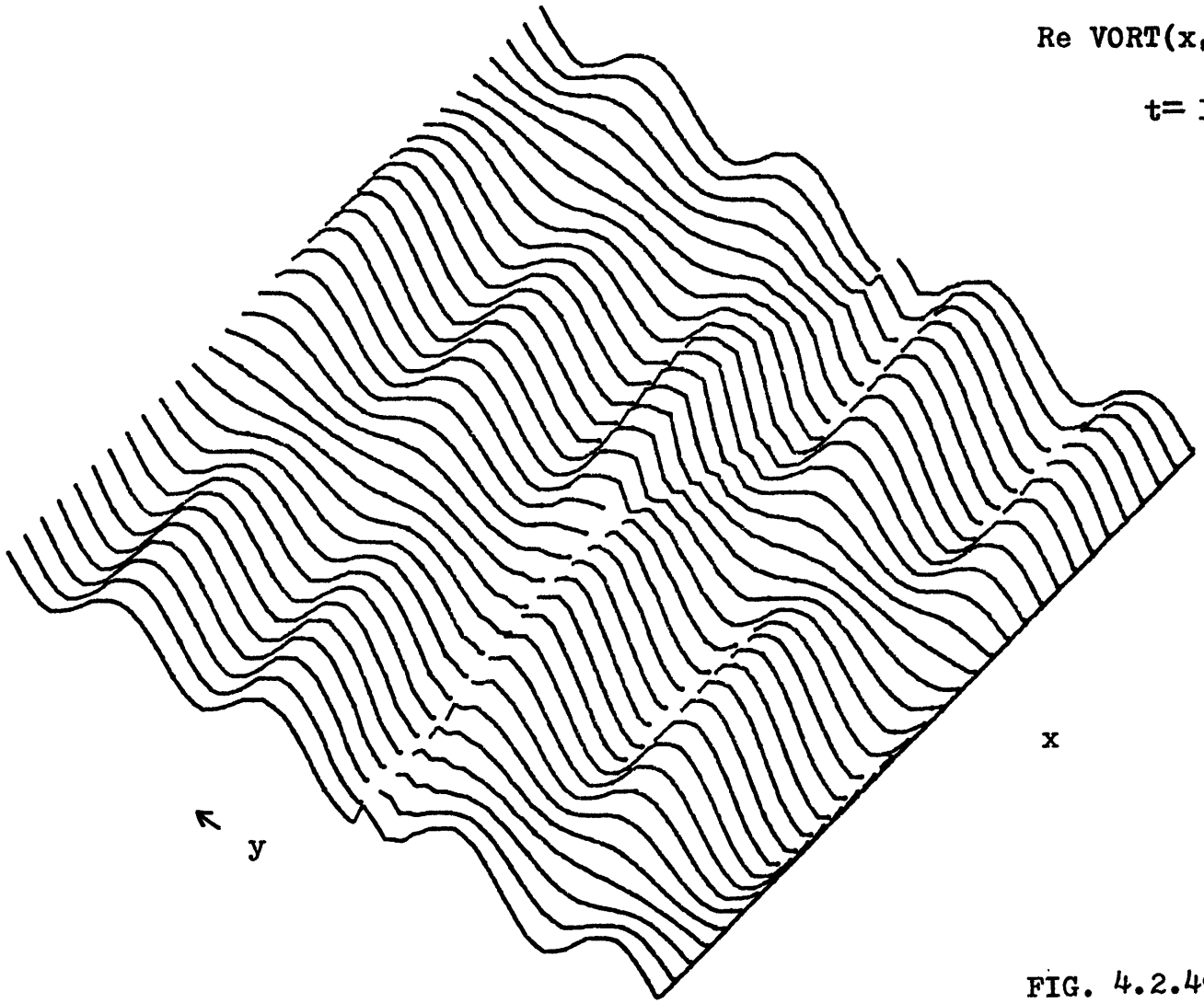

FIG. 4.2.49

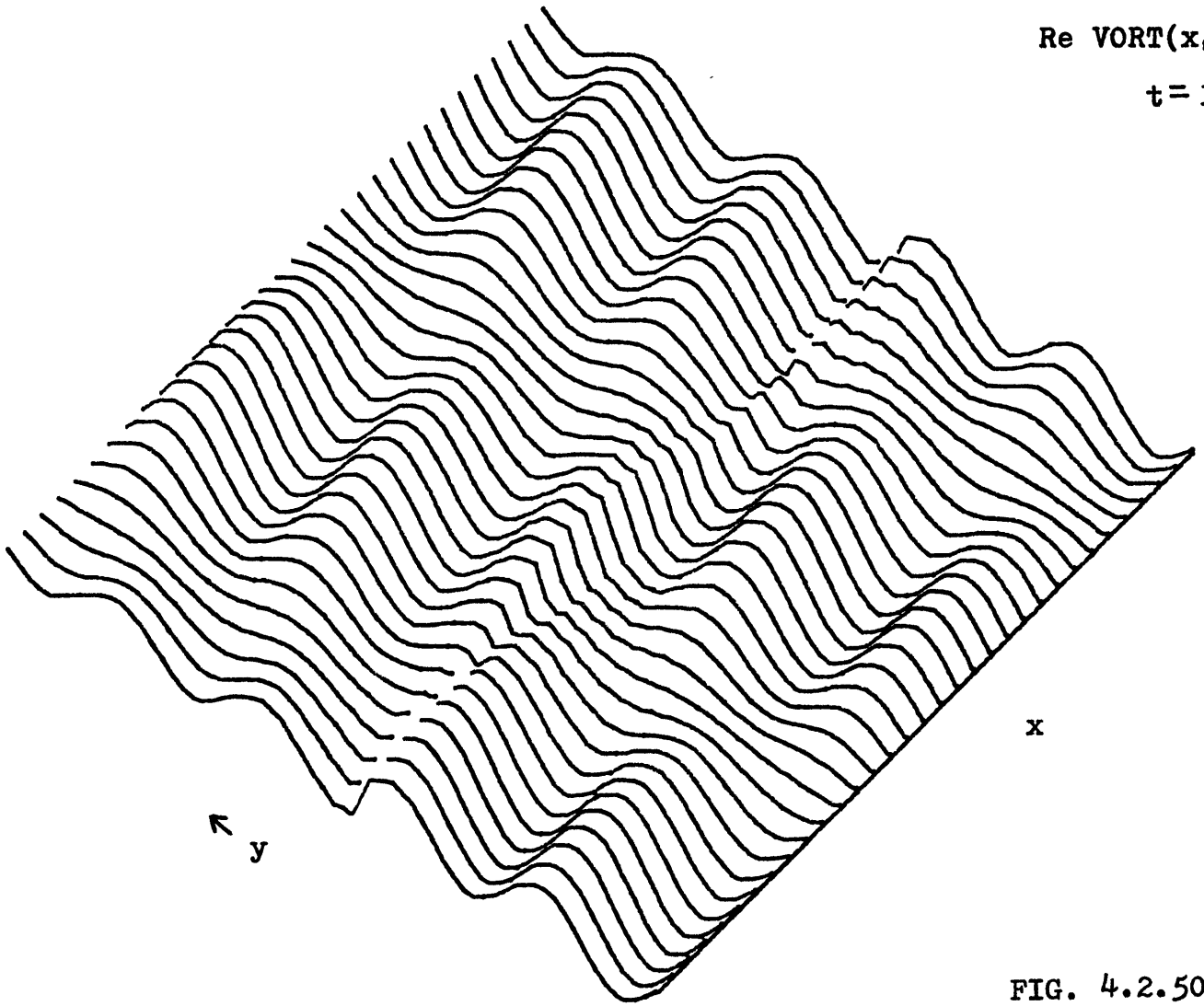

FIG. 4.2.50

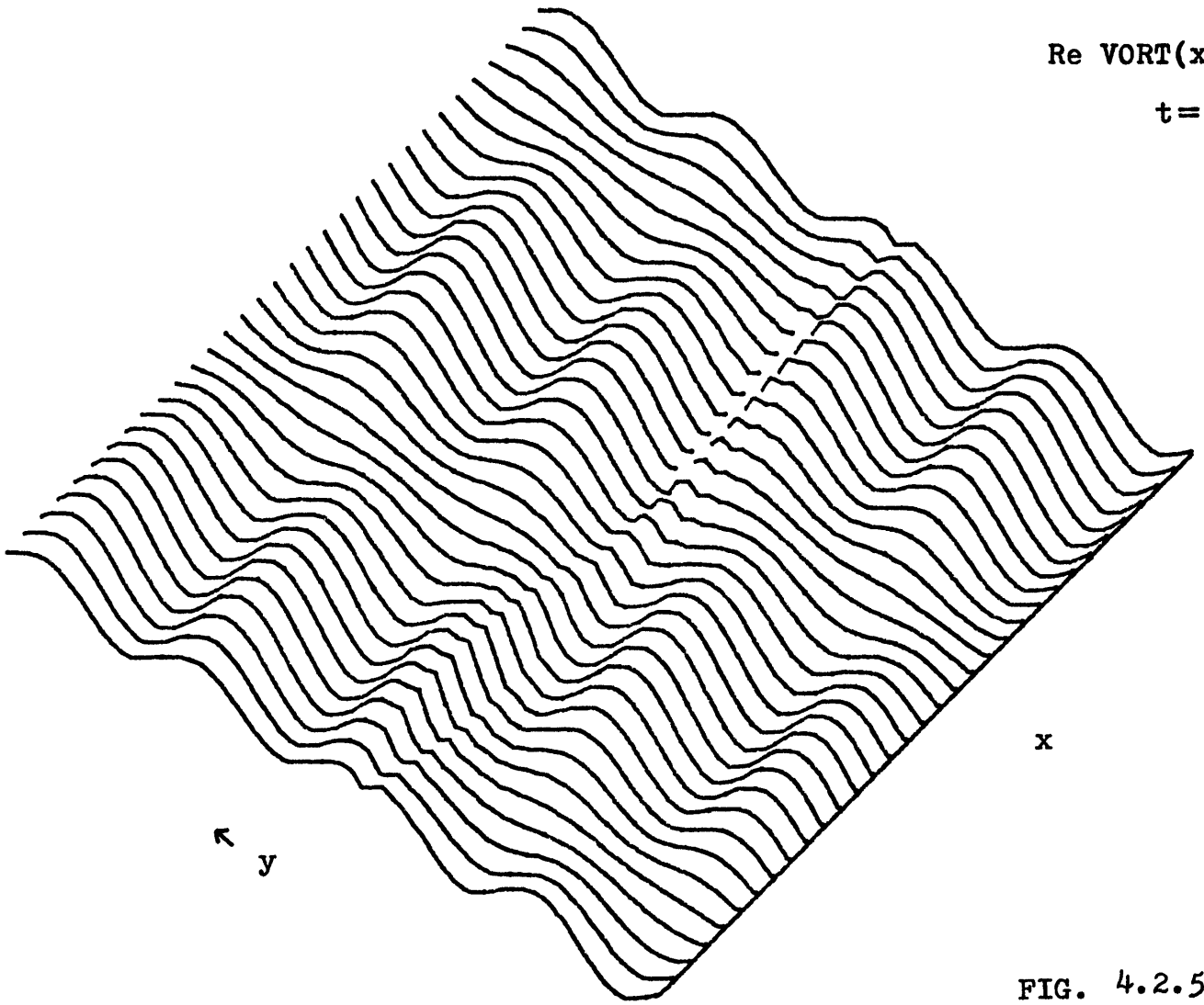

FIG. 4.2.51

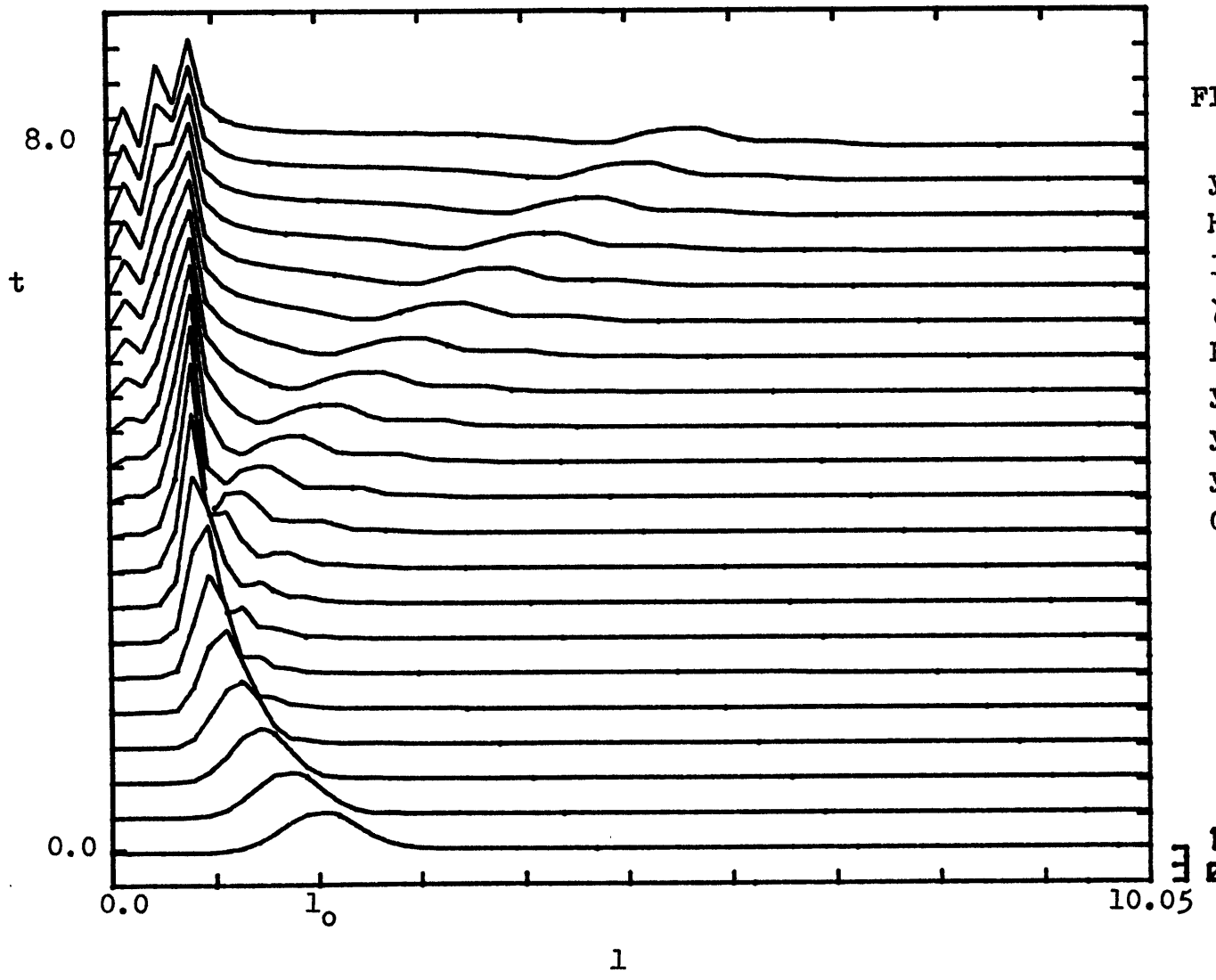

FIG. 4.2.52

$y_o = 11.0$
$H = 2.0$
$l_o = 2.0$
$\gamma = 1.5$
$B = -15.0$
$y_c \cong 10.7$
$y_{Tu} \cong 8.6$
$y_B = 10.0$
$C_{gy} \cong 0.24$
$k = 1.0$

|VORT(l,t)|

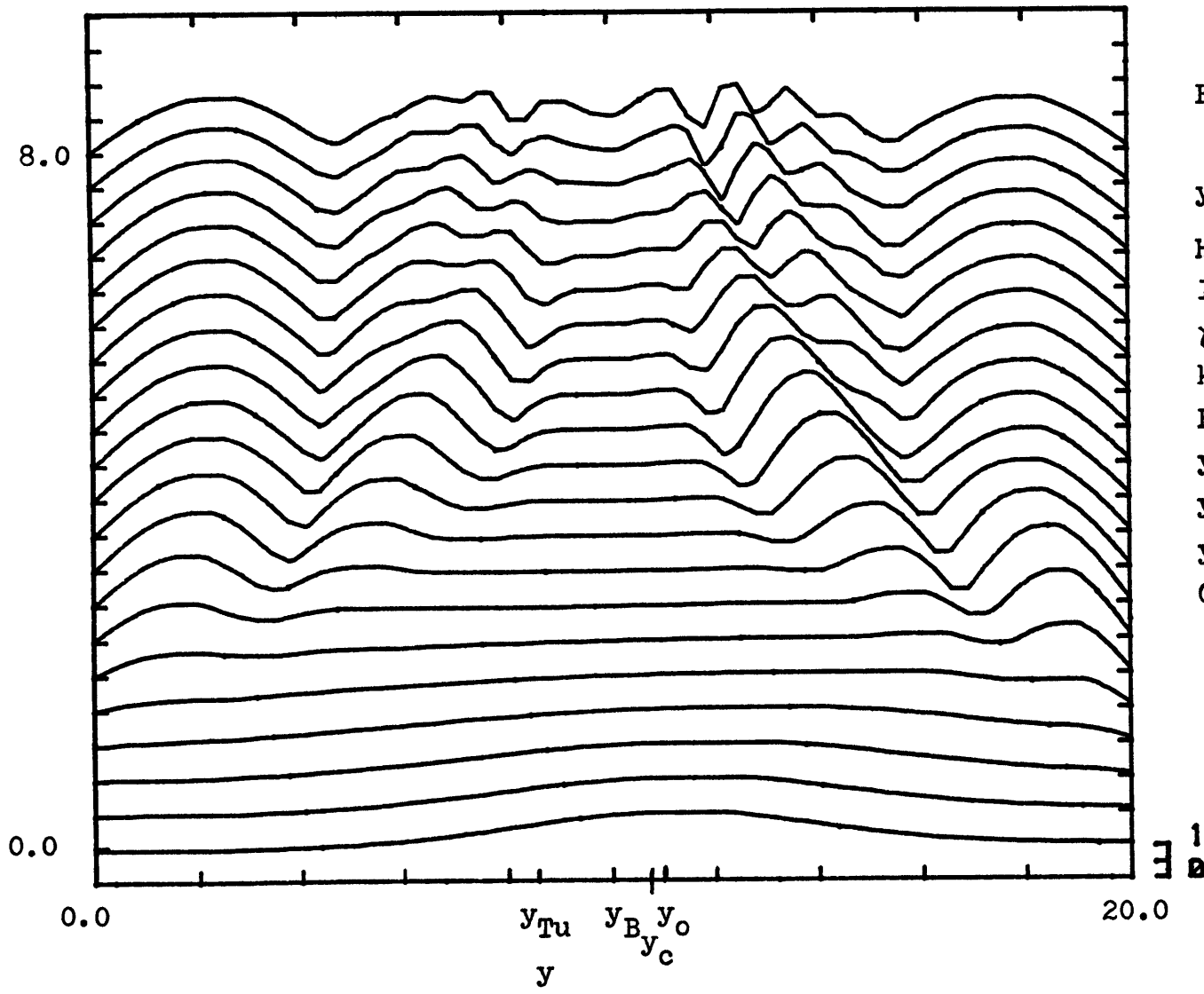

FIG. 4.2.53

$y_o = 11.0$
$H = 2.0$
$l_o = 2.0$
$\gamma = 1.5$
$k = 1.0$
$B = -15.0$
$y_c \cong 10.7$
$y_{Tu} \cong 8.6$
$y_B = 10.0$
$C_{gy} \cong 0.24$

|VORT(y,t)|

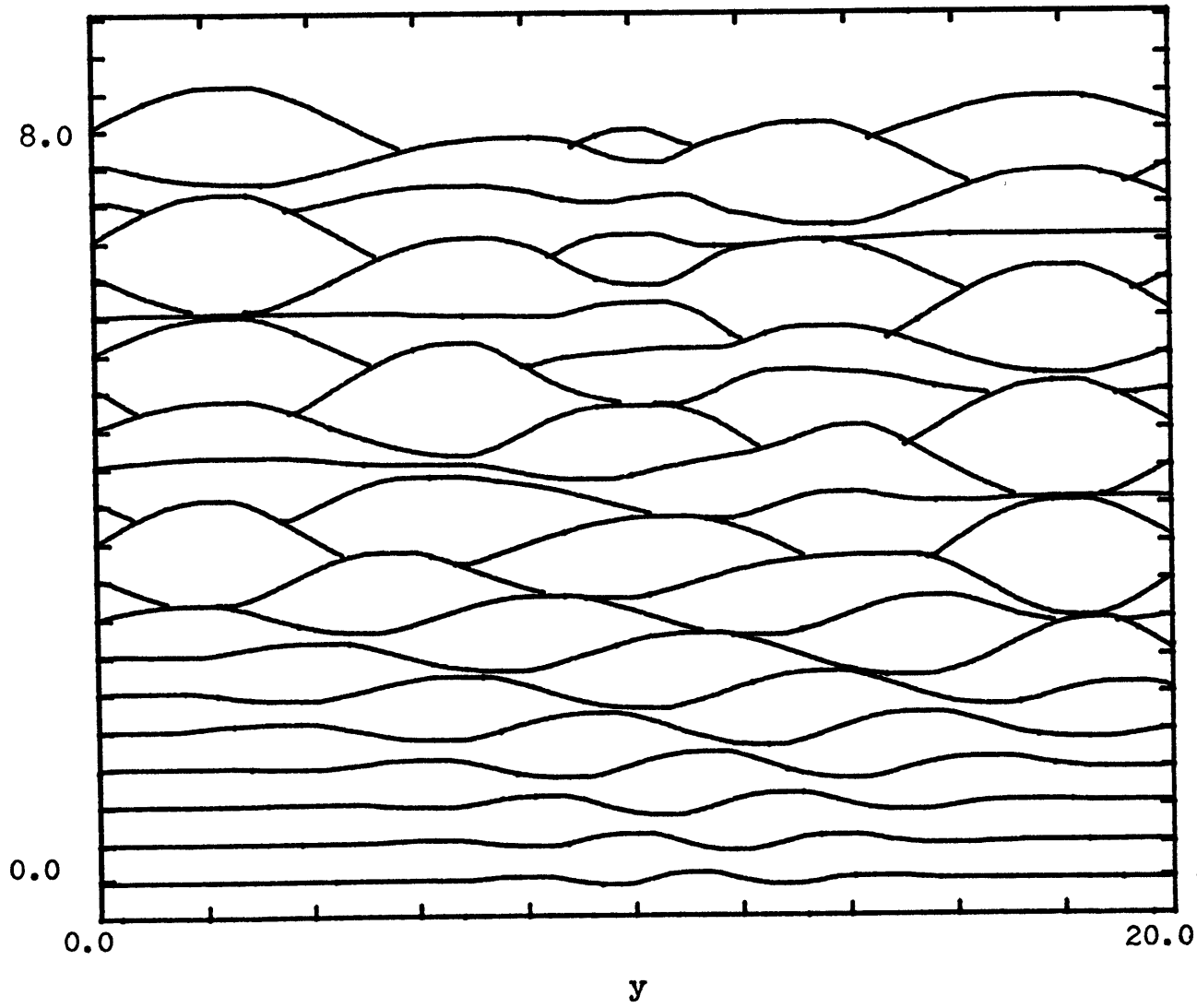

FIG. 4.2.54

$y_o = 11.0$
$H = 2.0$
$l_o = 2.0$
$\gamma = 1.5$
$k = 1.0$
$B = -15.0$
$y_c \cong 10.7$
$y_{Tu} \cong 8.6$
$y_B = 10.0$
$C_{gy} \cong 0.24$

Re (sf(y,t))

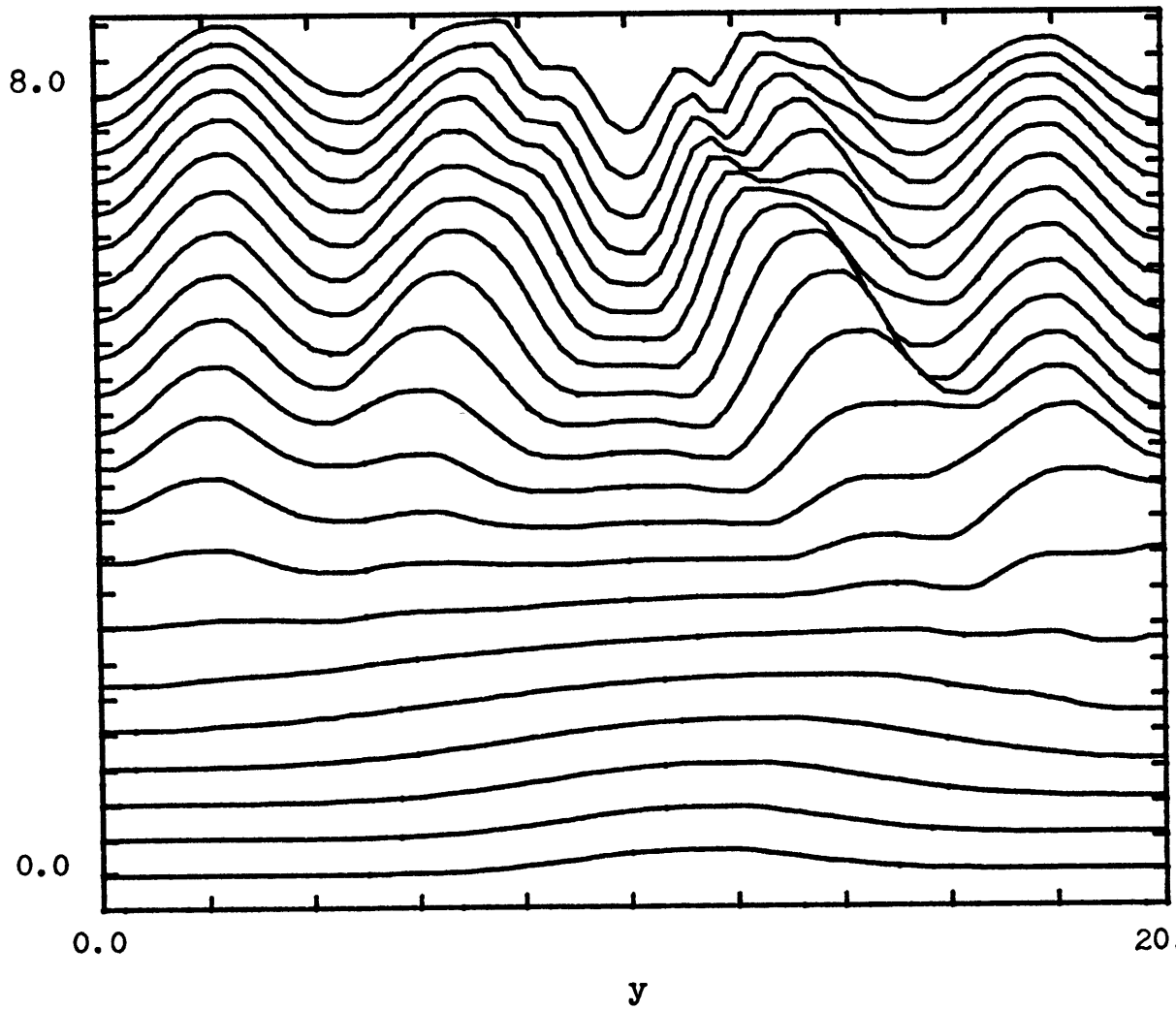

FIG. 4.2.55

$y_o = 11.0$
$H = 2.0$
$l_o = 2.0$
$\gamma = 1.5$
$B = -15.0$
$k = 1.0$
$y_c \cong 10.7$
$y_{Tu} \cong 8.6$
$y_B = 10.0$
$C_{gy} \cong 0.24$

E(y,t)

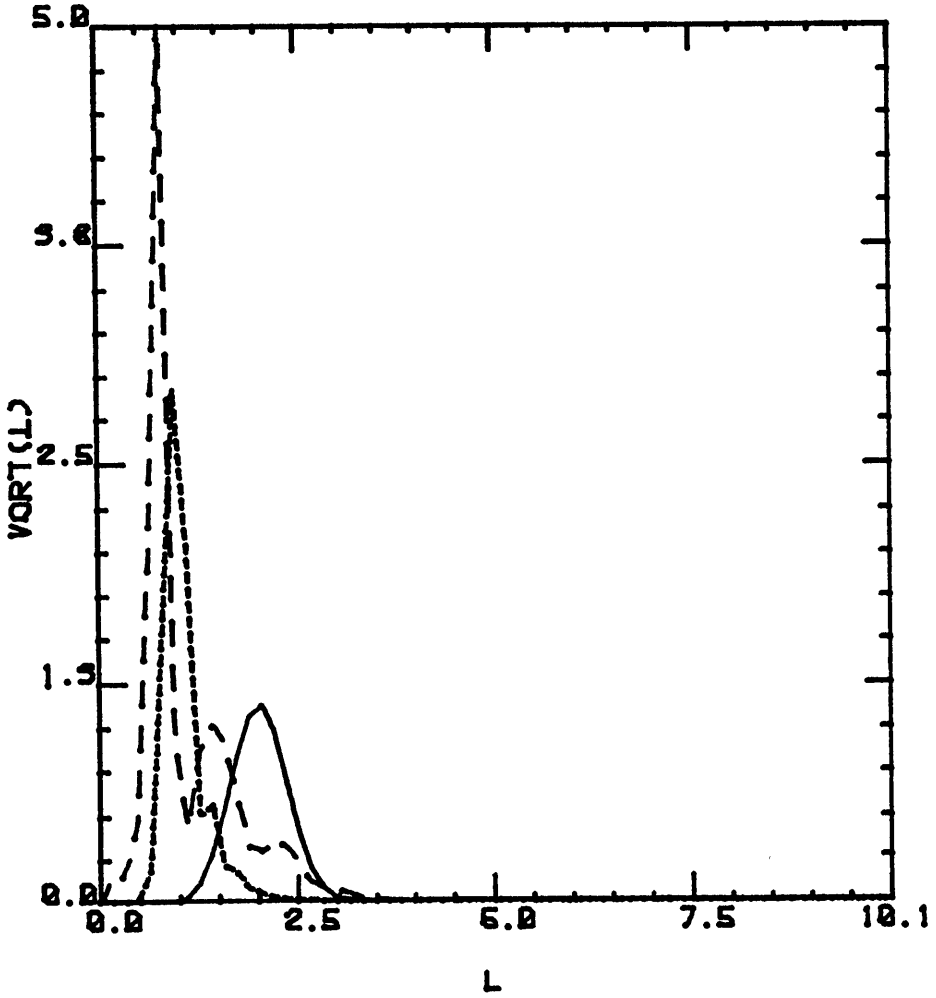

FIG. 4.2.56

$y_o = 11.0$
$H = 2.0$
$l_o = 2.0$
$\gamma = 1.5$
$k = 1.0$
$B = -15.0$
$y_c \cong 10.7$
$y_{Tu} \cong 8.6$
$y_B = 10.0$
$C_{gy} \cong 0.24$

—— T = 0.0
---- T = 2.0
– – – T = 4.0

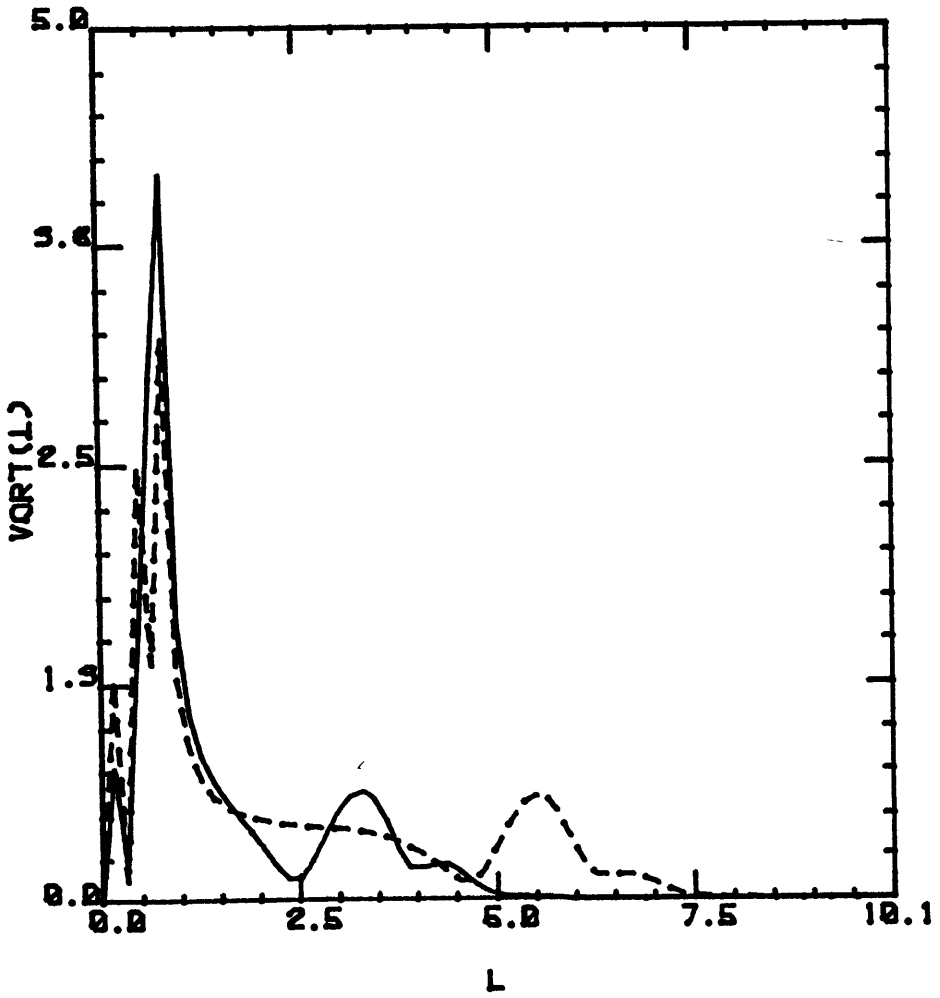

FIG. 4.2.57

$y_o = 11.0$
$H = 2.0$
$l_o = 2.0$
$\gamma = 1.5$
$k = 1.0$
$B = -15.0$
$y_c \cong 10.7$
$y_{Tu} \cong 8.6$
$y_B = 10.0$
$C_{gy} \cong 0.24$

——— T 6.0
----- T 8.0

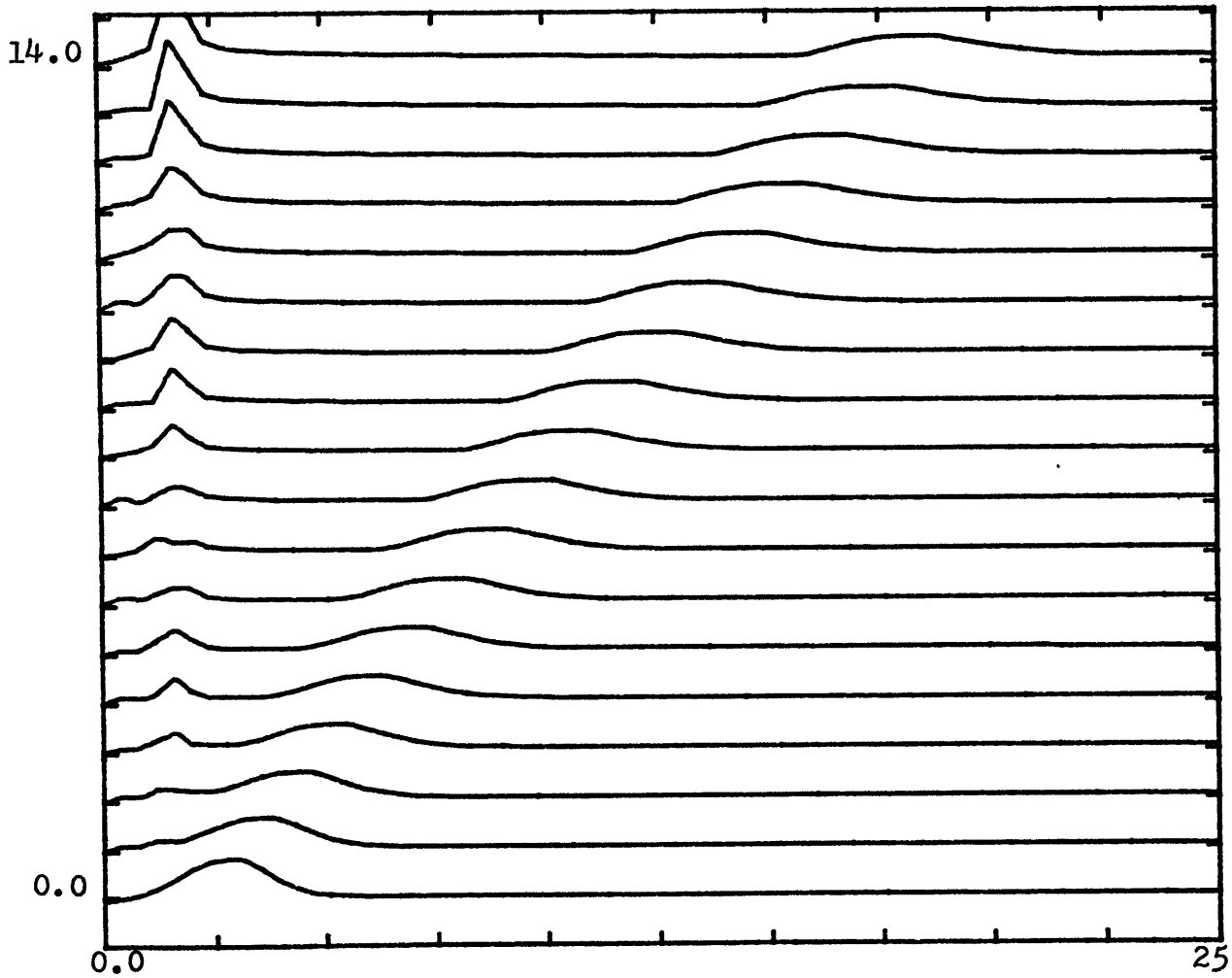

FIG. 4.2.58

$y_o = 5.0$
$H = 0.75$
$l_o = 2.67$
$\gamma = 4.06$
$k = -1.0$
$B = -12.17$
$y_c \cong 4.0$
$y_{Tu} \cong 2.67$
$y_B = 3.0$
$C_{gy} \cong -0.66$

|VORT(l,t)|

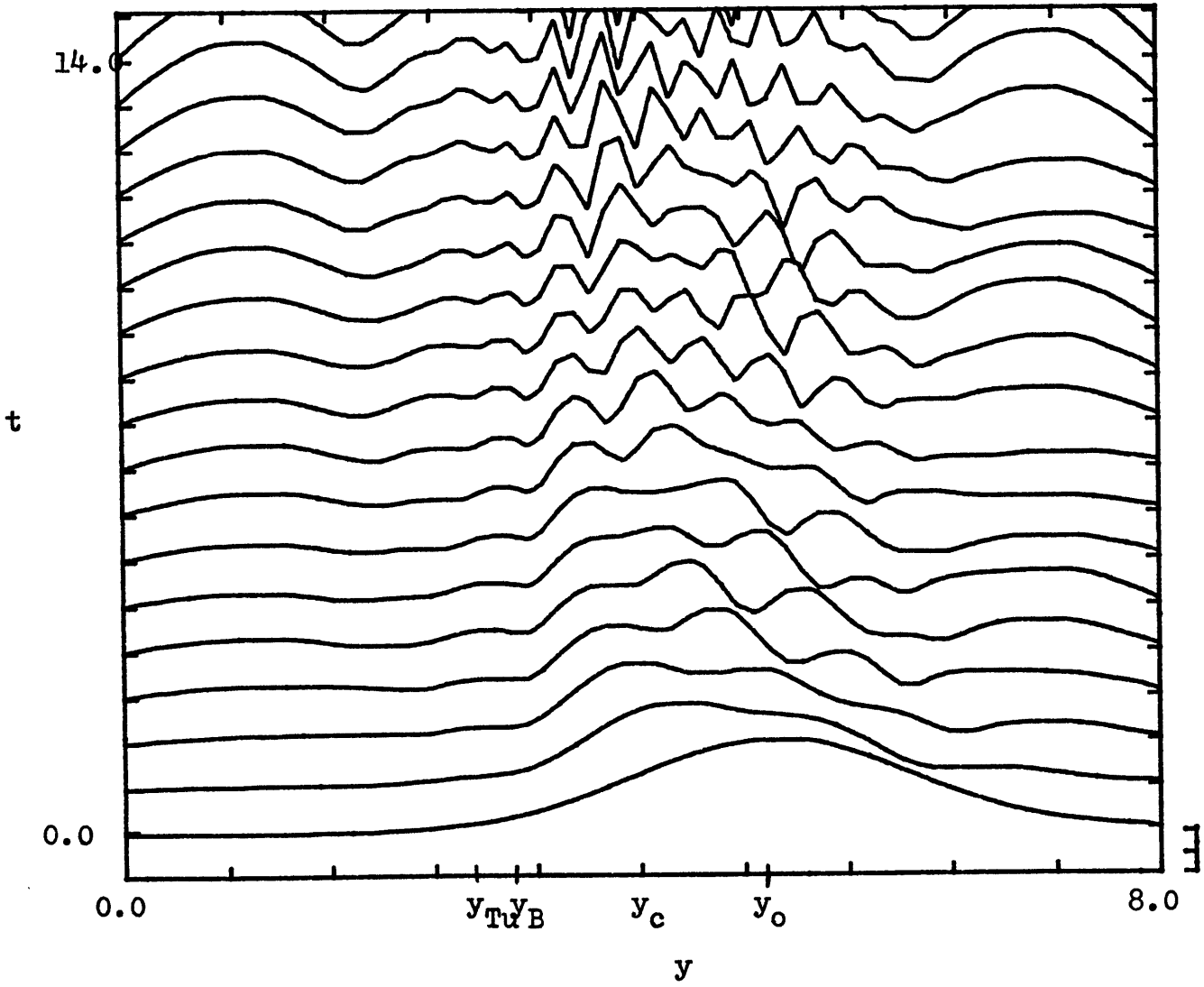

FIG. 4.2.59

$y_o = 5.0$
$H = 0.75$
$l_o = 2.67$
$\gamma = 4.06$
$k = -1.0$
$B = -12.17$
$y_c = 4.0$
$y_{Tu} = 2.67$
$y_B = 3.0$
$C_{gy} = -0.66$

|VORT(y,t)|

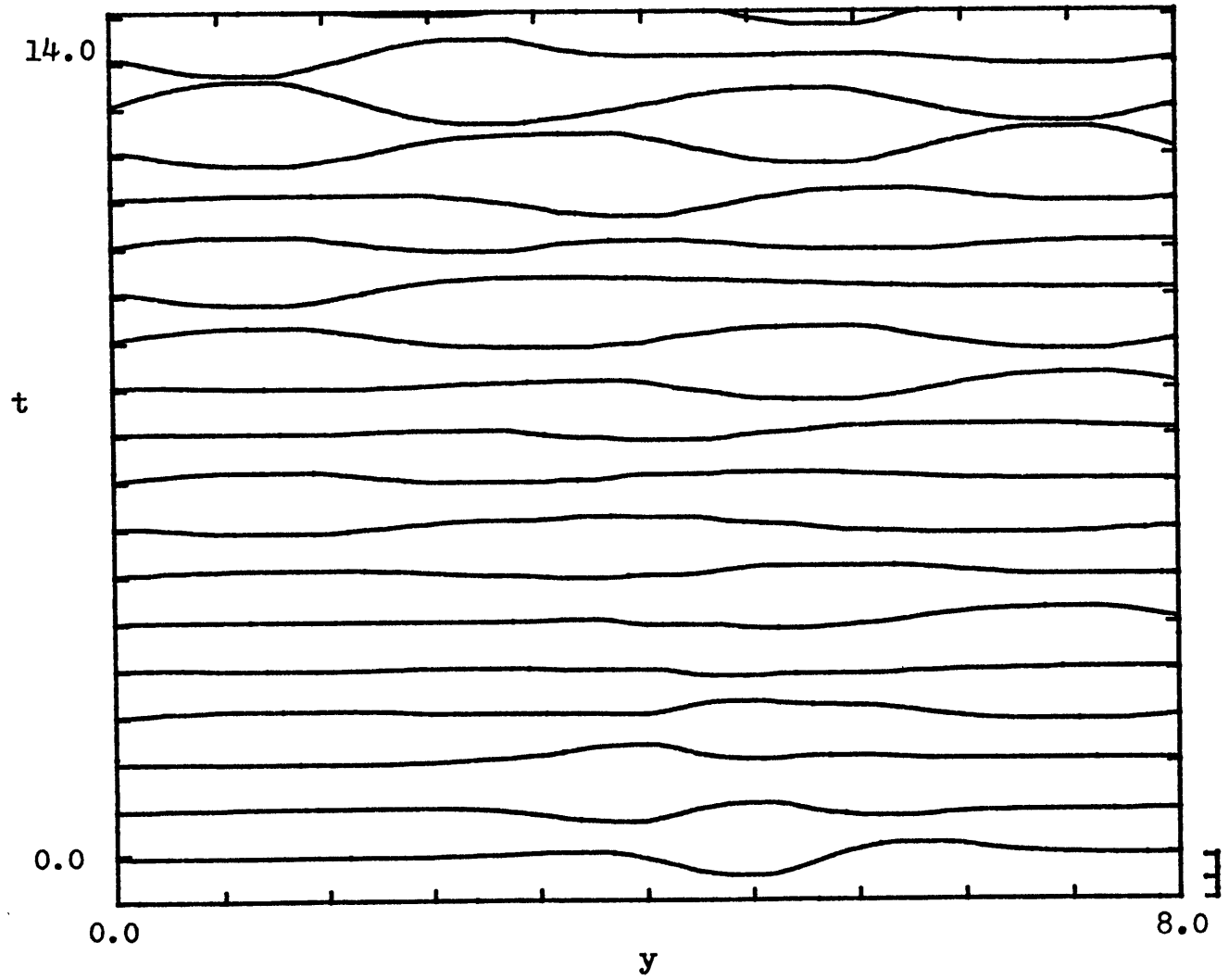

FIG. 4.2.60

$y_o = 5.0$
$H = 0.75$
$l_o = 2.67$
$\gamma = 4.06$
$k = -1.0$
$B = -12.17$
$y_c \cong 4.0$
$y_{Tu} \cong 2.67$
$y_B = 3.0$
$C_{gy} \cong -0.66$

Re (sf(y,t))

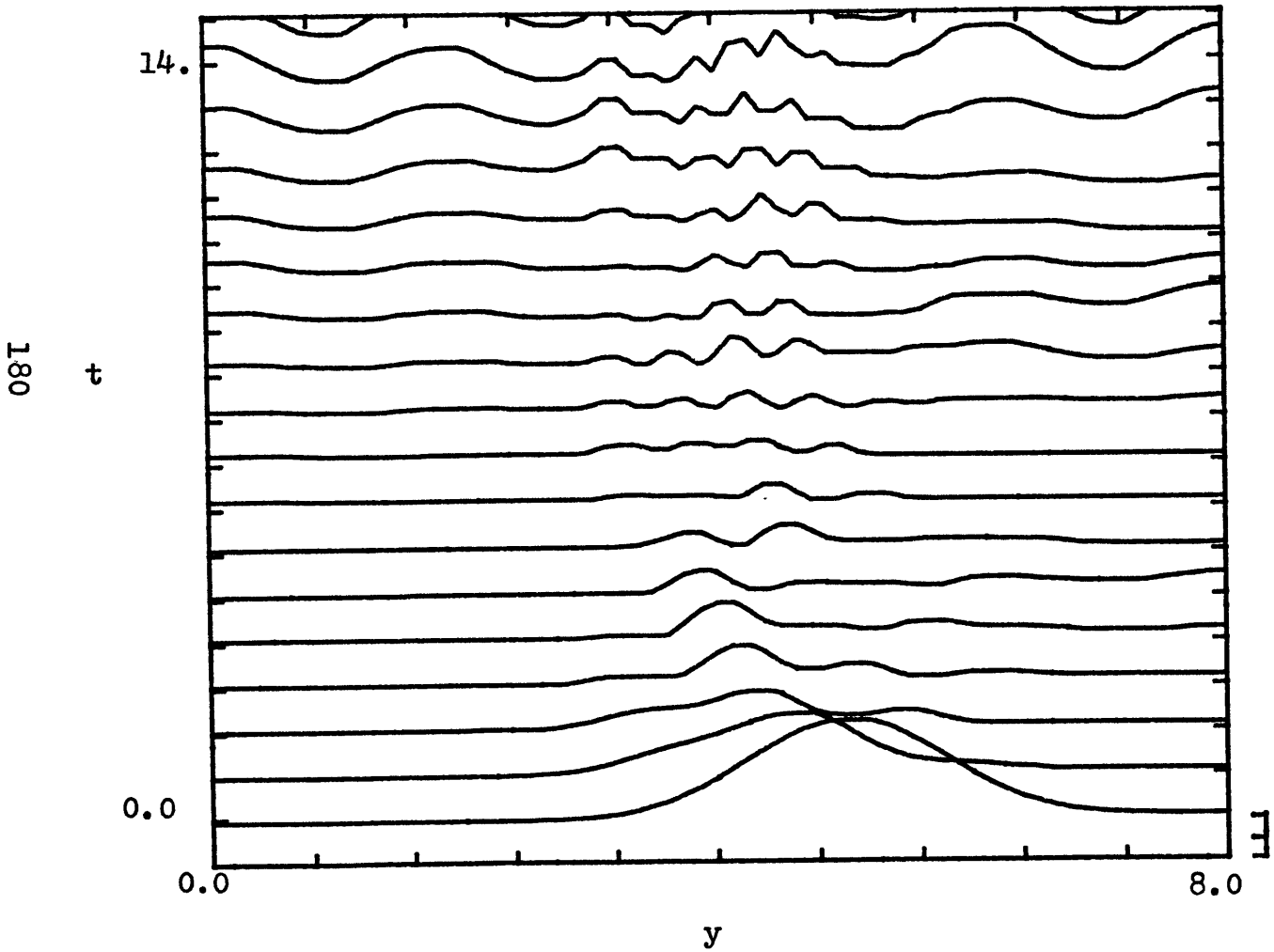

FIG. 4.2.61

$y_o = 5.0$
$H = 0.75$
$l_o = 2.67$
$\gamma = 4.06$
$k = -1.0$
$B = -12.17$
$y_c \cong 4.0$
$y_{Tu} \cong 2.67$
$y_B = 3.0$
$C_{gy} \cong -0.66$

E(y,t)

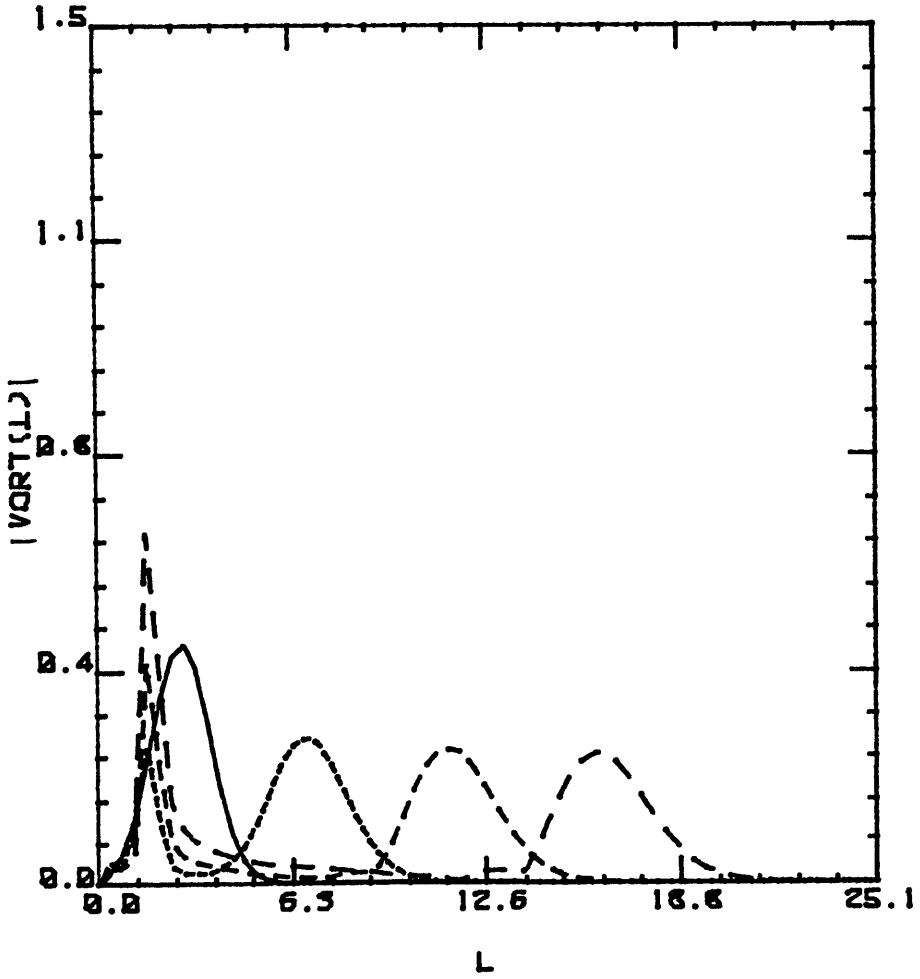

FIG. 4.2.62

$y_o = 5.0$
$H = 0.75$
$l_o = 2.67$
$\gamma = 4.06$
$k = -1.0$
$B = -12.17$
$y_c \cong 4.0$
$y_{Tu} \cong 2.67$
$y_B = 3.0$
$C_{gy} \cong -0.66$

—— T=0.0
---- T 4.0
--- T 8.0
—— T 12.0

V. CONCLUSION

For the Couette flow with and without β-effect, it has been shown that, provided the effect of the walls are not felt (i.e. there is first a turning point y_T and then a critical level on the trajectory of the wave or there is a critical level on the direct trajectory of the wave) then the solution in the finite domain is basically the same as the one obtained by Worsham (1983) and Tung (1983). The numerical values of y_c and y_T as predicted by Tung have been shown to be accurate. When the effect of the walls is not present, only transient waves make up the Fourier spectrum and the l-scale is continuously changing due to the effect of the shear. Transient waves which have l's increasing in time are associated with the decaying part of the wave. When the effect of the walls is present, i.e. when only y_T is inside the domain or when both y_c and y_T are outside the domain, it is possible for normal modes to be set up. Since there is no inflection point in the profile, only neutral waves with phase speed $c_r < U_{min}$ can develop.

The way in which the effect of the walls is shown in the Fourier spectrum is by the presence of the development of distinct peaks for fixed low wavenumbers indicating the presence of coherent structures in physical space. The waves in physical space change constantly with time and this is due to the presence of different phase speeds.

The part of the Fourier spectrum associated with the decay of the wave fades away with time.

For $U=\alpha y$ with β-effect and with an inflection point, the formulaes predicting y_c and the initial group velocity of the wave packet have been modified to contain the inflection point. The numerical estimates of y_c and C_{gy} have been shown to be accurate.

The prediction of y_c and the overreflection theory applied at $t=0$ have been shown to be able to predict qualitatively the time-evolution of the initial condition.

If one considers a wave-packet as a sum of delta functions, then to each l in the spectrum corresponds a $y_c(l)$. A necessary initial condition to have instability is that some l's will have propagating waves which will see the "inflection point" before seeing the critical level where overreflection takes place. This agrees with the fact that instability occurs provided there is a projection of the initial condition onto the normal mode.

It has also been shown that neutral modes (with c_r inside the range of U) have a wavenumber called l_φ which maximizes the function in Fourier space. l_φ can be estimated by using the same formula as for y_c (i.e. critical level located at the inflection point).

One can also estimate such a l_φ for unstable normal modes since then c_r is close to y_B (in non-dimensional

units).

If at t=0, there is no projection of the initial condition onto the normal modes (i.e. if l_φ is smaller than all the l's which make up the initial condition) and if $l_o/K>0$, then an unstable wave can still develop, although slowly, after the packet has a chance to reflect from the walls. The wall reflection produces new l's which have the correct configuration for overreflection.

When the waves grow unstable, a stationary part of the Fourier spectrum can be observed, giving stationary waves in the physical domain. Neutral waves which have c_r inside the limits of U also have a stationary part to the Fourier spectrum.

Further studies would be necessary to be able to find a way of observing how successive overreflections can quantize the waves.

TABLES 1-5
TOTAL ENERGY E(t)

TABLE#	1	2	3	4	5
TIME STEP	$t\epsilon(0,8)$	$t\epsilon(0,8)$	$t\epsilon(0,8)$	$t\epsilon(0,8)$	$t\epsilon(0,3)$
1	1.38 E-02	1.84 E-02	8.43 E-03	8.43 E-03	1.29 E-02
2	1.38 "	2.10 "	1.20 E-02	6.18 "	1.12 "
3	1.38 "	2.41 "	1.75 "	4.72 "	9.74 E-03
4	1.37 "	2.76 "	2.52 "	3.72 "	8.57 "
5	1.37 "	3.18 "	3.39 "	3.01 "	7.59 "
6	1.36 "	3.66 "	4.09 "	2.49 "	6.77 "
7	1.36 "	4.22 "	4.31 "	2.01 "	6.08 "
8	1.35 "	4.87 "	3.93 "	1.78 "	5.49 "
9	1.35 "	5.64 "	3.18 "	1.54 "	5.00 "
10	1.35 "	6.57 "	2.38 "	1.34 "	4.55 "
11	1.35 "	7.64 "	1.72 "	1.18 "	4.17 "
12	1.35 "	8.88 "	1.26 "	1.05 "	3.84 "
13	1.35 "	0.101	9.43 "	9.35 E-04	3.55 "
14	1.36 "	0.118	7.23 E-03	8.40 "	3.29 "
15	1.36 "	0.137	5.66 "	7.59 "	3.06 "
16	1.36 "	0.158	4.53 "	6.90 "	2.86 "
17	1.37 "	0.183	3.69 "	6.29 "	2.68 "
18	1.37 "	0.213	3.06 "	5.76 "	2.51 "
19	1.37 "	0.247	2.57 "	5.29 "	2.36 "
20	1.37 "	0.287	2.19 "	4.89 "	2.23 "
21	1.37 "	0.334	1.88 "	4.52 "	2.11 "
TOL	1.0 E-05	1.0 E-04	1.0 E-04	1.0 E-08	1.0 E-05

TABLES 6-10
TOTAL ENERGY E(t)

TABLE #	6	7	8	9	10
TIME STEP	$t\epsilon(0, 8)$	$t\epsilon(0, 6.8)$	$t\epsilon(0, 6.4)$	$t\epsilon(0, 6.8)$	$t\epsilon(0, 5.6)$
1	1.29 E-02	3.22 E-02	1.29 E-02	1.29 E-02	1.94 E-03
2	1.94 "	4.84 "	9.76 E-03	1.90 "	1.32 E-03
3	3.08 "	5.66 "	9.16 E-03	1.97 "	9.13 E-04
4	4.62 "	4.94 "	1.03 E-02	1.41 "	6.52 "
5	5.70 "	3.50 "	1.20 E-02	1.06 "	4.81 "
6	5.44 "	2.52 "	1.30 "	9.77 E-03	3.66 "
7	4.11 "	2.15 "	1.31 "	1.04 E-02	2.88 "
8	2.68 "	2.12 "	1.28 "	1.14 "	2.33 "
9	1.73 "	2.22 "	1.27 "	1.23 "	1.95 "
10	1.17 "	2.36 "	1.24 "	1.28 "	1.68 "
11	8.43 E-03	2.55 "	1.26 "	1.28 "	1.49 "
12	6.38 "	2.62 "	1.23 "	1.29 "	1.35 "
13	5.02 "	2.69 "	1.23 "	1.29 "	1.24 "
14	4.08 "	2.82 "	1.24 "	1.24 "	1.138 "
15	3.40 "	2.75 "	1.28 "	1.26 "	1.04 "
16	2.90 "	2.67 "	1.28 "	1.24 "	
17	2.52 "	2.86 "	1.21 "	1.23 "	
18	2.22 "	2.95 "		1.27 "	
19	2.00 "				
20	1.80 "				
21	1.64 "				
TOL	1.0 E-05	1.0 E-05	1.0 E-05	1.0 E-05	1.0 E-08

TABLES 11-14
TOTAL ENERGY E(t)

TABLE #	11	12	13	14a	14b
TIME STEP	$t\epsilon(0, 6)$	$t\epsilon(0, 15)$	$t\epsilon(0, 15)$	$t\epsilon(0, 16)$	$t\epsilon(16, 32)$
1	1.29 E-02	1.51 E-02	1.51 E-02	4.55 E-03	0.228
2	9.71 E-03	8.14 E-03	2.76 "	2.73 "	0.289
3	7.47 E-03	7.47 "	4.21 "	4.35 "	0.364
4	5.86 "	9.93 "	5.72 "	6.18 "	0.483
5	4.68 "	1.16 E-02	7.57 "	7.48 "	0.648
6	3.81 "	1.14 "	9.95 "	8.28 "	0.880
7	3.15 "	1.31 "	0.128	1.04 E-02	1.16
8	2.64 "	1.97 "	0.165	9.18 E-03	1.51
9	2.24 "	2.87 "	0.214	7.39 E-03	1.95
10	1.92 "	3.71 "	0.273	1.03 E-02	2.52
11	1.67 "	4.64 "	0.346	1.62 "	3.346
12	1.46 "	6.01 "	0.454	2.39 "	4.49
13	1.28 "	7.88 E-02	0.615	2.86 "	6.03
14	1.14 "	0.104	0.815	3.51 "	7.80
15	1.02 E-03	0.141	1.04	4.01 "	10.5
16	9.13 E-04	0.188	1.35	4.56 "	13.7
17		0.241	1.80	6.89 "	18.0
18		0.306	2.42	8.52 E-02	23.9
19		0.410	3.17	0.121	31.9
20		0.561	4.11	0.158	42.4
21		0.739	5.40	0.202	56.1
TOL	1.0 E-08	1.0 E-08	1.0 E-08	1.0 E-08	1.0 E-04

TABLES 15-16
TOTAL ENERGY E(t)

TABLE #	15	16
TIME STEP	$t \epsilon (0, 8)$	$t \epsilon (0, 13.6)$
1	1.29 E-02	8.43 E-03
2	1.93 E-02	4.61 "
3	2.96 "	3.17 "
4	4.55 "	2.92 "
5	6.85 "	2.87 "
6	9.89 "	2.79 "
7	0.135	2.18 "
8	0.172	2.04 "
9	0.206	2.21 "
10	0.234	3.49 "
11	0.254	4.68 "
12	0.267	5.54 "
13	0.276	5.22 "
14	0.280	5.36 "
15	0.280	7.32 E-03
16	0.277	1.15 E-02
17	0.269	1.56 "
18	0.257	1.82 "
19	0.241	
20	0.223	
21	0.202	
TOL	1.0 E-08	1.0 E-08

APPENDIX

Let $\psi(y,t) = \sum_{l=0}^{\infty} \sin(ly)\, \tilde{\psi}_l(t)$;

with $l = n\pi/2D$, $n = 0, 1, 2, 3\ldots$ and $0 \leqslant y \leqslant 2D$. The boundary conditions $\psi = 0$ at $y = 0, 2D$ are then identically satisfied.

Let $C_l \equiv (-i/2)\, \tilde{\psi}_l$, $l \geq 0$,

$C_l \equiv (i/2)\, \tilde{\psi}_l$, $l < 0$.

Then

$$\psi(y,t) = \sum_{l\geq 0} (1/2i)\,(e^{ily} - e^{-ily})\, \tilde{\psi}_l(t)$$

$$= \sum_{l\geq 0} e^{ily} C_l + \sum_{l<0} e^{ily} C_l$$

and $\psi(y,t) = \sum_{l=-\infty}^{\infty} C_l\, e^{ily}$.

Now, let's change this to a Fourier transform (in integral form):

$$\psi(y,t) = \int_{-\infty}^{\infty} e^{ily}\, C_l(t)\, dl\, (2D/\pi)$$

Also $\tilde{\psi}_l(t) = (1/D) \int_0^{2D} \sin ly\, \psi(y,t)\, dy$

$$\equiv I_l/D, \quad l>0$$

or $D\,\tilde{\psi}_l = I_l, \quad l > 0.$

Then $C_l = (-i/2)\,(I_l/D), \quad l \geq 0$

$= (i/2)\,(I_l/D), \quad l < 0.$

Substituting this in the Fourier transform, we obtain:

$$2DC_1 / \pi = -i\ (I_1/\pi),\quad l \geq 0$$

$$= i\ (I_1/\pi),\quad l < 0.$$

So the condition is then $\tilde{\psi}(-l, t) = -\tilde{\psi}(l, t)$.

REFERENCES

Lindzen, R. S. and Tung, K. K. 1978. Wave overreflection and shear instability. J. Atmos. Sci., 35, 1626-1632.

Pedlosky, J. 1979. Geophysical Fluid Dynamics, Springer - Verlag, Inc., New York.

Ralston, A. and Rabinowitz, P. 1978. A First Course in Numerical Analysis, McGraw-Hill, New York.

Tung, K.-K. 1983. Initial-value problems for Rossby waves in a shear flow with initial level. J. Fluid Mech., 133, 443-469.

Worsham, R. D. 1983. Time Development of Rossby Wave Instability in a Shear Flow, Master Thesis, Mathematics Department, M. I. T.